University of Liège – Faculty of Medicine
Laboratory of Biology of Tumor and Development (LBTD)

Experimental study of fertility alterations, immune microenvironment changes, and S1P pathway targeting in a murine model of adenomyosis.



Marlyne Squatrito

Promoter : Dr. Carine Munaut

Thesis submitted in fulfillment of the requirements for the degree of Doctor of Biomedical and Pharmaceutical Sciences

Academic Year 2025 – 2026

Remerciements/Acknowledgements

Cette thèse constitue l'aboutissement d'un parcours marqué par de nombreux apprentissages et défis. Sa réalisation n'aurait pas été possible sans le soutien de nombreuses personnes, tant sur le plan scientifique qu'humain. Je tiens à leur adresser ici mes sincères remerciements.

Avant de les formuler plus précisément, il convient de revenir brièvement sur les circonstances dans lesquelles ce travail a été entrepris. Me lancer dans un doctorat n'a jamais été une évidence pour moi. J'ai longtemps hésité avant d'accepter ce défi, portée par l'envie d'apprendre mais freinée par le doute — le doute de ne pas être à la hauteur, de ne pas en être capable, de ne pas avoir les épaules pour un projet aussi exigeant.

J'ai finalement fait ce choix sans certitude, avec plus de questions que de réponses. Ces années de thèse m'ont appris que le doctorat n'est ni un parcours linéaire ni une succession de réussites. Il est fait de remises en question, d'incertitudes et parfois, même souvent, d'échecs. Mais cette expérience m'a aussi appris l'importance des rencontres, du soutien des autres et de la confiance qui se construit tout au long du parcours. Si j'ai pu aller au bout de ce travail, ce n'est pas seule, mais grâce aux personnes qui m'ont accompagnée tout au long de ce chemin. Ces remerciements sont l'occasion d'exprimer ma reconnaissance à l'ensemble de ces personnes.

Je tiens tout d'abord à remercier les **membres du jury** pour avoir accepté d'évaluer ce travail et pour le temps consacré à sa lecture.

Je souhaite ensuite vous remercier, Prof. **Agnès Noël** et **Didier Cataldo**, de m'avoir accueillie au sein du laboratoire et de m'avoir donné l'opportunité d'entreprendre ce doctorat. **Agnès**, je tiens à vous remercier tout particulièrement. Vous avez été l'une de mes professeures lors de mes études en sciences biomédicales - Une de celles que l'on retient : toujours à l'écoute, profondément humaine et que l'on n'oublie pas. Retrouver ces mêmes qualités au sein du labo a été un véritable privilège.

Je souhaite également te remercier, Dr **Carine Munaut**, pour m'avoir accompagnée tout au long de ces quatre années de thèse. Ton encadrement, parfois exigeant, m'a poussée à dépasser mes limites, à affiner ma réflexion et à développer mon esprit critique. Même lorsque des manips n'étaient vraiment pas glorieuses, ton soutien et tes conseils m'ont permis d'avancer, de gagner en autonomie et de prendre confiance en moi. Merci pour ton accompagnement, pour avoir cru en moi et pour m'avoir guidée jusqu'au bout de ce projet.

Je remercie aussi les membres de mon comité de thèse - **Michaël Herfs**, **Nathalie Jacobs**, et **Laure Noël** - pour m'avoir suivie tout au long de ces quatre années, pour leur disponibilité, leurs remarques constructives et l'intérêt porté à mon travail. Je tiens aussi à remercier Dr **Michelle Nisolle**, qui a été ma co-promotrice pendant près de trois ans, ainsi que Dr **Marie-Madeleine Dolmans**, Dr **Jacques Donnez** et **l'ensemble de leur équipe**, pour les échanges scientifiques ponctuels et enrichissants.

Je tiens à remercier chaleureusement les technologues du laboratoire — **Nath**, **Laëti M-R**, **Erika**, **Sheila**, **Isa D**. et **Emilie**. Votre aide est précieuse et indispensable au quotidien. Votre efficacité, votre disponibilité et votre bonne humeur ont grandement facilité mon travail expérimental, et travailler à vos côtés a été un réel plaisir.

Je remercie les différentes plateformes du **GIGA** pour leur soutien technique, et tout particulièrement **Raafat Stephan**, qui m'a formée aux FACS, **Gaëtan Lefèvre** pour l'Incucyte, et **Alexandre Hego** pour l'imagerie 3D. Votre expertise et votre disponibilité ont été essentielles à la réalisation de ce travail.

Un grand merci à **Hélène Brisy**. Hélène, merci pour ta gentillesse, ta bienveillance et ton aide précieuse au quotidien, notamment pour la gestion des commandes. Ta présence rend le fonctionnement du labo beaucoup plus simple et tellement plus agréable.

Je tiens à adresser un remerciement tout particulier à Dr. **Silvia Blacher**, doyenne du laboratoire, pour avoir réalisé l'ensemble de mes quantifications d'images. Ce travail colossal a été d'une importance majeure pour cette thèse, et je te suis profondément reconnaissante pour ton investissement.

Ces années de thèse ont aussi été rythmées par le quotidien partagé avec d'autres doctorants et collègues, qui traversaient les mêmes doutes, les mêmes difficultés, mais aussi les mêmes fous rires. C'est à eux que je souhaite maintenant m'adresser.

Je remercie tout d'abord le « **bureau des six** », où l'ambiance a toujours été au rendez-vous. Merci pour ces moments partagés entre les manips, les pauses bien méritées et les marshmallows grillés sur le radiateur électrique. **Léa**, je tiens à te remercier tout particulièrement. Nous avons commencé cette aventure côte à côte et avons passé des heures à discuter de tout et de rien, parfois sans même nous rendre compte que le temps filait. Ces échanges ont accompagné mes premiers pas en doctorat et ont beaucoup compté pour moi.

Je souhaite ensuite m'adresser aux membres de mon équipe. **Jules**, merci pour ta patience face à mon anglais parfois (très souvent) approximatif. Malgré la barrière de

la langue, ton humour et ta joie de vivre ont rendu certaines journées difficiles un peu plus légères. Même si je râlais parfois lorsque tu remplissais la machine à café uniquement pour le tien, je garderai surtout le souvenir de ton énergie positive et contagieuse au quotidien. **Laëtitia B**., merci d'être arrivée à mi-parcours dans l'équipe et d'avoir créé si rapidement une si belle complicité. Merci pour ton écoute, ta bienveillance et ces longues pauses au bureau. Je suis vraiment heureuse d'avoir partagé avec toi le congrès à Amsterdam — la chambre en sous-sol de l'hôtel et un congrès sans boire ni manger resteront des souvenirs mémorables. **Julie**, je te remercie pour les échanges partagés au sein de l'équipe et je te souhaite le meilleur pour la suite de ton parcours. J'espère que tu mèneras le projet sur l'adénomyose aussi loin que possible – et je n'ai aucun doute sur ta capacité à le faire.

Je souhaite aussi remercier les membres de mon nouveau bureau. **Eva**, merci d'avoir toujours été une oreille attentive. Nos échanges ont largement dépassé le cadre du laboratoire, et je suis heureuse que nous continuions encore aujourd'hui à nous voir en dehors du labo. **Florence**, merci pour ta bonne humeur, ta tchatche inépuisable et tous ces moments partagés autour d'un café — ou parfois bien plus. Tu doutes souvent de toi, mais tu devrais vraiment te faire confiance, car ton enthousiasme et ta générosité rendent chaque journée plus agréable. Je dois avouer que j'ai encore un peu peur quand j'entends une porte claquer… un souvenir d'une Florence très en colère. **Manon**, merci à toi aussi pour ta bonne humeur, ton soutien et ton énergie incroyable. Même si notre aventure sportive commune n'a pas duré bien longtemps (du moins pour moi), je n'ai jamais cessé d'admirer ta rigueur et ta capacité à toujours être présente quand c'était important. Travailler à tes côtés a été un vrai plaisir.

Florence et **Manon**, je tiens à vous remercier tout particulièrement pour votre soutien lors d'une étape très importante de ma vie : ma première grossesse. Florence, merci d'avoir discrètement bu mes verres à ma place. Manon, merci de m'avoir supporté au quotidien, tâche pas toujours évidente. Votre présence et votre bienveillance m'ont été précieuses.

Je souhaite également m'adresser à **Vincenzo** et **Isabelle DDS**. Au-delà de votre gentillesse, votre soutien scientifique a été déterminant. Merci pour vos conseils, votre disponibilité et votre aide dans de nombreuses expériences, notamment pour les FACS. Vous avez largement contribué à me guider tout au long de ce travail.

Merci à tous les autres membres du LBTD — **Chloé, Louis, Fatine, Daphnée, Sébastien, Loïc R., Jonathan, Elitsa, Aimée, Sophie, Loïc C., Camille, Noémie, Thomas, Robin, Quentin** — pour l'ambiance exceptionnelle qui a régné au

laboratoire. J'ai pleinement conscience que je ne retrouverai probablement jamais ailleurs une atmosphère aussi humaine et chaleureuse. Je souhaite aussi remercier **les filles du +3**. Même si nous étions un peu moins proches, j'ai toujours apprécié nos échanges et votre gentillesse.

Je souhaite enfin m'adresser à ma famille. **Papa**, **Maman**, et toi aussi **ma sœur**, merci d'avoir toujours cru en moi. Même si vous n'avez sans doute jamais vraiment compris ce que j'ai fait pendant ces quatre années, vous m'avez toujours soutenue, encouragée et fait confiance. Votre présence et votre fierté ont été des repères essentiels tout au long de ce parcours. Savoir que vous étiez là, quoi qu'il arrive, m'a donnée la force de continuer, même dans les moments de doute. **Nathan**, mon amour de toujours. Toi, tu as vécu cette thèse avec moi, tout du long. Tu as partagé chaque étape : les longues soirées devant l'ordi, les week-ends au laboratoire, les moments difficiles et les doutes. Tu as été le soutien le plus constant, celui qui a tout traversé à mes côtés. Sans comprendre ce que je faisais toi non plus, tu as toujours compris ce dont j'avais besoin. Tu as essuyé chacune de mes larmes lorsque je rentrais à la maison après un sacrifice de souris, et tu as toujours su trouver les mots pour m'aider à continuer. Tu as été cette épaule sur laquelle je pouvais me reposer, un pilier dans les moments les plus exigeants de ce doctorat. Pour ta patience, ton amour et ton soutien sans faille, merci.

Et enfin je m'adresse à toi, **Juliette**, ma fille. Tu n'as évidemment pas contribué directement à l'écriture de cette thèse, et pourtant tu en es, sans aucun doute, l'une des raisons les plus fortes. Terminer un doctorat en parallèle d'une grossesse, puis d'une maternité, n'a pas été simple — loin de là. Reprendre le travail après ta naissance, te laisser chaque matin, apprendre à jongler entre les nuits écourtées, les émotions, la fatigue, et la pression de devoir encore rédiger deux articles scientifiques et une thèse, a été une épreuve particulièrement difficile. Il y a eu des moments de doute, d'épuisement, parfois même de découragement. Et pourtant, je n'ai aucun regret. Bien au contraire. Tu m'as appris à aller à l'essentiel, à relativiser ce qui me paraissait insurmontable. C'est toi qui m'as donné l'énergie de continuer lorsque je pensais ne plus en avoir, la motivation de terminer ce que j'avais commencé, et la force de mener cette thèse jusqu'au bout. Grâce à toi, j'ai compris que je pouvais être plus forte que je ne l'imaginais. Cette thèse s'est achevée avec toi à mes côtés, et pour cela, je te remercie.

List of abbreviations

Arg-1 – Arginase-1

ART – Assisted reproductive technologies

BMP15 – Bone morphogenetic protein 15

CD – Cluster of differentiation

DIE – Deep infiltrating endometriosis

DN – Double negative (T cells)

EMID – Endometrial–myometrial interface disruption

ERα / ERβ – Estrogen receptor alpha / beta

FDA – Food and Drug Administration

FOXP3 – Forkhead box P3

FOXL2 – Forkhead box L2

FSHR – Follicle-stimulating hormone receptor

FTY720 – Fingolimod

FTY720-P – Phosphorylated fingolimod

G-CSF – Granulocyte colony-stimulating factor

hEM3 – Human endometrial mesenchymal cell line

hESC – Human endometrial stromal cells

HoxA10 – Homeobox A10

ICSI – Intracytoplasmic sperm injection

IFN-γ – Interferon gamma

IL – Interleukin

IL6R – Interleukin-6 receptor

IVF – In vitro fertilization

JZ – Junctional zone

KIR – Killer-cell immunoglobulin-like receptor

LEF1 – Lymphoid enhancer-binding factor 1

LIF – Leukemia inhibitory factor

MAPK – Mitogen-activated protein kinase

MMP9 – Matrix metalloproteinase 9

MRI – Magnetic resonance imaging

MUSA – Morphological Uterus Sonographic Assessment

NK cells – Natural killer cells

NKT cells – Natural killer T cells

PBMCs – Peripheral blood mononuclear cells

PI3K – Phosphoinositide 3-kinase

PND – Postnatal day

PGR – Progesterone receptor

RNA-seq – RNA sequencing

RRMS – Relapsing–remitting multiple sclerosis

S1P – Sphingosine-1-phosphate

S1PR – Sphingosine-1-phosphate receptor

SGLP – Sphingosine-1-phosphate lyase

SGPP – Sphingosine-1-phosphate phosphatase

SKI-5C – Sphingosine kinase inhibitor 5C

SPHK – Sphingosine kinase

STAT3 – Signal transducer and activator of transcription 3

Tc cells – Cytotoxic T cells

TGF-β – Transforming growth factor beta

Th cells – T helper cells

Th17 – T helper 17 cells

TIAR – Tissue injury and repair

TNF – Tumor necrosis factor

TNF-α – Tumor necrosis factor alpha

Treg – Regulatory T cell

uNK – Uterine natural killer cells

uPA – Urokinase-type plasminogen activator

VEGF – Vascular endothelial growth factor

ABSTRACT

Résumé

L'adénomyose est une pathologie utérine fréquente, associée à des douleurs pelviennes, des ménorragies et une altération de la fertilité, alors qu'aucune thérapie médicale ciblée n'est actuellement approuvée et que l'hystérectomie demeure le seul traitement définitif, incompatible avec le désir de grossesse. La compréhension de sa physiopathologie reste entravée par la coexistence fréquente de comorbidités, notamment l'endométriose, qui rendent difficile l'identification des mécanismes propres à l'adénomyose. L'utilisation d'un modèle murin induit par le tamoxifène, dépourvu de pathologies gynécologiques associées, permet d'explorer de manière intégrée et isolée l'impact de l'adénomyose sur la fertilité, le microenvironnement immunitaire utérin et la signalisation sphingosine-1-phosphate (S1P).

Les résultats de ce travail suggèrent qu'une adénomyose diffuse est suffisante pour perturber la folliculogenèse, modifier les cycles œstraux et altérer précocement des marqueurs clés de la réceptivité endométriale, avant l'installation d'une résistance à la progestérone, conduisant à une diminution marquée du potentiel reproducteur. Parallèlement, le microenvironnement immunitaire utérin apparait profondément remanié dès les stades précoces, avec une reprogrammation des macrophages, une redistribution des sous-populations de lymphocytes T et une surexpression persistante de l'IL6, reflétant un état inflammation chronique et une rupture de l'homéostasie tissulaire. Enfin, la voie S1P montre une dérégulation dynamique étroitement liée à la progression de la maladie. Son inhibition pharmacologique par SKI-5C ou FTY720 réduit la sévérité et l'invasion des lésions de manière dépendante du stade et du moment d'intervention, sans normalisation globale de l'infiltrat immunitaire mais avec une modulation significative des voies cytokiniques et invasives, notamment via la réduction d'uPA.

En intégrant ces trois volets, cette thèse propose de considérer l'adénomyose non plus uniquement comme une anomalie structurelle, mais comme une affection centrée sur la zone jonctionnelle et le microenvironnement utérin, où interagissent dérégulation immunitaire, altération de la réceptivité endométriale et remodelage tissulaire S1P-dépendant. Sans prétende épuiser la complexité de la maladie, ces travaux mettent en évidence des processus et voies de signalisation susceptibles de guider le développement de stratégies thérapeutiques mieux adaptées au stade évolutif de la maladie et potentiellement compatibles avec la préservation de la fertilité.

Abstract

Adenomyosis is a frequent uterine disorder associated with pelvic pain, heavy menstrual bleeding, and impaired fertility, yet no targeted medical therapy is currently available, and hysterectomy remains the only definitive treatment, which is incompatible with the desire to conceive. Understanding its pathophysiology is hindered by the frequent coexistence of comorbid conditions, particularly endometriosis, making it difficult to isolate mechanisms specifically attributable to adenomyosis. The use of a tamoxifen-induced mouse model, free of associated gynecological diseases, provides the opportunity to investigate in an integrated and isolated manner the impact of adenomyosis on fertility, the uterine immune microenvironment, and sphingosine-1-phosphate (S1P) signaling.

Findings from this work show that diffuse adenomyosis is sufficient to disrupt folliculogenesis, alter estrous cyclicity, and induce early defects in endometrial receptivity markers, preceding the onset of progesterone resistance and ultimately leading to a marked reduction in reproductive potential. In parallel, the uterine immune microenvironment appears profoundly remodeled from the earliest stages, with macrophage reprogramming, redistribution of T-cell subsets, and persistent IL6 overexpression, consistent with chronic inflammation and disrupted tissue homeostasis. Finally, the S1P pathway exhibits dynamic dysregulation closely linked to disease progression. Pharmacological inhibition of this pathway using SKI-5C and FTY720 reduces lesion severity and invasion in a stage-dependent manner, without globally normalizing the immune infiltrate but significantly modulating cytokine and invasive pathways, including reducing uPA expression.

By integrating these three dimensions, this thesis proposes that adenomyosis should be considered not solely as a structural abnormality, but as a disorder centered on the junctional zone and the uterine microenvironment, where dysregulated immune signaling, impaired endometrial receptivity, and S1P-dependent tissue remodeling interact. While not claiming to exhaust the complexity of the disease, this work highlights several cellular processes and signaling pathways that may guide the development of more stage-adapted therapeutic strategies, potentially compatible with fertility preservation.

Table of contents

INTRODUCTION 1

1. Adenomyosis: clinical and epidemiological context 1

1.1. Definition 1

1.2. Prevalence 2

1.3. Symptoms and clinical features 3

1.4. Diagnosis approaches and challenges 4

2. From initiation to progression: Biological basis of adenomyosis 5

2.1. Hypotheses of lesion formation 5

2.1.1. Invagination theory 6

2.1.2. The Stem Cell/Metaplasia theory 6

2.1.3. Outside-to-inside hypothesis 7

2.2. Mechanisms of lesion development and progression 8

3. Preclinical models of adenomyosis 12

3.1. Major stages of mouse uterine development 13

3.2. Experimental models of adenomyosis 14

3.3.1. Effects of tamoxifen exposure in murine models 16

3.3.2. Reproductive and uterine effects of tamoxifen in humans 17

4. Adenomyosis and female fertility: impact on reproductive potential 21

4.1. Key elements of female reproductive physiology 21

4.2. Fundamental biological requirements for conception and pregnancy maintenance 23

4.2.1. Acquisition of a developmentally competent oocyte 24

4.2.2. Establishment of a receptive endometrium 25

4.2.3. A favorable uterine microenvironment 27

4.3. Comparative aspects of the reproductive system in female mice and women 28

4.3.1. Morphological comparison 29

4.3.2. Folliculogenesis and reproductive cycles 29

4.3.3. Implantation and decidualization 30

4.3.4. Translational considerations 31

4.4. Adenomyosis and infertility: mechanisms and clinical outcomes 32

4.4.1. Reproductive outcomes in natural and assisted conception 32

4.4.2. Potential mechanisms underlying infertility in adenomyosis 32
4.4.3. Comorbidities and confounding factors 33
5. Uterine immune landscape: immune cells and cytokine networks 34
5.1. The healthy uterine immune system 35
5.1.1. Macrophages 35
5.1.2. NK cells 36
5.1.3. T lymphocytes 37
5.1.4. B lymphocytes 37
5.2. Immune dysregulation in adenomyosis: initiation and lesion progression 38
5.2.1. Macrophages 38
5.2.2. NK cells 38
5.2.3. T and B lymphocytes 39
5.3. Disruption of implantation processes in adenomyosis 40
5.4. Therapeutic perspectives 41
6. The Sphingosine-1-phosphate pathway (S1P) 42
6.1. Metabolism, cellular sources, receptors, and gradient formation 42
6.2. Physiological roles of S1P in reproductive tissues 46
6.3. The S1P gradient: physiological significance and pathological relevance 46
6.4. Implications in endometriosis and other gynecological pathologies 48
6.5. Potential implication in adenomyosis 49
6.6. Therapeutic targeting of the S1P pathway 50
6.6.1. Targeting S1P synthesis 51
6.6.2. Targeting S1P receptors (S1PR modulators) 51
OBJECTIVES AND OUTLINES OF THE THESIS 53
RESULTS 57
DISCUSSION AND CONCLUSION 117
PERSPECTIVES 129
REFERENCES 135
APPENDIXES 171

INTRODUCTION

1. Adenomyosis: clinical and epidemiological context

1.1.Definition

Adenomyosis is a chronic, estrogen-dependent uterine disorder characterized by a disruption of the endometrial-myometrial interface – also known as the junctional zone (JZ) – and the presence of ectopic endometrial tissue within the myometrium. Although it was first described in the 19th century by Karl von Rokitansky (1), its histopathological definition was firmly established by Bird et al. (1972) (2), whose criteria remain widely accepted today.

Macroscopically, adenomyosis often manifests as a globular, enlarged uterus with asymmetric thickening of the myometrial walls, reflecting the diffuse remodeling of the myometrium that accompanies lesion development. Small cystic or hemorrhagic foci may be observed, although these features can be subtle and require correlation with histology or imaging (3).

Microscopically, adenomyotic lesions are characterized not only by the presence of ectopic endometrial glands and stroma within myometrium but also by marked remodeling of the adjacent smooth muscle compartment. The myometrial bundles surrounding the lesions typically exhibit hypertrophy, loss of their normal fascicular organization and alterations in cytoskeletal architecture. These structural modifications are thought to reflect a local response to repeated tissue injury and chronic exposure to cyclic estrogen-progesterone fluctuations (3). Stromal inflammation, microcyst formation, or localized fibrosis may appear in more advanced forms of the disease, further illustrating its progressive myometrial remodeling (3,4). The ectopic glands often display cyclical changes similar to those of the eutopic endometrium, which may contribute to symptoms such as pelvic pain and abnormal uterine bleeding (4). A schematic illustration of normal uterine anatomy and adenomyosis-associated architectural disruption is shown in Figure 1.

These histological and anatomical features form the basis of diagnosis, yet their visibility varies across diagnostic methods – ranging from histopathology to transvaginal ultrasound and MRI – contributing to the wide variability in reported prevalence estimates.

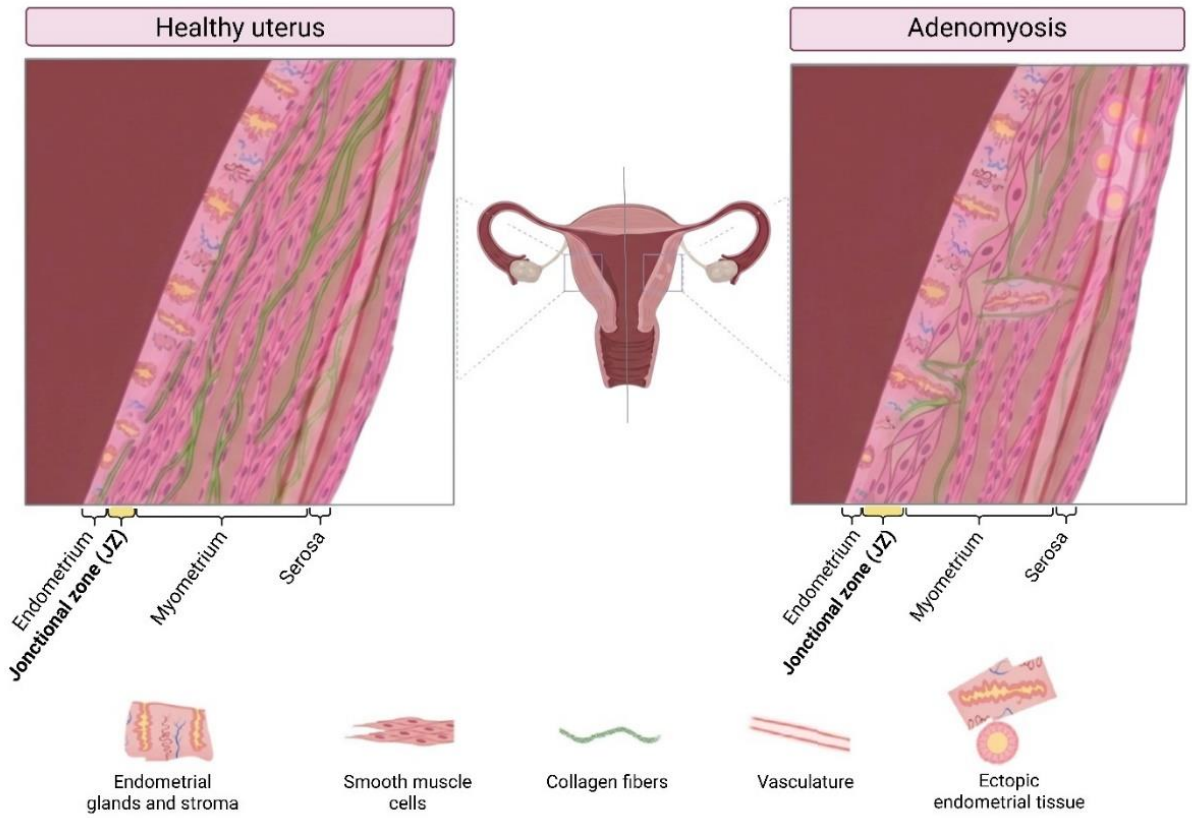


Figure 1. Morphological organization of the normal uterine wall and structural alterations in adenomyosis. *In healthy uterus, the uterine wall is organized into distinct layers comprising the endometrium, the junctional zone (JZ), the myometrium, and the serosa. The JZ corresponds to a specialized compartment at the endometrium-myometrium interface, which is involved in uterine contractility and tissue homeostasis. In adenomyosis, the overall organization of the endometrium is preserved, whereas major architectural alterations are observed within the JZ and the myometrium. The JZ exhibits structural disorganization, with altered smooth muscle cell arrangement, and ectopic endometrial glands and stromal tissue extend into the myometrium, disrupting normal tissue architecture. Adapted from Harmsen et al. (5) with BioRender.com*

1.2. Prevalence

Adenomyosis is a common gynecological condition, although its true prevalence remains highly variable due to differences in diagnostic criteria, study populations and the sensitivity of available detection methods. Population-based imaging studies have estimated that 10-30% of women of reproductive age are affected, whereas hysterectomy-based histological analyses report prevalence rates ranging from 8.8% to 61.5%, reflecting selection bias toward symptomatic women undergoing surgery. In addition, a substantial proportion of adenomyosis cases are asymptomatic and therefore incidentally diagnosed after hysterectomy performed for other indications, which may further inflate prevalence estimates in surgical cohorts compared with imaging-based studies (6–8). Consequently, the true population prevalence likely lies between these extremes and remains difficult to define precisely.

Historically, adenomyosis was considered a condition predominantly affecting multiparous women between 35 and 50 years old, with parity described as a significant risk factor, likely due to repeated trauma at the endometrial-myometrial interface during pregnancy and childbirth (8–10). However, with the advent of high-resolution MRI and standardized ultrasound criteria, adenomyosis is increasingly diagnosed in younger and nulliparous women (11–13). These observations suggest that the condition may also arise independently of obstetric history, indicating the involvement of genetic, hormonal, or inflammatory mechanisms. Early detection in younger women is therefore best regarded as potentially clinically relevant, as it may facilitate early symptom management and the consideration of potential fertility preservation strategies before disease progression.

Despite improved detection, adenomyosis remains underdiagnosed. Symptoms often overlap with those of uterine fibroids or endometriosis, variability in operator expertise, and the non-universal application of standardized MUSA criteria all contribute to missed or delayed diagnosis, ultimately impacting quality of life and delaying appropriate care (14). The real prevalence therefore remains uncertain, highlighting the need for reliable preclinical models to study the disease.

1.3.Symptoms and clinical features

Adenomyosis exhibits a broad spectrum of clinical manifestations, ranging from completely asymptomatic cases to severe, debilitating symptoms that markedly affect daily functioning. The most common presentation includes heavy menstrual bleeding (menorrhagia), painful menstruation (dysmenorrhea), chronic pelvic pain, and infertility (15). However, a substantial proportion of women may remain asymptomatic or present with non-specific symptoms, which can contribute to delayed diagnosis and under-recognition of the disease.

Menorrhagia is often the presenting complaint, with patients experiencing prolonged and abundant menstrual flow that can lead to iron-deficiency anemia (16). Dysmenorrhea typically presents as severe, progressively worsening pelvic pain during menstruation and may be accompanied by chronic, non-cyclic pelvic discomfort (17). Dyspareunia and lower back pain are also frequently reported (18).

Overall, these symptoms substantially impact the quality of life of women with adenomyosis, who often report fatigue, emotional distress, and limitations in social or occupational functioning due to chronic pain and heavy bleeding (19–21).

Infertility is another important clinical feature associated with adenomyosis. Its mechanisms are multifactorial and involve alterations in uterine contractility, endometrial receptivity,

inflammatory signaling, and hormonal imbalance (22). Because of its clinical relevance and translational implications, infertility constitutes a central focus of this thesis and will be addressed in detail in a dedicated chapter.

1.4.Diagnosis approaches and challenges

Historically, the diagnosis of adenomyosis relied almost exclusively on histological confirmation after hysterectomy, which inherently excluded women of reproductive age wishing to preserve fertility (2). With the introduction of advanced imaging modalities, particularly high-resolution transvaginal ultrasound and magnetic resonance imaging (MRI), adenomyosis can now be investigated in broader and younger populations, including women seeking fertility preservation (23).

In transvaginal sonography, the MUSA (Morphological Uterus Sonographic Assessment) group proposed standardized criteria, revised in 2022, to improve diagnostic reproducibility. They distinguish direct signs, such as intramyometrial cysts, hyperechogenic islands, or subendometrial echogenic lines and buds, from indirect signs, including asymmetrical myometrial thickening, globular uterine shape, fan-shaped acoustic shadowing, translesional vascularity, or irregularity of the JZ. Direct signs increase specificity, yet overall sensitivity remains moderate and strongly operator-dependent, underscoring the importance of expertise and standardized evaluation (24,25). The main MUSA features are summarized in Figure 2.

Magnetic resonance imaging (MRI) offers higher soft-tissue contrast and is particularly useful when ultrasound findings are inconclusive, or when fibroids coexist (26). A junctional zone thickness > 12 mm is a historically accepted diagnostic threshold and correlates with histological disease in several studies (27). Yet, this cut-off is no longer considered sufficient on its own as JZ thickness varies with age, hormonal status and menstrual cycle phase and may remain normal in focal adenomyosis. Recent MRI approaches therefore combine several parameters, such as JZ irregularity, asymmetric thickening, and the presence of intramyometrial cysts, to improve diagnostic accuracy (28).

Despite improvements in imaging and standardization efforts, adenomyosis remains challenging to diagnose consistently. Lesion heterogeneity, overlap with endometriosis or fibroids, variability in operator expertise, and the lack of universally adopted criteria continue to limit sensitivity, particularly in mild or focal disease.

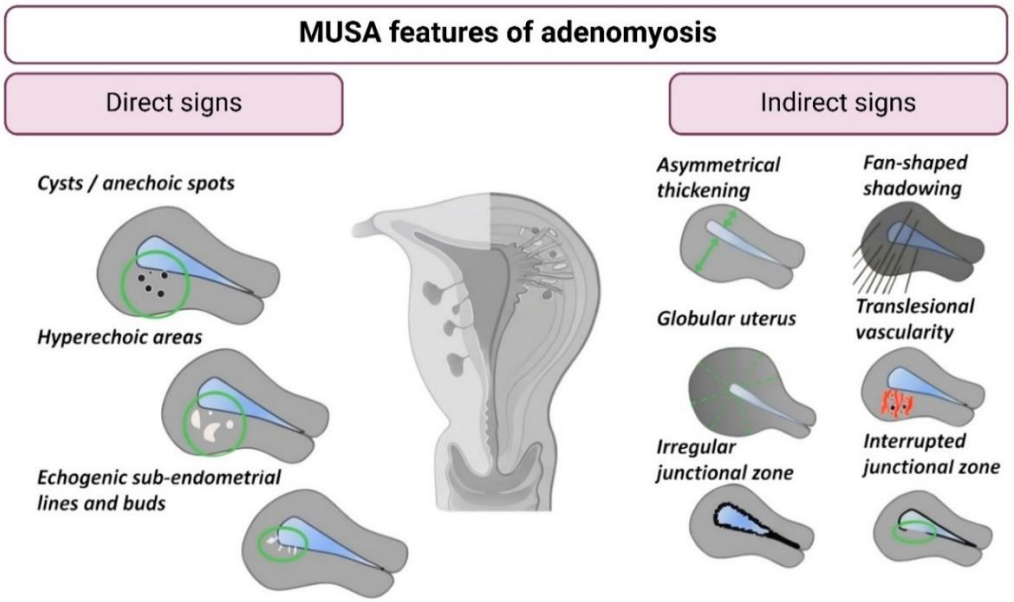


Figure 2. Summary of MUSA 2022 ultrasound criteria for the diagnosis of adenomyosis. *Direct signs include intramyometrial cysts, hyperechoic areas, and sub-endometrial echogenic lines or buds. Indirect signs include asymmetrical myometrial thickening, globular uterus, fan-shaped shadowing, translesional vascularity, and an irregular or interrupted junctional zone. Adapted from Harmsen et al. (24).*

2. From initiation to progression: Biological basis of adenomyosis

2.1. Hypotheses of lesion formation

Despite increasing recognition of adenomyosis as a distinct gynecological disorder, its origin remains incompletely understood. Several hypotheses have been proposed, the most prominent of which are the invagination theory, the stem cell/metaplasia theory and the outside-to-inside hypothesis (Figure 3). These models should not be viewed as mutually exclusive explanations but rather as complementary mechanisms that may contribute to the development of adenomyosis. Instead of representing distinct disease entities, they likely reflect different aspects of a shared pathological process, whose relative contribution may vary between patients. Such mechanistic diversity may help to explain the heterogeneity of lesion morphology, disease progression, and clinical presentation observed across individuals. For example, invagination might predominate in parous women with focal or diffuse adenomyosis of the inner myometrium, whereas metaplasia/stem cell driven mechanisms could underlie diffuse or juvenile forms typically seen in nulliparous adolescents or women without prior uterine surgery. In contrast, the outside-to-inside mechanism is thought to occur mainly in patients with deep infiltrating endometriosis. To provide an integrated understanding, the three main hypotheses are summarized below with balanced emphasis on their respective mechanisms.

2.1.1. Invagination theory

The invagination theory is the most widely cited model and proposes that adenomyosis originates from a direct infiltration of the endometrium basalis into the underlying myometrium through a disrupted or weakened junctional zone (JZ). JZ weakening is thought to result from recurrent mechanical stress and microtrauma associated with uterine hyperperistalsis and exaggerated contractility, which are characteristic of adenomyotic uteri (29,30).

This process is reinforced by the tissue injury and repair (TIAR) mechanism, whereby microlesions trigger a local cascade of inflammatory mediators, angiogenesis, and upregulation of aromatase activity, leading to increased local estradiol production. Estradiol, in turn, stimulates further contractility (via ERα-mediated oxytocin upregulation) and proliferation (via ERβ overexpression in adenomyotic lesions), thus establishing a self-perpetuating cycle of JZ disruption and tissue remodeling (29,30).

Beyond intrinsic uterine activity, physiological and iatrogenic events such as menstruation, childbirth, and uterine instrumentation (e.g. curettage, cesarean section, hysteroscopic procedures, …) may similarly compromise the integrity of the JZ. These events facilitate the downward migration of basal endometrial glands and stroma into the myometrium, providing an alternative pathway for lesion initiation. This may help explain the frequent clinical observation that adenomyosis often emerges or worsens after reproductive events (31,32).

2.1.2. The Stem Cell/Metaplasia theory

The second major hypothesis suggests that adenomyotic lesions may develop *de novo* within the myometrium, through the activity of stem or progenitor cells. The endometrial basalis layer is known to harbor adult stem cells capable of regenerating the endometrium after each menstrual cycle (33). Under conditions of local tissue disruption (e.g. microtrauma at the JZ), these progenitor cells may aberrantly migrate into the myometrium, where they differentiate into endometrial glands and stroma (31,34).

Additionally, embryonic remnants of Müllerian duct-derived cells, normally quiescent within the myometrium, may undergo metaplastic transformation into endometrial-like tissue under the influence of hormonal or inflammatory signals (34). This “stem cell/metaplasia theory” is supported by observations of adenomyotic foci in young patients or nulliparous women without prior uterine trauma, and by the detection of stem cell markers in adenomyotic lesions (34,35).

Overall, this theory reframes adenomyosis as a disorder of aberrant differentiation or misplaced stem cell activity, explaining cases not readily accounted for by JZ disruption alone.

2.1.3. Outside-to-inside hypothesis

A third, less frequent hypothesis proposes that adenomyosis may result from the migration of ectopic endometrial cells into the uterine wall, moving from the peritoneal cavity into the myometrium. This mechanism, which parallels theories of endometriosis development, appears to occur predominantly in women with coexisting deep infiltrating endometriosis, where ectopic implants may invade the outer myometrium and give rise to adenomyotic foci (35).

According to this model, ectopic endometrial cells originating from endometriotic implants could infiltrate the outer uterine wall, progressively extending inward to form adenomyotic foci. This theory is strongly supported by the frequent coexistence of adenomyosis and endometriosis, particularly in the posterior uterine wall adjacent to deep infiltrating endometriotic nodules (36). Several histopathological studies have reported direct continuity between endometriotic lesions and adjacent adenomyotic tissue, suggesting that outside-in invasion may represent a plausible mechanism in a subset of patients (37,38).

Thus, this mechanism may represent a relevant etiological route in patients with combined adenomyosis-endometriosis phenotypes.

These three theories likely represent complementary mechanisms rather than mutually exclusive pathways. Their relative contribution may differ according to age, reproductive history, lesion subtype (focal vs diffuse), and associated endometriosis. Recognizing this etiological heterogeneity is essential for understanding the diversity of clinical presentations and for interpreting findings from preclinical models of adenomyosis.

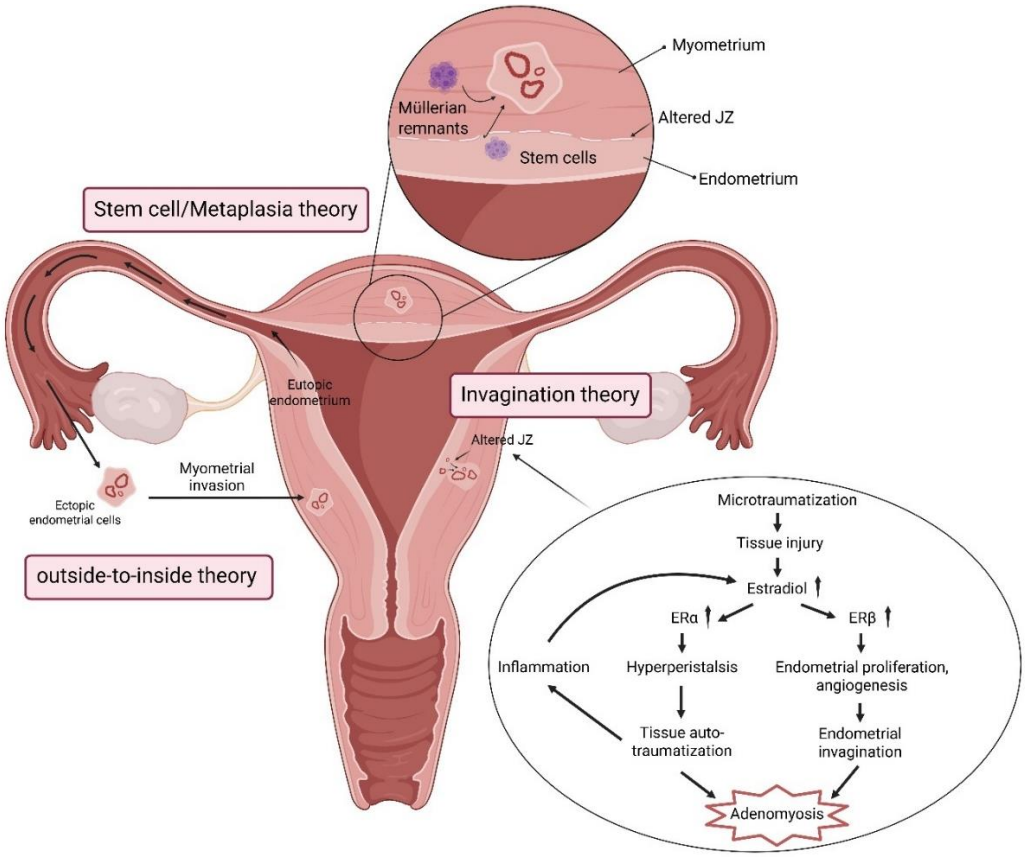


Figure 3. Main hypotheses proposed to explain adenomyotic lesion development*. The figure illustrates the three major theories of lesion formation: (1) invagination theory, describing the downward infiltration of the endometrial basalis into the myometrium, facilitated by junctional zone disruption and the tissue injury and repair (TIAR) mechanism; (2) stem cell/metaplasia theory, where endometrial or Müllerian progenitor cells differentiate de novo into endometrial-like tissue within the myometrium; (3) outside-to-inside theory, suggesting invasion of the uterine wall by ectopic endometrial cells originating from endometriotic implants. This latter mechanism likely applies to a subset of patients with coexisting deep infiltrating endometriosis and remains less widely accepted than the other two models. Adapted from Zhai et al.(39), designed with BioRender.com*

2.2.Mechanisms of lesion development and progression

The development and progression of adenomyotic lesions results from the interplay of several biological processes that collectively support lesion survival and contribute to symptom generation (40). After their initiation, adenomyotic foci exhibit enhanced epithelial and stromal proliferation, increased migratory and invasive capacity, and epithelial to mesenchymal transition (31,41,42). These processes represent the core mechanisms that drive lesion expansion and constitute the primary drivers of disease progression.

In parallel, chronic inflammation and altered innate and adaptive immune responses contribute to the establishment of a microenvironment that favors lesion persistence. Although multiple immune alterations have been reported (43), their temporal sequence and precise contribution to disease progression remain incompletely understood. Hormonal imbalance,

characterized by heightened local estrogenic activity and reduced progesterone responsiveness, amplifies proliferative and invasive cellular behavior (44,45).

Additional processes further sustain lesion maintenance. Angiogenesis and neuroangiogenesis provide the vascular and neural support required for ongoing lesion growth (46–48), while extensive extracellular matrix remodeling and progressive fibrosis alter uterine architecture and contribute to increased tissue stiffness (49,50). These processes are generally considered amplifying mechanisms.

Finally, disruptions in cell-death pathways, including altered apoptosis and incompletely defined role of autophagy, may also influence the persistence of ectopic endometrial cells, although current data remain contradictory (51,52).

Together, these interconnected mechanisms create self-reinforcing loops that drive lesion progression and underline the clinical manifestations of adenomyosis (Figure 4). Despite advances in understanding these pathways, important uncertainties remain regarding their respective contributions and interactions during disease evolution.

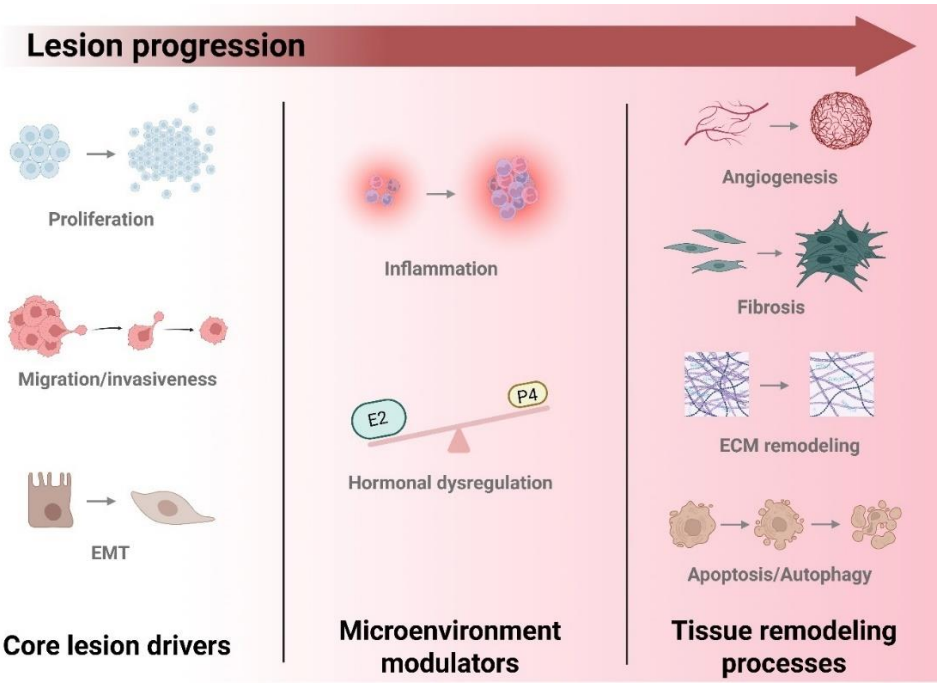


Figure 4. Biological processes contributing to the development and progression of adenomyotic lesions. *The schematic summarizes the major interconnected mechanisms involved in adenomyosis pathophysiology. Core drivers include enhanced epithelial and stromal proliferation, increased migratory and invasive behavior, and epithelial-to-mesenchymal transition (EMT), which together support lesion expansion. These primary mechanisms are reinforced by chronic inflammation, dysregulated innate and adaptive immune responses and local hormonal imbalance favoring estrogenic activity and progesterone resistance. Additional amplifying processes such as angiogenesis, extracellular matrix remodeling (ECM) and progressive fibrosis further promote lesion maintenance and tissue architectural changes. Finally, alterations in cell-death pathways, including disrupted apoptosis and autophagy may contribute to the persistence of ectopic endometrial cells. Created with BioRender.com*

2.3. Morphological subtypes and histopathological patterns

Adenomyosis is traditionally classified according to macroscopic, histopathologic, and imaging criteria, reflecting the heterogeneity of lesion architecture and depth of myometrial involvement. These systems provide complementary perspectives encompassed by the disease.

At the macroscopic level, the most common distinction is between diffuse and focal forms (Figure 5). Diffuse adenomyosis is characterized by widespread infiltration of ectopic endometrial glands and stroma throughout the myometrium, often resulting in a globally enlarged uterus. This diffuse pattern is the most commonly observed phenotype in preclinical tamoxifen-induced murine models, which typically develop full-thickness adenomyosis three months post-induction, thereby reproducing key morphological features observed in severe human disease.

In contrast, focal adenomyosis (also termed adenomyoma) corresponds to a localized, nodular form, surrounded by hypertrophic smooth muscle, and may mimic fibroids on imaging. MRI is particularly useful for differentiating focal adenomyosis from uterine fibroids due to its superior contrast resolution and visualization of the junctional zone (36).

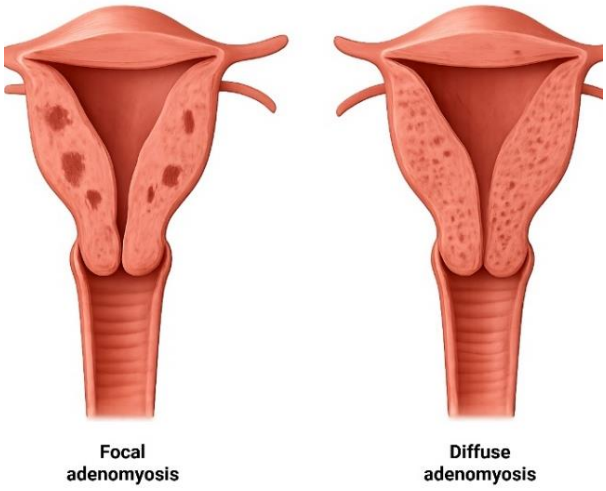


Figure 5. Comparison of focal and diffuse adenomyosis. *Created with BioRender.com*

However, the focal/diffuse dichotomy offers only a limited overview and does not fully capture the complexity of adenomyosis subtypes identified through modern imaging. MRI-based classifications now distinguish inner, outer, transmural, and indeterminate adenomyosis according to the location of lesions relative to the JZ (36). This imaging-based classification better reflects underlying pathophysiological mechanisms.

In addition to this morphological and anatomical distinctions, several histopathological grading systems have been proposed by Bird et al. to describe the depth and severity of myometrial infiltration. Grade 1 (mild) corresponds to superficial invasion confined to the inner third of the myometrium, grade 2 (moderate) involves up to two-thirds of the myometrial thickness, and grade 3 (severe) indicates deep or transmural infiltration extending toward the outer myometrium or even reaching the serosal surface (53). Although informative, this grading requires hysterectomy specimens and is therefore rarely used in clinical routine.

From a diagnostic standpoint, TVUS and MRI are the main tools for evaluating adenomyosis severity (54,55). MRI offers the highest diagnostic accuracy and allows assessment of lesion distribution within the myometrium, including inner, outer, or transmural involvement (36). This classification complements both morphological and histopathological systems and provides a more clinically applicable classification for characterizing disease severity.

2.4. Pathophysiological overlaps with endometriosis

Endometriosis and adenomyosis are both gynecological disorders characterized by the presence of ectopic endometrial-like tissue, but they differ in localization. In endometriosis, the ectopic tissue is found outside the uterine cavity, most commonly on the ovaries, peritoneum, or uterosacral ligaments, often forming deep infiltrating nodules or endometriomas. In contrast, adenomyosis affects the uterus internally, involving infiltration within the myometrium (29). Coexistence of the two conditions has been reported in up to 80% of patients with endometriosis (56–59). However, adenomyosis may also occur as an isolated condition without associated pelvic disease, and several studies have reported a substantial proportion of women presenting with adenomyosis in the absence of endometriosis or fibroids (60). Women affected by both conditions often exhibit more severe pain and poorer reproductive outcomes than those with either disease alone (61).

For many years, adenomyosis and endometriosis were often conflated, largely because diagnostic tools were not precise enough to distinguish them reliably. The two conditions share numerous clinical manifestations as well as several molecular and histological features. Both diseases exhibit ectopic glandular and stromal tissue, elevated local estrogen production, cellular hyperproliferation and resistance to cell death, along with increased migratory and invasive capacity (62,63). However, the notion that adenomy6osis and endometriosis share common pathogenic mechanisms is not universally accepted. Several studies emphasize that they represent two distinct diseases with different origins and clinical trajectories. Endometriosis is often linked to retrograde menstruation, metaplasia, and lymphatic or vascular dissemination. In contrast, adenomyosis appears to result from disruption of the

junctional zone, invagination of the endometrium, repeated mechanical or hormonal injury, or dysfunction of stem/progenitor cells (see "2. From initiation to progression: Biological basis of adenomyosis") (64,65). Thus, despite considerable overlap between the two conditions, important etiological and pathological differences remain. These distinctions are not only conceptual but also influence how experimental models should be interpreted, since models designed to capture one disease do not necessarily reproduce the biological processes driving the other. In this context, the murine model used in this thesis which is based on alterations of the junctional zone, is particularly relevant for investigating adenomyosis-specific mechanisms. While this model does not encompass all clinical phenotypes especially forms associated with deep infiltrating endometriosis, it provides a suitable framework to study the pathophysiological process intrinsic to adenomyosis. Whether the molecular similarities observed in adenomyosis and endometriosis reflect a shared origin or represent convergent pathogenic pathways driven distinct initiating events remain unresolved. Addressing this question will require further mechanistic investigation using disease-specific and comparative experimental models.

3. Preclinical models of adenomyosis

Experimental models – ranging from animal systems to cell-based approaches – have become essential tools to investigate both the pathogenesis of adenomyosis and the evaluation of potential therapies. Because research based on patient-derived tissue is limited by restricted access to uterine samples, marked inter-patient variability, and ethical constraints that preclude longitudinal or interventional analyses, preclinical systems provide controlled experimental conditions in which hormonal, molecular and cellular environments can be manipulated. Consequently, a wide spectrum of *in vivo*, *ex vivo* and *in vitro* models has been developed to overcome these challenges and to explore disease pathogenesis and treatment responses (66).

Because the experimental work presented in this thesis relies on a neonatal tamoxifen-induced murine model, it is important to consider the developmental context in which this exposure occurs. In mice, unlike in humans, a large part of uterine maturation takes place during the early postnatal period. This developmental window is characterized by rapid differentiation of uterine compartments and the initiation of endometrial gland formation, processes that are highly sensitive to endocrine perturbations. For this reason, the major stages of mouse uterine development are briefly outlined below to provide the biological context in which neonatal tamoxifen exposure occurs. The different experimental models currently used to study

adenomyosis are then presented, before focusing more specifically on the tamoxifen-induced murine model and the biological effects of tamoxifen.

3.1.Major stages of mouse uterine development

The mammalian uterus originates from the fusion of the two Müllerian ducts during embryonic development (67). In mice, however, although the basic uterine structure is specified prenatally, the majority of uterine differentiation and maturation occurs after birth.

At birth (postnatal day 0, P0), the mouse uterus consists of a simple tubular structure composed of a central lumen lined by luminal epithelial cells surrounded by undifferentiated mesenchymal cells (68,69). At this stage, the uterine wall remains largely immature and endometrial glands are absent. During the first postnatal week, major morphogenetic events progressively establish adult uterine architecture. Between postnatal days 3 and 5, epithelial invaginations originating from the luminal epithelium begin to penetrate the surrounding stroma, marking the onset of uterine gland formation in a process known as adenogenesis. These epithelial buds subsequently elongate and differentiate into tubular endometrial glands extending into the stromal compartment (68).

Concomitantly, the surrounding mesenchyme differentiates into distinct uterine compartments. The endometrial stroma becomes organized around the developing glands, while the myometrium differentiates into two smooth muscle layers: an inner circular layer and an outer longitudinal layer. By approximately postnatal days 10 to 15, uterine glands become more elongated and coiled, extending toward the myometrium, and the overall histological organization of the uterus begins to resemble that of the adult organ at P15 (68). As summarized in Figure 6, these sequential postnatal changes gradually establish the near-adult uterine architecture by the time of weaning.

Importantly, this perinatal period represents a critical developmental window during which epithelial–mesenchymal interactions and tightly regulated hormonal signaling pathways coordinate uterine morphogenesis. In particular, estrogen receptor-mediated signaling, especially through ERα, plays a central role in regulating epithelial proliferation and uterine development during the early postnatal period (70). During this time, uterine gland formations is initiated through the invagination of the luminal epithelium into the underlying stroma, a process that occurs predominantly after birth in rodents and is highly sensitive to hormonal perturbations (71). This morphogenetic process depends on coordinated signaling between epithelial and stromal compartments to ensure proper gland development and uterine maturation. In parallel, epigenetic programming events occurring during this

developmental window contribute to the long-term establishment of uterine cellular identity and hormone responsiveness (72). Disruption of these tightly coordinated processes, particularly through exposure to endocrine-active compounds, could lead to long-term alterations in uterine structure and reproductive function later in life. This developmental sensitivity is especially relevant for experimental models in which neonatal exposure to pharmacological agents, such as tamoxifen, is used to induce adenomyosis-like lesions.

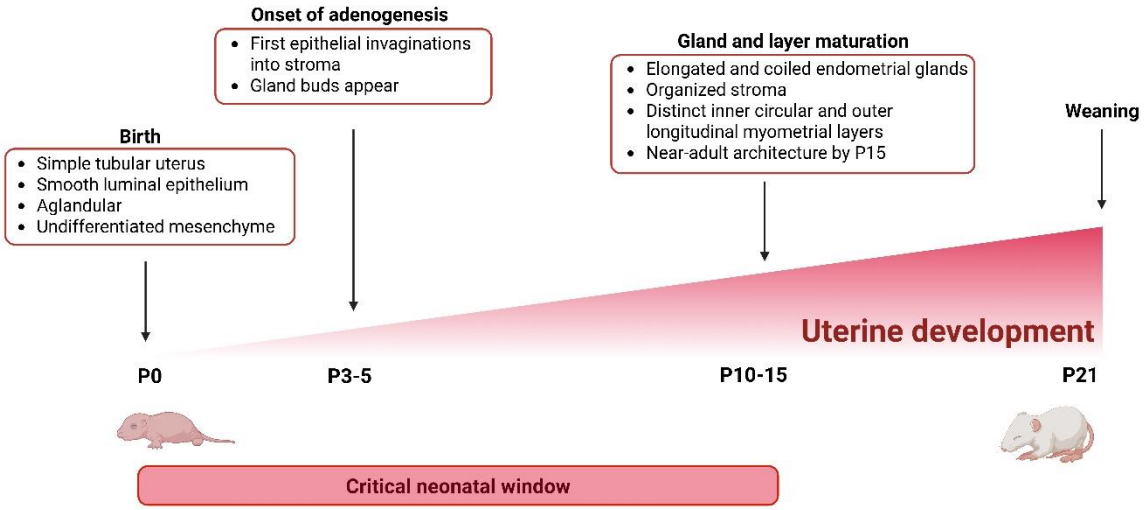


Figure 6. Postnatal development of the mouse uterus. *Schematic timeline illustrating key morphological events from birth (P0) to weaning (P21). At birth, the uterus is a simple tubular structure with a smooth luminal epithelium, no glands, and undifferentiated mesenchyme. During P3–P5, the onset of adenogenesis is characterized by the first epithelial invaginations into the stroma and the appearance of gland buds. By P10–P15, uterine gland and layer maturation are evident, with elongated and coiled endometrial glands, organized stroma, and distinct inner circular and outer longitudinal myometrial layers, resulting in a near-adult uterine architecture by P15. The shaded area indicates overall uterine development, and the bar at the bottom highlights the critical neonatal window during which the uterus is highly sensitive to endocrine and environmental perturbations. P= postnatal days. Created with BioRender.com*

3.2. Experimental models of adenomyosis

Among *in vivo* models, several experimental approaches have been developed to reproduce key aspects of adenomyosis pathogenesis. One recent approach is the uterine wall injury model, in which mechanical disruption of the endometrial-myometrial interface induces infiltration of endometrial glands into the myometrium, thereby mimicking the invagination process proposed in human disease (73,74). Another classical model is the pituitary graft model, where ectopic pituitary tissue is transplanted into rodents, leading to chronic hyperprolactinemia and the subsequent development of adenomyotic lesions (75–78). A third widely used strategy relies on pharmacological induction using neonatal tamoxifen exposure, which disrupts uterine development and leads to the appearance of adenomyosis-like lesions in adulthood (79,80). This tamoxifen-induced murine model, used as the experimental

framework throughout this thesis, has become one of the widely employed models for investigating pathophysiology due to its high reproducibility and its ability to recapitulate key histopathological hallmarks of the human disease, including the invasion of endometrial glands into the myometrium and the associated myometrial disorganization (81–84). Although it does not reproduce clinical symptoms such as dysmenorrhea or abnormal uterine bleeding, this model provides a useful framework to explore the cellular and molecular mechanisms involved in adenomyosis development and to evaluate therapeutic interventions in a controlled experimental setting.

While animal models provide crucial *in vivo* context, *ex vivo* and *in vitro* systems offer complementary mechanistic insights. Patient-derived explant (PDE) cultures, for example, are increasingly used in gynecological oncology as three-dimensional, patient-relevant models that preserve native tissue architecture and stromal-epithelial interactions, offering a more physiologically relevant study of drug response than traditional 2D cell cultures (85). In the context of adenomyosis, PDEs represent a potentially valuable approach to bridge mechanistic findings from murine models with patient-specific therapeutic testing. However, their application in this field remains challenging, as adenomyotic tissues are difficult to access, highly heterogeneous, and may vary depending on the depth of myometrial infiltration. In addition, limitations such as short-term viability, inter-patient variability, and the requirement for fresh surgical specimens further restrict their use. Thus, although technically feasible, patient derived explant culture remains a partial and short-lived model that does not recapitulate the invasive epithelial-myometrial interactions characteristic of adenomyosis (85).

Finally, cell-based models – including primary endometrial cells and, immortalized cell lines (e.g. hESC, 12Z, hEM3,..) enable tightly controlled assays of hormone signaling, proliferation, invasion, and candidate drug responses. Building on these 2D systems, 3D organoids derived from adenomyotic or eutopic endometrium recapitulate glandular architecture and epithelial polarity, thereby improving physiological relevance for mechanistic and pharmacologic studies. However, these models lack key features of the *in vivo* uterine environment, including systemic hormonal cyclicity, myometrial contractility, and vascularization, which may limit their ability to fully capture disease dynamics. Extending this concept, assembloids are composite 3D constructs generated by co-culturing epithelial organoids with stromal and/or myometrial cells to re-establish cell crosstalk and early extracellular matrix remodeling that are central to adenomyosis (85–92). While these *in vitro* models lack the complex immune, vascular, and mechanical context of the *in vivo* uterus, they represent an essential component of the experimental continuum for understanding adenomyosis pathophysiology and developing targeted therapies and may contribute to translational validation of preclinical

findings. Table 1 summarizes the main experimental models currently used to study adenomyosis, although other, less commonly used models have also been reported.

3.3. Tamoxifen-induced mouse model and biological effects of tamoxifen

Tamoxifen is a selective estrogen receptor modulator (SERM) widely used both in experimental biology and in clinical practice. In experimental systems, it is commonly employed to activate inducible genetic systems such as Cre-LoxP, enabling temporal control of gene recombination in transgenic mouse models (93). Beyond this technical application, tamoxifen also exerts intrinsic biological effects through its interaction with estrogen receptors, acting either as an antagonist or a partial agonist depending on the tissue context and developmental stage. These tissue-specific actions are particularly relevant in reproductive organs, where estrogen signaling plays a central role in uterine development and function. Tamoxifen exposure during critical developmental windows may therefore interfere with epithelial–mesenchymal interactions, stromal differentiation, and myometrial organization (94,95).

3.3.1. Effects of tamoxifen exposure in murine models

In rodents, neonatal tamoxifen exposure occurs during a critical window of uterine development and can disrupt the normal differentiation and organization of uterine tissues. Experimental studies have shown that early tamoxifen administration alters myometrial development, leading to disorganization of smooth muscle bundles and abnormalities in uterine architecture (95). These developmental alterations highlight the high sensitivity of the neonatal uterus to endocrine perturbations and the essential role of hormonal signaling in the establishment of uterine structure.

As a consequence of these developmental disruptions, neonatal tamoxifen exposure can promote the ectopic invasion of endometrial glands and stroma into the myometrium in adulthood, producing lesions that display key histopathological features comparable to those observed in human adenomyosis. These include well-defined ectopic endometrial glands within the myometrium, hypertrophy and thickening of the myometrial wall, and disruption of smooth muscle organization (79,80). However, susceptibility to lesion formation is strongly strain-dependent. CD1 mice are highly responsive to neonatal tamoxifen exposure, whereas C57BL/6 females are largely resistant, suggesting a genetic contribution to disease susceptibility (96). Moreover, CD1 mice are known to develop spontaneous adenomyosis with age, which further supports the use of this strain in experimental studies (95). Although this

intrinsic predisposition may also represent a potential confounding factor when interpreting outcomes.

Beyond its effects on uterine development, tamoxifen exposure has also been reported to influence ovarian physiology in adult rodents. Experimental studies have shown that tamoxifen may stimulate the premature activation of primordial follicles and alter ovarian reserve dynamics (97), although other studies suggest no significant effect on primordial and primary follicles pools but a reduction number of growing follicles (98). These apparently divergent findings likely reflect differences in experimental design, timing of exposure, and strain-specific ovarian sensitivity.

3.3.2. Reproductive and uterine effects of tamoxifen in humans

In humans, tamoxifen is widely used as adjuvant therapy for hormone receptor-positive breast cancer, most often in peri- or postmenopausal women. While it acts primarily as an estrogen receptor antagonist in breast tissue, tamoxifen behaves as a partial estrogen agonist in several other organs, including the female reproductive tract (99,100). As a result, its administration has been associated with multiple structural and functional changes in uterine tissues.

Clinical studies have reported that tamoxifen therapy can induce endometrial alterations such as increased endometrial thickness, endometrial polyps, and hyperplasia, reflecting its estrogen-like activity in the uterus (99–101). Prolonged exposure has also been associated with an increased risk of endometrial carcinoma and other uterine pathologies (99–101). In addition, several clinical observations have reported an increased prevalence of adenomyosis in women receiving tamoxifen therapy compared with untreated controls (102) although causality remains difficult to establish due to confounding factors such as age and parity.

In contrast, available evidence suggests that tamoxifen does not appear to have a major detrimental impact on ovarian reserve in women (103). Consistently, several studies indicate that fertility can often be preserved after treatment completion or temporary interruption of therapy in breast cancer survivors. Although women who receive tamoxifen are overall less likely to have a child after cancer diagnosis compared with women who did not receive the treatment, this difference does not appear to result from a further reduction in ovarian reserve attributable to tamoxifen exposure (104,105).

Beyond its endocrine effects, tamoxifen has also been shown to modulate immune cell function, including the activity of neutrophils, indicating that the drug may exert broader biological effects beyond estrogen receptor signaling (106,107). These immunomodulatory properties may contribute to shaping uterine tissue remodeling and inflammatory dynamics. In the endometrium, its exposure has been associated with the induction of angiogenic factors

such as vascular endothelial growth factor (VEGF) contributing to vascular remodeling and increased endometrial proliferation (108). In parallel, tamoxifen has been shown to modulate endothelial cell behavior by reducing migration and altering the expression of angiogenesis-related genes, thereby affecting endometrial angiogenesis and vascular integrity (109). Such alterations are closely linked to inflammatory processes, as changes in angiogenic signaling and tissue remodeling can influence immune cell recruitment and cytokine production. Together these findings suggest that tamoxifen may contribute to reshaping the uterine microenvironment through interconnected effects on immune regulations, angiogenesis and tissue remodeling- an aspect that must be considered in tamoxifen-based experimental models.

Importantly, tamoxifen exposure during pregnancy is contraindicated because of potential teratogenic effects and adverse fetal outcomes. Cases of congenital abnormalities and pregnancy complications following in utero exposure have been reported, highlighting the importance of effective contraception during treatment and appropriate washout periods before conception attempts (110). Consistent with these observations, experimental studies in mice have shown that tamoxifen administration during pregnancy can adversely affect both maternal physiology and embryonic development (111).

Taken together, these observations illustrate that tamoxifen can influence uterine physiology, ovarian function and reproductive outcomes through its tissue-specific modulation of estrogen receptor signaling. These effects should therefore be considered when interpreting results obtained from tamoxifen-based experimental models particularly in studies investigating uterine pathophysiology or fertility outcomes. Importantly, it should be noted that, in humans, tamoxifen exposure occurs predominantly in adult women after uterine maturation is complete, whereas in the present experimental model it is administered during a critical neonatal developmental window. This difference in timing may result in distinct biological outcomes and should be considered when extrapolating experimental findings to the clinical context.

Table 1. Summary of the main experimental models used on adenomyosis research.

Model type	Biological source	Induction method	Reproduced phenotypes	Advantages	Limits	Ref.
			In vivo			
Uterine wall injury	Mouse (BALB/c, C57BL/6)	Puncture with microcatheters or needle on uterine horn Thermal induction by electrocoagulation	JZ disruption, focal adenomyotic foci, myometrial fibrosis, local inflammation	Highly reproducible model to study tissue injury-repair mechanisms and early myometrial invasion	Artificial lesion induction; lacks spontaneous disease onset; acute injury-repair response rather than chronic disease; limited chronicity; limited immune and hormonal complexity	(73,74)
Pituitary graft model	Mouse (SHN, SLN, Balb/c, C3H, C57BL/6) Wistar rat	Pituitary graft under renal capsule or uterine horn	Disruption of myometrial layer, increased angiogenesis, hormonal imbalance	Useful to investigate hyperprolactinemia driven uterine remodeling	Requires surgery and complex procedures; systemic hormonal milieu differs from most clinical situations	(75–78)
Tamoxifen treatment	Mouse (CD1)	Oral gavage of neonatal mice (PND1-5)	JZ disruption, diffuse adenomyosis, myometrial fibrosis, local inflammation	Robust and reproductible model for diffuse adenomyosis, fertility studies, and longitudinal analyses	Slower disease chronology; Strain- and dose- dependent severity; partial representation of the clinical heterogeneity of adenomyosis	(79,80)
Spontaneous adenomyosis	Non-human primates	Naturally occurring lesions	Same as humans	Closest to human reproductive physiology; spontaneous disease	Ethical issues, high cost, restricted experimental manipulation	(112)
			Ex vivo			
Patient-derived explant	Fresh uterine or endometrial tissue culture	_	_	Preserves 3D tissue architecture, allows drug testing; retains stromal-epithelial interactions	Requires fresh biopsies; limited lifespan; donor variability; lacks systemic influences	(85)
			In vitro			
Primary endometrial cells	Isolated from eutopic or ectopic endometrium	Cells obtained from uterine tissues after surgery	_	Retain patient/animal-specific response; suitable for dissecting molecular pathways and testing targeted interventions	Variable phenotype; limited lifespan; loss of 3D organization and interaction with myometrium and immune cells	(92)
Immortalized endometrial cell lines	12Z, hESC, hEM3,…	Viral or telomerase immortalization	_	Long-term, stable; useful for mechanistic and drug studies	Altered gene expression vs primary cells; lack tissue context	(87,89,91)

Table 1. Summary of the main experimental models used on adenomyosis research.

Model type	Biological source	Induction method	Reproduced phenotypes	Advantages	Limits	Ref.
Organoids	3D culture from endometrial or stem cells	Organoid-forming culture from patient/animal tissue	_	Recapitulate glandular structure; hormone responsiveness	Lacks myometrial interaction; technically demanding; limited capacity to model tissue-scale invasion or uterine contractility	(85,88)
Assembloids	Combined organoids + stromal/myometrial cells	Co-culture	_	Models cell-cell communication and invasion	Complex; not yet standardized; still lack full uterine complexity	(86,90)

4. Adenomyosis and female fertility: impact on reproductive potential

Understanding how adenomyosis affects female fertility requires first revisiting the fundamental principles that govern normal reproductive physiology. In this chapter, an overview of the anatomy and function of the female reproductive system, the ovarian and menstrual cycles, and the essential biological requirement for conception is therefore provided to establish the physiological context in which reproductive disorders arise. Because the present thesis relies on a murine model, key comparative aspects of the reproductive system between women and mice are also outlined to further justify the use of this species as the experimental model chosen for this work. These elements form the basis needed to then explore in detail the current knowledge on adenomyosis-associated infertility and its underlying mechanisms.

4.1. Key elements of female reproductive physiology

The female reproductive system relies on the coordinated function of the ovaries, uterus and hormonal regulatory axes to support oocyte maturation, endometrial remodeling, and embryo implantation. Although these organs differ in structure, they operate as an integrated physiological unit whose cycle activity establishes the conditions required for fertilization and early pregnancy. The uterus consists of a hormonally responsive endometrium, a dynamic mucosa subdivided into a basal layer with regenerative capacity and functional layer that undergoes cyclical proliferation, differentiation and shedding. This tissue integrates endocrine, immune and vascular signals to create a receptive environment for implantation. Beneath it, the myometrium provides contractile activity essential for sperm transport, menstruation, and parturition, while the peritoneum forms the outer serosal surface.

The ovaries generate mature oocytes and produce steroid hormones, which regulate uterine cyclicity and reproductive potential (113,114). At birth, they contain a finite pool of follicles, each representing a potential oocyte (115,116). Folliculogenesis - the maturation of these follicles from a dormant pool to an ovulatory stage - begins with primordial follicles, composed of an immature oocyte surrounded by squamous granulosa cells. Upon activation, they transition into primary follicles, characterized by cuboidal granulosa cells, and then into secondary (preantral) follicles, which acquire multiple layers of granulosa cells and a developing theca layer. As fluid accumulates within the follicle, it becomes an antral follicle, a stage at which most follicles undergo atresia. Among the growing cohort, a single dominant

follicle emerges due to its superior growth capacity and steroidogenic activity. This follicle reaches the preovulatory (Graafian) stage, at which point the oocyte becomes competent for fertilization. Ovulation results from the rupture of the dominant follicle and the release of the oocyte-cumulus complex into the Fallopian tube, where the fertilization can occur (117–122).

These ovarian changes progress in parallel with the menstrual cycle, the sequence of endometrial events preparing the uterus for potential implantation. The cycle begins with menstruation, during which the functional layer of the endometrium is shed in response to falling ovarian hormone levels. During the proliferative phase, rising estradiol from developing follicles promotes rapid regeneration of the endometrium, expansion of the vascular network, and re-establishment of glandular architecture. Following ovulation, the secretory phase is dominated by progesterone produced by the corpus luteum, inducing stromal decidualization, enhanced glandular secretion, and establishment of the implantation window, a brief period, typically occurring in the mid-secretory phase, during which the endometrium acquires the molecular, structural, and immune features required to allow blastocyst attachment and invasion. If implantation does not occur, regression of the corpus luteum triggers a decline in progesterone, causing breakdown of the functional layer and initiation of a new cycle (121,123–126) (Figure 7).

Together, follicular maturation and menstrual cycle form an integrated system in which ovarian and uterine events are temporally aligned to optimize reproductive success. These principles provide the physiological foundation for understanding how disorders such as adenomyosis may disrupt ovulation, endometrial receptivity, or implantation, and they serve as a reference for comparative analyses with murine reproductive physiology.

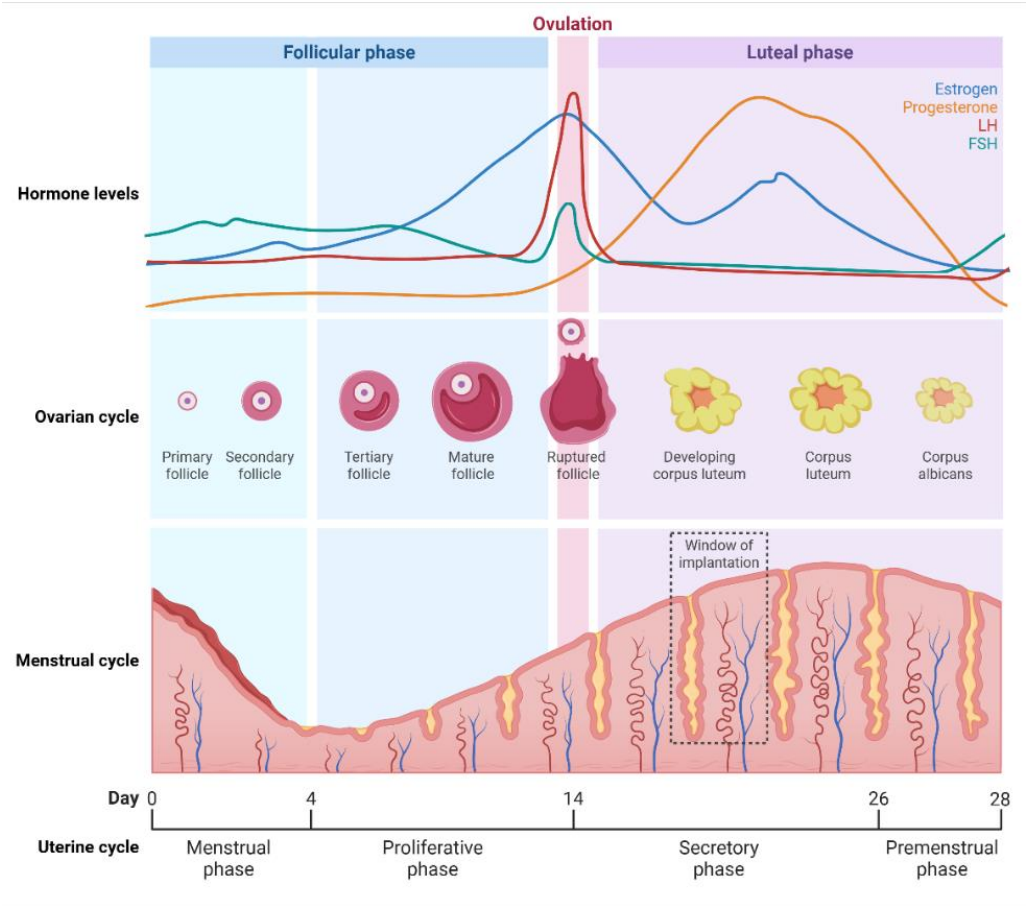


Figure 7. Hormonal, ovarian and menstrual cycle dynamics. *The diagram shows the coordinated changes in estradiol, progesterone, follicle-stimulating hormone (FSH), and luteinizing hormone (LH) throughout the menstrual cycle. These endocrine patterns are shown in parallel with the ovarian cycle as well as the corresponding endometrial changes during the menstrual, proliferative, and secretory phases. Created with BioRender.com*

4.2. Fundamental biological requirements for conception and pregnancy maintenance

Successful conception and pregnancy maintenance rely on a complex interplay between the oocyte, the endometrium, and the uterine microenvironment. Each of these elements must achieve a precise degree of maturation and synchronization to allow fertilization, embryo implantation, and early gestational development (127). The key physiological processes required for successful implantation are summarized in Figure 8, which outlines the coordinated contributions of oocyte competence, endometrial receptivity, and the uterine immune microenvironment. In our adenomyosis-induced mouse model, we specifically assess selected aspects of these processes, including estrous cycles, folliculogenesis, the expression of genes involved in ovarian function, markers of endometrial receptivity such as the progesterone receptor to evaluate progesterone resistance, pregnancy outcomes, and, in a subsequent step, features of the uterine immune microenvironment.

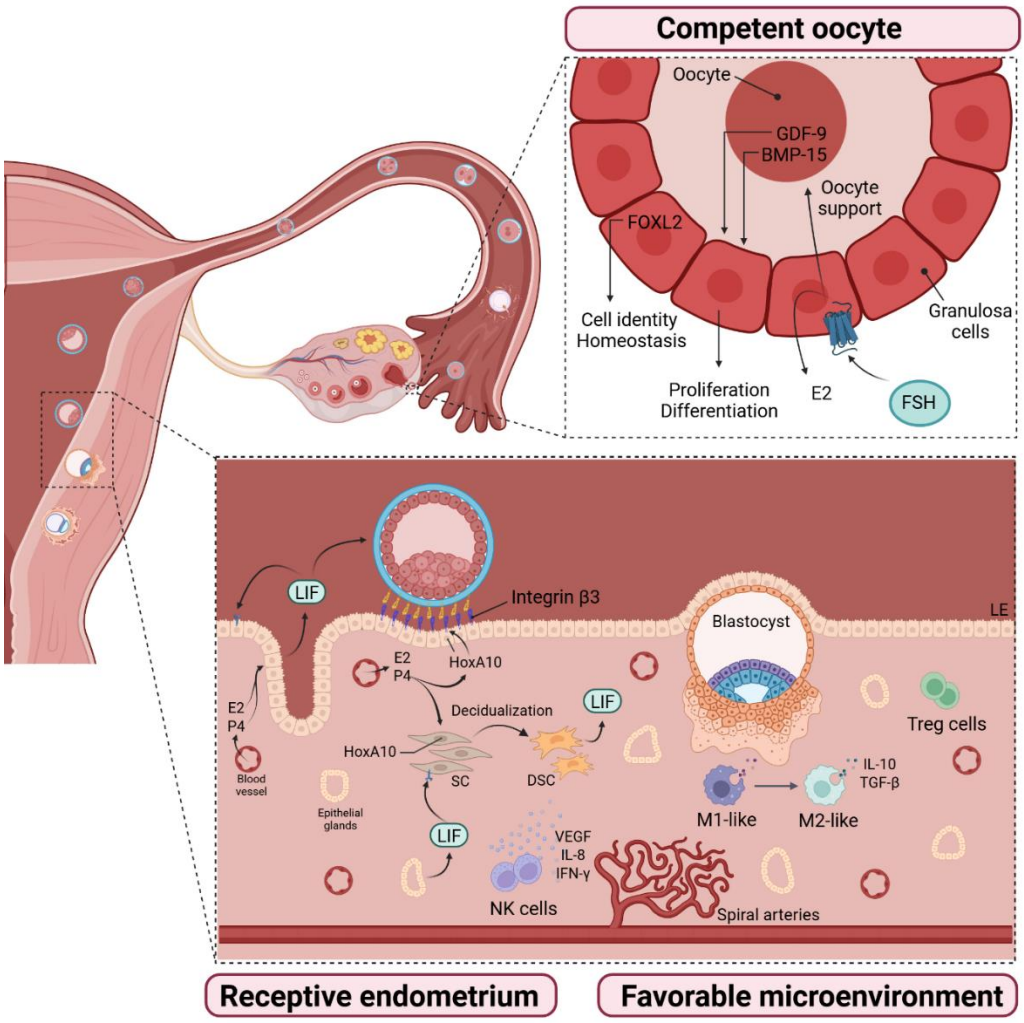


Figure 8. Key biological requirements for successful embryo implantation. *The illustration highlights the three essential components needed for implantation: a developmentally competent oocyte, a receptive endometrium, and a supportive uterine microenvironment. A magnified view on the ovary illustrates the cellular and molecular factors governing oocyte competence, while a focused view of the endometrium outlines the features underlying endometrial receptivity and the immune-modulated microenvironment required for embryo apposition, adhesion, and invasion. Created with BioRender.com*

4.2.1. Acquisition of a developmentally competent oocyte

The developmental competence of the oocyte represents a central determinant of female fertility. Rather than depending solely on the completion of folliculogenesis, oocyte quality reflects the successful integration of multiple cellular, molecular, and metabolic processes that occur within the ovarian follicle. The oocyte develops within a highly specialized microenvironment formed by granulosa and theca cells, whose continuous communication with the oocyte ensures proper coordination of growth and maturation (128). Through gap junctions and paracrine signaling, these somatic cells supply nutrients, metabolites, and regulatory molecules essential for chromatin organization, meiotic spindle assembly, and cytoplasmic maturation (129).

Several intrinsic regulators are critical for ensuring oocyte competence. The transcription factor FOXL2 maintains granulosa cell identity and homeostasis, preserving the steroidogenic function necessary for follicular health and the production of estradiol (130). The oocyte-derived growth factor BMP15, together with GDF9, modulates granulosa cell proliferation and differentiation, ensuring synchronized follicular development and communication (131). The FSH receptor (FSHR) expressed on granulosa cells mediates the effects of FSH, promoting estradiol synthesis and regulating the expression of genes involved in oocyte support and survival (132). Mitochondrial content and function are also essential, as they provide ATP for meiotic progression and early embryo development (133). Proper storage of maternal transcripts ensures successful embryonic genome activation (134,135).

Although adenomyosis is primarily regarded as a uterine disorder, it remains unclear whether it alters oocyte competence. This question is relevant because oocyte quality can be influenced by multiple external factors such as hormonal imbalance, inflammation or oxidative stress, that disrupt the equilibrium between follicular growth, atresia, and ovulation (136).

4.2.2. Establishment of a receptive endometrium

Endometrial receptivity represents the transient period during which the uterine lining acquires the capacity to support embryo attachment and invasion. This process depends on the cyclical modulation of estrogen and progesterone secreted by the ovaries. Estrogen promotes proliferation of the endometrial epithelium during the follicular phase, while progesterone, secreted after ovulation by the corpus luteum, induces secretory transformation and stromal differentiation (137). Following the luteal rise of progesterone, stromal fibroblasts differentiate into decidual cells in a process known as decidualization, which is essential for implantation and pregnancy maintenance. Decidual cells orchestrate vascular remodeling, regulate trophoblast invasion, and secrete a range of cytokines and growth factors that create an immune tolerant environment conducive to embryo survival (138). Because several of these processes are disrupted in adenomyosis, understanding their physiological basis helps contextualize the molecular defects observed in affected women and in our murine model.

4.2.2.1. Leukemia inhibitory factor (LIF) and embryo-endometrium signaling

LIF is a pleiotropic cytokine belonging to the interleukin-6 (IL-6) family and represents a key mediator of estrogens and progesterone action within the endometrium. LIF is secreted primarily by endometrial glands and stromal cells during the mid-secretory phase, when the endometrium attains maximal receptivity. Acting through its receptor complex LIF receptor

(LIFR) and gp130, it activates the JAK/STAT signaling pathway, which regulates epithelial receptivity, stromal decidualization, and trophoblast adhesion (139).

In both mouse and human models, LIF deficiency leads to implantation failure despite normal embryo development, underscoring its crucial role in establishing uterine receptivity (140–142). Low levels of LIF or LIFR expression have been consistently reported in infertile women suggesting that dysregulation of this cytokine contributes directly to the impaired embryo-endometrium communication characteristic of these conditions (141,142).

4.2.2.2. Integrin β3 and cell adhesion during implantation

Integrins are transmembrane receptors that mediate cell-extracellular matrix interactions, and their cyclic expression in the endometrium serves as a reliable marker of receptivity. Among these, Integrin β3 is of particular importance because it facilitates blastocyst adhesion to the luminal epithelium (143). Its expression is tightly regulated by HoxA10 and is normally restricted to the mid-secretory phase (144). In women with implantation defects, such as endometriosis, a marked reduction or delay in integrin β3 expression has been observed, contributing to poor embryo attachment and early pregnancy failure. Therefore, integrin β3 serves not only as a biomarker of receptivity but also as a functional mediator of uterine-embryo cross-talk (145–147).

4.2.2.3. The role of HoxA10 in uterine receptivity

The homeobox gene HoxA10 is a progesterone-responsive transcription factor that plays a key role in the structural and functional transformation of the endometrium during the window of implantation. Its expression peaks in the mid-secretory phase, particularly in the stromal compartment, where it regulates genes involved in adhesion, immune modulation, and extracellular matrix remodeling (148,149). Reduced expression of HoxA10 has been reported in the eutopic endometrium of patients with endometriosis, correlating with decreased fertility rates (150,151). Experimental studies have shown that HoxA10 directly controls the transcription of several implantation-associated molecules, including integrin β3 and LIF, thereby ensuring proper adhesion and communication between the embryo and the uterine epithelium (144,152).

4.2.2.4. The essential of progesterone in endometrial receptivity and the concept of progesterone resistance

Progesterone is the central regulator of secretory transformation and decidualization. Acting via its nuclear receptors PR-A and PR-B, it controls differentiation, immune tolerance, angiogenesis, and numerous implantation-related genes (138,153). Decidualization involves a

profound morphological and functional transformation of stromal cells into decidual cells, which acquire a secretory phenotype and produce key factors such as prolactin (PRL), and insulin-like growth factor binding protein 1 (IGFBP1) – two markers of successful decidualization (154). These decidual cells support early embryo development, regulate trophoblast invasion, and contribute to the establishment of a tolerogenic immune environment (155).

When the endometrium shows an insufficient response to progesterone – termed progesterone resistance – decidualization is defective and epithelial proliferation persists, leading to downregulation of progesterone-regulated genes (137,156). Mechanistically, progesterone resistance often results from an imbalance between PR-A and PR-B isoforms, reduced receptor signaling efficiency, or epigenetic modifications affecting progesterone-responsive promoters (157,158). Consequently, key molecules involved in implantation, such as HoxA10, LIF and Integrin β3, are insufficiently expressed, leading to a non-receptive endometrium and implantation failure (144,159,160).

Several studies in both humans and mice have demonstrated a direct relationship between decreased expression or dysregulation of PGR and implantation defects (161–163). Genome-wide mapping of PGR binding sites in the human endometrium has revealed that PGR occupancy dynamically changes between the proliferative and mid-secretory phases, controlling the expression of hundreds of genes essential for uterine receptivity (164). In translational models, the loss of epithelial PGR isoforms has been associated with reduced expression of LIF, defective stromal decidualization, and impaired embryo attachment (160,165). Similarly, a murine model has shown that maintaining epithelial PGR expression during the window of implantation disrupts embryo attachment and uterine receptivity, highlighting the necessity of finely tuned, cell-specific PGR regulation for successful implantation (166).

Reduced PGR expression and dysregulation of progesterone-dependent pathways in adenomyosis suggest that some degree of progesterone resistance may occur in this disease. Yet, current data remain fragmentary, and disentangling the intrinsic effects of adenomyotic lesions from those related to coexisting disorders represents an important gap in our understanding of implantation failure in adenomyosis.

4.2.3. A favorable uterine microenvironment

Successful implantation and maintenance of pregnancy require not only a receptive endometrium and a competent embryo but also finely tuned uterine microenvironment. This microenvironment is composed of various immune and non-immune cells, soluble mediators,

and extracellular matrix components that dynamically interact to promote tissue remodeling, vascular adaptation, and maternal-fetal tolerance (167). During the implantation window, the endometrium undergoes a controlled inflammatory state that facilitates tissue breakdown, embryo apposition, and trophoblast invasion. Early implantation requires a controlled pro-inflammatory response dominated by macrophages, dendritic cells, and uterine natural killer (uNK) cells, which remodel the extracellular matrix, increase vascular permeability, and facilitate the adhesion of the blastocyst to the receptive endometrial epithelium (167–171). This transient inflammatory phase is essential for initiating implantation but must be tightly regulated, as excessive or prolonged inflammation can hinder trophoblast attachment and damage the endometrial lining (172).

As trophoblast invasion progresses, this pro-inflammatory milieu must be rapidly shifted toward an anti-inflammatory and tolerogenic state to ensure maternal-fetal coexistence (173). During this transition, uNK remains non-cytotoxic, induces spiral artery remodeling and secrete angiogenic mediators; macrophages shift toward an M2-like profile; and Tregs expand to suppress excessive Th1/Th17 responses. This tightly regulated equilibrium enables both tissue remodeling and immune tolerance (168,169,174–177). Coordinated signaling among these innate and adaptive immune cells is essential to establish immune homeostasis, preventing both immune rejection and uncontrolled inflammation that could compromise implantation (178).

Altogether, these dynamic interactions establish a balanced immune environment that combines localized inflammation for tissue remodeling with systemic and local tolerance for embryo protection. Any perturbation in this finely tuned immune-endocrine network can impair decidualization, trophoblast invasion, and ultimately, implantation success. Because the uterine immune microenvironment is essential for reproductive success, and given increasing evidence of its dysregulation in adenomyosis, the following chapter (5. Uterine immune landscape: immune cells and cytokine networks) provides a detailed examination of immune-cell populations and cytokine networks in both healthy and adenomyotic uteri, with particular emphasis on their potential involvement in disease progression and implantation defects.

4.3. Comparative aspects of the reproductive system in female mice and women

Rodents, particularly mice, are the most commonly used models in reproductive research because they share genomic, physiological, and endocrine similarities with humans (179). These similarities allow key aspects of ovarian biology, uterine function, and implantation to

be modeled experimentally, while the divergences must be considered when interpreting findings relevant to human adenomyosis.

4.3.1. Morphological comparison

The murine reproductive tract differs anatomically from the human system primarily in uterine architecture: mice possess a bicornuate uterus composed of two lateral uterine horns and a single uterine body, whereas humans exhibit a simple uterus with a single cavity. Each mouse ovary is enclosed within an ovarian bursa - absent in humans - and the oviducts are long and coiled (180) (Figure 9). Despite these structural differences, the overall organization and function of the reproductive organs are highly conserved, ensuring that essential ovarian and uterine processes can be modeled effectively.

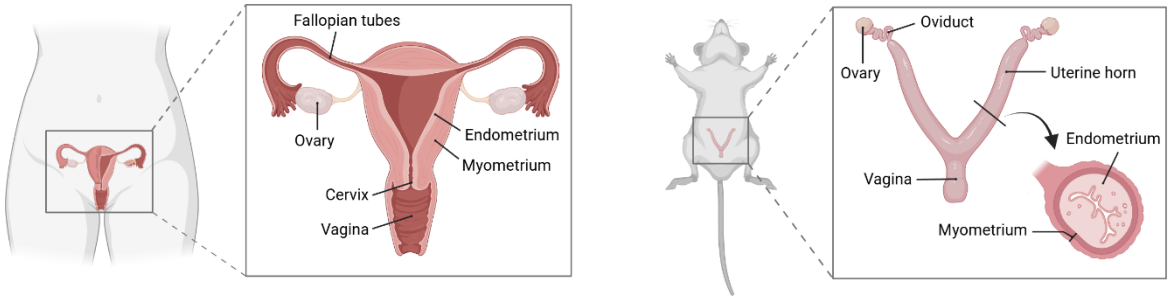


Figure 9. Comparative anatomy of the female reproductive tract in humans and mice. *The human reproductive system includes paired ovaries, Fallopian tubes, a single uterus composed of myometrium and endometrium, the cervix and the vagina. In mice, the system features two elongated uterine horns, along with a transverse uterine section highlighting the layered uterine wall. Created with BioRender.com*

4.3.2. Folliculogenesis and reproductive cycles

At birth, the mouse ovary contains approximately 8,000 primordial follicles, compared with 1-2 million in humans (115,181). Mice reach sexual maturity at around 4 weeks of age, whereas menarche in humans occurs between 10 and 16 years (180). Follicular growth is also much faster in mice – approximately three weeks compared with six months in women – reflecting species-specific differences in follicle recruitment and endocrine regulation (182).

The mouse estrous cycle lasts 4-6 days and is divided into proestrus, estrus, metestrus and diestrus, roughly paralleling the proliferative and secretory phases of the human menstrual cycle, which spans about 28 days. Unlike women, mice do not menstruate: the endometrium is resorbed rather than shed (180). Despite these differences, both species exhibit similar hormonal regulation through the HPO axis to drive folliculogenesis and ovulation (183) (Figure 10).

Another key difference between the two species lies in their reproductive output and gestation. In mice, multiple oocytes are typically ovulated per cycle, resulting in litters of 2-12 pups on average, whereas in humans, usually a single dominant follicle reaches ovulation, producing one oocyte per cycle (180,184). Consequently, mice exhibit multiple births per gestation, while humans exhibit 1 to 3 births per gestation. The gestation period in mice is also considerably shorter – approximately 18.5-21 days – compared to around 37-42 weeks in humans (180).

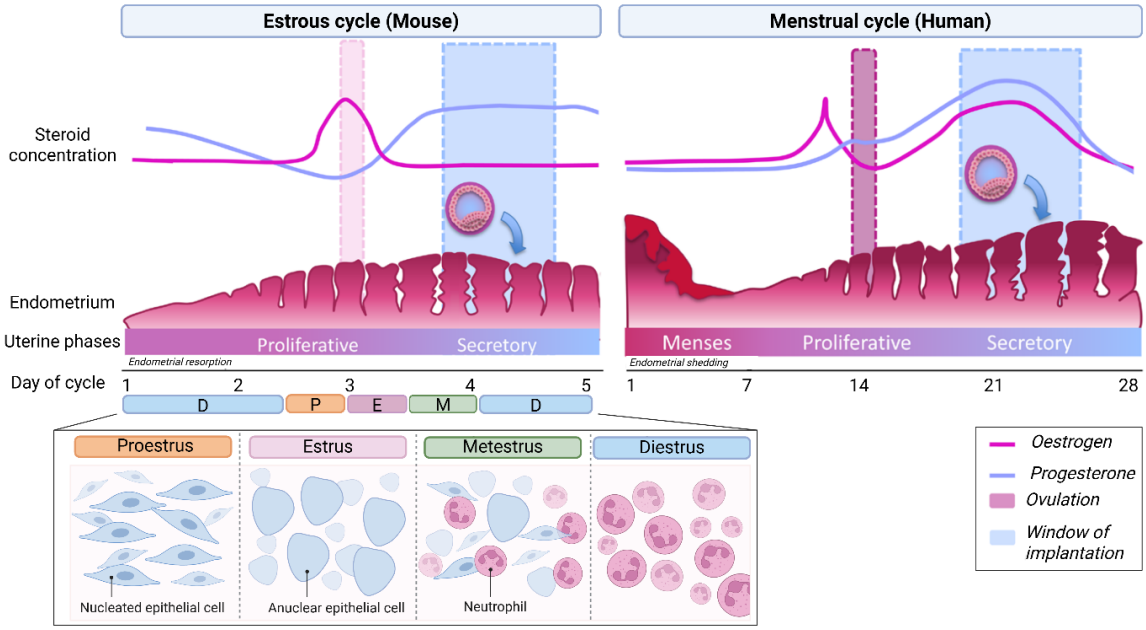


Figure 10. Comparative overview of the murine estrous cycle and the human menstrual cycle. *The figure illustrates the temporal dynamics of steroid hormone fluctuations and associated endometrial remodeling in mice and humans. In mice, the four stages (proestrus, estrus, metestrus, and diestrus) are distinguished based on vaginal smear cytology and cyclic endometrial remodeling through resorption rather than menstruation. In humans, cyclical variations in estrogen and progesterone regulate the menstrual, proliferative, and secretory phase, including the window of implantation. Adapted from Bellofiore et al.(185), modified with BioRender.com*

4.3.3. Implantation and decidualization

Perhaps the most striking divergence between the species lies in the process of implantation and decidualization. In humans, decidualization of endometrial stromal cells begins spontaneously during the mid-secretory phase under progesterone influence, even before embryo arrival. This pre-decidualization prepares the uterine lining for implantation and ensures an optimal environment for trophoblast invasion. By contrast, in mice, decidualization is induced only after embryo implantation, triggered by the attachment of the blastocyst to the uterine epithelium (186).

Implantation in humans is interstitial, meaning the blastocyst completely embeds within the endometrium, while in mice, implantation is superficial, with the embryo partially penetrating

the stroma. Consequently, human implantation involved more extensive tissue remodeling, angiogenesis, and immune modulation (187). Despite these differences, molecular markers of uterine receptivity such as LIF, HoxA10, and integrin β3 are conserved (188).

4.3.4. Translational considerations

Although mice recapitulate key reproductive mechanism – such as follicular development, hormonal regulation, and uterine remodeling – their short reproductive cycles, induced decidualization, and limited trophoblast invasion restrict their direct extrapolation to human physiology. Therefore, while murine models are ideal for dissecting molecular and cellular pathways, human studies remain indispensable for validating the clinical relevance of findings related to endometrial receptivity and implantation disorders. Integrating both systems provides a powerful comparative framework for understanding normal and pathological reproductive processes (189). A comprehensive comparison of anatomical and reproductive characteristics between mice and humans is provided in Table 2.

Table 2. Key anatomical and reproductive differences between mice and humans.

	Mouse	***Human***
Uterine anatomy	Bicornuate with two uterine horns	Single-cavity uterus
Oviduct structure	Long, thin, highly coiled	Shorter, not coiled
Ovarian position and shape	Spherical ovary inside an ovarian bursa	Ovoid ovary, not coiled
Primordial follicles at birth	~8 000	1-2 million
Duration of folliculogenesis	~3 weeks	~6 months
Sexual maturity/puberty	~4 weeks	10-16 years
Reproductive cycle	Estrus cycle, 4-6 days	Menstrual cycle, ~28 days
Menstruation	None	Present
Ovulation per cycle	Multiple oocytes	Usually one oocyte
Gestation length	18.5-21 days	37-42 weeks
Decidualization	Induced after embryo implantation	Occurs spontaneously before implantation
Implantation type	Superficial	Interstitial
Reproductive lifespan	6-8 months	38 years

4.4. Adenomyosis and infertility: mechanisms and clinical outcomes

As discussed in the general overview, the epidemiology of adenomyosis has shifted considerably, with the disease increasingly detected in young women due to advances in imaging techniques and better recognition of its clinical presentation. This shift underscores the importance of understanding its potential impact on fertility, particularly as the condition is no longer considered exclusive to multiparous or late-age women (11). However, current knowledge remains limited, as studies on adenomyosis-associated infertility are hindered by diagnostic heterogeneity and by the lack of standardized preclinical models capable of isolating the specific reproductive effects of the disease.

4.4.1. Reproductive outcomes in natural and assisted conception

Among women facing fertility difficulties, adenomyosis has gained increasing attention as a potential contributor to reproductive failure. In infertile populations, establishing precise epidemiological estimates remains challenging because of heterogeneous diagnostic criteria and frequent coexistence of other gynecological conditions. Despite these limitations, reported prevalence rates range from approximately 7.5% to 22%, suggesting that adenomyosis may represent a clinically relevant, yet still underrecognized, factor for subfertility (190,191).

Clinically, adenomyosis has been associated with reduced fertility potential, higher miscarriage rates, and poorer reproductive outcomes (192). These reproductive difficulties extend to assisted conception. In a retrospective analysis of 973 IVF cycles, Sharma et al. found that adenomyosis was associated with significantly lower clinical pregnancy and live birth rates compared with controls, even after adjusting for age and concomitant gynecological pathologies (193).

Despite these poorer outcomes, ART remains a recommended and viable fertility option for patients with adenomyosis, particularly when spontaneous conception does not occur or when additional infertility factors are present. Current clinical reviews emphasize that treatment should be individualized, aiming to optimize uterine receptivity before ART (194,195).

4.4.2. Potential mechanisms underlying infertility in adenomyosis

Although the details molecular mechanisms are still being elucidated, multiple pathological alterations have been proposed to explain reduced fertility in adenomyosis. These include: (1) altered oocyte maturation and lower quality embryos; (2) Structural disruptions of the myometrium and junctional zone thickening caused by uterine hyperperistalsis leading to impaired embryo transport; (3) Local hyperestrogenism and progesterone resistance, resulting

in defective endometrial receptivity and impaired decidualization; (4) Altered expression of implantation-related molecules, which are critical for embryo attachment and uterine receptivity; (5) Dysregulated immune and inflammatory responses within the endometrium, contributing to an inhospitable implantation environment; (6) Increased angiogenesis, neuroinflammation, and fibrosis that may interfere with vascular remodeling and placentation (196,197) (Figure 11). These alterations disrupt the synchronized communication between embryo and endometrium, potentially leading to implantation failure, early pregnancy loss, or obstetric complications.

4.4.3. Comorbidities and confounding factors

Interpreting the reproductive consequences of adenomyosis remains challenging as this disease frequently coexists with other uterine pathologies such as endometriosis (in up to 80% of cases) and uterine fibroids (up to 50%), both of which can independently compromise fertility (56–59). This overlap complicates the delineation of adenomyosis-specific effects. For instance, the miscarriage rate has been reported to be significantly higher in women affected by both adenomyosis and endometriosis (28.5%) than in those with adenomyosis alone (11.3%) (198). Similarly, in a large cohort of women undergoing IVF/ICSI, combined adenomyosis and endometriosis results in markedly reduced live birth and ongoing pregnancy compared with isolated disease, suggesting additive or synergistic detrimental effects on reproductive outcomes (199). A systematic review and meta-analysis in subfertile populations reported that approximately 6% of women present adenomyosis with endometriosis, while isolated adenomyosis is found in around 10% of cases (60).

Although adenomyosis has been associated with altered endometrial function, its precise contributions to impaired fertility remain incompletely understood. In particular, it is unclear whether the disease alone is sufficient to induce progesterone resistance or to compromise endometrial receptivity through altered expression of implantation-related genes or disrupted decidualization.

While these uterine-specific alterations have been the main focus of research, a largely unexplored question concerns the potential impact of adenomyosis on ovarian function. Although adenomyosis is primarily a uterine disorder, it is still unknown whether it can influence oocyte quality and folliculogenesis, potentially impairing fertility through mechanisms extending beyond the uterine environment. Addressing these gaps is essential to disentangle the independent effects of adenomyosis from those of comorbidities and to define the full spectrum of reproductive alterations associated with the disease.

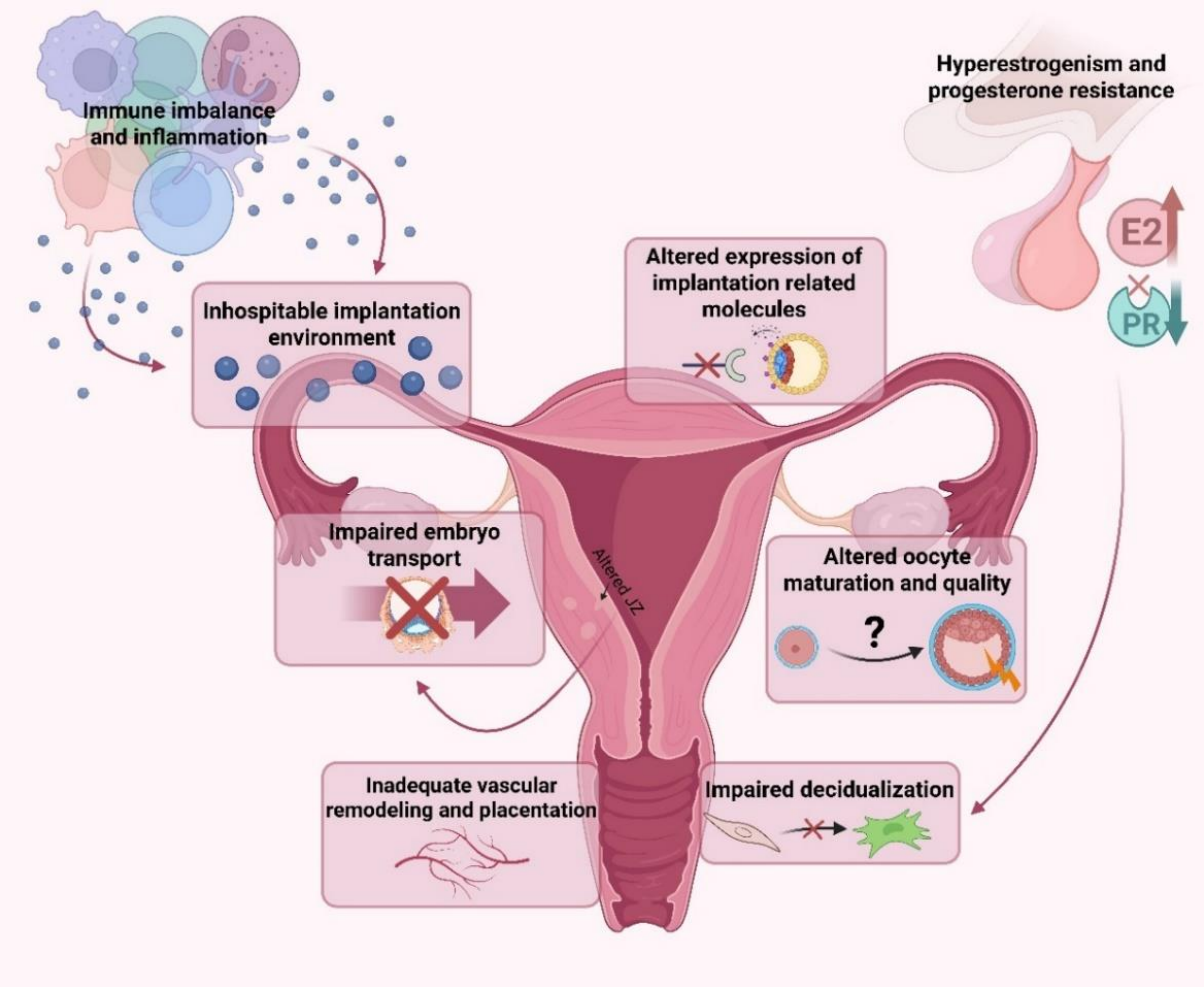


Figure 11. Proposed mechanisms by which adenomyosis may contribute to infertility
This schematic highlights how adenomyosis can interfere with key steps of the reproductive process. Altered oocyte maturation and embryo quality together with junctional zone disruption and abnormal uterine peristalsis, may disturb gamete and embryo transport. Local hyperestrogenism and progesterone resistance impair endometrial receptivity and decidualization and are accompanied by dysregulated expression of implantation-related molecules. In parallel, immune imbalance and chronic inflammation create an inhospitable implantation environment, while aberrant angiogenesis, neuroinflammation and fibrosis can compromise vascular remodeling and placentation, ultimately reducing the chance of successful implantation and ongoing pregnancy. These mechanisms are synthesized from experimental and clinical literature on adenomyosis, but their level of evidence is heterogeneous and should be interpreted as indicative rather than definitive.

5. Uterine immune landscape: immune cells and cytokine networks

Beyond its implications for fertility, adenomyosis is increasingly recognized as a condition in which local uterine homeostasis is profoundly altered. In the healthy uterus, immune cells orchestrate cyclical tissue breakdown and repair, support embryo implantation, and regulate early pregnancy through tightly coordinated interactions with hormonal, stromal, and epithelial signals (200). Emerging evidence suggests that this balance is altered in

adenomyosis, with changes in immune-cell composition and cytokine signaling (201–203). Nevertheless, the extent and biological significance of these alterations remain incompletely defined.

To contextualize these findings and to introduce the rationale for examining immune remodeling in our murine model, I first summarize the immune cell types most relevant for uterine physiology and those most frequently reported as dysregulated in adenomyosis.

5.1. The healthy uterine immune system

5.1.1. Macrophages

Macrophages are among the most abundant immune cells (20%) in the endometrium and are essential for cyclical tissue repair, clearance of apoptotic cells, and regeneration (204). Their function relies on a high degree of plasticity, allowing polarization across an inflammatory-repair continuum. In this context, the historical M1/M2 paradigm is now recognized as an oversimplification (205), but the terms *M1-like* and *M2-like* remain useful shorthand to describe predominant activation profiles rather than mutually exclusive lineages. Classically, activated M1-like macrophages, typically expressing CD86, display antigen-presenting and pro-inflammatory activities, including the production of mediators such as TNF-α, IL1-β, and IL-6, which support menstrual shedding and early tissue defense. In contrast, M2-like macrophages, typically associated with CD163 and/or CD206 expression, are more frequently linked to regulatory and tissue-repair-oriented functions, including the secretion of IL-10, TGF-β, and VEGF, that promote regeneration and angiogenesis (206) (Figure 12).

This dynamic balance between macrophage activation states is central to normal uterine homeostasis. Because several studies have suggested altered macrophage density and polarization in adenomyosis, this population represents a key immune axis for understanding disease-associated tissue remodeling.

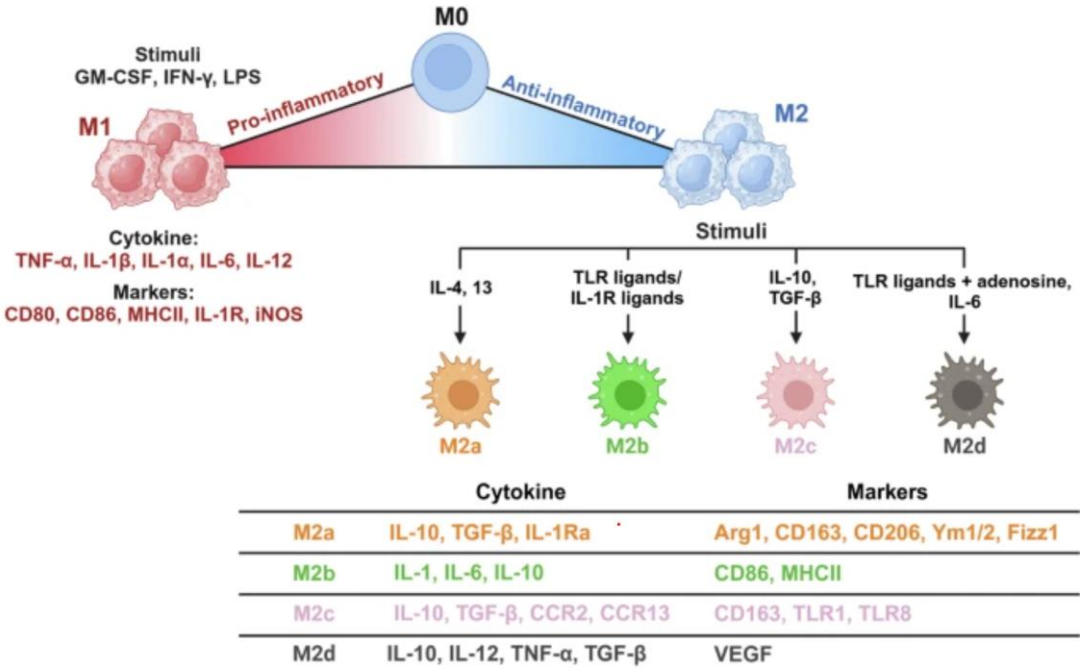


Figure 12. Conceptual representation of macrophage polarization states and associated stimuli, markers, and cytokine profiles. *This schematic illustrates the classical M1/M2 polarization framework, in which macrophages adopt a spectrum of activation states in response to environmental cues. Pro-inflammatory (M1-like) and alternatively activated (M2-like) phenotypes are depicted together with commonly reported stimuli, surface markers, and cytokines, as well as proposed M2 subcategories (M2a–d). This classification is primarily derived from in vitro studies and should be regarded as a simplified conceptual model, as macrophage phenotypes in vivo—particularly within the uterine microenvironment—are highly plastic and context-dependent. From Park et al. (207)*

5.1.2. NK cells

Uterine natural killer (uNK) cells constitute the predominant lymphocyte population during the secretory phase and early pregnancy (208). Unlike peripheral NK cells, which are primarily cytotoxic, uNK cells exhibit low intrinsic cytotoxicity and are instead specialized in supporting angiogenesis, tissue remodeling, and immune regulation (208–210). Through receptors such as NKp46, NKG2D, NKp30, and inhibitory killer-cell immunoglobulin-like receptors (KIRs), uNK cells finely balance activation and tolerance within the uterine microenvironment (211). Functionally, uNK secrete a range of cytokines and growth factors that orchestrate vascular remodeling, angiogenesis, and stromal differentiation during the menstrual cycle and implantation. Their controlled activation ensures the maintenance of endometrial homeostasis, promoting tissue renewal while preventing excessive cytotoxicity toward trophoblast or endometrial cells (212).

Altered uNK density or phenotype could therefore participate in defective implantation or aberrant tissue remodeling. For this reason, uNK cells represent a relevant immune population to examine when investigating immune changes in adenomyosis.

5.1.3. T lymphocytes

T lymphocytes constitute a major component of the adaptive immune system within the endometrium and are essential for maintaining mucosal homeostasis across the menstrual cycle. The endometrial T-cell pool is mainly composed of CD3+CD4+ and CD3+CD8+ T lymphocytes, along with smaller subsets of natural killer T (NKT) cells, each contributing to tissue homeostasis and implantation (213).

Within the CD4+ population, several functional subsets coexist, including T helper cells (Th1, Th2 and Th17 subsets) and regulatory T cells (Tregs), that regulate immune surveillance, tissue repair and tolerance, as well as host defense through cytokine secretion. Estrogen tends to enhance recruitment and activation of effector T cells, whereas progesterone promotes a tolerogenic, pregnancy-compatible profile, enriched in Tregs (213,214). CD8+T cells maintain cytolytic surveillance during the proliferative phase but display reduced cytotoxic activity during the secretory phase, lowering the risk of embryo rejection without necessarily decreasing in number (215). Natural killer T (NKT) cells, bridging innate and adaptive immunity, also contribute to local immune tolerance and balanced cytokine production, helping to promote a receptive endometrial environment (216).

Because shifts in T-cell subsets can be involved in inflammation and tissue repair, characterizing T-cell dynamics provides a useful framework for understanding how immune imbalance may contribute to adenomyosis progression.

5.1.4. B lymphocytes

B cells are less abundant in the healthy endometrium, but they contribute to local humoral immunity through antibody production and antigen presentation (217). Although minor in abundance, they help maintain tissue homeostasis and defend against pathogens.

In contrast to other uterine immune populations, the role of B cells in adenomyosis has been scarcely investigated, and available data remain extremely limited. Several studies have reported an increased density of B cells in both eutopic and ectopic endometrium along with the presence of circulating auto-antibodies in women affected by endometriosis (218,219). These findings support the hypothesis that B-cell activation may contribute to chronic inflammation or altered immune regulation. Given this background, assessing B-cell modulation in adenomyosis is of particular interest, as it may help clarify whether similar immune deviations occur in the adenomyotic uterus or whether B-cell involvement represents a distinguishing feature between the two pathologies.

5.2. Immune dysregulation in adenomyosis: initiation and lesion progression

5.2.1. Macrophages

Macrophages are among the most abundant immune cells in adenomyotic tissues, with increased density reported in both eutopic and ectopic compartments (220). Their activation state appears heterogeneous. In human lesions, M2-like macrophages accumulate in eutopic endometrium and *in vitro*, these cells enhance endometrial cell invasiveness through MMP9 (203). Additionally, co-culture experiments further show that macrophage-stromal interactions amplify inflammatory signaling via IL-6 (221). In a tamoxifen-induced mouse model of adenomyosis, Bourdon et al. observed by mRNA analysis an early increase in M1 macrophage markers and a transient decrease in the M2 marker Arginase-1 thirty days post-induction, while no significant changes in M2 markers were detected at later stages (201). Because lesion onset is experimentally timed in this model, these profiles capture a controlled kinetic sequence of macrophage activation that is rarely accessible in human studies, which usually provide only cross-sectional observations at variable and often unknown stages of disease.

Insights from endometriosis models suggest that macrophage polarization is functionally relevant for lesion control. Therapeutic strategies that experimentally shift macrophages toward a more M1-like profile have been associated with a reduction in lesion burden (222). Rather than indicating that a single, fixed polarization state is intrinsically beneficial or deleterious, these observations support the idea that the balance and temporal evolution of macrophage activation states critically influence lesion behavior. Together, these findings underscore that macrophage polarization may play a central role in adenomyosis pathophysiology, influencing tissue remodeling, invasion and inflammation, but the temporal dynamics of this polarization remain poorly characterized.

5.2.2. NK cells

In adenomyosis, alterations in uNK phenotype and function have been described. Quantitative analyses have reported increased numbers of CD56+ NK cells in the eutopic endometrium of women with adenomyosis, particularly in those presenting severe form of disease (223). In a tamoxifen-induced mouse model, a transient upregulation of Nrc1, encoding the activating receptor NKp46, was observed thirty days post-treatment, suggesting early modulation of NK cell abundance or activity (201). More recent immunophenotyping studies using flow cytometry and multiplex imaging confirm accumulation of uNK cells

within ectopic adenomyotic foci, displaying reduced NKp46 and NKG2D expression, together with an upregulation of inhibitory KIRs, indicating a shift toward a less cytotoxic and more tolerant phenotype (211,220,224,225). These changes may impair local immune surveillance, facilitating the persistence of ectopic endometrial cells. However, current data remain fragmentary regarding the temporal evolution of uNK subsets and their receptor repertoire during disease progression, underscoring the need for longitudinal analyses in well-controlled experimental models.

5.2.3. T and B lymphocytes

Altered T-cell infiltration characterizes the endometrium in women with adenomyosis. Several studies report elevated numbers of T cells (CD3+) in the eutopic endometrium of patients compared to unaffected controls (226,227). Beyond quantity, the activation state and functional phenotype of T-cell subsets, such as CD4+ helper and CD8+ cytotoxic T cells, are critical for understanding immune dysregulation in adenomyosis. However, reports on their abundance remain inconsistent, with some studies showing elevated CD4+ and CD8+ T-cell levels in adenomyosis tissues (227), while others found no significant differences compared with controls (226,228). Cytokine-driven polarization of CD4+ T cells generates opposing subsets: pro-inflammatory Th17 and immunosuppressive Treg cells. Their reciprocal differentiation maintains immune balance, but in adenomyosis, reduced FOXP3+ Tregs and elevated IL-17A+ Th17 cells indicate a Th17/Treg imbalance. This disequilibrium correlated with dysmenorrhea observed in affected women (229). Evidence on Th1/Th2 balance in adenomyosis is limited, though increased IFN-γ in endometrial cells points to Th1 involvement (230).

Data on B cells are likewise limited. Most studies showing minimal infiltration in endometrium, but one report noted a marked increase in myometrial B cells, suggesting a possible contribution of humoral immunity to disease progression (43,227). These results are inconsistent with the study of Bourdon et al. on a mouse model who showed a persistent decrease in CD19 mRNA expression at all stages, indicating reduced B-cell presence in this model (201). Rather than excluding a biological role for B lymphocytes, these discrepancies may reflect differences in disease stage, tissue compartment analyzed, or experimental methodology, underscoring the need for more standardized and longitudinal studies.

Taken together, these observations indicate that while T and B lymphocytes constitute a minor component of the uterine immune landscape, quantitative and functional alterations may create a microenvironment that supports adenomyotic lesion persistence and associated clinical symptoms. However, most available data have been generated in the presence of established lesions, and it remains unclear whether lymphocyte alterations precede lesion

formation or arise as a secondary response to tissue damage. Clarifying how early immune changes develop in relation to lesion onset will be essential to understand whether adaptive immunity participates in the initiation of adenomyosis or mainly modulates its chronic progression.

5.3.Disruption of implantation processes in adenomyosis

As described earlier, successful embryo implantation depends on a finely regulated dialogue between the embryo and the endometrium, involving hormonal signals, decidual transformation of stromal cells, and controlled activation of uterine immune populations. As previously mentioned, during the peri-implantation period, a short pro-inflammatory phase supports blastocyst attachment and invasion, followed by a shift toward an tolerogenic environment driven by progesterone-dependent decidualization (171,172). Macrophages, uNK, dendritic cells, and Tregs are central actors of this transition, ensuring vascular adaptation, stromal differentiation, and maternal-fetal immune tolerance (231).

In the context of adenomyosis, the immune microenvironment of the endometrium and myometrium undergoes significant perturbations precisely during the window of implantation. The controlled sequence of events that ordinarily fosters embryo attachment, invasion, and maternal tolerance is compromised in several key ways.

First, alterations in the timing of endometrial receptivity are observed – window of implantation shifts have been documented in adenomyosis, undermining synchrony between blastocyst and endometrium (232). The cytokine milieu of the mid-luteal endometrium is also modified, with increased pro-inflammatory cytokines such as IL-6 and MCP-1 and reduced concentrations of regulatory mediators including IL-10 (233). This elevated and persistent inflammation contrasts with the tightly controlled, transient activation normally required to initial implantation. Moreover, reduced IL-10 in the eutopic endometrium has been shown to downregulate HOXA10 via impaired STAT3 signaling, directly compromising the molecular machinery of endometrial receptivity (234).

Additional perturbations of endometrial-immune communication have been described, including loss of IL-33 and dysregulation of IL-18 signaling, both of which impair decidualization and embryo adhesion (235,236). At the level of immune-cell populations, transcriptomic studies indicate altered interferon-induced and TNF-related pathways while experimental models show persistent shift toward M1 macrophages and reduced total numbers of macrophages, uNK and dendritic cells during early implantation (237,238).

Overall, the adenomyotic uterus appears unable to transition from inflammation to immune tolerance, resulting in impaired decidualization and suboptimal conditions for embryo invasion.

Despite increasing knowledge on immune alterations in adenomyosis, most studies have focused on established disease or on samples collected at or after conception. Consequently, pre-conception immune changes in the endometrium remain poorly characterized, leaving a critical gap in understanding the earliest events that may predispose to lesion initiation or progression. Similarly, the temporal dynamics and functional status of specific immune cell populations have not been fully delineated during disease development. Addressing these gaps is essential for identifying early pathogenic mechanisms, refining our understanding of disease progression, and ultimately for developing interventions aimed at restoring immune homeostasis before implantation.

5.4. Therapeutic perspectives

Growing evidence suggests that modulating the uterine immune microenvironment may offer therapeutic opportunities in adenomyosis, particularly for women facing infertility. Several strategies including corticosteroids, low-molecular weight heparin, intralipid infusion, or anti-TNFα therapies – have shown the ability to reduce excessive inflammation, modulate NK-cell cytotoxicity, facilitate uterine vascular remodeling, or favor Th2/Treg immune profile, thereby promoting a more receptive and tolerogenic endometrial environment (239–244). Other interventions, such as G-CSF administration or intrauterine infusion of autologous peripheral blood mononuclear cells (PBMCs), seek to enhance endometrial receptivity by supporting angiogenesis, macrophage differentiation, and local production of anti-inflammatory cytokines (245,246).

While these treatments may partially correct immune dysregulation associated with adenomyosis and could theoretically improve implantation success, their capacity to modify or regress adenomyotic lesions themselves remain unclear, as most evidence focuses on functional rather than structural outcomes and is largely derived from empirical or preclinical observations rather than controlled clinical trials. Such emerging strategies underscore the potential of targeting key molecular pathways involved in immune regulation and tissue remodeling. Although most mechanistic insights into S1P signaling have been derived from endometriosis, the striking overlap in inflammatory, fibrotic, vascular and immune alterations between endometriosis and adenomyosis strongly suggests that similar S1P-driven mechanisms may operate within the adenomyotic uterus.

6. The Sphingosine-1-phosphate pathway (S1P)

Building on the immune dysregulation, chronic inflammation, and tissue remodeling described in the previous chapters, increasing evidence supports the sphingosine-1-phosphate (S1P) signaling axis as a central regulator of immune cell trafficking, inflammation, fibrosis, and vascular remodeling in gynecological disorders, including adenomyosis.

In adenomyosis, where immune imbalance, fibrotic remodeling, and altered uterine homeostasis coexist, S1P signaling emerges as a particularly relevant non-hormonal pathway to investigate. In this thesis, we therefore examine whether targeting S1P signaling can modulate uterine immune remodeling and disease progression in a murine model of adenomyosis.

6.1. Metabolism, cellular sources, receptors, and gradient formation

S1P originates from the complex metabolism of ceramides, which are structural components of cell membranes. Ceramidases convert ceramide into sphingosine, which is subsequently phosphorylated by either one of the two sphingosine kinases, SPHK1 or SPHK2, to generate S1P (247). SPHK1 is predominantly cytosolic but translocate to the plasma membrane in response to extracellular stimuli, while SPHK2 is localized within the nucleus, mitochondria, and endoplasmic reticulum, where it participates in the apoptosis regulation, transcription and mitochondrial function (247,248). The balance between ceramide, sphingosine and S1P, often described as a "sphingolipid rheostat", determines whether cells undergo apoptosis, differentiation, or adopt proliferation and migratory phenotypes. S1P levels are controlled not only by synthesis but also by degradation through sphingosine-1-phosphate lyase (SGLP), which irreversibly cleaves S1P, and by S1P phosphatases (SGPP1 and SGPP2), which recycle S1P back into sphingosine, contributing to ceramide regeneration (247). The major steps of the sphingolipid metabolic pathway are illustrated in Figure 13.

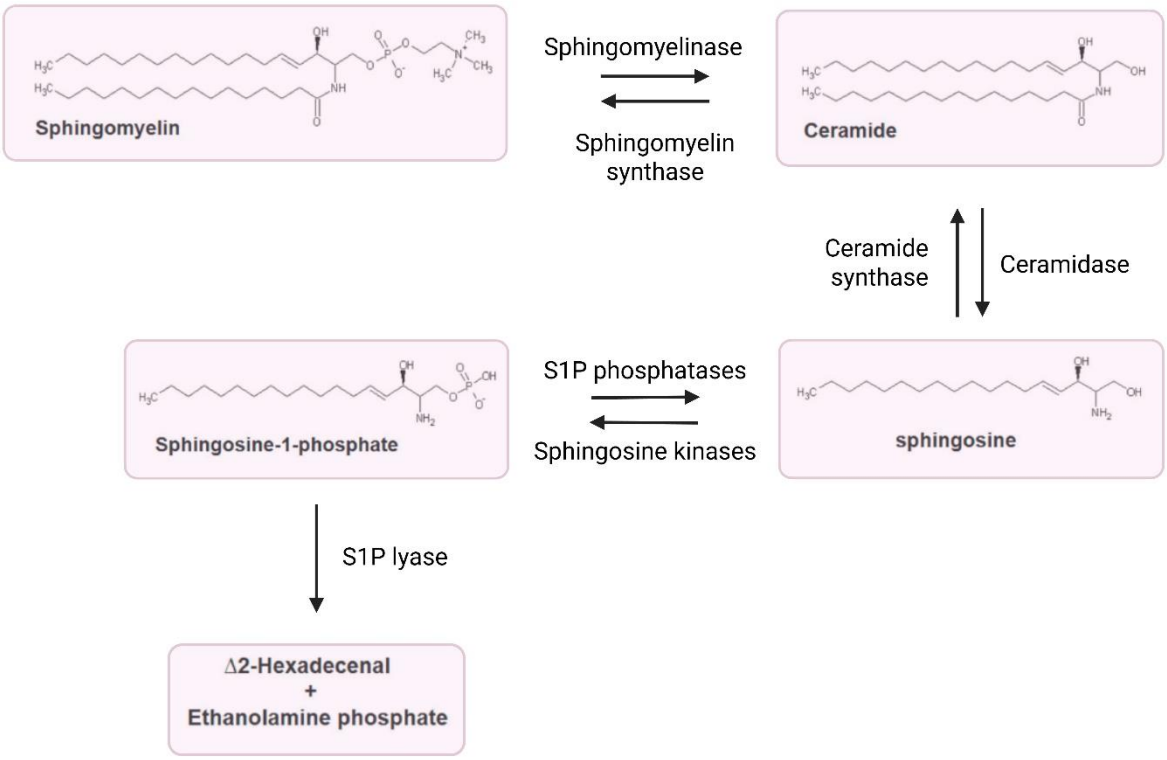


Figure 13. Simplified overview of the sphingolipid metabolic pathway. *Sphingomyelin can be hydrolyzed by sphingomyelinase to generate ceramide, whereas sphingomyelin synthase catalyzes the reverse reaction. Ceramide can be converted into sphingosine through the action of ceramidase, while ceramide synthase regenerates ceramide from sphingosine. Sphingosine is phosphorylated by sphingosine kinases to produce sphingosine-1-phosphate (S1P), a bioactive lipid mediator. S1P can be dephosphorylated back to sphingosine by S1P phosphatases or irreversibly degraded by S1P lyase into Δ2-hexadecenal and ethanolamine phosphate. This pathway illustrates the dynamic interconversion between sphingolipid species that regulate cellular processes. Adapted from Diaz Escarcega et al. (249), designed with BioRender.com*

Multiple cell types contribute to extracellular S1P production. Erythrocytes constitute a major source due to their high sphingosine kinase activity and absence of S1P-degrading enzymes. Platelets release S1P upon activation particularly during coagulation (250), while endothelial cells continuously synthesize and export S1P, thereby maintaining a stable circulating pool (251,252). In the uterus, components of the sphingosine-1-phosphate (S1P) signaling pathway are expressed in both endometrial and myometrial tissues, suggesting that local production of S1P may contribute to autocrine and paracrine regulatory mechanisms (253–255). While direct evidence of S1P production by uterine immune cells remains limited, macrophages are well known to express SPHK2 and secrete S1P in inflammatory contexts, suggesting a potential contribution to the local S1P pool (256,257). These immune populations also express various S1P receptors in other tissues, implying that reciprocal communication between immune and resident uterine cells through S1P signaling is likely (258), although this requires further confirmation in uterine models.

Once produced, S1P can act as a second messenger, regulating pathways involved in cell survival, proliferation, and calcium homeostasis or can be exported from cells through specific transporters, primarily spinster homolog 2 (SPNS2), a membrane transporter that mediates the release of intracellular S1P into the extracellular space (259). Circulating S1P is then carried by plasma proteins, mainly high-density lipoproteins (HDL) associated with apolipoprotein M (ApoM) or by albumin (250). Extracellular S1P signals through a family of five G protein-coupled receptors (S1PR1-5), each with distinct tissue distribution and downstream signaling properties (260). Within the female reproductive system, several S1PR subtypes are expressed and participate in the regulation of key physiological processes such as angiogenesis, inflammatory signaling and uterine contractility. S1P signaling has been identified in ovarian granulosa cells, where activation of S1PR1-3 contributes to endothelial barrier stabilization and vascular homeostasis (261). In endometrium, S1PR1, S1PR2 and S1PR3 are the predominant subtypes expressed, suggesting a central role in endometrial remodeling (255). For example, S1PR3 expression has been reported in endometriotic lesions, where its modulation influences fibrotic remodeling and inflammation, suggesting potential implications for uterine pathophysiology (262). This sequence of enzymatic conversions and regulatory steps is summarized in Figure 14, which provides overview of S1P synthesis, export and receptor-mediated signaling.

Despite these emerging findings, our understanding of uterine S1P signaling remains fragmentary, particularly regarding the specific roles of individual S1P receptors subtypes in endometrial remodeling, implantation and immune homeostasis. Table 3 provides the main characteristics of the five S1P receptor subtypes and their reported expression in reproductive tissues. Importantly, S1PR expression is highly context-dependent and can vary according to cell type, hormonal milieu, and activation state, which must be considered when interpreting function data from reproductive tissues.

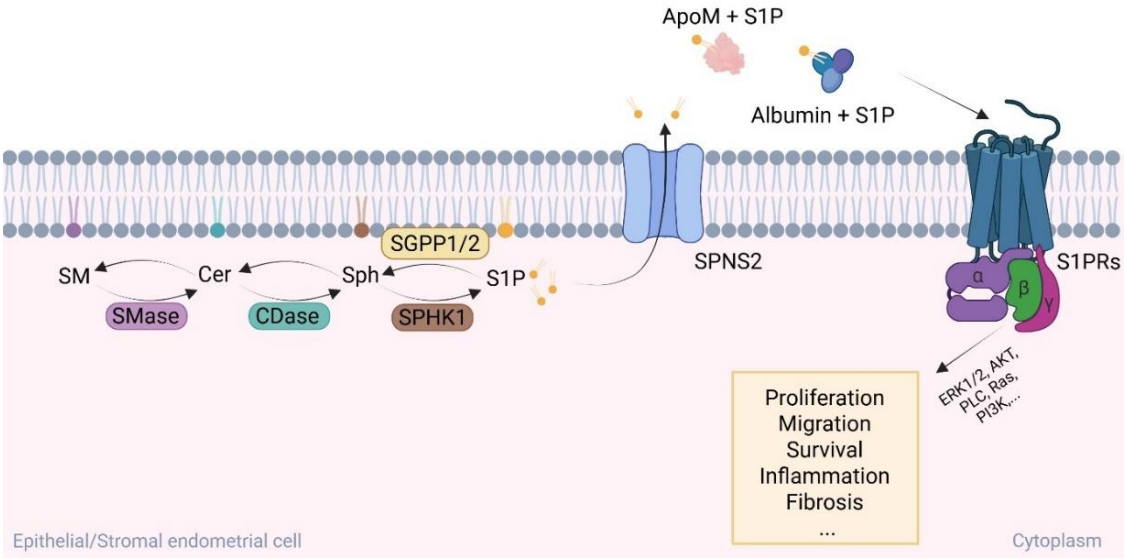


Figure 14. Overview of the sphingosine-1-phosphate signaling pathway. *Within endometrial epithelial and/or stromal cells, sphingomyelin (SM) is hydrolyzed into ceramide (Cer) by sphingomyelinase (SMase), then converted to sphingosine (Sph) via ceramidase (CDase). Sphingosine is phosphorylated by sphingosine kinase SPHK1, the main source of extracellular biologically active S1P. Cytosolic S1P is exported by the transporter SPNS2 and circulates bound to Apolipoprotein M (ApoM) or albumin. Extracellular S1P activates S1P receptors (S1PRs) at the plasma membrane, triggering downstream pathways involved in the regulation of proliferation, migration, survival, inflammation and fibrotic remodeling. Adapted from Hu et al.(263), designed with BioRender.com*

Table 3. Main characteristics of S1P receptor subtypes *(264–266)*

Receptor	Main tissue/Cell localization	Coupled G proteins	Principal signaling pathways	Main biological function
S1PR1	Endothelial cells, lymphocytes, smooth muscle cells, endometrium	Gi	PI3K-Akt, Rac, MAPK/ERK	Promotes endothelial barrier integrity; egression from lymph nodes;…
S1PR2	Smooth muscle, endothelial cells, macrophages, endometrium	G12/13, Gq, Gi	Rho/ROCK, PLC-Ca2+	Increases vascular permeability and contractility
S1PR3	Endothelial cells, smooth muscle, endometrium	Gi, Gq, G12/13	ERK/MAPK, PLC-Ca2+, Rho	Regulates endothelial barrier and vascular tone; involved in inflammatory responses; may influence uterine tone and fibrosis
S1PR4	Lymphoid tissues	Gi, G12/13	ERK, Rho	Modulates immune cell activation and cytokine production
S1PR5	NK cells	Gi, G12/13	Akt, Rho	NK cell migration

6.2. Physiological roles of S1P in reproductive tissues

The reproductive tract is subject to cyclic remodeling, angiogenesis, immune modulation, and phases of regression and regeneration (267,268). Within this dynamic environment, the S1P signaling axis plays essential roles at multiple levels.

Within the ovary, S1P acts as a potent pro-survival factor, protecting oocytes and follicles from apoptosis induced by stressors such as chemotherapy or irradiation. This anti-apoptotic role preserves the ovarian reserve and supports fertility. Additionally, S1P signaling contributes to luteal cell function and corpus luteum maintenance, thereby influencing progesterone synthesis and endocrine support of early pregnancy (269–271). Together, these ovarian effects highlight the capacity of S1P to modulate reproductive potential through survival and endocrine pathways.

In the uterus, S1P orchestrates tissue remodeling and neovascularization, with its expression and signaling tightly regulated in a temporal and spatial manner during the menstrual cycle and pregnancy. S1P promotes angiogenesis necessary for endometrium regeneration and for establishing the utero-placental blood supply during pregnancy (272–275).

A crucial physiological process regulated by S1P is decidualization. In murine models, upregulations of S1PR1, S1PR3 and S1PR5 have been observed in the uterine decidua during the peri-implantation period, spatially correlating with vascularized regions and suggesting coordination of decidual growth and angiogenesis (275). In human tissues, increased expression of SPHK1, S1P lyase, and S1PR3 has been reported in decidual samples during late pregnancy, further supporting a role for S1P signaling in endometrial remodeling and vascular adaptation (274). By integrating vascular, stromal and immune cues, S1P supports the dynamic changes required for menstrual regeneration, implantation, and early placentation. These physiological functions are particularly relevant in the context of adenomyosis, a condition characterized by disrupted vascular adaptation, altered stromal differentiation and immune balance.

6.3. The S1P gradient: physiological significance and pathological relevance

The coordinated regulation of synthesis, export, degradation, and receptor activation generates a concentration gradient between the bloodstream and peripheral tissues, a distinctive feature of the S1P signaling system. In blood, S1P levels are maintained at micromolar concentrations through continuous release by erythrocytes, platelets and endothelial cells, whereas tissue and interstitial levels remain in the nanomolar range due to

active degradation by S1P lyase and phosphatases (276). This gradient is essential for immune cell trafficking, vascular permeability control, and inflammatory responses (252).

The physiological significance of this gradient extends to reproductive tissues, where vascular remodeling, cyclic inflammatory changes, and endometrial regeneration depend on finely tuned S1P signaling. In the endometrium and myometrium, endothelial cells constitute the major sources and sensors of S1P, allowing coordinated control of angiogenesis, vascular permeability, and immune cell recruitment. Disruption of this spatial S1P distribution is therefore expected to profoundly alter local vascular and inflammatory dynamics (254,275,277).

In pathological contexts, such as endometriosis, this finely regulated gradient is markedly disrupted. Elevated peritoneal S1P concentrations, primarily released by erythrocytes and platelets activation, reduce the normal vascular-to-tissue differential. This altered gradient favors immune cell retention, chronic inflammation, and the persistence of ectopic endometrial lesions through pro-survival and pro-angiogenic mechanisms (Figure 15). This model of a flattened or reversed S1P gradient in endometriosis provides an important conceptual framework for other uterine conditions characterized by chronic inflammation. Although data in adenomyosis remain scarce, the strong biological parallels between the two diseases suggest that a similar disruption of local S1P distribution is plausible. Such a hypothesis is particularly relevant given the fibrotic remodeling, altered vascular features, and immune imbalance that characterize adenomyosis (278).

By drawing on the mechanistic insights established in endometriosis, the endometriotic S1P gradient model provides a useful conceptual framework to generate hypotheses about S1P dynamics in adenomyosis and to explore whether analogous alterations might contribute to its pathophysiology. At present, however, this extension remains a working hypothesis rather than an established mechanism and will require dedicated experimental validation in adenomyosis.

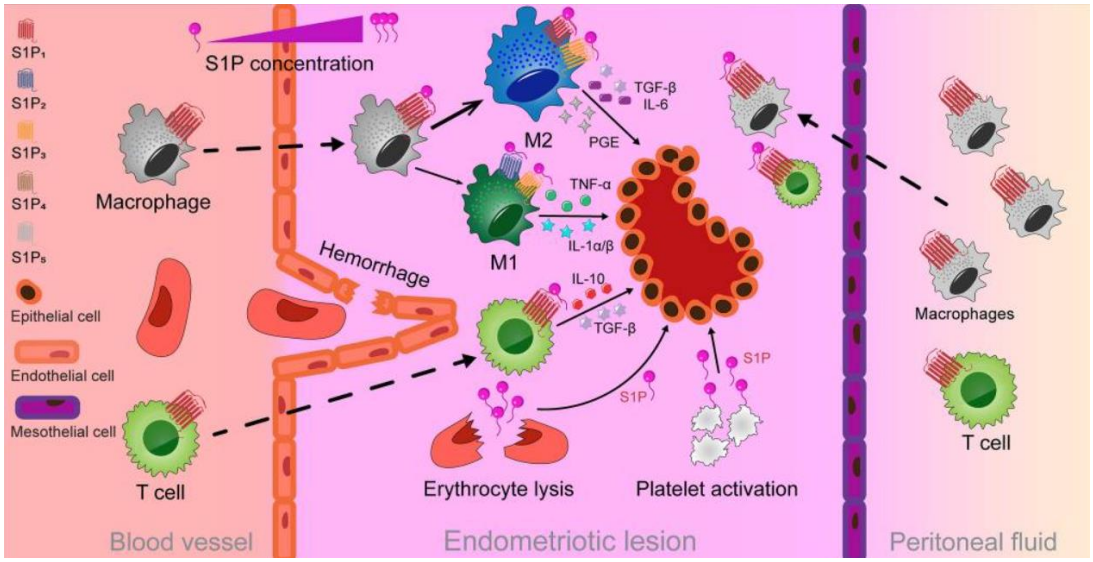


Figure 15. S1P-dependent regulation of immune cell recruitment and macrophage polarization in endometriotic lesions*. Endometriotic lesions recruit macrophages and T cells from the bloodstream and peritoneal fluid. The sphingosine-1-phosphate (S1P) signaling axis plays a central role in this process: S1P1-S1P5 (also referred to as sphingosine-1-phosphate receptors (S1PR1-S1PR5) regulate immune cell trafficking and activation. In particular, S1P1 regulates the trafficking of T cells and macrophages in response to local S1P gradients, while S1P2 and S1P3 modulate macrophage activation states and contribute to the balance between pro-inflammatory and pro-fibrotic phenotypes Local erythrocyte lysis and platelet activation increase S1P concentrations within the lesion, thereby amplifying inflammatory signaling through the release of cytokines and chemokines that support lesion persistence. From Zhang et al. (278)*

6.4. Implications in endometriosis and other gynecological pathologies

The S1P signaling pathway has emerged as a pivotal regulator in gynecological disorders. Altered expression of sphingosine kinases and S1P receptors has been reported in several reproductive pathologies, including endometriosis, ovarian cancer, uterine fibroids, and adenomyosis (271).

Most mechanistic insights into S1P signaling in gynecological pathology come from endometriosis. In peritoneal fluid of affected women, S1P concentrations are elevated due to release by activated platelets and macrophages. This S1P produced promotes an M2-polarized phenotype that facilitates tissue remodeling and immune tolerance within lesions (279). This macrophage-derived S1P amplifies the inflammatory cascade in endometrial stromal cells, upregulating cytokines such as IL-6 through ERK and Akt activation, thereby promoting proliferation and survival (280). Additionally, S1P induces a reactive oxygen species (ROS)-dependent proinflammatory response mediated by ERK5 in human endometrial stromal cells, reinforcing the chronic inflammatory state typical of endometriotic tissues (281).

Beyond inflammation, S1P participates in the neuroangiogenic and fibrotic remodeling of endometriosis lesions through the S1P/S1PR3 axis (282,283). Dysregulation of S1P receptors,

particularly S1PR2 and S1PR3, has been implicated in TGFβ-induced fibrosis, identifying S1PR3 as a potential non-hormonal therapeutic target against endometriosis-associated fibrotic remodeling (262,284,285). Omics-based analyses further confirm global deregulation of the sphingolipid metabolic network in endometriotic tissues, reinforcing the centrality of this pathway in disease pathogenesis (255). These mechanisms reflect processes that are also active in adenomyosis, including inflammation, fibrosis and aberrant stromal-myometrial interactions.

Other gynecological disorders show similar dysregulation. Uterine fibroids exhibit increased SPHK1 and S1PR3 expression correlates with smooth muscle cell proliferation and extracellular matrix deposition (286). In ovarian cancer, S1P signaling contributes to tumor growth, invasion, and chemoresistance. SPHK1 overexpression enhances proliferation and angiogenesis, while its inhibition sensitizes tumor cells to apoptosis underscoring its potential as a therapeutic target (287). Interestingly, metformin suppresses SPHK1 expression and S1P levels, reducing migration and invasion under hypoxia, suggesting a metabolic link between S1P signaling and cancer aggressiveness (288). Although these conditions differ in etiology, they collectively highlight the recurrent involvement of S1P signaling in pathological uterine tissue remodeling.

6.5.Potential implication in adenomyosis

Given the pathophysiological parallels between endometriosis and adenomyosis (63), S1P signaling is likely to contribute to adenomyosis through overlapping molecular mechanisms. To date, only one study has specifically explored the involvement of the S1P pathway in human adenomyosis, providing preliminary evidence that this bioactive lipid may influence disease development (289).

Available data suggest that adenomyotic tissues exhibit a profound dysregulation of S1P signaling, characterized by a marked increase in S1PR3 expression and a concomitant reduction in S1PR2 compared with healthy endometrium. This receptor shift is consistent with a transition toward pro-survival, pro-inflammatory and extracellular matrix remodeling pathways, all key processes implicated in the progression of adenomyosis. Notably, elevated S1PR3 levels positively correlate with increased α-SMA (ACTA2) levels, suggesting S1P-mediated myofibroblast activation and contractile transformation within the myometrium (289).

Although these observations point toward a potentially central role for the S1P/SPHK1/S1PR3 axis in adenomyotic fibrosis, inflammation and tissue remodeling, the mechanistic evidence remains poor. The scarcity of human data and the lack of functional experiments leave major

gaps in our understanding. Elucidating how S1P metabolism and receptor signaling shape the adenomyotic microenvironment represents a critical avenue for future research, with significant implications for pathophysiology. Altogether, these findings support the hypothesis that the SPHK1/S1PR3 axis may drive myometrial fibrosis and immune remodeling in adenomyosis, which we will explore in our murine model.

6.6. Therapeutic targeting of the S1P pathway

Given the extensive involvement of the S1P axis in inflammation, angiogenesis, fibrosis, and pathological tissue remodeling, pharmacological targeting of this pathway represents a promising strategy for gynecological disorders such as adenomyosis and endometriosis. Experimental models of endometriosis have demonstrated that inhibition of key components including sphingosine kinases and S1P receptors, reduces lesion growth, cytokine production and fibrosis, supporting their therapeutic potential in adenomyosis (290,291). These pharmacological interventions and their expected effects on S1P signaling in adenomyosis are summarized in Figure 16, which illustrates the hypothesized pathogenic role of S1P and how SKI-5C and FTY720 modulate this pathway.

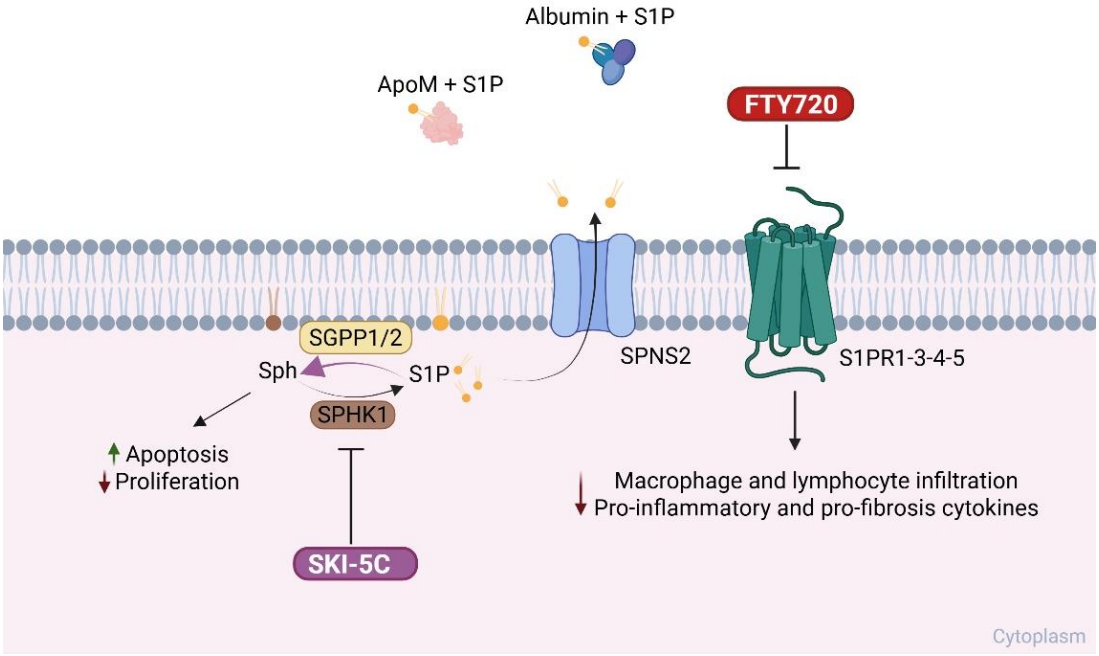


Figure 16. Therapeutic targeting of the sphingosine-1-phosphate (S1P) signaling pathway in adenomyosis *Schematic representation of the hypothesized role of S1P signaling and its pharmacological modulation. SKI-5C selectively inhibits sphingosine kinase 1 (SPHK1), thereby reducing intracellular S1P synthesis and shifting the sphingolipid balance toward pro-apoptotic ceramides, thus limiting S1P-dependent cell survival and proliferation. FTY720, following phosphorylation, functionally antagonizes S1P receptors, primarily S1PR1, by inducing receptor internalization, resulting in reduced macrophage and lymphocyte trafficking and decreased production pro-inflammatory and pro-fibrotic cytokines within adenomyotic lesions. Created with BioRender.com*

6.6.1. Targeting S1P synthesis

Sphingosine kinase 1 (SPHK1) catalyzes the conversion of sphingosine to sphingosine-1-phosphate (S1P) and acts as a "sphingolipid rheostat", determining the balance between apoptosis and survival (292). SPHK1 overactivation promotes pro-survival and pro-fibrotic pathways, making it an appealing therapeutic target in conditions characterized by pathological tissue remodeling. Its overexpression in multiple cancers has been associated with poor prognosis and chemoresistance, reinforcing its pathological relevance (293).

SKI-5C (2-(p-hydroxyanilino)-4-(p-chlorophenyl)thiazole) is a small-molecule compound that selectively inhibits SPHK1, first described in 2009, with negligible activity against SPHK2. SPHK1 normally phosphorylates sphingosine to generate S1P. Inhibition of this enzyme therefore reduces intracellular S1P levels and shifts the sphingolipid balance toward ceramide. This shift in the sphingolipid balance – from pro-survival S1P toward pro-apoptotic ceramides – promotes apoptosis and limits cellular proliferation (294).

In murine models of endometriosis, administration of SKI-5C has demonstrated clear therapeutic potential. Treated animals showed reduced lesion size, diminished vascularization and microvessel density, and downregulation of proliferative and angiogenic pathways (290). Together, these findings suggest that inhibiting SPHK may counteract multiple S1P-driven mechanisms including abnormal cell survival, excessive proliferation, and pathological angiogenesis, highlighting SPHK1 inhibition as a promising therapeutic strategy.

6.6.2. Targeting S1P receptors (S1PR modulators)

Fingolimod, also known as FTY720, is a synthetic analog of sphingosine originally derived from the fungal metabolite myriocin (ISP-I), a metabolite of the fungus *Isaria sinclairii*. Its structural similarity to sphingosine enables it to participate in sphingolipid metabolic pathways. Once administered, fingolimod undergoes phosphorylation primarily by SPHK2 to form the active metabolite fingolimod-phosphate (FTY720-P). This phosphorylated form structurally mimics endogenous S1P and binds with high affinity to several S1P receptor subtypes, particularly S1PR1, S1PR3, S1PR4 and S1PR5, but not significantly S1PR2 (295).

The principal pharmacological mechanism of FTY720-P is functional antagonism of S1PR1. Upon receptor binding, FTY720-P induces receptor internalization and degradation, thereby preventing lymphocytes from responding to S1P gradients between lymphoid organs and blood. As a result, lymphocytes become sequestered in secondary lymphoid tissues, leading to lymphopenia and decreased autoimmune reactivity. This mechanism underlies its therapeutic efficacy in autoimmune diseases characterized by aberrant lymphocyte trafficking

(296). FTY720 was approved by the U.S. Food and Drug Administration (FDA) in 2010 as the first oral disease-modifying therapy for relapsing-remitting multiple sclerosis (RRMS) (295,297).

In experimental models of endometriosis, FTY720 has been shown to exert strong anti-inflammatory and anti-lesion effects. The treatment markedly reduced the size of endometriotic lesions and lowered the infiltration of macrophage and lymphocyte, two key immune cell populations that sustain chronic inflammation. In parallel, FTY720 decreased the expression of major pro-inflammatory and pro-fibrotic cytokines, including IL1-β, TNF-α, and TGF-β1 (291). Together, these findings indicate that altering S1P receptor signaling can dampen the persistent inflammatory responses and pathological tissue remodeling that characterize endometriosis.

Despite its efficacy, FTY720 presents dose-dependent adverse effects, including transient bradycardia, atrioventricular block, lymphopenia, macular edema, headache and increased susceptibility to viral infections (298).

Given its ability to modulate lymphocyte trafficking and to reduce inflammatory lesion burden in endometriosis models, FTY720 represents an attractive tool to test the contribution of S1P signaling to adenomyosis progression in our murine model.

Overall, pharmacological targeting of the S1P pathway, through SPHK1 inhibitors or SP1PR modulators, has shown promising effects in preclinical models of endometriosis. However, the therapeutic relevance in adenomyosis remains largely unexplored. This gap highlights the need for dedicated studies specifically addressing the role of S1P signaling in adenomyosis pathophysiology and fertility impairment, which forms the basis of the objectives developed in this thesis.

OBJECTIVES AND OUTLINES OF THE THESIS

Objectives

Adenomyosis is increasingly diagnosed in young women of reproductive age and frequently associated with infertility, yet the specific biological mechanisms linking the disease to impaired reproductive outcomes remain poorly defined. Current knowledge is limited by the frequent coexistence of other gynecological disorders, which prevents the isolation of adenomyosis-specific features, and by the lack of studies addressing the role of the uterine immune microenvironment during the earliest stages of disease development.

The general objective of this thesis was to investigate the mechanisms by which adenomyosis may affect fertility and promote disease initiation and progression, and to identify molecular pathways that may represent targets for fertility-preserving therapeutic strategies.

To achieve this goal, four complementary objectives were defined:

1. To investigate reproductive outcomes and underlying mechanisms in a controlled mouse model of adenomyosis, thereby characterizing adenomyosis-specific effects on cyclicity, folliculogenesis, fertility and implantation independently of coexisting pathologies.
2. To characterize the uterine immune microenvironment at both pre-lesional and advanced stages of disease development, with the aim of identifying early immune alterations contributing to lesion initiation and progression.
3. To explore the involvement of the sphingosine-1-phosphate signaling pathway in adenomyosis, by assessing its deregulation at pre-lesional and advances stages of disease.
4. To evaluate the therapeutic potential of pharmacological S1P pathway inhibition using SKI-5C and FTY720 in preventive and therapeutic settings, and assessing their effects on lesion development, immune dysregulation, and cell migration mechanisms.

Outlines

This thesis is structured around three original research articles that together address the four objectives defined above. Each article constitutes an independent scientific study and is presented in its published or submitted form.

Article 1 focuses on reproductive outcomes in a controlled mouse model of adenomyosis, providing a comprehensive characterization of estrous cyclicity, folliculogenesis, fertility, and implantation defects associated with the disease.

Article 2 addresses immune remodeling in adenomyosis by characterizing the uterine immune microenvironment at pre-lesional and established stages, with particular emphasis on early immune alterations potentially involved in lesion initiation and progression.

Article 3 examines the deregulation of the sphingosine-1-phosphate (S1P) signaling pathway during adenomyosis development and evaluates the preventive and therapeutic potential of pharmacological S1P pathway inhibition, focusing on immune modulation and tissue remodeling.

Additional research contributions completed during this PhD are presented in the appendixes.

RESULTS

ARTICLE 1

Impaired fertility in adenomyosis: a murine model reveals endometrial receptivity and progesterone resistance imbalances

Marlyne Squatrito, Julie Vervier, Jules Bindels, Silvia Blacher, Michelle Nisolle and Carine Munaut.

Reproduction (2024) 167 e240019

In this study, we demonstrated that adenomyosis alone is sufficient to impair fertility in a controlled murine model. By inducing adenomyosis neonatally with tamoxifen, we showed that affected mice develop severe lesions and exhibit profound reproductive defects. We observed disrupted estrous cyclicity, impaired folliculogenesis, and a marked reduction in litter number and size. At the uterine level, we identified decreased expression of key implantation markers, together with a significant loss of progesterone receptor expression, revealing the presence of progesterone resistance. Altogether, our work clarifies how adenomyosis compromises ovarian function and endometrial receptivity, providing mechanistic evidence for its causal role in fertility.

Reproduction

Reproduction (2024) **167** e240019
https://doi.org/10.1530/REP-24-0019

Received 12 January 2024
Accepted 7 March 2024
Available online 7 March 2024
Version of Record published 17 April 2024

RESEARCH

Impaired fertility in adenomyosis: a murine model reveals endometrial receptivity and progesterone resistance imbalances

Marlyne Squatrito[1], Julie Vervier[1,2], Jules Bindels[1], Laëtitia Bernet[1], Silvia Blacher[1], Michelle Nisolle[2] and Carine Munaut[1]

[1]Laboratory of Biology of Tumor and Development, GIGA-Cancer, University of Liège, Liège, Belgium
[2]Department of Obstetrics and Gynecology, Hôpital de la Citadelle, University of Liège, Liège, Belgium

Correspondence should be addressed to C Munaut; Email: c.munaut@ulg.ac.be

Abstract

In brief: The impact of adenomyosis on reproductive health needs to be fully understood. By using a murine model, this study provides novel insights into the nuanced mechanisms associated with fertility challenges and offers a foundation for targeted interventions.

Abstract: This study investigates the intricate relationship between adenomyosis and reproductive health using a murine model, offering novel insights into this prevalent gynecological disorder. Adenomyosis, characterized by the invasive growth of endometrial tissue into the myometrium, is believed to negatively impact fertility. However, the challenge lies in disentangling this influence, as adenomyosis often coexists with other gynecological diseases. A tamoxifen-induced mice model presents a significant advantage by enabling the specific study of adenomyosis, devoid of confounding influences of concurrent gynecological diseases such as endometriosis. Focusing exclusively on adenomyosis, our study aims to elucidate pathogenic mechanisms underlying fertility issues, focusing on estrous cyclicity, ovarian follicle development, and overall fertility. Our findings uncover disruptions in estrous cyclicity, characterized by an increased duration of time spent in the estrus phase in adenomyosis-induced mice. These disturbances are potentially linked to observed compromised folliculogenesis and the remarkable reduction in litter number and size in mice affected by adenomyosis. Moreover, this study unveils potential drivers of subfertility such as progesterone resistance and altered endometrial receptivity. Within the uteri of mice with adenomyosis, reduced expression of the progesterone receptor and a decreased expression of two implantation-related markers (HoxA10 and integrin β3) were observed. This comprehensive examination sheds light on the nuanced complexities of adenomyosis-associated reproductive challenges, providing a foundation for targeted interventions in addressing fertility issues related to this disease.

Introduction

Adenomyosis is a benign estrogen-dependent uterine disease characterized by ectopic endometrial glands and stroma within the myometrium and surrounded by smooth-muscle hyperplasia reaction (Bird *et al.* 1972). Two principal forms of the disease, focal and diffuse, are generally described depending on the distribution pattern of the ectopic endometrial implants in the myometrium. Focal adenomyosis is a circumscribed

Published by Bioscientifica Ltd.
https://rep.bioscientifica.com
© 2024 the author(s)

Downloaded from Bioscientifica.com at 04/18/2024 11:35:24AM
via Open Access. This work is licensed under a Creative Commons Attribution 4.0 International License.
This work is licensed under a Creative Commons Attribution 4.0 International License.
http://creativecommons.org/licenses/by/4.0/

Reproduction (2024) **167** e240019
https://doi.org/10.1530/REP-24-0019

nodular collection whereas diffuse adenomyosis is characterized by different groups of endometriotic glands and stroma distributed throughout the myometrium. This gynecological disorder is often associated with pain (dysmenorrhea, pelvic pain, or dyspareunia), abnormally heavy menstrual bleeding, and poor pregnancy outcomes (infertility, repeated implantation failure, miscarriage, or obstetric complications). However, up to one-third of patients can be asymptomatic (Levgur *et al.* 2000). Accurate prevalence assessment remains challenging due to the lack of standardized diagnostic criteria, protocols, and patient populations (Abbott 2017, Loring *et al.* 2021). Nevertheless, numerous studies suggest a prevalence ranging from 20% to 35% (Abbott 2017). Historically, the gold standard for the diagnosis of adenomyosis was through histological examination of the uterus after hysterectomy. Therefore, it was considered to be a disease affecting mainly multiparous women over 40 years old. Recent advances in imaging techniques, such as transvaginal ultrasound (TVS) and magnetic resonance imaging (MRI), have led to increased diagnoses in young women of reproductive age (Vannuccini & Petraglia 2019) as well as in a population of women undergoing assisted reproductive technologies (Puente *et al.* 2016). One of the most determinant fertility factors is age. In Europe, we observed for the past years a trend to delay the first pregnancy (mean age 29.4 years old) (Fertility statistics – Statistics Explained (europa.eu)). Since adenomyosis could further affect the fertility of those women, understanding the mechanisms underlying adenomyosis development and addressing its impact on fertility outcomes is now crucial (Donnez *et al.* 2021).

Given that adenomyosis often coexists with other gynecological diseases such as endometriosis (20-80%) and uterine fibroids (15-57%), the direct causal relationship between adenomyosis and infertility remains challenging to establish (Sharma *et al.* 2019, Vannuccini & Petraglia 2019, Yu *et al.* 2020, Szubert *et al.* 2021). Furthermore, it is uncertain whether these concurrent conditions act independently or cumulatively to affect fertility (Vercellini *et al.* 2023). For instance, a meta-analysis by Vercellini *et al.*, including 1865 women, indicated that adenomyosis could reduce clinical pregnancy rates and increase miscarriage risk in IVF/ICSI outcomes (Vercellini *et al.* 2014). In addition, among infertile women and, more specifically, those experiencing recurrent miscarriages or repeated implantation failure in Assisted Reproductive Technology (ART), the prevalence of adenomyosis was estimated at 25%. These observations support the possibility that adenomyosis may have a deleterious impact on human reproduction (Puente *et al.* 2016). Various mechanisms have been proposed to explain subfertility and poor reproductive outcomes in adenomyosis, including aberrant uterotubal sperm transport and contractility, altered endometrial function and receptivity, excessive free radical formation affecting oocyte quality and embryo development as well as uterine immune imbalances (Harada *et al.* 2016, Sharma *et al.* 2019). However, the potential confounding effect of endometriosis could not be excluded (Vercellini *et al.* 2014). The use of a murine model of adenomyosis is beneficial for studying fertility outcomes associated with adenomyosis without associated pathologies such as myomas or endometriosis. Among the various models available to induce adenomyosis, neonatal treatment of CD1 mice with tamoxifen, a selective estrogen receptor modulator, is a model of choice because it appears to reliably produce severe adenomyosis lesions in a high proportion of mice and has been used extensively for examining adenomyosis pathogenesis and drug screening (Green *et al.* 2005, Yen *et al.* 2017*a*, Marquardt *et al.* 2020).

In this study, we aimed to elucidate the potential pathogenic mechanisms through which adenomyosis, in the absence of associated gynecological disorders, could impact pregnancy outcomes negatively. We assessed estrous cycles, folliculogenesis, and the expression of genes related to endometrial receptivity as well as progesterone resistance in a murine model. This would allow us to explore the multifactorial factors contributing to infertility associated with adenomyosis.

Materials and methods

Mouse model of adenomyosis

Animal experiments in this study were approved by the Animal Ethics Committee of the University of Liège (#2387) and conducted following relevant guidelines and regulations. In total, 69 female neonatal CD1 mice (born from pregnant mice provided by Charles River Laboratories (Italy)) were orally dosed with 2,7 µmol/kg tamoxifen (= 1 mg/kg) (Sigma, T5648) suspended in a peanut oil/lecithin/condensed milk mixture (2:0.2:3, v/v) on days 2 through 5 after birth (day of birth = day 1) at a dose volume of 5 µL/g body weight (Green *et al.* 2005). Seventy-eight female neonatal control mice received vehicle only. All mice were housed under controlled temperature (+/- 21°C) and light (12-h light–12-h darkness cycle) with ad libitum access to food and water. Animals were euthanized either at 1-month-old (CTL, $n = 12$; ADM, $n = 14$) or 3-month-old (CTL, $n = 66$; ADM, $n = 55$). Ovaries were collected and weighed; one was fixed in 4% formalin while the second was snap-frozen in liquid nitrogen. Uteri from 1 and 3-month-old mice were also removed and weighted. One of the uterine horns was divided into 2 (1-month-old mice) or 3 parts (3-month-old mice) and snap-frozen for RNA and protein extraction. The second horn was fixed in 4% formalin. Complete autopsies were performed. Histopathological examinations of ovaries and uteri were conducted using standard histological sections prepared from formalin-fixed material and stained with hematoxylin and eosin.

Downloaded from Bioscientifica.com at 04/18/2024 11:35:24AM
via Open Access. This work is licensed under a Creative Commons Attribution 4.0 International License.
http://creativecommons.org/licenses/by/4.0/

Reproduction (2024) **167** e240019
https://doi.org/10.1530/REP-24-0019

To study progesterone resistance and implantation gene expression, only mice in the proliferative phase of the estrus cycle (proestrus or estrus phase) were included. To synchronize the phase of the cycle of the mice included in this aim, we injected them subcutaneously for 3 consecutive days with 17β-estradiol (100 ng/100 µL) before sacrifice.

Vaginal smears analysis

The estrous cycle phase was determined once daily (between 08:00 and 10:00 h) for 14 consecutive days by collecting samples via vaginal lavage as previously described by Caligioni *et al.* (Caligioni 2010). Briefly, the vagina was gently flushed with 30 µL sterile PBS using a sterile 200 µL pipette tip. The collected PBS was deposited on a glass slide as a drop, dried, and fixed for 30 min in 100% ethanol. Ethanol-fixed smears were then rehydrated and stained with hematoxylin–eosin. The estrous cycle stage was determined by examining the proportion and morphology of leukocytes and epithelial cells under a 40× objective light microscope. When the female is in proestrus, mostly nucleated epithelial cells are present. More cornified epithelial cells are present as the cycle stage advances to estrus. If the female is not pregnant, metestrus will begin. Metestrus is a brief stage during which the uterine lining will begin to slough, and leads to the presence of cornified epithelial cells and leukocytes present in vaginal smears. Diestrus is the longest stage characterized by leukocytes in a very high density. If a smear appears to contain more than one cell type, the stage representing the majority cell type is selected (Byers *et al.* 2012). In total, 18 mice in the adenomyosis group and 25 in the control group were subjected to vaginal lavage for our first experiment. We repeated the experiment with vaginal smears on 19 other adenomyosis-induced mice and 25 control mice to validate our results.

Fertility and litter size analysis

To analyze the fertility, 12 female mice (3-month-old) tamoxifen-treated ($n=6$) or vehicle-treated ($n=6$) during the neonatal period were bred with CD1 fertility-proven male mice (1:1). Mice were mated continuously for 3 months, and litter number and size were monitored. To calculate the average litter size at weaning, the total number of pups born during the breeding trial was divided by the total number of litters. To ensure that a lack of conception was not due to male subfertility, male mice breaded with control mice were exchanged with male mice mated with tamoxifen-treated mice after a first successful mating cycle.

Immunohistochemistry

Ovarian sections were assessed by immunostaining serial sections with antibodies against Lhx8 to facilitate the quantification of follicles. Uterine sections of 1- or 3-month-old mice were stained in visible light with three markers of implantation (HoxA10, integrin β3, and LIF). Progesterone resistance was also assessed by double immunofluorescence staining for αSMA and PGR. Briefly, ovarian and uterine sections were deparaffinized and rehydrated, followed by antigen retrieval using an autoclave (11 min, 126°C, 1.3 bar). After cooling down for 20 min, endogenous peroxidase activity was blocked by incubating the sections in 3% hydrogen peroxide for 20 min at room temperature (RT). Non-specific binding sites were blocked by incubation in the 'Animal-Free Blocking Solution' (Cell Signaling) for 20 min at RT. Primary antibodies (Table 1) were diluted at different concentrations in the 'REAL antibody diluent' (Dako) and incubated for 1 h at RT except for cleaved HoxA10, integrin β3, and LIF which were incubated overnight at 4°C. For double immunostaining, the anti-PGR and anti-αSMA antibodies were mixed as well as for anti-EpCAM and anti-αSMA antibodies. Afterward, sections were incubated with the secondary antibody linked to horseradish peroxidase (ENVISION/HRP ready to use, Dako) for 30 min at RT. For staining in visible, the revelation was revealed using DAB + (Dako) followed by hematoxylin counterstaining, and sections were mounted using Entellan new mounting medium (Sigma-Aldrich). For fluorescent staining, the fluorescein tyramide kit (PerkinElmer) was used for 10 min and sections were mounted with DAPI Fluoromount-G mounting medium (SouthernBiotech, Birmingham, AL, USA). Stained sections were then scanned using the NanoZoomer2.0HT digital slide scanner (Hamamatsu, Photonics, K.K., Japan) or the SLIDEVIEW VS200 research

Table 1 Antibodies for immunostaining.

Primary antibody	Conjugate	Catalogue number	Dilution†	Secondary antibody*
Lhx8	–	Abcam, ab51519	1:100	ENVISION/HRP
EpCAM	–	Cell Signaling, 93790	1:400	ENVISION/HRP
PGR A/B	–	Cell Signaling, 3153	1:100	ENVISION/HRP
HoxA10	–	Cell ignaling, 58891	1:100	ENVISION/HRP
Integrin β3	–	Affinity, AF6086	1:200	ENVISION/HRP
LIF	–	Affinity, DF13730	1:50	ENVISION/HRP
αSMA	FITC	Sigma, F3777	1:400	–

†Dilution of primary antibody; *Anti-rabbit secondary antibody ENVISION/HRP ready to use.

Downloaded from Bioscientifica.com at 04/18/2024 11:35:24AM
via Open Access. This work is licensed under a Creative Commons Attribution
4.0 International License.
http://creativecommons.org/licenses/by/4.0/

Reproduction (2024) **167** e240019
https://doi.org/10.1530/REP-24-0019

slide scanner (Olympus, Anvers, Belgium) equipped with a UPlan-XApo 20× 0.8 NA objective (Olympus).

Quantification of PGR immunostaining

Image processing and automatic quantification of PGR expression in the endometrium were performed using the image analysis toolbox of MATLAB R2021b according to the following steps: the original images were registered in the full-color red, green, and blue (RGB) space where PGR labeling appeared in red, αSMA in green and DAPI nuclear staining in blue (Fig. 1A). Three regions of interest were drawn manually: (a) the total studied region (b) the external border of the luminal epithelium, and (c) the glands. This allows to decompose the original image into three ones corresponding to the luminal epithelium (Fig. 1B), the glands (Fig. 1C), and the stroma (Fig. 1D). For each image, blue and red components were binarized independently using an automatic threshold (Otsu *et al.* 1979), and the area occupied by the blue and red cells were calculated. Finally, the ratio between red and blue cells was determined (area occupied by red cell/area occupied by blue cells).

Follicle quantification

Fixed ovarian samples were embedded in paraffin and then sectioned into 5 µm thickness pieces. One in every ten sections was stained for LIM-homeobox protein 8 (Lhx8) transcription factor for differential follicle counts. Lhx8 is an oocyte-specific transcription factor that is essential in regulating postnatal folliculogenesis, especially in the earliest stages of primordial follicle activation. It can be used as a biomarker for rapid assessment of follicle pool in the mouse ovary. Scanned sections labeled for Lhx8 were analyzed using the NDP.view2 software (Hamamatsu Photonics K.K., Hamamatsu, Japan). Follicles were classified into primordial, primary, and secondary or more growing according to morphological mouse follicle classification described by Myers *et al.* (Myers *et al.* 2004). Total follicle density was defined as the number of follicles per mm^2 (n/mm^2) after manually calculating the ovarian surface. Results are expressed as the number of each follicle type per mm^2. At least six sections per ovary were quantified blindly. The number of corpora lutea was determined across sections encompassing the eight sections of the ovary to avoid double counting. Raw counts of corpora lutea were not adjusted.

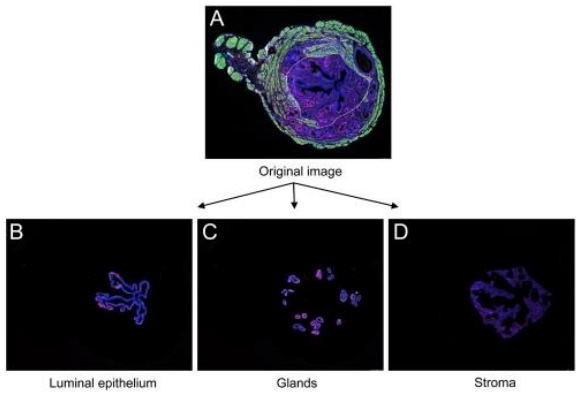


Figure 1

Image processing workflow to quantify endometrial PGR expression in uterus. Original image (A) from the whole scanned image registered in RGB space decomposes in uterine surface epithelium (B), endometrial glands (C), and stroma (D).

Western blot analysis

Follicular development was assessed by Western blot analysis of folliculogenesis factors. One ovary per mouse was used for protein extraction. The protein extraction was performed with radioimmunoprecipitation assay (RIPA) buffer containing 4% of a protease and phosphatase inhibitor (Roche). Lysate was collected, and protein concentrations were determined using a protein assay kit (Bio-Rad Laboratories). Equal amounts of protein (20 µg) were denatured and separated by electrophoresis on SDS–polyacrylamide gels. According to standard procedures, proteins were transferred onto a polyvinylidene difluoride membrane (PerkinElmer). The membrane was then blocked using 5% non-fat milk solution during 2 h on a shaker, then incubated with respective primary antibodies (Cell Signaling), at a dilution of 1/1000, in the blocking solution, overnight at 4°C. Primary antibodies used were anti-FOXL2 (Novus, NB100-1277), anti-BMP15 (Biorbyt, Orb247897), and anti-FSHR (Proteintech, 22665-1-AP). The appropriate horseradish peroxidase-conjugated secondary antibody was added to the membrane, followed by a 1h incubation at RT. After sequential washing of the membranes to remove excess secondary antibodies, signals were detected using an enhanced chemiluminescence (ECL) kit (PerkinElmer) according to the manufacturer's instructions in a LAS4000 imager (Fujifilm, Tokyo, Japan). The intensities of the protein bands were quantified using QuantityOne Analysis software. Data are expressed as the fold-change compared to the control group. HSP70 expression was measured to verify equal loading.

Real-time PCR analysis of mRNA

The expression of *Pgr*, *HoxA10*, integrin β3 (*Itgb3*), and *Lif* mRNA in uterine tissues (one-third of one horn for 3-month-old mice and half horn for 1-month-old mice) was determined by real-time PCR. According to the manufacturer's instructions, RNA from individual mice was isolated using an RNeasy® mini kit (Qiagen). For each sample, 1 µg of RNA was converted to cDNA using the FastGene Scriptase II Ready Mix (Nippon Genetics, Düren, Germany). The quantitative RT-PCR was performed

Downloaded from Bioscientifica.com at 04/18/2024 11:35:24AM
via Open Access. This work is licensed under a Creative Commons Attribution 4.0 International License.
http://creativecommons.org/licenses/by/4.0/

Reproduction (2024) **167** e240019
https://doi.org/10.1530/REP-24-0019

Table 2 Primers for RT-qPCR.

Gene name	GenBank number	Primer sequences (5'–3') Forward	Reverse	Product size (bp)
Pgr	NM_008829.2	CTACTCGCTGTGCCTTACCATG	CTGGCTTTGACTCCTCAGTCCT	139
Hoxa10	NM_008263.4	GGCAGTTCCAAAGGCGAAAAT	GTCTGGTGCTTCGTGTAAGGC	86
Itgb3	NM_016780.2	GGCGTTGTTGTTGGAGAGTC	CTTCAGGTTACATCGGGGTCA	138
Lif	NM_008501.3	GCTGTATCGGATGGTCGCATA	CACAGACGGCAAAGCACATT	156
Gapdh	NM_001289726.2	GGTGGACCTCATGGCCTACA	CTCTCTTGATCAGTGTCCTTGCT	82
Rplp0	NM_007475.5	GGACCCGAGAAGACCTCCTT	GCACATCACTCAGAATTTCAATGG	85

using SYBR Green PCR Master Mix and specific primers (Table 2) in a Fast Real-time PCR (QuantStudio 3, Thermo Fisher Scientific). Relative gene expression was analyzed according to the $2^{-\Delta\Delta Ct}$ method. All samples were assayed in duplicate reactions. The *Rplp0* and *Gapdh* genes were used as housekeeping genes to normalize the expression level, as Lin *et al.* advised for mouse uterus (Lin *et al.* 2013).

Statistical analysis

Statistical analyses were performed using GraphPad Prism software (GraphPad), using a Mann–Whitney test to compare two groups or a two-way ANOVA to calculate the cumulative number of pups over time. All data are presented as mean ± S.E.M. or median with interquartile range. A probability of $P \leq 0.05$ was considered to be statistically significant.

Results

Most female mice develop severe adenomyosis 3 months after neonatal tamoxifen treatment

The grade of adenomyosis was evaluated using criteria previously described by Bird *et al.* (Bird *et al.* 1972). This classification is based on the depth of myometrial infiltration of adenomyotic foci on histological sections by grading the severity according to adenomyotic involvement of the inner third (grade I, superficial adenomyosis), two-thirds (grade II), or entire myometrium (grade III, deep adenomyosis). In our mice model, we observed a disruption and a distortion of the myometrium of all 3-month-old adenomyosis-induced mice. The invasion of the muscle layer by epithelial and/or stromal endometrial cells was observed in 98.53% of neonatally treated females. Contrary to what is observed in mice with adenomyosis, the myometrium of control mice is composed of two well-defined layers without discontinuity (Fig. 2A). Immunofluorescence analysis of EpCAM co-staining with αSMA allowed us to determine the percentage of each 3-month-old mouse by stage of disease. Only 1.47% of treated mice did not develop adenomyosis. 2.94% and 4.41% have grade I and II adenomyosis, respectively (Fig. 2B, C, and E). Most of the mice (91.18%) are affected by grade III adenomyosis (Fig. 2D and E), which confirmed the successful establishment of the mouse adenomyosis model. The grade of adenomyosis was not assessed using these criteria in 1-month-old mice because of the thin myometrium at this age. In this case, we only considered the presence or absence of myometrial invasion. All 1-month-old tamoxifen-treated mice have developed myometrial disruption (data not shown).

Adenomyosis-induced mice present disrupted estrous cyclicity

To study the potential effects of adenomyosis on estrous cyclicity, daily vaginal smears were performed two months after birth in each group of mice (the adenomyosis-induced group and the control group). The smears were collected for 14 consecutive days to assess estrous cycles (Fig. 3A). Adenomyosis-induced

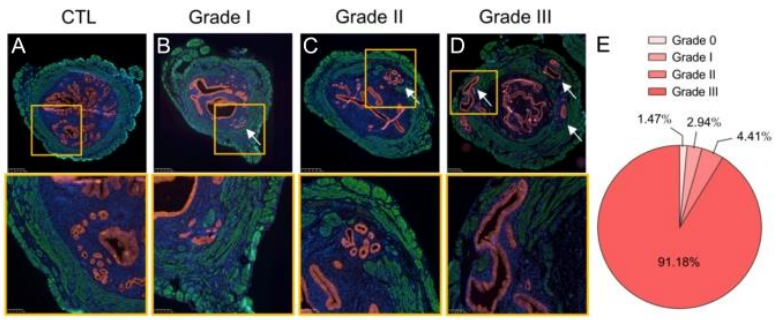


Figure 2

Classification of adenomyosis progression in an experimentally induced mouse model. Representative microscopic images of the uterus from (A) untreated mice, (B) grade I, (C) grade II, and (D) grade III adenomyosis. Red staining = EpCAM; green staining = αSMA; blue staining = DAPI. The arrow marks the ectopic endometrium. (E) Pie chart representing the proportion of mice who have developed adenomyosis with grade 0, I, II, or III.

Downloaded from Bioscientifica.com at 04/18/2024 11:35:24AM
via Open Access. This work is licensed under a Creative Commons Attribution 4.0 International License.
http://creativecommons.org/licenses/by/4.0/

Reproduction (2024) **167** e240019
https://doi.org/10.1530/REP-24-0019

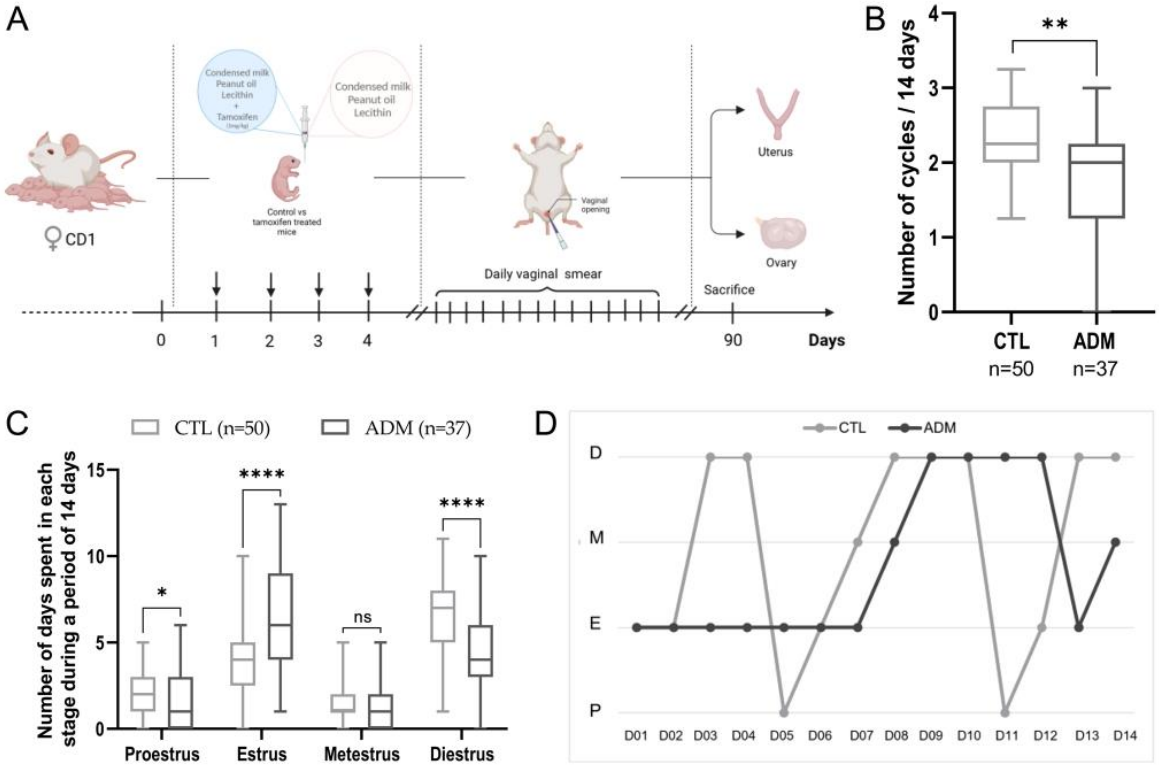


Figure 3

Impact of adenomyosis on estrous cycles. (A) Schematic diagram of the experiment performed on adenomyosis-induced mice model to assess estrous cyclicity. (B) Graph representing the number of cycles during 14 days in tamoxifen-treated mice compared to control mice. (C) Effects of tamoxifen treatment on total number of days spent in each stage during the same period. (D) Representative estrous cycles of control and treated mice as measured by vaginal cytology at 2 months of age (P, pro-estrus; E, estrus; M, metestrus; D, diestrus). The values are the median with the interquartile range. Statistical significance (Mann–Whitney test): *$P \leq 0.05$; **$P \leq 0.01$; ****$P \leq 0.0001$; ns, non-significant.

females underwent less regular cycles than control mice ($P = 0.0012$) (Fig. 3B). Furthermore, a significant increase in the percentage of days spent in estrus ($P \leq 0.0001$) and a concomitant decrease in the rate of days spent in proestrus ($P = 0.0466$) and diestrus ($P \leq 0.0001$) phase was observed in adenomyosis-induced mice (Fig. 3C). As represented in Fig. 3D, mice with adenomyosis exhibited a prolonged estrous cycle compared to control mice, mainly due to the increased duration of the estrus phase. These data suggested that adenomyosis negatively impacts estrous cyclicity.

Adenomyosis-induced mice show impaired ovarian follicle development

To determine if the disruption in estrous cyclicity was related to altered follicular development, we first analyzed the ovaries of 3-month-old mice. There were no apparent differences in ovarian weight ($P = 0.1411$) and surface area on histological sections ($P = 0.4397$) between adenomyosis-induced and control mice (Fig. 4A and B). Nevertheless, follicular quantification analyses after Lhx8 immunodetection on ovarian sections reveal a reduction in the total number of primordial ($P = 0.0356$), primary ($P = 0.0393$) and secondary or more growing follicles ($P = 0.0407$) per mm^2 in adenomyosis-induced ovaries (Fig. 4D and E) compared to control ones (Fig. 4C and E). No difference in the number of corpora lutea ($P = 0.0862$) was observed (Fig. 4F). To further investigate how folliculogenesis was impaired in mice affected by adenomyosis, we performed western blot analysis to evaluate the expression of three crucial oocyte-derived factors involved in follicular development: BMP15, FOXL2, and FSHR. The protein levels of all these factors were lower in adenomyosis mice compared with control (FOXL2, $P = 0.0499$; FSHR, $P = 0.0044$; BMP15, $P = 0.0207$; Fig. 5A, B, and C). Both histological and protein analysis suggest that adenomyosis may impair follicle development and reduce ovarian reserve despite preserved ovulation. Adenomyosis-related infertility could therefore be linked to reduced oocyte quality or embryo implantation defects.

Downloaded from Bioscientifica.com at 04/18/2024 11:35:24AM
via Open Access. This work is licensed under a Creative Commons Attribution
4.0 International License.
http://creativecommons.org/licenses/by/4.0/

Reproduction (2024) **167** e240019
https://doi.org/10.1530/REP-24-0019

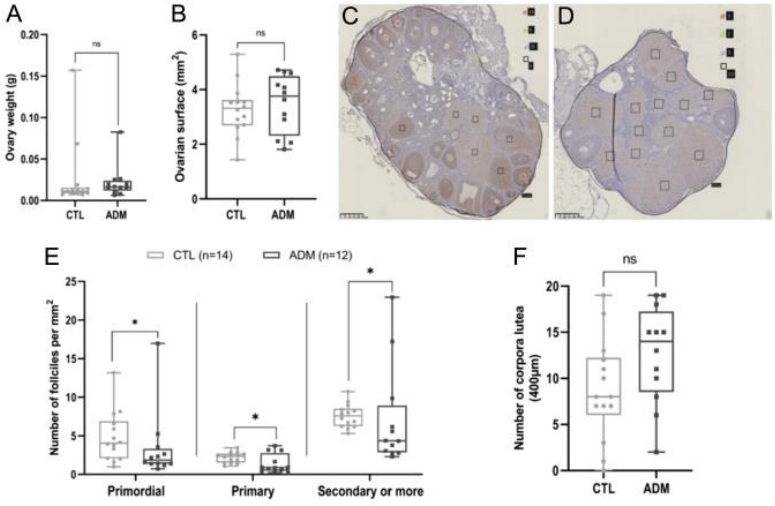


Figure 4

Comparison of ovarian weight, surface, and follicle density between control mice and adenomyosis-induced mice. Comparison of ovary weight (A) and surface (B) between control and mice with adenomyosis. Representative images of Lhx8 staining of (C) control and (D) adenomyosis-induced mice ovaries. Red pins indicate primordial follicles, green pins primary follicles, blue pins secondary or more growing follicles and black rectangle corpora lutea. Follicle density was expressed as the total number of each follicle type per mm² (E). The number of corpora lutea was evaluated on ovarian section of 400 µm (F). The values are the median with the interquartile range. Statistical significance; ns, non-significant; *$P \leq 0.05$.

Adenomyosis causes female subfertility

To further investigate the effect of adenomyosis on fertility, 3-month-old CD1 control and adenomyosis-induced mice were pair-bred with sexually mature (8-week-old) males continuously for 3 months. The number of females giving birth, the mean number of litters and average litter sizes were recorded (Fig. 6A). During this period, 100% of control females have given birth at least once, while only 33.33% of mice in the pathology-induced group delivered (Fig. 6B). In addition, compared with controls, females affected by adenomyosis had reduced litter numbers ($P = 0.0065$) and sizes (Figs 6C and D). Indeed, control mice gave birth to an average of 12.94 ± 0.98 pups, while the average litter size of adenomyosis-induced mice was 6.33 ± 1.20 ($P = 0.0155$) (Fig. 6D). These numbers include only pups that are still alive at weaning. The cumulative number of pups per dam indicates a lower number in the adenomyosis-induced group than in the control group, starting after month 1 of mating ($P = 0.0007$) and persisting until the end of the experiment ($P = 0.0003$) (Fig. 6E).

Progesterone resistance is a potential mechanism leading to adenomyosis-related infertility

To assess progesterone responsiveness in the uterus of adenomyosis-induced mice, we examined progesterone

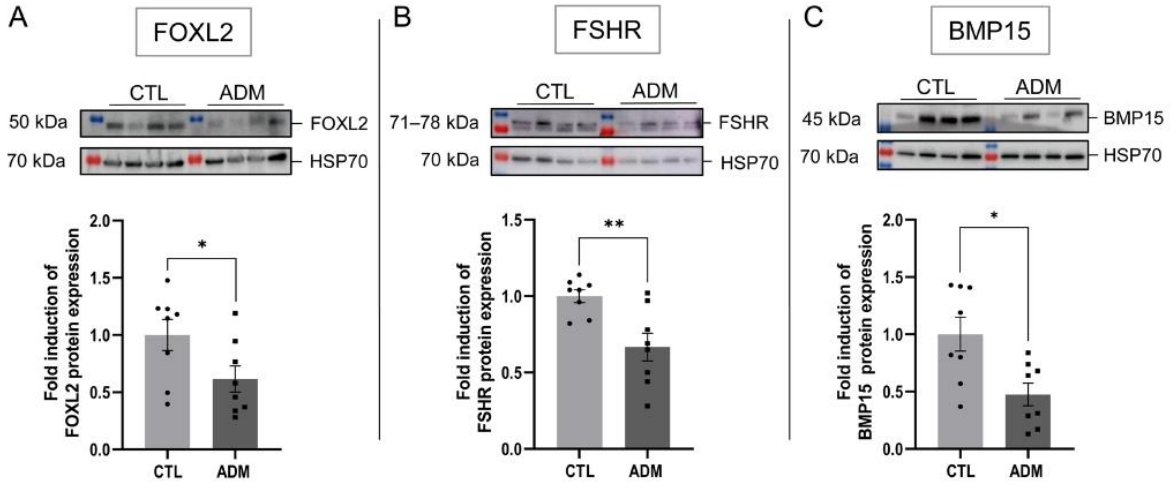


Figure 5

Comparison of ovarian follicle development between control and adenomyosis-induced mice. Representative immunoblots and quantification of FOXL2 (A), FSHR (B), and BMP15 (C) expression in uterus of control and adenomyosisinduced mice. Control group: $n = 8$; adenomyosis group: $n = 8$. The data are mean ± S.E.M.; *$P \leq 0.05$; **$P \leq 0.01$.

Downloaded from Bioscientifica.com at 04/18/2024 11:35:24AM
via Open Access. This work is licensed under a Creative Commons Attribution 4.0 International License.
http://creativecommons.org/licenses/by/4.0/

Reproduction (2024) **167** e240019
https://doi.org/10.1530/REP-24-0019

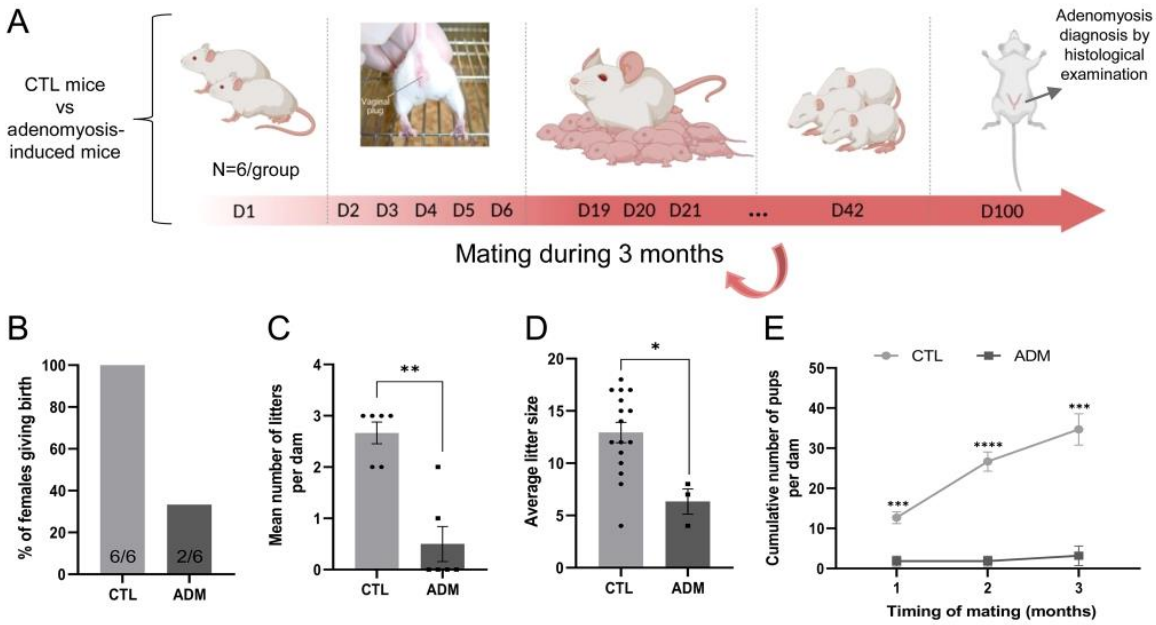


Figure 6

Impact of adenomyosis on fertility outcomes. Schematic diagram of the mating experiment to evaluate how fertility is affected in adenomyosis-induced mice (A). Reduction of the number of pregnant females (B) as well as the litter number (C), litter size (D), and cumulative number of pups (E) of adenomyosis-induced mice. The values are the mean ± S.E.M. Statistical significance (Mann–Whitney test or two-way ANOVA): *$P \leq 0.05$; **$P \leq 0.01$; ***$P \leq 0.001$; ****$P \leq 0.0001$.

receptor expression in the eutopic endometrium of the two groups of mice by immunofluorescence. We observed that PGR was expressed in the stromal and epithelial luminal and glandular cell nuclei (Fig. 7A). The results indicate a reduced proportion of PGR-positive stromal ($P = 0.0048$) and glandular ($P = 0.0178$) cells in eutopic endometrium of 3-month-old adenomyosis-induced mice than in control mice. Nevertheless, no difference in PGR expression in luminal epithelial cells was observed (Fig. 7B). The *Pgr* gene expression analysis of entire uteri from 3-month-old mice confirmed the results obtained by immunofluorescence. The progesterone receptor was lower expressed in the uteri of adenomyosis-induced mice compared to control mice ($P = 0.0101$) (Fig. 7C). It can be inferred that subfertility in mice with adenomyosis may be caused by progesterone resistance.

Adenomyosis impairs endometrial receptivity and implantation

The expression of implantation-related markers was measured to explore the mechanisms leading to impaired endometrial receptivity and implantation caused by adenomyosis. The results indicated a reduction of endometrial receptivity-related genes in the 1-month-old mice of the adenomyosis group. In this group, we observed a significant decrease in the expression of *HoxA10* ($P = 0.0011$) and integrin β3 ($P = 0.0002$) mRNA levels in comparison to those in the control group. Those reduced levels of expression are maintained over time for *HoxA10* ($P = 0.0433$) but not for integrin β3 ($P = 0.2110$) (Fig. 8A, B, and C). The IHC staining of these implantation-related markers confirmed the decreased protein expression in the adenomyosis group but also revealed differences in localization. Indeed, *HoxA10* is mainly located in endometrial luminal epithelial cells and glandular epithelial cells. On the contrary, control mice do not express *HoxA10* in epithelial endometrial cells but rather in stromal cells (Fig. 8D). IHC staining of integrin β3 revealed no significant difference between the healthy and adenomyosis mice groups (Fig. 8D). Surprisingly, the uterine mRNA expression of *Lif* was increased in 1-month-old adenomyosis-induced mice (1 month: $P = 0.0056$; 3 months: $P = 0.0630$) (Fig. 8C). These results were confirmed by IHC analysis, which showed an apparent increase in *Lif* expression levels in the glandular and luminal epithelium of the endometrium of mice with adenomyosis compared with control mice (Fig. 8D). Taken altogether, these results suggested that adenomyosis may alter endometrial receptivity through downregulation of implantation-related genes.

Downloaded from Bioscientifica.com at 04/18/2024 11:35:24AM
via Open Access. This work is licensed under a Creative Commons Attribution
4.0 International License.
http://creativecommons.org/licenses/by/4.0/

Reproduction (2024) **167** e240019
https://doi.org/10.1530/REP-24-0019

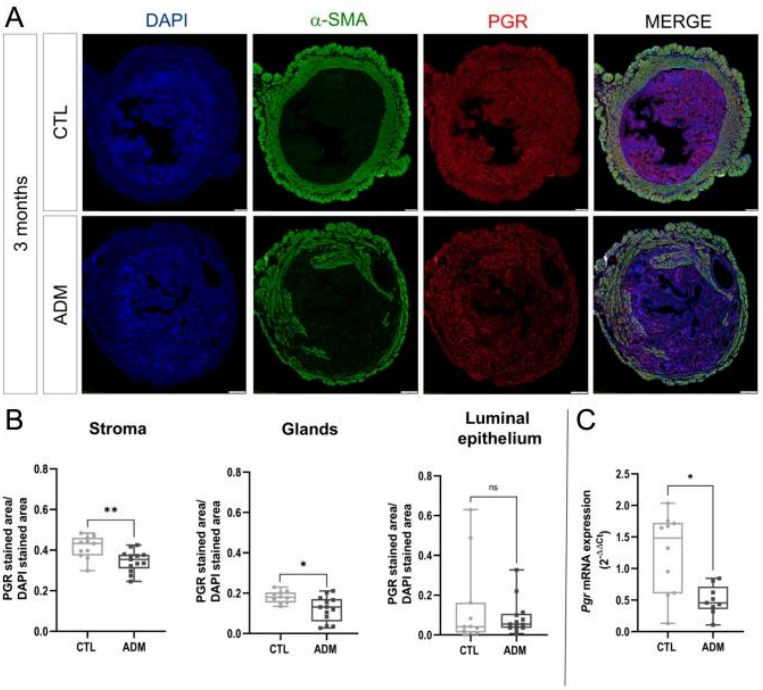


Figure 7

Progesterone receptor (PGR) expression in the uteri of control and adenomyosis-induced mice. Immunofluorescence (A) and computer-assisted quantification (B) of PGR expression in the uteri of 3-month-old control and adenomyosis-induced mice. Bar scale = 200 µm. The mRNA expression levels of Pgr were also assessed (C). The values are the median with the interquartile range. Statistical significance (Mann–Whitney test): $*P \leq 0.05$; $**P \leq 0.01$; ns, non-significant.

Discussion

The results of this study shed light on the complex relationship between adenomyosis and female reproductive health, encompassing disease severity, estrous cyclicity, ovarian follicle development, fertility, progesterone responsiveness, and endometrial receptivity. These findings contribute to a better understanding of the potential mechanisms underlying adenomyosis-related infertility and the multifactorial impact of this condition.

The analysis of the severity of the adenomyosis induced in our mouse model revealed a high incidence of deep adenomyosis, with over 90% of the treated mice exhibiting grade III adenomyosis. Unlike the well-defined myometrial layers in the healthy uterus, the affected mice displayed a disruption and distortion of the myometrium due to the invasion of epithelial and stromal endometrial cells. Furthermore, all 3-month-old mice developed diffuse adenomyosis. According to Park *et al.*, symptoms experienced by women with diffuse adenomyosis are more pronounced than those with focal adenomyosis (Park *et al.* 2016). This extensive myometrial disruption is also described in human uteri affected by adenomyosis. Those results ensure the successful establishment of the model and its value in simulating the human condition without any associated comorbidities (Upson & Missmer 2020, Loring *et al.* 2021).

In women with adenomyosis, abnormal levels of free radicals have been found in the uterine cavity, which can also negatively impact oocyte quality and inhibit embryo development and implantation, resulting in reduced pregnancy rates (Barroso *et al.* 1998, Harada *et al.* 2016, Vercellini *et al.* 2014). While endometriosis and adenomyosis share similarities, research on the involvement of these mechanisms in adenomyosis is limited (Maruyama *et al.* 2020). Recent studies have primarily focused on endometrial receptivity and function (Hiraoka *et al.* 2023), with little investigation into folliculogenesis and menstrual cycles. In our model, adenomyosis-induced mice displayed disrupted estrous cyclicity, characterized by irregular cycles and prolonged periods in the estrus phase. Furthermore, our analysis of ovarian follicular yield revealed a significant reduction in primordial, primary, and secondary or more growing follicles per unit area in adenomyosis-induced mice compared to controls. In addition to the impact of adenomyosis on folliculogenesis and ovarian reserve, ovarian function may also be impaired. The reduced expression of critical oocyte-derived factors, including Foxl2, BMP15, and FSHR, further indicates ovarian dysfunction in adenomyosis. Several studies have shown that female mice with a deletion of these genes experience subfertility (Desai *et al.* 2013, Abir *et al.* 2014, Zhou *et al.* 2022). In our study, reduced expression of these genes in the ovaries of mice with adenomyosis could partially explain the observed fertility outcomes in the mice model, with only 33.33% of the experimental group giving birth compared to 100% in the control group. The mice with adenomyosis had smaller litter sizes and reduced number of litters. The cumulative number of pups born from adenomyosis-affected mice

Downloaded from Bioscientifica.com at 04/18/2024 11:35:24AM
via Open Access. This work is licensed under a Creative Commons Attribution 4.0 International License.
http://creativecommons.org/licenses/by/4.0/

Reproduction (2024) **167** e240019
https://doi.org/10.1530/REP-24-0019

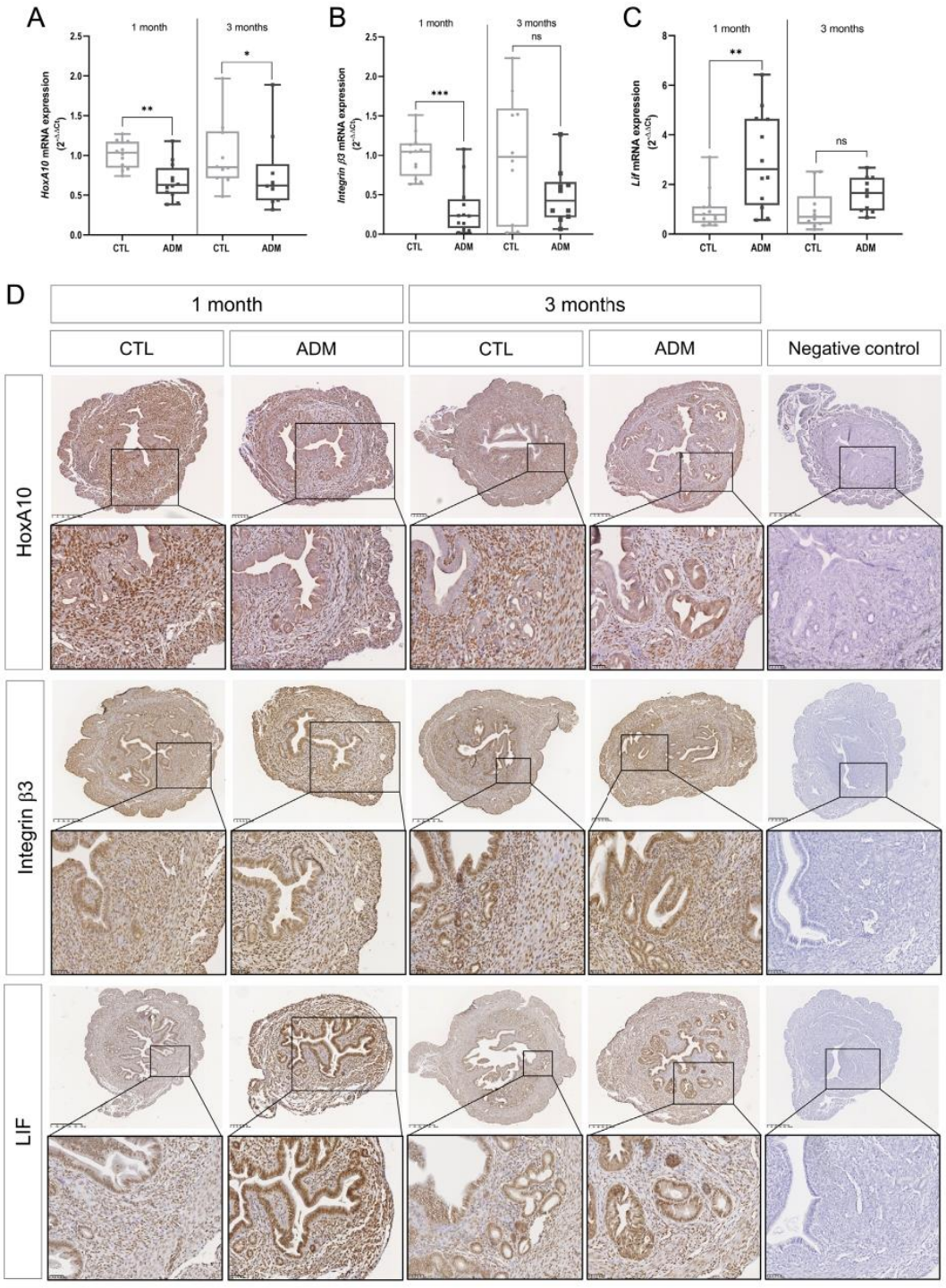


Figure 8

Implantation-related markers expression in the uteri of healthy and adenomyosis-induced mice. The mRNA expression levels of *HoxA10* (A), *Itgb3* (B), and *Lif* (C) in the uteri of 1-month-old and 3-month-old control and adenomyosis-induced mice. Representative immunohistochemistry of *HoxA10*, Itgb3, and *Lif* uterine expression (D). The values are the median with the interquartile range. Statistical significance (Mann–Whitney test): *$P \leq 0.05$; **$P \leq 0.01$; ***$P \leq 0.001$; ns, non-significant.

Downloaded from Bioscientifica.com at 04/18/2024 11:35:24AM
via Open Access. This work is licensed under a Creative Commons Attribution
4.0 International License.
http://creativecommons.org/licenses/by/4.0/

Reproduction (2024) **167** e240019
https://doi.org/10.1530/REP-24-0019

was, indeed, consistently lower throughout the mating period. These findings align with clinical observations of decreased fertility in women with adenomyosis highlighting the profound impact of the condition on reproductive outcomes (Liang *et al.* 2022).

An essential role of the ovaries is to produce sex hormones in response to stimulation from the pituitary gland. Estrogens and progesterone are key hormones that regulate healthy endometrium physiology and are essential for creating a microenvironment conducive to embryo implantation. Adenomyosis is thought to be caused by an imbalance in hormonal signaling between these two hormones (Rossi *et al.* 2022, Vannuccini & Petraglia 2022). Although hyperestrogenism is commonly cited as a significant factor in the development of adenomyosis, few studies have investigated the role of progesterone resistance in adenomyosis-related infertility (Vannuccini & Petraglia 2022, d'Argent *et al.* 2023). One proposed molecular cause of progesterone resistance is a reduced expression of progesterone receptors, found in endometriotic lesions and eutopic endometrium from women with endometriosis (Nie *et al.* 2009, Shen *et al.* 2015, Wölfler *et al.* 2016). This endometrial progesterone unresponsiveness may negatively influence both the proliferation of endometrial cells and the decidualization of stromal cells, leading to both lesion growth and a non-receptive endometrium (Maclean & Hayashi 2022, Zhang & Wang 2023). In our mice affected by adenomyosis, the PGR expression was reduced in the stromal and glandular cells of the uterus of 3-month-old mice affected by adenomyosis. This finding suggests that it could be a potential mechanism leading to adenomyosis-related infertility, which was previously observed in the study of Mehasseb *et al.* (Mehasseb *et al.* 2011). Additionally, their research revealed that women with adenomyosis exhibit an inadequate response to progesterone during the secretory phase, leading to an estrogen-driven hyperproliferation of endometrium due to an insufficient response to progesterone. By analyzing the expression of PGR in uterine stromal cells from 1-month-old mice (Supplementary Data, Fig. 1, see section on supplementary materials given at the end of this article), we indirectly investigate whether progesterone resistance plays a role in adenomyosis at an earlier stage of the disease. At 1 month of age, the mice respond appropriately to progesterone signaling, suggesting that progesterone unresponsiveness appears later in disease progression. Impaired progesterone responsiveness could contribute to endometrial dysfunction and the subsequent reduction in endometrial receptivity, vital for implantation and successful pregnancy. This phenomenon warrants further investigation to understand its mechanistic underpinnings and clinical implications. Further studies are needed to confirm progesterone resistance in this mice model, notably through evaluating the response of endometrial cells to progesterone stimulation.

Adenomyosis can also impair endometrial receptivity, a disorder associated with a lack of adequate expression of adhesion molecules, reduced expression of implantation markers, and altered function of genes involved in embryonic development (Vannuccini *et al.* 2017). Our analysis of implantation-related markers during the estrous phase revealed decreased *HoxA10* and *Itgb3* mRNA levels in adenomyotic uteri, particularly in 1-month-old mice. The reduction of *HoxA10* expression continued over time. Interestingly, the homeobox gene, known to be involved in the development of the female genital tract during the embryonic period and in regulating endometrial receptivity in adulthood, is a target of progesterone (Du & Taylor 2016). Decreased *HoxA10* endometrial expression correlates with lower endometrial receptivity, leading to reduced implantation rates (Zanatta *et al.* 2010). In previously published studies with adenomyosis-induced mice, *HoxA10* expression was assessed and shown to decrease during the implantation window when the endometrium is receptive to the embryo (Guo *et al.* 2018, Guan *et al.* 2022). Our present study provides evidence that *HoxA10* is decreased outside the implantation window, and the expression levels could be insufficient to ensure effective implantation and therefore successful pregnancy.

Epigenetic changes are thought to be responsible for reduced expression of progesterone receptor and homeobox genes in endometriosis (Wu *et al.* 2005, 2006). Further studies are needed to determine whether these epigenetic changes are also accountable for progesterone resistance and reduced *HoxA10* expression in adenomyosis. The transcription factor *HoxA10*, in response to progesterone, can enhance integrin *β*3 expression during the luteal phase of menstrual cycle (Joshi *et al.* 2021). Integrin β3 is a cell adhesion molecule indispensable for successful implantation during uterine receptivity and therefore overexpressed in the endometrium during the receptive window (Lessey *et al.* 1994). Just as with the analysis of *HoxA10*, we similarly observed a decrease in the gene expression of integrin β3 in the uteri of 1-month-old mice with adenomyosis when compared to the control group during the estrous phase, mirroring what was observed during the implantation window in mice induced for adenomyosis (Guo *et al.* 2018, Guan *et al.* 2022). For patients undergoing ART, analysis of endometrial integrin β3 expression is critical, as it has been shown that ART is less effective if the endometrial level of integrin β3 is low (Joshi *et al.* 2021). Another essential key factor for embryo implantation is *Lif*. This cytokine has multiple roles: it influences endometrial receptivity, affects trophoblastic function, and participates in placental vascular formation (Xu *et al.* 2012). Our data indicate a significant increase in *Lif* expression in the uterus of adenomyosis-induced mice during the estrus phase of the estrous cycle. This result contrasts those found in previous works reporting lower *Lif* expression in the endometrium of mice or women with adenomyosis during the implantation

Downloaded from Bioscientifica.com at 04/18/2024 11:35:24AM
via Open Access. This work is licensed under a Creative Commons Attribution 4.0 International License.
http://creativecommons.org/licenses/by/4.0/

Reproduction (2024) **167** e240019
https://doi.org/10.1530/REP-24-0019

window, potentially explaining the low implantation rate in these experimental groups (Yen *et al.* 2017*b*, Guo *et al.* 2018). In our results, the increase in *Lif* mRNA expression could suggest a compensatory response that may reflect the uterus' attempt to counteract the diminished implantation markers such as *HoxA10* and integrin β3. A study on adenomyosis-derived organoids showed the same trend as that in our adenomyosis mice, i.e. increased *Lif* expression (Juárez-Barber *et al.* 2022). The authors hypothesized that *Lif* could play a role not only in the implantation process but also in epithelial–mesenchymal transition through the regulation of the Wnt/b-catenin pathway (Rosario & Stewart 2016, Juárez-Barber *et al.* 2022). These findings are crucial for understanding the various mechanisms involved in the physiopathology of adenomyosis and associated symptoms such as infertility and thus finding suitable therapeutic regimens. In our study, the expression of implantation-related markers was evaluated outside the implantation window, revealing dysregulation of these genes before any potential pregnancy.

This study's major challenge was identifying whether all the described effects are the consequence of adenomyosis or caused by neonatal tamoxifen treatment. Neonatal treatment with tamoxifen (TAM) has been used extensively for examining adenomyosis pathogenesis and drug screening (Parrott *et al.* 2001, Yen *et al.* 2017*a*, Marquardt *et al.* 2020). While it is true that TAM could impair adult rodent ovarian function, results from the literature are controversial. TAM administration in adult mice did not affect the number of primordial and primary follicles but decreased the number of growing follicles (Akduman *et al.* 2014). TAM was also shown to activate dormant primordial follicles transiently (Wei *et al.* 2022). No alteration of the follicle number or prevalence of granulosa apoptosis was found in rats (Nynca *et al.* 2023). These results do not reflect the neonatal TAM treatment to induce adenomyosis in mice. To our knowledge, no study has demonstrated the negative effect of neonatal tamoxifen administration on ovarian function. Interestingly, TAM-treated breast cancer survivors did not have decreased ovarian reserve compared to TAM non-users (Shandley *et al.* 2017). Therefore, the direct or indirect impacts of observed alterations on fertility reduction remain unanswered. Nevertheless, adenomyosis has been reported in 60% of postmenopausal women taking tamoxifen therapy for an extended period, suggesting the promotional effect of tamoxifen in establishing adenomyosis lesions (Harada *et al.* 2016). We are confident in the fact most features found in women suffering from adenomyosis, such as the decrease in menstrual cycle length, the earlier age of the menarche, and the effect on ovarian reserve are reflected in the murine model (Templeman *et al.* 2008, Guo *et al.* 2018).

In conclusion, our study provides insights into adenomyosis' impact on female reproductive health. The disrupted estrous cyclicity, the compromised ovarian follicle development, the reduced fertility and progeny, the decreased expression of endometrial progesterone receptor and receptivity-related genes collectively suggest a potential contribution to the subfertility observed in adenomyosis. These findings underscore the need for further research into the mechanisms underlying these effects and the potential development of targeted interventions to improve fertility outcomes in women affected by adenomyosis.

Supplementary materials
This is linked to the online version of the paper at https://doi.org/10.1530/REP-24-0019.

Declaration of interest
The funders had no role in the design of the study; in the collection, analyses, or interpretation of data; in the writing of the manuscript; or in the decision to publish the results.

Funding
This research was funded by the Fonds de la Recherche Scientifique – (F.R.S.-FNRS, Belgium), grant number T.0171.21 and J.0143.22, the Foundation Léon Fredericq (University of Liège), grant number FSR-F-2022-FM.

Author contribution statement
Conceptualization, C.M. and M.S.; methodology, C.M. and M.S.; validation, M.S., J.V and C.M.; formal analysis, investigation, M.S., J.V., S.B., J.B., and L.B.; resources, M.S., J.V., J.B., L.B., and C.M., writing – original draft preparation, M.S. and C.M.; writing – review and editing, M.S., C.M., J.B., L.B., M.N., and J.V.; supervision, C.M., project administration, M.S., J.V., and C.M.; funding acquisition, C.M. and M.N. All authors read and agreed to the final version of the manuscript.

Acknowledgements
The authors acknowledge Emilie Feyereisen, Isabelle Dasoul, Erika Kondarawski, and Nathalie Lefin for their excellent technical assistance.

References

Abbott JA 2017 Adenomyosis and abnormal uterine bleeding (AUB-A)—pathogenesis, diagnosis, and management. *Best Practice and Research* **40** 68–81. (https://doi.org/10.1016/j.bpobgyn.2016.09.006)

Abir R, Fisch B & Johnson MH 2014 BMP15, fertility and the ovary. *Reproductive Biomedicine Online* **29** 525–526. (https://doi.org/10.1016/j.rbmo.2014.09.007)

Akduman AT, Özerkan K, Zik B, Peker S, Avcı B & Ata B 2014 Effect of tamoxifen on ovarian reserve: a randomized controlled assessor-blind trial in a mouse model. *Journal of the Turkish German Gynecological Association* **15** 228–232. (https://doi.org/10.5152/jtgga.2014.14166)

Barroso RP, Osuamkpe C, Nagamani M & Yallampalli C 1998 Nitric oxide inhibits development of embryos and implantation in mice. *Molecular Human Reproduction* **4** 503–507. (https://doi.org/10.1093/molehr/4.5.503)

Bird CC, McElin TW & Manalo-Estrella P 1972 The elusive adenomyosis of the uterus-revisited. *American Journal of Obstetrics and Gynecology* **112** 583–593. (https://doi.org/10.1016/0002-9378(72)90781-8)

Downloaded from Bioscientifica.com at 04/18/2024 11:35:24AM
via Open Access. This work is licensed under a Creative Commons Attribution 4.0 International License.
http://creativecommons.org/licenses/by/4.0/

Byers SL, Wiles MV, Dunn SL & Taft RA 2012 Mouse estrous cycle identification tool and images. *PLoS One* **7** e35538. (https://doi.org/10.1371/journal.pone.0035538)

Caligioni C 2010 Study of estrous cyclicity in aging C57BL / 6J I. Cycle frequency, length and vaginal Cytology1 mice: of san at the. *Current Protocols in Neuroscience* 1–11.

d'Argent M, Stratopoulou CA, Cussac S, Camboni A, Jadoul P, Donnez J & Dolmans MM 2023 Are lower levels of apoptosis and autophagy behind adenomyotic lesion survival? *Reproductive Biomedicine Online* **47** 103248. (https://doi.org/10.1016/j.rbmo.2023.06.003)

Desai SS, Roy BS & Mahale SD 2013 Mutations and polymorphisms in FSH receptor: functional implications in human reproduction. *Reproduction* **146** R235–R248. (https://doi.org/10.1530/REP-13-0351)

Donnez J, Donnez O, Tourniaire J, Brethous M, Bestel E, Garner E, Charpentier S, Humberstone A & Loumaye E 2021 Uterine adenomyosis Treated by Linzagolix, an Oral gonadotropin-releasing hormone receptor Antagonist: a Pilot Study with a New hit Hard First and Then Maintain Regimen of Administration. *Journal of Clinical Medicine* **10** 1–13. (https://doi.org/10.3390/jcm10245794)

Du H & Taylor HS 2016 The Role of Hox Genes in Female Reproductive Tract development, adult function, and fertility. *Cold Spring Harbor Perspectives in Medicine* **6** a023002. (https://doi.org/10.1101/cshperspect.a023002)

Juárez-Barber E, Francés-Herrero E, Corachán A, Vidal C, Giles J, Alamá P, Faus A, Pellicer A, Cervelló I & Ferrero I 2022 Establishment of adenomyosis organoids as a preclinical model to study infertility. *Journal of Personalized Medicine* **12** 219. (https://doi.org/10.3390/jpm12020219)

Green AR, Styles JA, Parrott EL, Gray D, Edwards RE, Smith AG, Gant TW, Greaves P, Al-Azzawi F & White IN 2005 Neonatal tamoxifen treatment of mice leads to adenomyosis but not uterine cancer. *Experimental and Toxicologic Pathology* **56** 255–263. (https://doi.org/10.1016/j.etp.2004.10.001)

Guan X, Liu D, Zhou H, Dai C, Wang T, Fang Y, Jia Y & Li K 2022 Melatonin improves pregnancy outcomes in adenomyosis mice by restoring endometrial receptivity via NF-KB/apoptosis signaling. *Annals of Translational Medicine* **10** 1317–1317. (https://doi.org/10.21037/atm-22-5493)

Guo S, Li Z, Yan L, Sun Y & Feng Y 2018 GnRH agonist improves pregnancy outcome in mice with induced adenomyosis by restoring endometrial receptivity. *Drug Design, Development and Therapy* **12** 1621–1631. (https://doi.org/10.2147/DDDT.S162541)

Harada T, Khine YM, Kaponis A, Nikellis T, Decavalas G & Taniguchi F 2016 The impact of adenomyosis on women's fertility. *Obstetrical and Gynecological Survey* **71** 557–568. (https://doi.org/10.1097/OGX.0000000000000346)

Hiraoka T, Hirota Y & Osuga Y 2023 How does adenomyosis impact endometrial receptivity? An updated systematic review of clinical and molecular insights. *F and S Reviews* **4** 15–25. (https://doi.org/10.1016/j.xfnr.2022.11.004)

Joshi NR, Kohan-Ghadr H, Roqueiro DS, Yoo JY, Fru K, Hestermann E, Yuan L, Ho S, Jeong J, Young SL, *et al.* 2021 Genetic and epigenetic changes in the eutopic endometrium of women with endometriosis: association with decreased endometrial Avβ3integrin expression. *Molecular Human Reproduction* **27** 1–4. (https://doi.org/10.1093/molehr/gaab018)

Lessey BA, Castelbaum AJ, Sawin SW, Buck CA, Schinnar R, Bilker W & Strom BL 1994 Aberrant integrin expression in the endometrium of women with endometriosis. *Journal of Clinical Endocrinology and Metabolism* **79** 643–649. (https://doi.org/10.1210/jcem.79.2.7519194)

Levgur M, Abadi MA & Tucker A 2000 Adenomyosis: symptoms, histology, and pregnancy terminations. *Obstetrics and Gynecology* **95** 688–691. (https://doi.org/10.1016/s0029-7844(99)00659-6)

Liang T, Zhang W, Pan N, Han B, Li R & Ma C 2022 Reproductive outcomes of in vitro fertilization and fresh embryo transfer in infertile women with adenomyosis: a retrospective cohort study. *Frontiers in Endocrinology* **13** 865358. (https://doi.org/10.3389/fendo.2022.865358)

Lin PF, Lan X, Chen F, Yang Y, Jin Y & Wang A 2013 Reference gene selection for real-time quantitative PCR analysis of the mouse uterus in the peri-implantation period. *PLoS One* **8** e62462. (https://doi.org/10.1371/journal.pone.0062462)

Loring M, Chen TY & Isaacson KB 2021 A systematic review of adenomyosis: it is time to reassess what we thought we knew about the disease. *Journal of Minimally Invasive Gynecology* **28** 644–655. (https://doi.org/10.1016/j.jmig.2020.10.012)

Maclean JA & Hayashi K 2022 Progesterone actions and resistance in gynecological disorders. *Cells* **11**. (https://doi.org/10.3390/cells11040647)

Marquardt RM, Jeong JW & Fazleabas AT 2020 Animal models of adenomyosis. *Seminars in Reproductive Medicine* **38** 168–178. (https://doi.org/10.1055/s-0040-1718741)

Maruyama S, Imanaka S, Nagayasu M, Kimura M & Kobayashi H 2020 Relationship between adenomyosis and endometriosis; different phenotypes of a single disease? *European Journal of Obstetrics, Gynecology, and Reproductive Biology* **253** 191–197. (https://doi.org/10.1016/j.ejogrb.2020.08.019)

Mehasseb MK, Panchal R, Taylor AH, Brown L, Bell SC & Habiba M 2011 Estrogen and progesterone receptor isoform distribution through the menstrual cycle in uteri with and without adenomyosis. *Fertility and Sterility* **95** 2228–2235.e1. (https://doi.org/10.1016/j.fertnstert.2011.02.051)

Myers M, Britt KL, Wreford NG, Ebling FJ & Kerr JB 2004 Methods for quantifying follicular numbers within the mouse ovary. *Reproduction* **127** 569–580. (https://doi.org/10.1530/rep.1.00095)

Nie J, Lu Y, Liu X & Guo SW 2009 Immunoreactivity of progesterone receptor Isoform B, nuclear factor KB, and IκBα in adenomyosis. *Fertility and Sterility* **92** 886–889. (https://doi.org/10.1016/j.fertnstert.2009.01.084)

Nynca A, Swigonska S, Molcan T, Petroff BK & Ciereszko RE 2023 Molecular action of tamoxifen in the ovaries of rats with mammary neoplasia. *International Journal of Molecular Sciences* **24**. (https://doi.org/10.3390/ijms242115767)

Otsu N, *et al.* 1979 Otsu_1979_otsu_method. *IEEE Transactions on Systems, Man, and Cybernetics Part C* **1** 62–66.

Park CW, Choi MH, Yang KM & Song IO 2016 Pregnancy rate in women with adenomyosis undergoing fresh or frozen embryo transfer cycles following gonadotropin-releasing hormone agonist treatment. *Clinical and Experimental Reproductive Medicine* **43** 169–173. (https://doi.org/10.5653/cerm.2016.43.3.169)

Parrott E, Butterworth M, Green A, White IN & Greaves P 2001 Adenomyosis: a result of disordered stromal differentiation. *American Journal of Pathology* **159** 623–630. (https://doi.org/10.1016/S0002-9440(10)61733-6)

Puente JM, Fabris A, Patel J, Patel A, Cerrillo M, Requena A & Garcia-Velasco JA 2016 Adenomyosis in infertile women: prevalence and the role of 3D ultrasound as a marker of severity of the disease. *Reproductive Biology and Endocrinology* **14** 60. (https://doi.org/10.1186/s12958-016-0185-6)

Rosario GX & Stewart CL 2016 The multifaceted actions of leukaemia inhibitory factor in mediating uterine receptivity and embryo implantation. *American Journal of Reproductive Immunology* **75** 246–255. (https://doi.org/10.1111/aji.12474)

Rossi M, Vannuccini S, Capezzuoli T, Fambrini M, Vannuzzi V, Donati C & Petraglia F 2022 Mechanisms and pathogenesis of adenomyosis. *Current Obstetrics and Gynecology Reports* **11** 95–102. (https://doi.org/10.1007/s13669-022-00326-7)

Downloaded from Bioscientifica.com at 04/18/2024 11:35:24AM
via Open Access. This work is licensed under a Creative Commons Attribution 4.0 International License.
http://creativecommons.org/licenses/by/4.0/

Shandley LM, Spencer JB, Fothergill A, Mertens AC, Manatunga A, Paplomata E & Howards PP 2017 Impact of tamoxifen therapy on fertility in breast cancer survivors. *Fertility and Sterility* **107** 243–252.e5. (https://doi.org/10.1016/j.fertnstert.2016.10.020)

Sharma S, Bathwal S, Agarwal N, Chattopadhyay R, Saha I & Chakravarty B 2019 Does presence of adenomyosis affect reproductive outcome in IVF cycles? A retrospective analysis of 973 patients. *Reproductive Biomedicine Online* **38** 13–21. (https://doi.org/10.1016/j.rbmo.2018.09.014)

Shen F, Yan C, Liu M, Feng Y & Chen Y 2015 Decreased expression of Mucin-1 in endometriosis endometrium correlated with progesterone receptor B involved in infertility. *Archives of Gynecology and Obstetrics* **291** 439–445. (https://doi.org/10.1007/s00404-014-3419-x)

Szubert M, Koziróg E, Olszak O, Krygier-Kurz K, Kazmierczak J & Wilczynski J 2021 Adenomyosis and infertility—review of medical and surgical approaches. *International Journal of Environmental Research and Public Health* **18** 1–12. (https://doi.org/10.3390/ijerph18031235)

Templeman C, Marshall SF, Ursin G, Horn-Ross PL, Clarke CA, Allen M, Deapen D, Ziogas A, Reynolds P, Cress R, *et al.* 2008 Adenomyosis and endometriosis in the California teachers study. *Fertility and Sterility* **90** 415–424. (https://doi.org/10.1016/j.fertnstert.2007.06.027)

Upson K & Missmer SA 2020 Epidemiology of adenomyosis. *38 Seminars in Reproductive Medicine* **38** 89–107.

Vannuccini S & Petraglia F 2019 Recent advances in understanding and managing adenomyosis [Version 1; peer review: 2 approved]. *F1000Research* **8** 1–10.

Vannuccini S & Petraglia F 2022 Adenomyosis: is an endocrine-related uterine dysfunction? *Gynecological Endocrinology* **38** 1017–1018. (https://doi.org/10.1080/09513590.2023.2172156)

Vannuccini S, Tosti C, Carmona F, Huang SJ, Chapron C, Guo SW & Petraglia F 2017 Pathogenesis of adenomyosis: an update on molecular mechanisms. *Reproductive Biomedicine Online* **35** 592–601. (https://doi.org/10.1016/j.rbmo.2017.06.016)

Vercellini P, Consonni D, Dridi D, Bracco B, Frattaruolo MP & Somigliana E 2014 Uterine adenomyosis and in vitro fertilization outcome: a systematic review and meta-analysis. *Human Reproduction* **29** 964–977. (https://doi.org/10.1093/humrep/deu041)

Vercellini P, Consonni D, Dridi D, Bracco B, Frattaruolo MP & Somigliana E 2023 Association of endometriosis and adenomyosis with pregnancy and infertility. *Fertility and Sterility* **119** 727–740. (https://doi.org/10.1016/j.fertnstert.2023.03.018)

Wei W, Komatsu K, Osuka S, Murase T, Bayasula B, Nakanishi N, Nakamura T, Goto M, Iwase A, Masubuchi S, *et al.* 2022 Tamoxifen activates dormant primordial follicles in mouse ovaries. *Reproductive Sciences* **29** 3404–3412. (https://doi.org/10.1007/s43032-022-00896-0)

Wölfler MM, Küppers M, Rath W, Buck VU, Meinhold-Heerlein I & Classen-Linke I 2016 Altered expression of progesterone receptor Isoforms A and B in human eutopic endometrium in endometriosis patients. *Annals of Anatomy* **206** 1–6. (https://doi.org/10.1016/j.aanat.2016.03.004)

Wu Y, Halverson G, Basir Z, Strawn E, Yan P & Guo SW 2005 Aberrant methylation at HOXA10 may be responsible for its aberrant expression in the endometrium of patients with endometriosis. *American Journal of Obstetrics and Gynecology* **193** 371–380. (https://doi.org/10.1016/j.ajog.2005.01.034)

Wu Y, Halverson G, Basir Z, Strawn E, Yan P & Guo SW 2006 Promoter hypermethylation of progesterone receptor Isoform B (PR-B) in endometriosis. *Epigenetics* **1** 106–111. (https://doi.org/10.4161/epi.1.2.2766)

Xu B, Sun X, Li L, Wu L, Zhang A & Feng Y 2012 Pinopodes, leukemia inhibitory factor, integrin-B3, and Mucin-1 expression in the peri-implantation endometrium of women with unexplained recurrent pregnancy loss. *Fertility and Sterility* **98** 389–395. (https://doi.org/10.1016/j.fertnstert.2012.04.032)

Yen CF, Huang SJ, Lee CL, Wang HS & Liao SK 2017*a* Molecular characteristics of the endometrium in uterine adenomyosis and its biochemical microenvironment. *Reproductive Sciences* **24** 1346–1361. (https://doi.org/10.1177/1933719117691141)

Yen CF, Liao SK, Huang SJ, Tabak S, Arcuri F, Lee CL, Arici A, Petraglia F, Wang HS & Kayisli UA 2017*b* Decreased endometrial expression of leukemia inhibitory factor receptor disrupts the STAT3 signaling in adenomyosis during the implantation window. *Reproductive Sciences* **24** 1176–1186. (https://doi.org/10.1177/1933719116681515)

Yu O, Schulze-Rath R, Grafton J, Hansen K, Scholes D & Reed SD 2020 Adenomyosis incidence, prevalence and treatment: United States population-based study 2006–2015. *American Journal of Obstetrics and Gynecology* **223** 94.e1–94.e10. (https://doi.org/10.1016/j.ajog.2020.01.016)

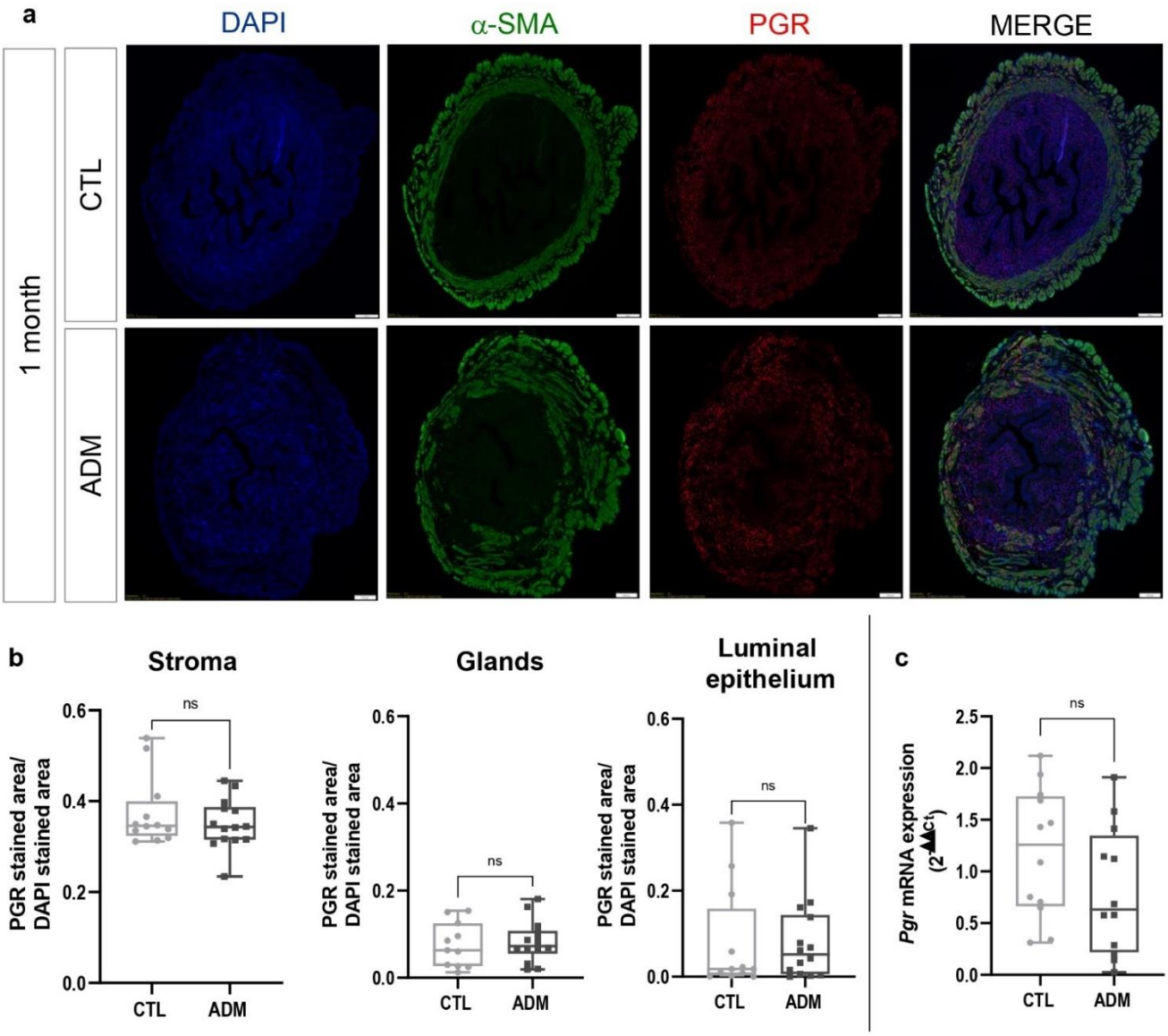
Zanatta A, Rocha AM, Carvalho FM, Pereira RM, Taylor HS, Motta EL, Baracat EC & Serafini PC 2010 The role of the Hoxa10/HOXA10 gene in the etiology of endometriosis and its related infertility: a review. *Journal of Assisted Reproduction and Genetics* **27** 701–710. (https://doi.org/10.1007/s10815-010-9471-y)

Zhang P & Wang G 2023 Progesterone resistance in endometriosis: current evidence and putative mechanisms. *International Journal of Molecular Sciences* **24**. (https://doi.org/10.3390/ijms24086992)

Zhou J, Jiang X, Wu H, Zhang L, Chen M, Chen M, Shen Z, Guo X, Wang H & Gao F 2022 Dissecting the fate of Foxl2-expressing cells in fetal ovary using lineage tracing and single-cell transcriptomics. *Cell Discovery* **8** 139. (https://doi.org/10.1038/s41421-022-00492-1)

Downloaded from Bioscientifica.com at 04/18/2024 11:35:24AM
via Open Access. This work is licensed under a Creative Commons Attribution 4.0 International License.
http://creativecommons.org/licenses/by/4.0/

SUPPLEMENTARY DATA



Supplementary data. Figure 1. Progesterone receptor (PGR) expression in uteri of 1 month-old control and adenomyosis-induced mice.

Immunofluorescence **(a)** and computer-assisted quantification **(b)** of PGR expression in uteri of 1-month-old control and adenomyosis-induced mice. Bar scale = 200μm (CTL), Bar scale = 100μm (ADM). The mRNA expression levels of *Pgr* were also assessed **(c)**. The values are the median with the interquartile range. Statistical significance (Mann-Whitney test): ns = non-significant

ARTICLE 2

Temporal dynamics of uterine immune microenvironment remodeling in a murine model of adenomyosis.

Marlyne Squatrito, Julie Vervier, Laëtitia Bernet, Alessandra Camboni, Marie-Madeleine Dolmans, Carine Munaut.

Molecular Human Reproduction (2025)

In this study, we addressed the major knowledge gap that most uterine immunological data in adenomyosis come from women studied during implantation window or early pregnancy, living little insight into how uterine immune microenvironment behaves outside gestation or before lesions appear. Using the same tamoxifen-induced murine model as in Article 1, we analyzed uterine immune cell populations at 4 weeks (pre-lesional stage) and 12 weeks (established disease). We showed that immune remodeling begins early, before any detectable lesions, with changes in macrophages and T-cell subsets, and then evolved toward a more pronounced adaptive immune involvement and altered macrophage phenotype as disease progresses. In parallel, early and persistent IL6 expression, together with only transient IL10 induction, links local cytokine signaling to this evolving immune imbalance. Overall, these findings indicate that adenomyosis is associated with stage-dependent immune alterations that appear before lesion formation, supporting a contributory role of immune dysregulation in disease initiation and, potentially, later fertility impairment.

OXFORD molecular human reproduction

Molecular Human Reproduction, 2025, **31(4)**, gaaf057
https://doi.org/10.1093/molehr/gaaf057
Advance Access Publication Date: November 26, 2025
Original Research

Temporal dynamics of uterine immune microenvironment remodeling in a murine model of adenomyosis

Marlyne Squatrito[1], Julie Vervier[1,2], Laëtitia Bernet[1], Alessandra Camboni[3,4], Marie-Madeleine Dolmans[3,5], and Carine Munaut[1,*]

[1]Laboratory of Biology of Tumor and Development, GIGA-Cancer, University of Liège, Liège, Belgium
[2]Department of Obstetrics and Gynecology, Hôpital de la Citadelle, University of Liège, Liège, Belgium
[3]Gynecology Research Unit, Institut de Recherche Expérimentale et Clinique, Université Catholique de Louvain, Brussels, Belgium
[4]Anatomopathology Department, Cliniques Universitaires Saint-Luc, Brussels, Belgium
[5]Gynecology Department, Cliniques Universitaires Saint-Luc, Brussels, Belgium

*Correspondence address. Laboratory of Biology of Tumor and Development, GIGA-Cancer, University of Liège, Avenue Hippocrate 13, 4000 Liège, Belgium.
E-mail: c.munaut@uliege.be https://orcid.org/0000-0003-4952-9637

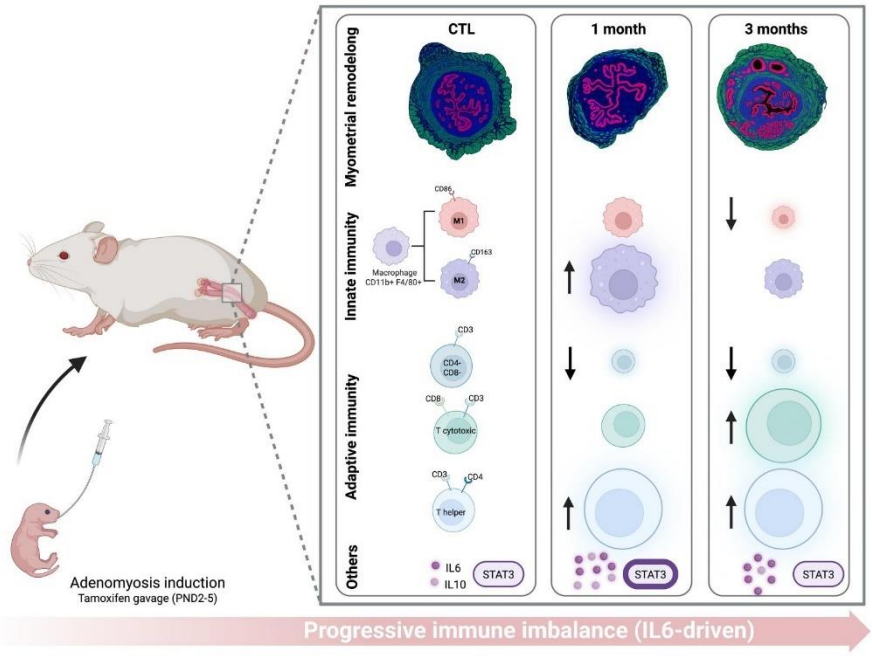
ABSTRACT

Adenomyosis—the ectopic presence of endometrial glands and stroma within the myometrium—affects reproductive-age women and is associated with pain, bleeding, and subfertility, yet the immune events that precede pregnancy remain poorly defined. To address this, we investigated how the uterine immune microenvironment evolves before conception in a tamoxifen-induced murine model of adenomyosis. At 1- and 3-months post-induction, we analyzed uterine tissue by immunofluorescence, flow cytometry, and quantitative polymerase chain reaction. We found that adenomyotic uteri exhibited a sustained elevation of interleukin-6 messenger RNA, a transient interleukin-10 rise at 1 month, and stable cyclooxygenase-2 levels. Interleukin-6 receptor messenger RNA and signal transducer and activator of transcription 3 messenger RNA were both transiently downregulated at 1 month and returned to control levels by 3 months. Early in disease development, total macrophage numbers declined and displayed an alternative (M2) activation phenotype, followed by a selective loss of classically activated (M1) macrophages at later stages. B lymphocytes were consistently enriched, indicating enhanced humoral activity. Although overall T-cell counts remained stable, the $CD3^+$ compartment underwent a marked shift from double-negative T lymphocytes toward T-helper and cytotoxic subsets, coinciding with the transient signaling changes. Limitations of our study include reliance on a single animal model, analysis at only two timepoints, and a lack of functional assessment of regulatory T cells. Future work should incorporate finer temporal profiling, single-cell transcriptomics, and validation in human tissues. These findings highlight dynamic innate–adaptive crosstalk as an early driver of adenomyosis pathology and suggest that targeting interleukin-6-mediated pathways may inform biomarker development and novel immunomodulatory interventions.

Keywords: adenomyosis / murine model / uterine immune microenvironment / macrophage polarization / T-cell subset reprogramming / interleukin-6/STAT3 signaling

Received: August 11, 2025. **Revised:** November 4, 2025. **Accepted:** November 24, 2025.
© The Author(s) 2025. Published by Oxford University Press on behalf of European Society of Human Reproduction and Embryology.
This is an Open Access article distributed under the terms of the Creative Commons Attribution License (https://creativecommons.org/licenses/by/4.0/), which permits unrestricted reuse, distribution, and reproduction in any medium, provided the original work is properly cited.

GRAPHICAL ABSTRACT



Adenomyosis progression in mice is associated with macrophage M2 shift, altered T-cell subsets, and IL-6/STAT3–driven immune imbalance. CTL, mice treated with vehicle; "1 month" and "3 months" refer to the time post-tamoxifen treatment. Created in BioRender. Munaut, C. (2025) https://BioRender.com/t13843g

Introduction

Adenomyosis was first identified at the end of the 19th century in uteri examined post-hysterectomy (Bird *et al.*, 1972). More recently, advances in medical imaging have enabled non-invasive diagnosis, underscoring that adenomyosis also affects younger, reproductive-age women (Pinzauti *et al.*, 2015; Chapron *et al.*, 2017; García-Solares *et al.*, 2018). Clinically, the condition is often associated with pelvic pain, abnormal uterine bleeding, and multiparity (Vannuccini and Petraglia, 2019; Vercellini *et al.*, 2025). Since the initial theory positing that endometrial tissue penetrates the myometrium through a compromised junctional zone (Bergeron *et al.*, 2006; Stratopoulou *et al.*, 2021), numerous molecular pathways have been explored to elucidate pathogenesis.

Over the past decade, murine models, particularly tamoxifen-induced models, have emerged as key research platforms for dissecting adenomyosis mechanisms (Parrott *et al.*, 2001; Green *et al.*, 2005). Although multiple mechanisms contribute to lesion progression, immune dysregulation has emerged as a critical driver (Li *et al.*, 2024). Bourdon *et al.* highlighted immunological disturbances and aberrant Notch1 signaling near or during the implantation window (Bourdon *et al.*, 2021, 2024). However, our group was the first to demonstrate a direct fertility impairment in tamoxifen-induced adenomyosis mice, documenting disrupted estrous cyclicity, prolonged estrus, impaired folliculogenesis, and notably smaller litter sizes and numbers (Squatrito *et al.*, 2024). We further linked these reproductive defects to progesterone resistance and reduced endometrial receptivity, as evidenced by downregulation of progesterone receptor expression, HoxA10, and integrin β3.

Despite these advances, the precise pathways by which adenomyosis impairs fertility remain incompletely defined. Several studies have implicated eutopic-endometrial immune dysregulation as a key contributor (Barrier *et al.*, 2004; Campo *et al.*, 2012; Bourdon *et al.*, 2021; Stratopoulou *et al.*, 2023), and mounting evidence indicates that inflammation disrupts processes crucial for successful implantation and pregnancy maintenance (Guo *et al.*, 2018). However, most work has focused on immune changes at or after conception, leaving a gap in our understanding of pre-conception immune alterations.

Addressing this gap is crucial for identifying early pathogenic events and for pinpointing the most effective strategies to safeguard fertility. Therefore, the aim of the present study was to investigate the uterine immune environment prior to pregnancy during the development of the pathology in tamoxifen-induced adenomyosis mice. By defining the timing and nature of immune dysregulation in adenomyosis, we aim to refine our understanding of its pathogenesis and highlight potential avenues for intervention. Ultimately, pinpointing the onset of these immune disturbances may pave the way for preventive measures to counteract the reduced fertility often observed in adenomyosis.

Materials and methods

Mouse model of adenomyosis (experimental design)

Animal experiments in this study were approved by the Animal Ethics Committee of the University of Liege (approval number # 2387) and conducted following ARRIVE guidelines. In total, 70 neonatal female CD1 mice were included in the study and divided into two groups. The first group received an oral administration of vehicle from postnatal day (PND) 1–5, while the second group received an oral administration of tamoxifen (2.7 μmol/

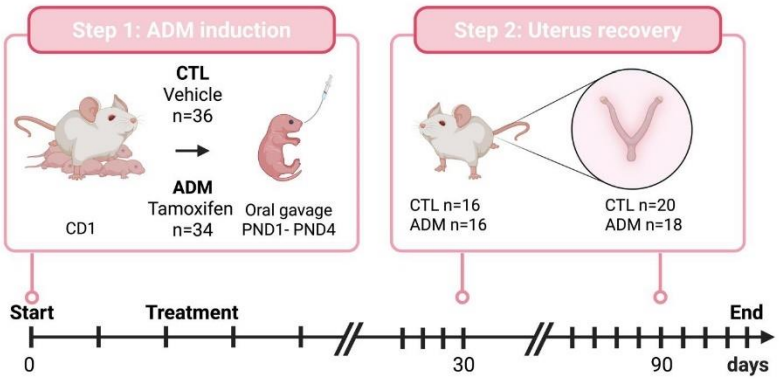


Figure 1. Experimental design. Schematic overview of the experimental design and analysis workflow in control (CTL) and adenomyosis (ADM) mice at 1- and 3-month post-induction. Created in BioRender. Munaut, C. (2025) https://BioRender.com/3l3vb9j.

kg = 1 mg/kg) (Sigma, T5648, St Louis, MO, USA) suspended in a peanut oil/lecithin/condensed milk mixture (2:0.2:3, v/v) at a dose volume of 5 µl/g body weight. This tamoxifen treatment was used to induce adenomyosis as previously described (Green *et al.*, 2005) (Fig. 1).

All mice were housed under controlled conditions, with a temperature maintained at approximately 21°C and a 12-h light/dark cycle, with ad libitum access to food and water. Mice were sacrificed at two different time points: an early stage, 4 weeks after treatment initiation, where 16 mice per group were euthanized, and an advanced stage, 12 weeks after treatment initiation, where 20 mice from the vehicle group and 18 mice from the tamoxifen group were sacrificed (Fig. 1). These time points were selected based on our previous characterization of this model: at 1-month post-induction, mice consistently display early disruption of the myometrium without invasive adenomyotic lesions (pre-lesional stage), whereas by 3-month post-induction, adenomyotic lesions are confirmed in nearly all animals, with the majority reaching grade 3 severity (Squatrito *et al.*, 2024). These two windows thus allow capturing both the onset of uterine alterations and the established disease stage, providing a relevant framework to study temporal immune remodeling.

To minimize variability related to the estrous cycle, mice were synchronized by subcutaneous injection of 17β-estradiol (100 ng/100 ml) for three consecutive days before sacrifice, as previously described (De Clercq *et al.*, 2017).

Mice were first anesthetized with isoflurane inhalation (5% in oxygen) until loss of pedal reflex, and subsequently euthanized by cervical dislocation, in accordance with the AVMA Guidelines for the Euthanasia of Animals (Leary *et al.*, 2020) and the approved institutional protocol.

Following euthanasia, uterine tissues were collected for further analysis. To ensure enough immune cells for flow cytometry analysis, one-half uterine horn from two mice were pooled. The remaining uterine horn from each mouse was divided into two (1-month-old mice) or three (3-month-old mice) parts: one portion was snap-frozen in liquid nitrogen and then stored at −80°C for RNA extraction and quantitative real-time PCR (RT-qPCR) analyses, while the other was fixed in 4% formalin and embedded in paraffin for immunohistochemistry (IHC) analyses.

Histochemical analysis

To confirm the presence or absence of adenomyotic lesions, double immunofluorescence staining was performed on uterine sections using αSMA-FITC (Sigma, F3777, 1/400, St Louis, MO, USA) and EpCAM (Cell Signaling, 93790, 1/400, Danvers, MA, USA) antibodies. αSMA antibody was directly conjugated to FITC, allowing visualization of the myometrium in green, while EpCAM was detected using a tyramide amplification system conjugated to Cy3, marking the epithelial glands in red.

Briefly, paraffin-embedded uterine sections were first deparaffinized and rehydrated, followed by antigen retrieval using an autoclave (11 min, 126°C, 1.3 bar). After cooling for 20 min at room temperature (RT), endogenous peroxidase activity was blocked by incubating the sections in 3% hydrogen peroxide for 20 min at RT. To prevent non-specific binding, sections were incubated for 20 min at RT in the 'Animal-Free Blocking Solution' (Cell Signaling).

Primary antibodies were diluted in REAL antibody diluent (Dako, Santa Clara, CA, USA) and incubated for 1 h at RT. After primary antibody incubation, sections were incubated with a secondary antibody conjugated to horseradish peroxidase (EnVision/HRP, Dako) for 30 min at RT. The revelation of EpCAM was performed using a tyramide amplification system conjugated to Cy3 (PerkinElmer, Shelton, CT, USA), allowing visualization of the epithelial glands in red. Sections were then mounted using DAPI Fluoromount-G mounting medium (SouthernBiotech, Birmingham, AL, USA).

Fluorescently labeled sections were scanned using the SLIDEVIEW VS200 research slide scanner (Olympus, Antwerp, Belgium) equipped with a Uplan-XApo 20× 0.8 NA objective (Olympus).

Flow cytometry analysis

Uterine tissue fragments from CD1 mice were placed in a digestion solution composed of Hank's balanced salt solution (HBSS) and collagenase type Ia (2.5 mg/ml) and incubated at 37°C with agitation for 1 h. To facilitate tissue dissociation, pipetting (40 up-and-down motions with a P1000) was performed every 15 min. Following digestion, EDTA (1:100) was added, and additional pipetting was performed for 2 min to ensure complete tissue dissociation. The resulting cell suspension was filtered through a 70 µm mesh and centrifuged at 310*g* for 10 min at 4°C. The supernatant was discarded, and the pellet was resuspended in FACS buffer (HBSS supplemented with 2% FBS and 1% penicillin/streptomycin). To prevent non-specific binding, cells were incubated for 20 min at 4°C with a blocking solution (Fc block; 1:500 dilution in HBSS) prior to antibody staining. A mixture of primary antibodies, targeting various cell populations (Table 1), was prepared in FACS buffer. Each sample was incubated with appropriate

Table 1. Antibodies and viability dye used for flow cytometric analysis of mouse uterine immune cells.

Target (antigen)	Fluorochrome	Company	City	Country	Catalogue No.
CD45	PeCy7	BioLegend	San Diego, CA	USA	103114
F4/80	BV605	BioLegend	San Diego, CA	USA	123133
CD11b	BV785	BioLegend	San Diego, CA	USA	101243
CD86	Pe-Dazzle594	BioLegend	San Diego, CA	USA	105041
CD163	APC	BioLegend	San Diego, CA	USA	156705
CD19	FITC	BioLegend	San Diego, CA	USA	152404
CD3	BB700	BD Biosciences	San Jose, CA	USA	742175
NKp46	BV650	BioLegend	San Diego, CA	USA	137635
CD4	BV711	BioLegend	San Diego, CA	USA	100447
CD8	APC-Cy7	BD Biosciences	San Jose, CA	USA	561967
Live/dead fixable aqua	—	Thermo Fisher Scientific	Waltham, MA	USA	L34957
Fc block	—	BD biosciences	San Jose, CA	USA	553142

Table 2. Primers for RT-qPCR.

Gene	Forward primer (5′–3′)	Reverse primer (5′–3′)	Amplicon size (bp)
Il6	ACCTGGAGTACATGAAGAACAACTT	GCTCTTGGTTGAAGATATGAATTAGA	102
Il6r	TGCAGTTCCAGCTTCGATACCG	TGCTTCACTCCTCGCAAGGCAT	112
Il10	GCTCTTACTGACTGGCATGAG	CGCAGCTCTAGGAGCATGTG	105
Stat3	CAATACCATTGACCTGCCGAT	GAGCGACTCAAACTGCCCT	109
Ptgs2	GCGACATACTCAAGCAGGAGCA	AGTGGTAACCGCTCAGGTGTTG	132

dilution of antibody mix in the dark, on ice, for 30 min, with gentle vortexing every 10 min. After incubation, cells were washed with FACS buffer and centrifuged at 250*g* for 5 min at 4°C. To exclude dead cells, a viability dye (Zombie Aqua) was used according to the manufacturer's instructions (Biolegend, San Diego, CA, USA). To correct for spectral overlap between fluorophores, a compensation matrix was generated using single-stained beads labeled with individual fluorochromes. Fluorescence minus one (FMO) controls were systematically included for key markers to define gating thresholds. A uniform gating strategy was applied consistently across all samples within each experimental group, ensuring reliable discrimination of positive and negative subsets for each immune population. After staining, samples were filtered through 40 μm filters into fresh FACS tubes prior to analysis.

Cell sorting was performed using an Aria III flow cytometer (BD Biosciences, San Jose, CA, USA), with all available cells from each sample being analyzed and sorted to maximize recovery of the targeted immune cell populations. Specifically, M1- and M2-like macrophage subsets were sorted with the initial aim of performing downstream RT-qPCR analyses to further characterize their polarization profiles. However, due to the low number of recovered cells in several samples, these downstream assays could not be reliably performed, and the present work therefore focuses on the flow cytometry-based characterization of the uterine immune microenvironment. One pooled sample (two uteri) was excluded from the analysis because the total number of recovered cells was abnormally low (<30 000 cells), whereas all other samples yielded a minimum of 600 000 cells analyzed. Flow cytometry data were analyzed using FlowJo software (version 10, Ashland, OR, USA). The gating strategies used for the flow cytometry analysis are shown in Supplementary Fig. S1.

Real-time PCR analysis

Gene expression was assessed by RT-qPCR. Total RNA was extracted from individual samples using the RNeasy Mini kit (Qiagen, Hilden, Germany) following the manufacturer's instructions.

For each sample, 1 μg of total RNA was reverse transcribed into complementary DNA (cDNA) using the FastGene Scriptase II Ready Mix (Nippon Genetics, Düren, Germany). RT-qPCR was performed using SYBR Green PCR Master Mix and specific primers (Table 2) on a QuantStudio 3 Real-Time PCR System (Thermo Fisher Scientific, Waltham, MA, USA).

Gene expression levels were analyzed using the $2^{-\Delta\Delta Ct}$ method, with all samples measured in duplicate. To minimize variability related to the estrous cycle, only mice in estrus were selected for RT-qPCR analyses, since the expression of several genes, including inflammation-related genes, may fluctuate depending on cycle stage. To normalize gene expression, *Rplp0* and *Gapdh* were used as housekeeping genes, as recommended by Lin *et al.* for gene expression studies in the mouse uterus (Lin *et al.*, 2013).

Statistical analysis

All statistical analyses were performed using GraphPad Prism (version 9.0, San Diego, CA, USA).

For mouse and uterine weights, data were normally distributed, as assessed by the Shapiro–Wilk test and visual inspection of QQ plots. Therefore, results are presented as mean ± SD, and parametric unpaired two-tailed *t*-tests were used to compare groups.

For flow cytometry (FACS) and RT-qPCR analyses, the non-parametric Mann–Whitney *U* test (two-tailed) was applied. In these cases, results are presented as medians (interquartile ranges).

Exact *P*-values are reported in the text. A *P*-value was considered statistically significant when $P < 0.05$. The number of replicates (biological or technical) is specified in each figure legend.

Results

Development of adenomyosis after neonatal tamoxifen treatment

To assess adenomyosis progression, we analyzed uterine morphology in control (CTL) and tamoxifen-treated (ADM) mice at 1- and 3-month post-treatment.

At both time points, none of the control mice exhibited signs of adenomyosis, confirming that the condition does not spontaneously develop in 'young' untreated animals. In contrast, uteri

from ADM mice sacrificed 30-day post-treatment displayed early signs of myometrial remodeling, characterized by tissue disorganization and structural alterations. However, in most cases, these modifications had not yet progressed into fully developed adenomyotic lesions, suggesting an initial phase of disease establishment without substantial glandular invasion.

By 90-day post-treatment, ADM mice exhibited prominent adenomyosis lesions, with the majority classified as grade 3, consistent with previously published data (Squatrito *et al.*, 2024). This progressive histopathological transformation supports the hypothesis that neonatal tamoxifen exposure induces sustained uterine alterations that gradually lead to advanced adenomyosis (Fig. 2).

In addition to morphological changes, physiological parameters were also affected. At 1-month post-treatment, body weight was significantly lower in ADM mice (22.86 ± 2.34 g) compared to controls (24.71 ± 1.55 g; $P = 0.0133$). However, this difference was no longer observed at 3 months (ADM: 34.98 ± 5.00 g vs CTL: 33.52 ± 3.45 g; n.s.), suggesting a transient growth delay. In contrast, uterine weight remained significantly reduced in ADM mice at both time points. At 1 month, ADM mice exhibited a dramatic reduction (0.036 ± 0.013 g) compared to controls (0.096 ± 0.010 g; $P < 0.0001$). A significant difference persisted at 3 months (ADM: 0.093 ± 0.036 g vs CTL: 0.145 ± 0.044 g; $P = 0.0004$), indicating sustained disruption of uterine homeostasis following neonatal tamoxifen exposure. Consistently, the uterine weight-to-body weight ratio was also significantly lower in ADM compared to CTL mice at both 1 month (ADM: 0.0016 ± 0.0006 vs CTL: 0.004 ± 0.0004; $P < 0.0001$) and 3 months (ADM: 0.0028 ± 0.001 vs CTL: 0.0044 ± 0.001; $P = 0.0002$), further confirming impaired uterine development (Table 3).

Together, these findings provide insight into the temporal dynamic of adenomyosis development following neonatal tamoxifen exposure and highlight key histopathological and physiological alterations that precede the establishment of severe disease.

Temporal modulation of innate and adaptive immune responses in a mouse model of adenomyosis

Adenomyosis induces profound modulation of the uterine immune microenvironment, a phenomenon suspected to impair fertility. To characterize these immunological alterations, we profiled innate and adaptive immune cell subsets in uteri from CTL and ADM mice at 1 month (early stage) and 3 months (advanced stage) post-induction. Multiparametric flow cytometry enabled precise quantification of each subset and revealed time-dependent alterations in both innate and adaptive immune compartments, as detailed below.

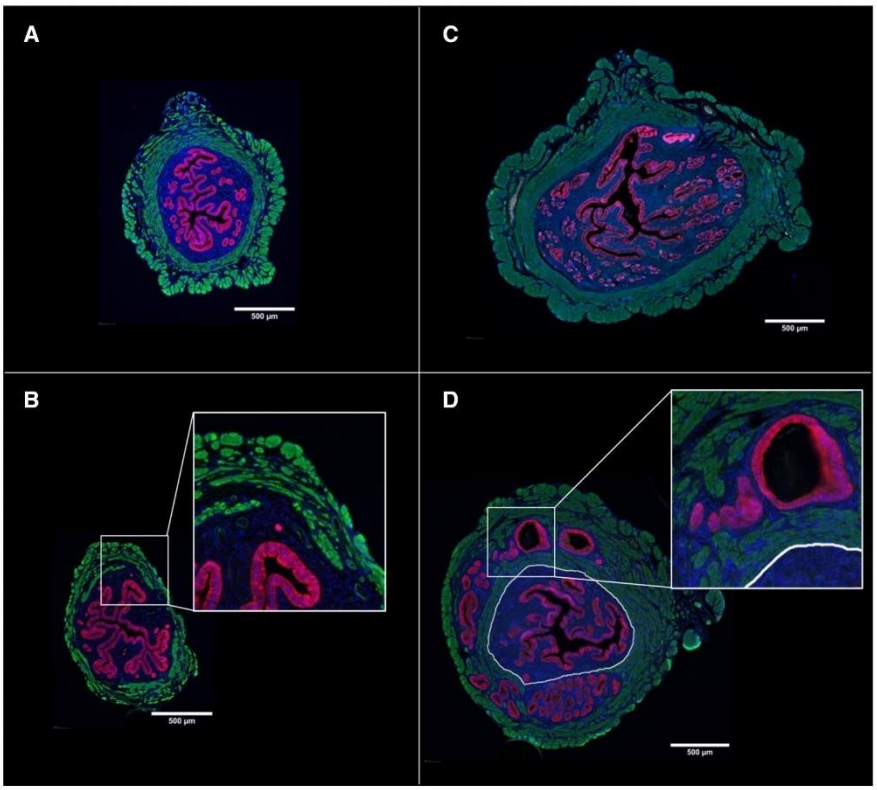


Figure 2. Uterine morphology in control (CTL) and adenomyosis (ADM) mice. Representative immunofluorescence staining of transverse uterine sections at 1 and 3 months. aSMA (green) marks the myometrium, EpCAM (red) labels epithelial glands, and DAPI (blue) stains cell nuclei. At 1 month, CTL uteri display normal morphology (**A**), whereas ADM uteri show disrupted myometrium (**B**, higher magnification). At 3 months, CTL uteri remain normal (**C**), while ADM uteri present adenomyotic lesions (**D**, higher magnification). In (D), the myometrium–endometrium boundary is delineated (white circle). Scale bar, 500 µm.

Table 3. Body and uterine weights in control (CTL) and tamoxifen-treated (ADM) mice at 1- and 3-month post-treatment.

Weight (g)	1 month			3 months		
	CTL (n = 16)	ADM (n = 16)	P	CTL (n = 20)	ADM (n = 18)	P
Body (B)	24.71 ± 1.55	22.86 ± 2.34	*	33.52 ± 3.45	34.98 ± 5.00	n.s.
Uterus (U)	0.096 ± 0.010	0.036 ± 0.013	****	0.145 ± 0.044	0.093 ± 0.035	***
Ratio U/B	0.004 ± 0.0004	0.0016 ± 0.0006	****	0.0044 ± 0.001	0.0028 ± 0.001	***

Data are expressed as mean ± standard deviation (SD). Statistical significance was assessed using unpaired two-tailed t-tests.
* $P < 0.05$, *** $P < 0.001$, **** $P < 0.0001$; n.s. = not significant.

Modulation of macrophages and other innate immune subsets in the adenomyotic uterus

NK cells

At both early (1 month) and advanced (3 months) stages, the proportion of uterine NK cells ($CD3^-$ $NKp46^+$) remained comparable between ADM and CTL mice (Fig. 3A–C, M–O), with no statistically significant differences ($P = 0.2440$ and $P = 0.237$, respectively). These findings suggest that adenomyosis does not substantially impact NK-cell-mediated immune surveillance at either time point.

Macrophages and subtypes

At the early stage, the proportion of total macrophages ($CD11b^+$ $F4/80^+$) was significantly reduced in ADM mice compared to CTL (median 9.27% vs 23.35%, $P = 0.0093$; Fig. 3D–F). This reduction was accompanied by a marked shift toward an increased frequency of M2-like macrophages ($CD11b^+$ $F4/80^+$ $CD163^+$) in ADM mice (median 20.9% vs 5.18%, $P = 0.0012$, Fig. 2G–L), while M1-like macrophages ($CD11b^+$ $F4/80^+$ $CD86^+$) remained comparable between groups.

At the advanced stage, the total macrophage population was no longer significantly different between ADM and CTL mice (median 15.70% vs 20.05%, $P = 0.189$, Fig. 3P–R). However, a significant decrease in M1-like macrophages was observed in the uteri of ADM mice compared to CTL mice (median 20.40% vs 31.85%, $P = 0.035$, Fig. 3S–U), whereas M2-like macrophages remained similar between groups (Fig. 3V–X).

Together, these results demonstrate a time-dependent modulation of macrophage polarization in ADM mice, with a significant reduction of M1-like macrophages and relatively stable levels of M2-like cells. This evolving macrophage profile is consistent with a progressive shift toward an anti-inflammatory immune environment in the adenomyotic uterus.

Changes in adaptive immune cells

B cells

At the early stage (1 month), the proportion of uterine B cells ($CD3^-CD19^+$) was significantly increased in ADM mice compared to CTL (median 0.56% vs 0.30%, $P = 0.029$). This elevation persisted at the advanced stage (3 months), with B-cell frequencies remaining significantly higher in ADM mice (median 1.36% vs 0.68%, $P = 0.026$, Fig. 4A–C, J–L). These findings indicate a sustained enrichment of B cells in the adenomyotic uterus, suggesting a long-lasting modulation of the humoral immune response in this pathological context.

T cells and subtypes

We first quantified total T lymphocytes ($CD3^+CD19^-$) in uteri from CTL and ADM mice at 1 month (early stage) and 3 months (advanced stage) post-induction. The overall proportion of $CD3^+$ T cells did not differ significantly between ADM and CTL groups at either time point, indicating that adenomyosis does not affect total T-cell infiltration (Fig. 4A–C, J–L).

We then analyzed the distribution of four $CD3^+$ T-cell subsets based on CD4 and CD8 expression: double-negative (DN, $CD4^-CD8^-$), CD4 single-positive ($CD4^+CD8^-$), CD8 single-positive ($CD4^-CD8^+$), and double-positive ($CD4^+CD8^+$) cells (Figs 4D–F, M–O and 5).

Across all groups, DN T cells represented the predominant subset, as shown by the 100% stacked bar graph (Fig. 5). However, this population was significantly reduced in ADM mice compared to CTL both at 1 month (median 51.4% vs 68.85%; $P = 0.0084$) and at 3 months (median 47.3% vs 80.6%; $P < 0.0001$, Table 4). Conversely, the frequency of $CD4^+CD8^-$ T cells was significantly increased in ADM mice at both time points (1 month: $P = 0.0093$; 3 months: $P = 0.0002$), as was the proportion of $CD4^+CD8^+$ double-positive cells (1 month: $P = 0.5335$; 3 months: $P = 0.0128$, Table 4). No significant difference was observed in the $CD8^+CD4^-$ subset at 1 month ($P = 0.5358$), although a moderate increase was detected at 3 months in ADM mice ($P = 0.0006$).

In addition, natural killer T cells (NKT, $CD3^+$ $NKp46^+$), a unique population bridging innate and adaptive immunity through rapid cytokine secretion, were also assessed. Their frequency remained low and did not differ significantly between ADM and CTL groups at either time point, suggesting that NKT cell involvement in the uterine immune response to adenomyosis is limited under these conditions.

Expression of *Il6*, *Il6R*, *Il10*, *Stat3*, and *Ptgs2* mRNA in control and adenomyotic uteri

To assess the cytokine and signaling profile associated with the altered immune landscape in adenomyotic uteri, we measured *Il6*, *Il6R*, *Il10*, *Stat3*, and *Ptgs2* mRNA levels by RT-qPCR in CTL and ADM mice at 1- and 3-month post-induction (Fig. 6).

At 1 month, *Il6* and *Il10* transcripts were significantly upregulated in ADM uteri compared to CTL (*Il6:* $P = 0.0014$; *Il10:* $P = 0.0003$), whereas *Il6R* and *Stat3* expression were significantly downregulated (*IL6R:* $P = 0.0132$; *Stat3:* $P = 0.0205$). In contrast, *Ptgs2* levels remained unchanged ($P > 0.9999$). At 3 months, *Il6* remained elevated in ADM mice (*Il6:* $P = 0.003$), but *Il6R*, *Stat3* and *Il10* expression were no longer different from CTL ($P = 0.7759$; $P = 0.1431$; $P = 0.1564$), and *Ptgs2* still showed no significant change ($P = 0.7959$).

Together, these data reveal a dysregulated cytokine signaling in adenomyotic uteri, marked by sustained *Il6* and *Il10* induction despite transient *Stat3* repression and no alteration of *Ptgs2* expression.

Discussion

General overview of immune remodeling

In this study, we investigated the temporal remodeling of the uterine immune microenvironment in a murine model of adenomyosis, integrating cellular and molecular analyses. Although flow cytometry was performed prior to gene expression analysis,

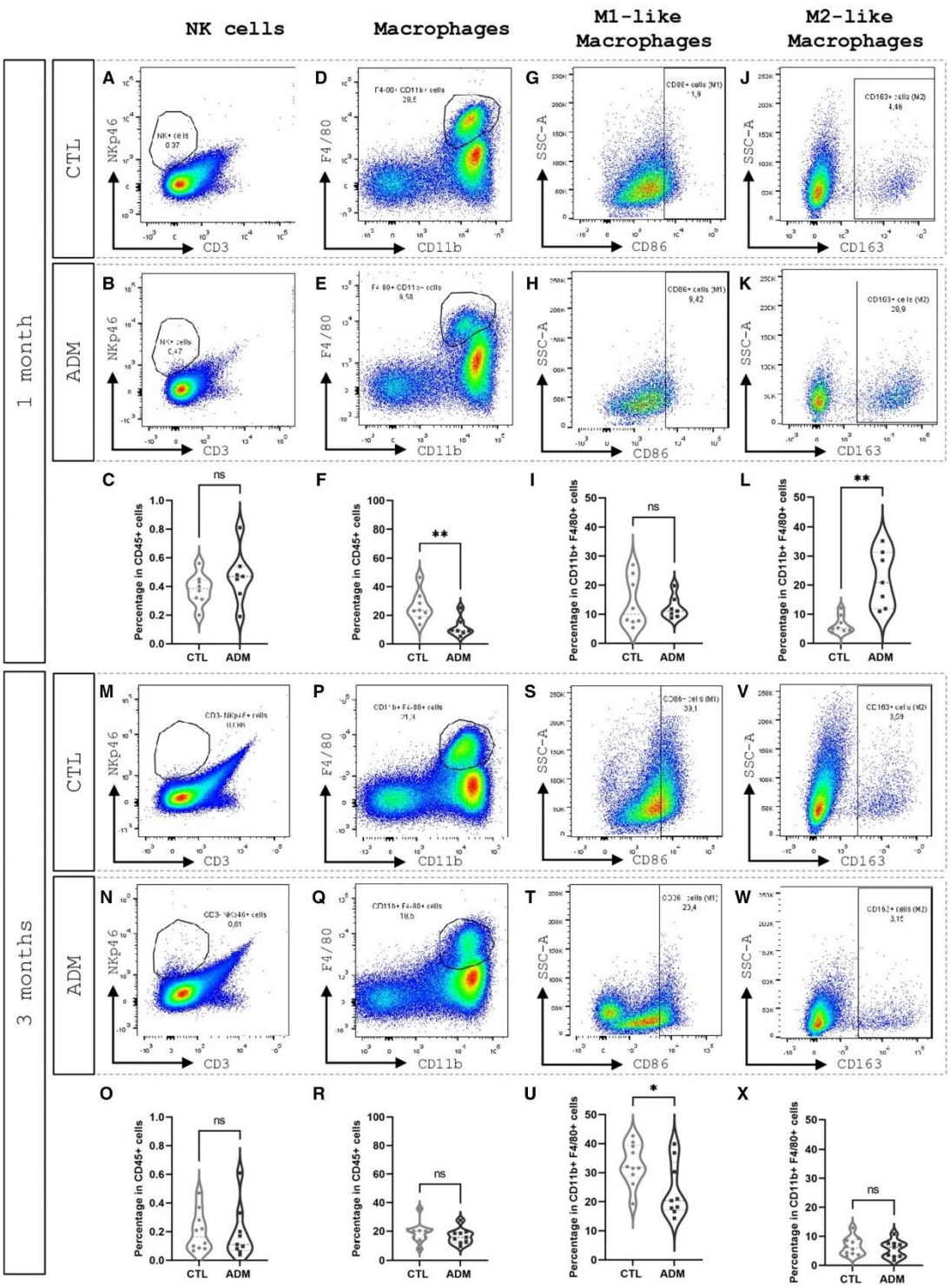


Figure 3. Innate immune cells in control (CTL) and adenomyosis (ADM) uteri. Representative flow cytometry dot plots and violin plots showing the percentage of natural killer (NK) cells ($CD3^-$ $NKp46^+$) (**A–C**, **M–O**), total macrophages ($CD11b^+$ $F4/80^+$) (**D–F**, **P–R**), M1-like macrophages ($CD11b^+$ $F4/80^+$ $CD86^+$) (**G–I**, **S–U**), and M2-like macrophages ($CD11b^+$ $F4/80^+$ $CD163^+$) (**J–L**, **V–X**) at 1 and 3 months. Adenomyosis induced an early reduction of total macrophages with an increase in the M2-like subset, followed by a decrease in M1-like macrophages 3-month post-tamoxifen treatment; NK-cell frequencies remained unchanged across time points. Sample sizes: 1 month (CTL 16 mice pooled (n = 8); ADM 16 mice pooled with one exclusion (n = 7)); 3 months (CTL 20 mice pooled (n = 10); ADM 18 mice pooled (n = 9)). Statistical significance was determined using the Mann–Whitney *U* test: $^*P < 0.05$, $^{**}P < 0.01$; ns, not significant.

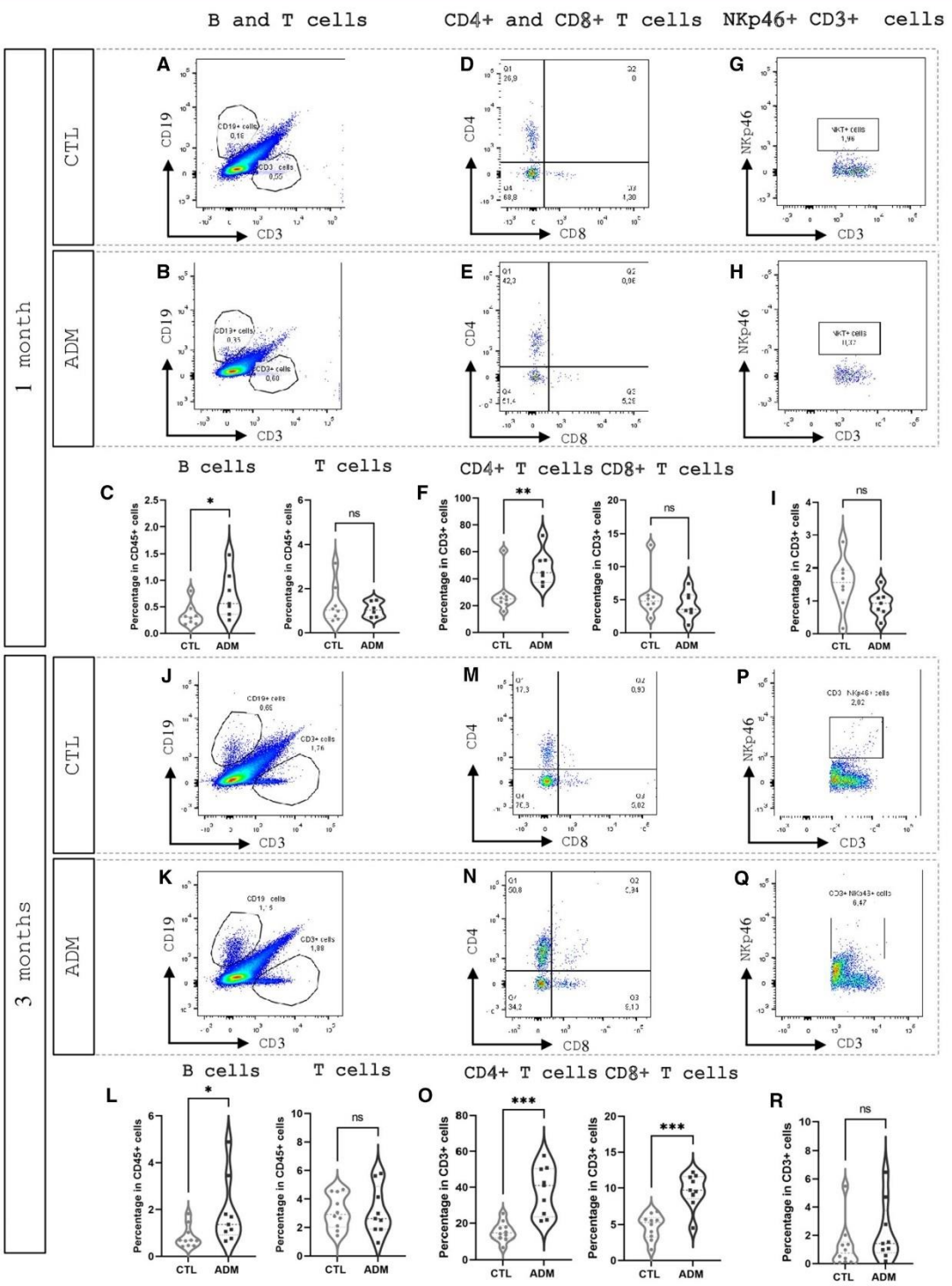


Figure 4. Adaptive immune cells in control (CTL) and adenomyosis (ADM) uteri. Representative flow cytometry dot plots and violin plots showing the percentage of B cells ($CD19^+$) and total T cells ($CD3^+$) (**A–C**, **J–L**), helper T cells ($CD4^+$) and cytotoxic T cells ($CD8^+$) (**D–F**, **M–O**), and NKT cells ($NKp46^+$ $CD3^+$) (**G–I**, **P–R**) at 1 and 3 months. ADM uteri showed increased B-cell percentage and higher $CD4^+$ T-cell levels at both time points, while $CD8^+$ T cells increased only 3-month post-tamoxifen treatment; total T and NKT cells remained unchanged. Sample sizes: 1 month (CTL 16 mice pooled (n = 8); ADM 16 mice pooled with one exclusion (n = 7)); 3 months (CTL 20 mice pooled (n = 10); ADM 18 mice pooled (n = 9)). Statistical significance was determined using the Mann–Whitney *U* test: $^*P < 0.05$, $^{***}P < 0.001$; ns, not significant.

Table 4. Quantitative comparison of $CD3^+$ T-cell subsets in the murine uterus at 1- and 3-month post-induction.

Time	Group	$CD4^-CD8^-$ (IQR)	$CD4^+CD8^-$ (IQR)	$CD4^-CD8^+$ (IQR)	$CD4^+CD8^+$ (IQR)
1 month	CTL	68.85 (66.55–70.50)	25.15 (21.63–28.55)	4.80 (3.78–5.61)	0.48 (0.41–1.48)
	ADM	51.40** (38.8–8.30)	44.70** (37.60–53.50	3.54 (3.04–5.70)	0.56 (0.47–1.35)
3 months	CTL	80.60 (74.08–82.53)	14.6 (11.83–18.68)	5.28 (3.25–5.95)	0.53 (0.25–1.00)
	ADM	47.30**** (38.40–60.95)	41.00*** (23.55–50.45)	9.70*** (8.58–11.60)	1.96* (1.12–4.25)

Median values (% of $CD3^+$) with interquartile ranges (IQR) are presented. Statistical comparisons were performed using the Mann–Whitney *U* test between control (CTL) and adenomyosis (ADM) groups at each timepoint.
* $P < 0.05$, ** $P < 0.01$, *** $P < 0.001$, **** $P < 0.0001$.

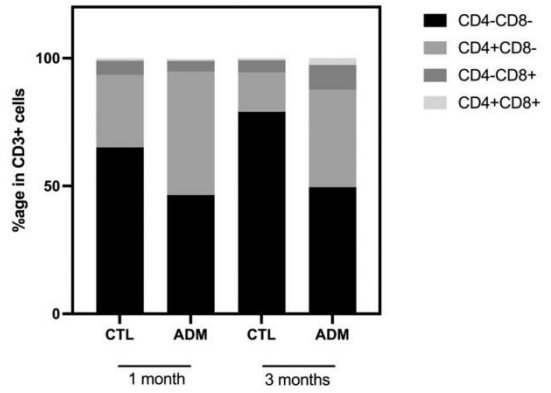


Figure 5. Distribution of uterine $CD3^+$ T-cell subsets. Relative distribution of $CD4^-CD8^-$ (double-negative, DN), $CD4^+CD8^-$, $CD4^-CD8^+$, and $CD4^+CD8^+$ (double-positive, DP) T-cell subsets within the $CD3^+$ compartment at 1 and 3 months. ADM uteri showed a reduction of DN T cells and increased $CD4^+$ single-positive cells at both time points, while $CD8^+$ single-positive and DP T cells increased only 3-month post-tamoxifen treatment. Each bar represents the mean of individual percentages. Sample sizes: 1 month, CTL (16 pooled, n = 8), ADM (16 pooled, one exclusion, n = 7); 3 months, CTL (20 pooled, n = 10), ADM (18 pooled, n = 9). ADM, adenomyosis; CTL, control.

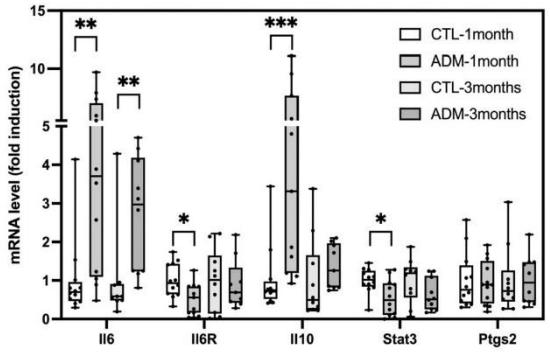


Figure 6. Expression levels of inflammatory and immunoregulatory transcripts. Relative mRNA expression of *Il6*, *Il6r*, *Il10*, *Stat3*, and *Ptgs2* in uterine tissues of control (CTL) and adenomyosis (ADM) mice at 1 and 3 months (RT-qPCR). At 1 month, ADM uteri showed increased expression of *Il6* and *Il10* with decreased expression of *Il6r* and *Stat3*, while *Ptgs2* expression remained unchanged; at 3 months, only *Il6* expression remained elevated. Bars represent median with interquartile range. Sample sizes: 1 month, CTL and ADM n = 12; 3 months, CTL and ADM n = 10. *P*-values were calculated using the Mann–Whitney *U* test: *$P < 0.05$, **$P < 0.01$, ***$P < 0.001$.

the following overview synthesizes both datasets to provide a comprehensive picture of immune dynamics.

Our data revealed coordinated alterations in both innate and adaptive compartments. Early adenomyosis was characterized by reduced macrophage numbers with a skewing toward M2-like polarization, while later stages showed selective depletion of M1-like macrophages. In parallel, B cells were consistently elevated, and $CD3^+$ T cells, although stable in total numbers, underwent a marked redistribution across subsets. At the molecular level, *Il6* mRNA was persistently upregulated, while *Il10* showed only transient elevation, and *Ptgs2* remained unchanged. Collectively, these findings suggest that adenomyosis provoked a progressive disruption of the innate–adaptive balance, shifting from an early compensatory anti-inflammatory response to a state of unresolved inflammation that may impair uterine homeostasis.

Time-dependent redistribution of $CD3^+$ T-cell subsets

Flow cytometry revealed a pronounced reshaping of $CD3^+$ T-cell subsets in the ADM uterus. The proportion of double-negative ($CD4^-CD8^-$) cells significantly declined at both 1 and 3 months, consistent with a progressive depletion of this subset. In parallel, $CD4^+$ T cells increased significantly at both timepoints, suggesting early activation of helper T-cell responses. $CD8^+$ T cells showed a delayed but robust expansion at 3 months, indicative of cytotoxic effector engagement.

Notably, $CD4^+CD8^+$ double-positive T cells emerged significantly at 3 months. These cells, typically rare in peripheral tissues, may represent transitional or activated phenotypes associated with chronic immune stimulation (Parel and Chizzolini, 2004; Hagen *et al.*, 2023). This time-dependent redistribution of T-cell subsets coincides with transient *Stat3* downregulation, suggesting that dampened STAT3 signaling may influence lineage commitment toward $CD4^+$ and $CD8^+$ effector functions. Similar alterations affecting $CD8^+$ T cells have been reported in the endometrium of patients with adenomyosis and/or endometriosis, highlighting changes in cytotoxic T-cell populations associated with disease severity (Kisovar *et al.*, 2023; Liu *et al.*, 2023). Together, these data support the hypothesis of an evolving adaptive immune response in adenomyosis, potentially contributing to lesion persistence and fertility impairment.

Physiological correlates of immune dysregulation

In addition to immune remodeling, we also observed significant physiological alterations. ADM mice exhibited a transient reduction in body weight at 1-month post-induction, which normalized

by 3 months. This early growth delay may reflect systemic effects of neonatal exposure or early inflammatory stress. More strikingly, uterine weight remained significantly reduced in ADM mice at both 1 and 3 months, suggesting a sustained disruption of uterine growth and tissue homeostasis. These changes parallel our molecular findings and support the idea that chronic immune imbalance may impair uterine remodeling, even beyond the acute lesion phase. These physiological observations are consistent with previous studies using neonatal tamoxifen to induce adenomyosis. Several reports have shown that uterine weight is significantly reduced in tamoxifen-treated mice at both early and late timepoints, even when body weight is unaffected (Parrott *et al.*, 2001; Green *et al.*, 2005). Our observation suggests that neonatal tamoxifen exposure disrupts uterine growth more specifically than systemic development.

Together, these immunological and physiological alterations underscore a coordinated disruption of uterine homeostasis in adenomyosis, prompting us to consider the underlying mechanisms by which IL6–driven inflammation and STAT3 modulation impair tissue growth and remodeling.

Macrophage polarization and IL-6/IL-10 imbalance

Our data suggest that early innate changes establish the inflammatory context for adaptive responses. The reduction in macrophage numbers paired with M2 polarization may hinder clearance of ectopic endometrial cells while promoting tissue remodeling and fibrosis (Gordon, 2003). Loss of M1-like macrophages 3 months after adenomyosis induction may further diminish classical inflammatory functions necessary for lesion resolution (Ota *et al.*, 1998; Riccio *et al.*, 2018).

Paralleling endometriosis literature—where M2-polarized macrophages accumulate in lesions and promote tissue invasion (Bacci *et al.*, 2009; Nie *et al.*, 2018), while studies on M1/M2 prevalence yield mixed findings (Itoh *et al.*, 2013; Takebayashi *et al.*, 2015)—our adenomyosis model similarly exhibits an early M2 dominance followed by M1 loss. This dualistic concept has recently been challenged: macrophages can undergo 'trained immunity' and display hybrid M1/M2 signatures that defy a simple polarization framework (Martinez and Gordon, 2014). These observations are consistent with human studies showing accumulation of M2 macrophages in adenomyotic lesions, where they contribute to tissue remodeling and lesion invasiveness (Stratopoulou *et al.*, 2023).

These macrophage dynamics appear to be closely tied to evolving cytokine environment. M1-like macrophages are known sources of pro-inflammatory cytokines such as IL-6, whereas M2-like macrophages secrete anti-inflammatory mediators like IL-10 (Martinez and Gordon, 2014). At 1 month, we observed increased M2-like macrophages and elevated *Il10* mRNA, suggesting an early anti-inflammatory response. However, *Il6* was already significantly upregulated despite unchanged M1-like macrophage numbers, implying non-immune sources such as stromal or epithelial cells may contribute. By 3 months, M1-like macrophages were reduced and *Il10* levels normalized, whereas *Il6* remained elevated, pointing to a shift toward chronic, unresolved inflammation in the ADM uterus. Elevated *IL6* and altered *IL10* dynamics have also been reported in human endometrial tissues from patients with adenomyosis, supporting the translational relevance of these cytokine patterns, which are known to influence endometrial receptivity and implantation success (Zhihong *et al.*, 2016; Wang *et al.*, 2018).

These local and systemic immune changes have been associated with impaired fertility in a murine adenomyosis model, coinciding with alterations in local and systemic immune cells observed during the implantation window (Bourdon *et al.*, 2024).

IL-6/STAT3 axis: chronic inflammation and therapeutic targeting

Our observation of a sustained increase in *Il6* mRNA in ADM uteri at both 1- and 3-month post-adenomyosis induction aligns with clinical reports of elevated IL-6 in the peritoneal fluid and lesional endometrium of patients with adenomyosis and endometriosis (Incognito *et al.*, 2023; Cao *et al.*, 2025). IL-6 is a pleiotropic cytokine that drives chronic inflammation by promoting STAT3 phosphorylation, leukocyte recruitment, angiogenesis, and stromal cell proliferation (Tanaka *et al.*, 2014; West, 2019).

As an activator of the JAK–STAT signaling pathway, IL-6 can act in both a pro-inflammatory and anti-inflammatory manner. Deregulation of IL-6 production can cause severe disease, such as rheumatoid arthritis, psoriasis, arteriosclerosis, and cancer. Therapeutically, monoclonal antibodies targeting IL-6 (e.g. tocilizumab) or JAK inhibitors (e.g. ruxolitinib) have already been tested in other inflammatory diseases and may represent candidate agents for repurposing in adenomyosis models (Taskin *et al.*, 2016; El-Zayadi *et al.*, 2020; Li *et al.*, 2025; Parisi *et al.*, 2025). Furthermore, accumulating evidence shows that IL-6 can interact with WNT/β-catenin signaling. For example, hypoxia-induced IL-6 secretion can activate WNT signaling in rat mesenchymal stem cells (MSCs) through the JAK2/STAT3 signaling (Mao *et al.*, 2019; Chen *et al.*, 2024). Although we did not detect sustained *Stat3* mRNA elevation—likely due to negative feedback by SOCS3 (Gao *et al.*, 2018)—the persistent *Il6* mRNA overexpression suggests that post-transcriptional activation of STAT3 or alternative pathways (e.g. MAPK) may underlie lesion progression in adenomyosis. Interestingly, both *Stat3* and *Il6r* mRNA levels were significantly reduced in ADM uteri at 1 month but returned to baseline by 3 months. This coordinated downregulation of receptor and downstream effector suggests a transient suppression of IL-6 signaling, potentially as a homeostatic brake against acute inflammatory activation. The latter normalization may reflect a loss of this regulation, allowing sustained IL-6 activity to drive chronic tissue remodeling. Although we did not directly assess regulatory T-cell (Treg) populations—a limitation of our work—it is plausible that reduced STAT3 signaling also impairs Treg maintenance. Future studies should include $FoxP3^+$ cell quantification to determine whether Treg deficiency contributes to the skewing toward $CD4^+$ and $CD8^+$ effector phenotypes observed in our adenomyosis model.

Anti-inflammatory feedback and the IL-10 paradox

Concomitant with lL-6 upregulation, we detected a transient rise in *Il10* mRNA at 1 month, which normalized by 3 months. Similar patterns have been reported in chronic endometrial inflammation models, where initial IL-10 increases serve to limit tissue damage (Yang *et al.*, 2017; Park *et al.*, 2025). IL-10, produced primarily by M2 macrophages and regulatory T cells, suppresses pro-inflammatory cytokine secretion and downregulates antigen presentation (Moore *et al.*, 2001). In the context of adenomyosis, early IL-10 induction may represent a host attempt to counterbalance IL-6–driven inflammation and prevent excessive fibrosis. However, prolonged IL-10 signaling can also foster immunotolerance, facilitating lesion survival by inhibiting cytotoxic responses (Couper *et al.*, 2008). Thus, the dynamic IL-6/IL-10 interplay we observe likely reflects a bidirectional push–pull between inflammation and regulation that shapes disease outcome. Notably, the sustained IL-6 upregulation and shifts in $CD3^+$ T-cell subset

composition observed here could serve as candidate biomarkers for disease staging or monitoring if validated in patient samples. Their detection in endometrial biopsies or peripheral blood may provide minimally invasive tools for clinical stratification.

COX-2 expression and technical considerations

In contrast to *Il6* and *Il10*, *Ptgs2* mRNA expression remained unchanged in ADM uteri at both 1 and 3 months. This finding diverges from a preclinical study using tamoxifen-induced adenomyosis in mice, where immunohistochemical analysis revealed high-level COX-2 protein expression in adenomyosis lesions, and pharmacological inhibition by selective COX-2 inhibitor celecoxib markedly reduced adenomyosis severity, including lesion depth, fibrosis, and epithelial–mesenchymal transition (EMT) markers (Jin *et al.*, 2020). The discrepancy may stem from methodological differences: our whole-uterus PCR approach likely dilutes localized expression seen in lesion-restricted IHC. These findings suggest that COX-2 may still play a functional role in adenomyosis progression, and protein-level analyses will be needed to clarify its contribution.

Bridging murine models and clinical fertility impairment

Our current murine data both align with and expand recent work in adenomyosis. Previously, using the same murine model, we documented compromised reproductive capacity, thereby establishing a functional readout of lesion impact on fertility (Squatrito *et al.*, 2024). The immune alterations we now describe offer a mechanistic bridge: early M2 dominance and *Il10* rise may initially buffer tissue damage yet predispose to chronic inflammation, while later loss of M1-like macrophages and skewed T-cell differentiation (linked to transient *Stat3* downregulation) could underlie the uterine dysfunction and subfertility observed in that study.

Translational implications and future directions

These findings resonate with other studies. Indeed, Bourdon *et al.* showed that infiltrating immune cells cooperate with Notch1 signaling to drive epithelial-to-mesenchymal transition during lesion development in mice (Bourdon *et al.*, 2021). Building on this, they also found that reduced fertility in the same murine adenomyosis model is associated with an altered uterine immune profile at the implantation period (Bourdon *et al.*, 2024). Disrupted uterine NK-cell distribution and altered macrophage phenotypes have also been associated with lower pregnancy success in adenomyosis patients undergoing ART (Bourdon *et al.*, 2025). A recent study also evidenced that M2 macrophages accumulate within human adenomyotic lesions and actively promote endometrial cell invasiveness (Stratopoulou *et al.*, 2023). Collectively, these murine and human studies support a model in which dynamic innate–adaptive immune remodeling not only drives lesion progression but also translates into the fertility impairments we first characterized in our reproductive-outcome study (Squatrito *et al.*, 2024). Whether these immune and structural changes translate into altered uterine contractility, receptivity, or implantation dynamics remains to be functionally addressed. Future *in vivo* or *ex vivo* assays, such as uterine peristalsis tracking or embryo transfer experiments, could help establish causality between immune remodeling and reproductive dysfunction.

Strengths and limitations of the current approach

A major strength of our study is the use of a well-validated murine adenomyosis model (Parrott *et al.*, 2001; Marquardt *et al.*, 2020) that isolates the effects of adenomyotic lesions from other uterine pathologies such as endometriosis or fibroids. We have characterized, for the first time, time-dependent immune remodeling in the uterus, including shifts in macrophage polarization, T-cell subsets, and cytokine expression.

Nevertheless, several limitations should be acknowledged. First, species differences and the simplified nature of the model may limit direct extrapolation to human adenomyosis, which often presents with heterogeneous lesions and coexists with endometriosis. Second, although mice were synchronized with β-estradiol, incomplete responses in some controls and disrupted cyclicity in ADM mice may have introduced residual variability, despite uniform synchronization across groups. Moreover, our analysis was restricted to two time points (1 and 3 months), which capture pre-lesional and established phases but do not resolve intermediate disease dynamics.

Technical factors should also be considered. Gene expression was assessed on whole uterine horns, which may dilute lesion-specific signals, and flow cytometry required pooling of uteri prior to histological confirmation, precluding one-to-one correlation with lesion grade. Furthermore, molecular analyses were limited to mRNA; protein-level validation and functional readouts remain to be performed.

Finally, our immune profiling was limited in resolution. Flow cytometry did not assess T-cell activation markers (e.g. FoxP3, CD69) or cytokine production at the protein level, which may overlook important functional diversity. A finer characterization of macrophage polarization states (e.g. M2a, M2b, M2c) and $CD4^+$ T-helper subtypes (e.g. Th1, Th2, Th17, Treg), as well as the inclusion of additional cytokines such as TNF-α, IFN-γ, IL-17, and TGF-β, will be essential to provide a more comprehensive picture of immune remodeling in adenomyosis.

Conclusion

In conclusion, adenomyosis induction in mice provokes a stepwise immune remodeling, beginning with M2 macrophage dominance and culminating in adaptive T-cell reprogramming underpinned by cytokine signaling shifts. These results identify immune alterations that may represent candidate markers for future investigation. Although intriguing, the translational relevance of these findings remains to be confirmed, and targeting IL6/STAT3 signaling should be considered a hypothesis-generating observation that requires further validation. Translating these findings to patients could enable immune-based stratification and personalized interventions aimed at restoring uterine immune homeostasis.

Supplementary data

Supplementary data are available at *Molecular Human Reproduction* online.

Data availability

The data underlying this article will be shared upon reasonable request to the corresponding author.

Acknowledgements

We gratefully acknowledge Prof. Michelle Nisolle for her support at the outset of this project, particularly in helping to secure the initial funding. The authors thank Prof. Jacques Donnez for his scientific input during discussions and Emilie Feyereisen and

Isabelle Dasoul for their excellent technical assistance. We also acknowledge the Flow cytometry platform at the University of Liège for their valuable support.

Authors' roles

Conceptualization: C.M. and M.S. Methodology: C.M. and M.S. Validation, M.S., J.V., and C.M. Formal analysis and investigation: M.S., J.V., and L.B. Resources: M.S., J.V., L.B., and C.M. Writing—original draft preparation: M.S. and C.M. Writing—review and editing: M.S., C.M., L.B., and J.V. Supervision: C.M. Project administration: C.M., A.C., and M.-M.D. Funding acquisition: C.M., A.C., and M.-M.D. All authors have read and agreed to the published version of the manuscript.

Funding

This research was funded by the Fonds de la Recherche Scientifique (F.R.S.-FNRS, Belgium), grant numbers T.0171.21, J.0169.25, F 5/4/130/5 (J.V.) and F 5/4/150/5 (awarded to M.-M.C.), the Fondation contre le Cancer grant 2018-072 awarded to A.C. and the Foundation Léon Fredericq (University of Liège), grant numbers 2023-016 and 2023-171. The funders had no role in the design of the study; in the collection, analyses, or interpretation of data; in the writing of the manuscript; or in the decision to publish the results.

Conflict of interest

The authors declare no conflict of interest.

References

Bacci M, Capobianco A, Monno A, Cottone L, Di Puppo F, Camisa B, Mariani M, Brignole C, Ponzoni M, Ferrari S *et al.* Macrophages are alternatively activated in patients with endometriosis and required for growth and vascularization of lesions in a mouse model of disease. *Am J Pathol* 2009;**175**:547–556.

Barrier BF, Malinowski MJ, Dick EJ, Hubbard GB, Wright Bates G. Adenomyosis in the baboon is associated with primary infertility. *Fertil Steril* 2004;**82**:1091–1094.

Bergeron C, Amant F, Ferenczy A. Pathology and physiopathology of adenomyosis. *Best Pract Res Clin Obstet Gynaecol* 2006;**20**:511–521.

Bird CC, McElin TW, Manalo-Estrella P. The elusive adenomyosis of the uterus-revisited. *Am J Obstet Gynecol* 1972;**112**:583–593.

Bourdon M, Maget AS, Jeljeli M, Doridot L, Marcellin L, Thomas M, Chene C, Chouzenoux S, Batteux F, Chapron C *et al.* Reduced fertility in adenomyosis mouse model is associated with an altered immune profile in the uterus during the implantation period. *Hum Reprod* 2024;**39**:119–129.

Bourdon M, Mimouni A, Maignien C, Casalechi M, Vigano P, Bordonne C, Millisher AE, Patrat C, Marcellin L, Chapron C *et al.* Reduced live birth rates following ART in adenomyosis patients: a matched control study. *Hum Reprod* 2025;**40**:855–864.

Bourdon M, Santulli P, Doridot L, Jeljeli M, Chêne C, Chouzenoux S, Nicco C, Marcellin L, Chapron C, Batteux F. Immune cells and Notch1 signaling appear to drive the epithelial to mesenchymal transition in the development of adenomyosis in mice. Mol Hum Reprod 2021;**27**:gaab053.

Bourdon M, Santulli P, Jeljeli M, Vannuccini S, Marcellin L, Doridot L, Petraglia F, Batteux F, Chapron C. Immunological changes associated with adenomyosis: a systematic review. *Hum Reprod Update* 2021;**27**:108–129.

Campo S, Campo V, Benagiano G. Adenomyosis and infertility. *Reprod Biomed Online* 2012;**24**:35–46.

Cao Y, Yang D, Cai S, Yang L, Yu S, Geng Q, Mo M, Li W, Wei Y, Li Y *et al.* Adenomyosis-associated infertility: an update of the immunological perspective. *Reprod Biomed Online* 2025;**50**:104703.

Chapron C, Tosti C, Marcellin L, Bourdon M, Lafay-Pillet MC, Millischer AE, Streuli I, Borghese B, Petraglia F, Santulli P. Relationship between the magnetic resonance imaging appearance of adenomyosis and endometriosis phenotypes. *Hum Reprod* 2017;**32**:1393–1401.

Chen Y, Guo Y, Li S, Xu J, Zhao C, Wang J, Yang J, Ning W, Qu Y, Zhang M *et al.* Tumor-derived IL-6 promotes chordoma invasion by stimulating tumor-associated macrophages M2 polarization and TNFα secretion. *Int Immunopharmacol* 2024;**143**:113315.

De Clercq K, Hennes A, Vriens J. Isolation of mouse endometrial epithelial and stromal cells for in vitro decidualization. *JoVE* 2017;**2017**:55168

Couper KN, Blount DG, Riley EM. IL-10: the master regulator of immunity to infection. *J Immunol* 2008;**180**:5771–5777.

El-Zayadi AA, Mohamed SA, Arafa M, Mohammed SM, Zayed A, Abdelhafez MS, Badawy AM. Anti-IL-6 receptor monoclonal antibody as a new treatment of endometriosis. *Immunol Res* 2020;**68**:389–397.

Gao Y, Zhao H, Wang P, Wang J, Zou L. The roles of SOCS3 and STAT3 in bacterial infection and inflammatory diseases. *Scand J Immunol* 2018;**88**:e12727.

García-Solares J, Donnez J, Donnez O, Dolmans MM. Pathogenesis of uterine adenomyosis: invagination or metaplasia? *Fertil Steril* 2018;**109**:371–379.

Gordon S. Alternative activation of macrophages. *Nat Rev Immunol* 2003;**3**:23–35.

Green AR, Styles JA, Parrott EL, Gray D, Edwards RE, Smith AG, Gant TW, Greaves P, Al-Azzawi F, White INH. Neonatal tamoxifen treatment of mice leads to adenomyosis but not uterine cancer. *Exp Toxicol Pathol* 2005;**56**:255–263.

Guo S, Li Z, Yan L, Sun Y, Feng Y. GnRH agonist improves pregnancy outcome in mice with induced adenomyosis by restoring endometrial receptivity. *Drug Des Devel Ther* 2018;**12**:1621–1631.

Hagen M, Pangrazzi L, Rocamora-Reverte L, Weinberger B. Legend or Truth: Mature CD4+CD8+ Double-Positive T Cells in the Periphery in Health and Disease. *Biomedicines* 2023;**11**:2702.

Incognito GG, Di Guardo F, Gulino FA, Genovese F, Benvenuto D, Lello C, Palumbo M. Interleukin-6 as a useful predictor of endometriosis-associated infertility: a systematic review. *Int J Fertil Steril* 2023;**17**:226–230.

Itoh F, Komohara Y, Takaishi K, Honda R, Tashiro H, Kyo S, Katabuchi H, Takeya M. Possible involvement of signal transducer and activator of transcription-3 in cell-cell interactions of peritoneal macrophages and endometrial stromal cells in human endometriosis. *Fertil Steril* 2013;**99**:1705–1713.

Jin Z, Wu X, Liu H, Xu C. Celecoxib, a selective COX-2 inhibitor, markedly reduced the severity of tamoxifen-induced adenomyosis in a murine model. *Exp Ther Med* 2020;**19**:3289–3299.

Kisovar A, Becker CM, Granne I, Southcombe JH. The role of $CD8^+$ T cells in endometriosis: a systematic review. *Front Immunol* 2023;**14**:1225639.

Leary S, Underwood W, Anthony R, Cartner S, Grandin T, Greenacre C, Gwaltney-Brant S, McCrackin MA, Meyer R, Miller D *et al.* AVMA guidelines for the euthanasia of animals: 2020 edition. Members of the Panel on Euthanasia AVMA Staff Consultants. 2020. Available from: https://www.avma.org/sites/default/files/2020-02/Guidelines-on-Euthanasia-2020.pdf

Li J, Wang R, Chen J, Xu A, Fu Y, Lin Y, Wang X, Ye S, Yuan Y, Du F *et al.* Efficacy and safety of ruxolitinib in adult patients with refractory rheumatic disease-associated macrophage activation syndrome. *Front Immunol* 2025;**16**:1604648.

Li Q, Shi J, Yi D, Li X, Gu Z, Yan H, Leng J. The pathogenesis of endometriosis and adenomyosis: insights from single-cell RNA sequencing. *Biol Reprod* 2024;**110**:854–865.

Lin PF, Lan XL, Chen FL, Yang YZ, Jin YP, Wang AH. Reference gene selection for real-time quantitative PCR analysis of the mouse uterus in the peri-implantation period. *PLoS One* 2013;**8**:e62462.

Liu W, Sheng S, Zhu C, Li C, Zou Y, Yang C, Chen ZJ, Wang F, Jiao X. Increased $NKG2A^{+}CD8^{+}$ T-cell exhaustion in patients with adenomyosis. *Mucosal Immunol* 2023;**16**:121–134.

Mao Q, Liang XL, Wu YF, Pang YH, Zhao XJ, Lu YX. ILK promotes survival and self-renewal of hypoxic MSCs via the activation of lncTCF7-Wnt pathway induced by IL-6/STAT3 signaling. *Gene Ther* 2019;**26**:165–176.

Marquardt RM, Jeong JW, Fazleabas AT. Animal models of adenomyosis. *Semin Reprod Med* 2020;**38**:168–178.

Martinez FO, Gordon S. The M1 and M2 paradigm of macrophage activation: time for reassessment. *F1000Prime Rep* 2014;**6**:13.

Moore KW, De Waal Malefyt R, Coffman RL, O'Garra A. Interleukin-10 and the interleukin-10 receptor. *Annu Rev Immunol* 2001;**19**:683–765.

Nie MF, Xie Q, Wu YH, He H, Zou LJ, She XL, Wu XQ. Serum and ectopic endometrium from women with endometriosis modulate macrophage M1/M2 polarization via the Smad2/Smad3 pathway. *J Immunol Res* 2018;**2018**:6285813.

Ota H, Igarashi S, Hatazawa J, Tanaka T. Is adenomyosis an immune disease? *Hum Reprod Update* 1998;**4**:360–367.

Parel Y, Chizzolini C. $CD4^{+}$ $CD8^{+}$ double positive (DP) T cells in health and disease. *Autoimmun Rev* 2004;**3**:215–220.

Parisi S, Ditto MC, Ghellere F, Panaro S, Piccione F, Borrelli R, Fusaro E. Update on tocilizumab in rheumatoid arthritis: a narrative review. *Front Immunol* 2025;**16**:1470488.

Park W, Lim W, Kim M, Jang H, Park SJ, Song G, Park S. Female reproductive disease, endometriosis: from inflammation to infertility. *Mol Cells* 2025;**48**:100164.

Parrott E, Butterworth M, Green A, White IN, Greaves P. Adenomyosis-a result of disordered stromal differentiation. *Am J Pathol* 2001;**159**:623–630.

Pinzauti S, Lazzeri L, Tosti C, Centini G, Orlandini C, Luisi S, Zupi E, Exacoustos C, Petraglia F. Transvaginal sonographic features of diffuse adenomyosis in 18-30-year-old nulligravid women without endometriosis: association with symptoms. *Ultrasound Obstet Gynecol* 2015;**46**:730–736.

Riccio LdGC, Santulli P, Marcellin L, Abrão MS, Batteux F, Chapron C. Immunology of endometriosis. *Best Pract Res Clin Obstet Gynaecol* 2018;**50**:39–49.

Squatrito M, Vervier J, Bindels J, Bernet L, Blacher S, Nisolle M, Munaut C. Impaired fertility in adenomyosis: a murine model reveals endometrial receptivity and progesterone resistance imbalances. *Reproduction* 2024;**167**:e240019.

Stratopoulou CA, Cussac S, d'Argent M, Donnez J, Dolmans M-M. M2 macrophages enhance endometrial cell invasiveness by promoting collective cell migration in uterine adenomyosis. *Reprod Biomed Online* 2023;**46**:729–738.

Stratopoulou CA, Donnez J, Dolmans MM. Origin and pathogenic mechanisms of uterine adenomyosis: what is known so far. *Reprod Sci* 2021;**28**:2087–2097.

Takebayashi A, Kimura F, Kishi Y, Ishida M, Takahashi A, Yamanaka A, Wu D, Zheng L, Takahashi K, Suginami H *et al.* Subpopulations of macrophages within eutopic endometrium of endometriosis patients. *Am J Reprod Immunol* 2015;**73**:221–231.

Tanaka T, Narazaki M, Kishimoto T. IL-6 in inflammation, immunity, and disease. *Cold Spring Harb Perspect Biol* 2014;**6**:a016295.

Taskin MI, Gungor AC, Adali E, Yay A, Onder GO, Inceboz U. A humanized anti-interleukin 6 receptor monoclonal antibody, tocilizumab, for the treatment of endometriosis in a rat model. *Reprod Sci* 2016;**23**:662–669.

Vannuccini S, Petraglia F. Recent advances in understanding and managing adenomyosis. *F1000Res* 2019;**8**:283.

Vercellini P, Buffo C, Bandini V, Cipriani S, Chiaffarino F, Viganò P, Somigliana E. Prevalence of adenomyosis in symptomatic adolescents and young women: a systematic review and meta-analysis. *F&S Rev* 2025;**6**:2666–5719.

Wang J, Huang C, Jiang R, Du Y, Zhou J, Jiang Y, Yan Q, Xing J, Hou X, Zhou J *et al.* Decreased endometrial IL-10 impairs endometrial receptivity by downregulating HOXA10 expression in women with adenomyosis. *Biomed Res Int* 2018;**2018**:2549789.

West NR. Coordination of immune-stroma crosstalk by IL-6 family cytokines. *Front Immunol* 2019;**10**:1093.

Yang HL, Zhou WJ, Chang KK, Mei J, Huang LQ, Wang MY, Meng Y, Ha SY, Li DJ, Li MQ. The crosstalk between endometrial stromal cells and macrophages impairs cytotoxicity of NK cells in endometriosis by secreting IL-10 and TGF-β. *Reproduction* 2017;**154**:815–825.

Zhihong N, Yun F, Pinggui Z, Sulian Z, Zhang A. Cytokine profiling in the eutopic endometrium of adenomyosis during the implantation window after ovarian stimulation. *Reprod Sci* 2016;**23**:124–133.

© The Author(s) 2025. Published by Oxford University Press on behalf of European Society of Human Reproduction and Embryology.
This is an Open Access article distributed under the terms of the Creative Commons Attribution License (https://creativecommons.org/licenses/by/4.0/), which permits unrestricted reuse, distribution, and reproduction in any medium, provided the original work is properly cited.
Molecular Human Reproduction, 2025, 31, 1–13
https://doi.org/10.1093/molehr/gaaf057
Original Research

ARTICLE 3

Stage-dependent sphingosine-1-phosphate pathway modulation as a therapeutic strategy in a murine model of adenomyosis.

Marlyne Squatrito, Silvia Blacher, Julie Vervier, Laëtitia Bernet, Alessandra Camboni, Marie-Madeleine Dolmans, Carine Munaut.

Molecular Human Reproduction (2026)

In this study, we investigated whether the sphingosine-1-phosphate (S1P) signaling pathway, already known to be involved in inflammation, fibrosis and angiogenesis, is dynamically altered in adenomyosis and whether its pharmacological inhibition can limit disease progression. Using the same neonatal tamoxifen-induced mouse model as in our previous articles, we first characterized S1P receptors and metabolic enzymes at a pre-lesional stage and at established disease, then evaluated two complementary pathway inhibitors: FTY720 and SKI-5C. The results suggested that S1P signaling is dynamically dysregulated over time in adenomyosis and that pharmacological blockade can mitigate key features of the disease. Preventive FTY720 treatment reduced the development and depth of lesions when given before they appeared, while therapeutic inhibition with SKI-5C in established disease decreased lesion invasion. Both drugs also lowered expression of uPA, suggesting a shared effect on tissue invasion. Altogether, these exploratory findings support the S1P pathway as a stage-sensitive, fertility-preserving therapeutic target that may help limit adenomyosis progression.

Molecular Human Reproduction, 2026, **32(1)**, gaag009
https://doi.org/10.1093/molehr/gaag009
Advance Access Publication Date: February 16, 2026
Original Research

Stage-dependent sphingosine-1-phosphate pathway modulation as a therapeutic strategy in a murine model of adenomyosis

Marlyne Squatrito[1], Silvia Blacher[1], Julie Vervier[1,2], Laëtitia Bernet[1], Alessandra Camboni[3,4], Marie-Madeleine Dolmans[3,5], and Carine Munaut[1,*]

[1]Laboratory of Biology of Tumor and Development, GIGA-Cancer, University of Liège, Liège, Belgium
[2]Department of Obstetrics and Gynecology, Hôpital de la Citadelle, University of Liège, Liège, Belgium
[3]Gynecology Research Unit, Institut de Recherche Expérimentale et Clinique, Université Catholique de Louvain, Brussels, Belgium
[4]Anatomopathology Department, Cliniques Universitaires Saint-Luc, Brussels, Belgium
[5]Gynecology Department, Cliniques Universitaires Saint-Luc, Brussels, Belgium

*Correspondence address. Laboratory of Biology of Tumor and Development, GIGA-Cancer, University of Liège, Avenue Hippocrate 13, 4000 Liège, Belgium.
E-mail: c.munaut@uliege.be https://orcid.org/0000-0003-4952-9637

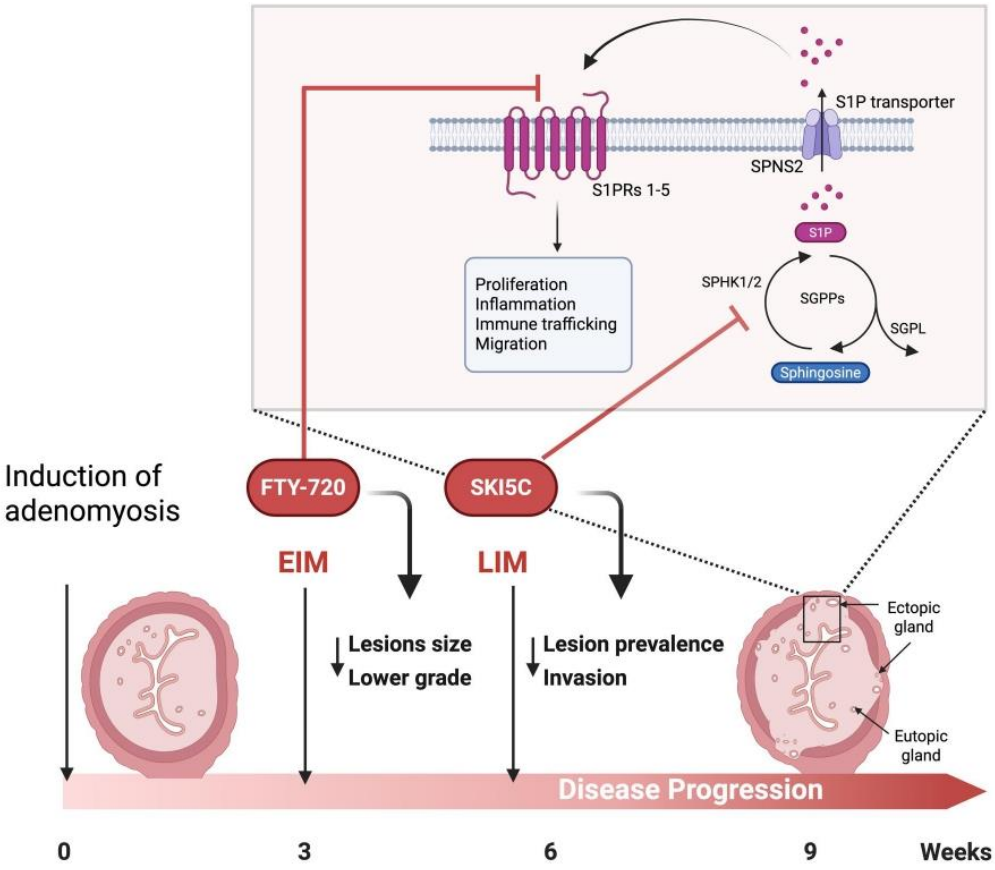
ABSTRACT

Adenomyosis is characterized by chronic inflammation, myometrial remodeling, and subfertility, yet therapeutic options that preserve reproductive potential remain limited. Sphingosine-1-phosphate (S1P) signaling regulates immune-cell trafficking, vascular remodeling, and tissue invasion, but its contribution to adenomyosis remains poorly defined. This study investigated the temporal regulation of this pathway in a tamoxifen-induced murine model of adenomyosis and evaluated whether its pharmacological inhibition alters uterine immune profiles and lesion severity. A total of 122 female CD1 mice were used (79 adenomyosis, 43 control). Preventive treatment (with FTY720) started at weaning, while therapeutic interventions (with FTY720 and SKI-5C) were initiated at 6 weeks. Outcomes included body/uterine weight, lesion prevalence, grading and depth, immune-cell phenotyping by flow cytometry, and uterine expression of inflammatory, angiogenic, and invasion-associated genes. Early disease (at 4 weeks) was marked by increased expression of S1PR1/2 and downregulation of SGPL, while established disease (at 12 weeks) showed that S1PR1 remained elevated with additional upregulation of SPHK1 and S1PR4. Preventive FTY720 reduced lesion depth and grade, whereas therapeutic SKI-5C decreased lesion prevalence and invasion. Uterine weight remained reduced across adenomyosis groups and was not restored by treatment. Immune profiling revealed no major differences in total T-cell abundance between the control and adenomyosis groups. However, SKI-5C treatment was associated with the most pronounced modulation of uterine immune cells, particularly affecting T- and NK-cell-related subsets. Gene expression analyses demonstrated increased interleukin-6 in early disease and modulation of urokinase-type plasminogen activator associated with the treatments. Study limitations included constraints related to immune-cell recovery from uterine tissue, the relatively short duration of treatment, and translational differences between murine and human adenomyosis. Overall, these findings indicate that S1P signaling contributes to immune microenvironment remodeling and lesion progression in adenomyosis. These results support S1P pathway modulation as a promising therapeutic strategy meriting evaluation in human studies.

Keywords: adenomyosis / murine model / sphingosine-1-phosphate signaling / FTY720 / SKI-5C / uterine immune profiling / myometrium remodeling

Received: October 22, 2025. **Revised:** January 21, 2026. **Accepted:** February 6, 2026.
© The Author(s) 2026. Published by Oxford University Press on behalf of European Society of Human Reproduction and Embryology. All rights reserved.
For commercial re-use, please contact reprints@oup.com for reprints and translation rights for reprints. All other permissions can be obtained through our RightsLink service via the Permissions link on the article page on our site—for further information please contact journals.permissions@oup.com.

GRAPHICAL ABSTRACT



Stage-dependent modulation of sphingosine-1-phosphate (S1P) signaling in a murine adenomyosis model reveals distinct preventive and therapeutic effects of FTY720 and SKI-5C on lesion progression and uterine immune remodeling. S1P, sphingosine-1-phosphate; S1PR, sphingosine-1-phosphate receptor; SPHK, sphingosine kinase; SGPL, sphingosine-1-phosphate lyase; EIM, early intervention model; LIM, late intervention model. Created in BioRender. Munaut, C. (2026) https://BioRender.com/w3cc3a6.

Introduction

Adenomyosis is a chronic gynecological disorder characterized by the ectopic presence of endometrial glands and stroma within the myometrium (Bird *et al.*, 1972). This condition is frequently associated with dysmenorrhea, heavy menstrual bleeding, and infertility, with a substantial impact on women's quality of life (Vannuccini *et al.*, 2017). Epidemiological studies estimate a prevalence of up to 20% among women of reproductive age, though the true rates may be underestimated due to diagnostic challenges and overlap with other gynecological disorders such as endometriosis (Abbott, 2017; Loring *et al.*, 2021). Adenomyosis severity is often classified histologically based on the depth of myometrial invasion: grade 1 involves the inner third of the myometrium, grade 2 extends to the mid-myometrium, and grade 3 corresponds to deep or full-thickness invasion, with more extensive lesions typically associated with more severe symptoms (Bird *et al.*, 1972; Moawad *et al.*, 2023). Despite its frequency, current treatments are limited to hormonal therapies or hysterectomy (Vannuccini *et al.*, 2018; Sharara *et al.*, 2021), which may not be suitable for women wishing to preserve fertility, highlighting the urgent need for alternative therapeutic strategies (Vannuccini and Petraglia, 2019).

Emerging evidence implicates chronic local inflammation, immune dysregulation, and abnormal tissue remodeling as central mechanisms driving adenomyosis progression (Zhai *et al.*, 2020). In our previous study using a tamoxifen-induced mouse model of adenomyosis, we reported alterations in uterine immune cell populations, notably in T lymphocytes and macrophages, pointing to local immune imbalance as a driver of disease progression (Squatrito *et al.*, 2025). Furthermore, transcriptomic and proteomic studies have identified dysregulation of inflammatory mediators, extracellular matrix components, and immune-related genes in adenomyotic tissues (Xiaoyu *et al.*, 2013; Bourdon *et al.*, 2021b; Liu *et al.*, 2021; Lin *et al.*, 2022). These findings suggest that crosstalk between immune responses and tissue remodeling sustains disease progression.

Among the signaling pathways potentially involved in these processes, the sphingosine-1-phosphate (S1P) axis is of particular interest (Di Paolo *et al.*, 2022). S1P is a bioactive lipid mediator that regulates immune cell trafficking, angiogenesis, vascular integrity, fibrosis, and cell migration (Spiegel and Milstien, 2011; Donati *et al.*, 2021; Gomez-Larrauri *et al.*, 2025). It is synthesized intracellularly by sphingosine kinases (SPHK1 and SPHK2) and signals through five G protein-coupled receptors (S1PR1–5),

whose expression is cell type- and context-dependent (Maceyka *et al.*, 2012). While the specific roles of S1P receptors and enzymes in the human uterus remain incompletely characterized, alterations in this pathway have been reported in uterine tissues of women with adenomyosis (Vannuzzi *et al.*, 2022). Aberrant S1P signaling has been implicated in several chronic inflammatory and fibrotic diseases, as well as in endometriosis, but its role in adenomyosis remains poorly explored (Bernacchioni *et al.*, 2021, 2024; Zhang and Lu, 2023; Zhang *et al.*, 2023).

Here, we investigated the temporal dynamics of the S1P signaling in a murine model of adenomyosis and assessed the impact of two inhibitors acting at distinct regulatory levels. FTY720 (fingolimod), a functional antagonist of S1P receptors, which is a pro-drug that requires phosphorylation by sphingosine kinase-2 (SPHK2) to generate its biologically active form, and SKI-5C, a selective SPHK1 inhibitor. By comparing preventive (pre-lesional) and therapeutic (post-lesional) interventions, we provide the first preclinical evidence that pharmacological modulation of the S1P pathway can attenuate adenomyotic lesion progression.

Materials and methods

Animals

All animal procedures were approved by the Animal Ethics Committee of the University of Liège (approval numbers: 2387 and 2590) and conducted following ARRIVE guidelines. Female CD1 mice (Charles River Laboratories, Calco, Italy) were housed under controlled temperature (±21 °C) and 12-h light/dark cycle, with 3–4 animals per cage. Food and water were available *ad libitum*.

Adenomyosis induction

Adenomyosis was induced as previously described (Green *et al.*, 2005). A total of 79 neonatal CD1 females (postnatal day 1 = day of birth) received daily oral administration of tamoxifen (2.7 µmol/kg, equivalent to 1 mg/kg; Sigma-Aldrich, T5648, St. Louis, MO, USA) from postnatal days 2 to 5. Tamoxifen was suspended in a vehicle composed of peanut oil, lecithin, and condensed milk (2:0.2:3, v/v). The dosing volume was standardized at 5 µl per gram of body weight and administered with a calibrated micropipette using a soft plastic feeding tube (Instechlabs, FTP-22-25, Plymouth Meeting, PA, USA). Control pups (n = 43) received vehicle alone. All pups remained with their dams until weaning at Day 21. In our hands, neonatal tamoxifen administration induces adenomyosis in 92–95% of CD1 females at 12 weeks, consistent with previously published rates (Green *et al.*, 2005).

Experimental design and pharmacological interventions

To assess temporal S1P modulation, animals were sacrificed at 4 weeks (early stage) or 12 weeks (late stage) after tamoxifen/vehicle treatment.

To assess S1P inhibitors, two experimental timelines were applied. In an early intervention model (EIM), mice received daily intraperitoneal injections of FTY720 (5 mg/kg in DMSO; MedChemExpress, HY-12005) or DMSO vehicle for 3 weeks starting at weaning (3 weeks of age). Groups included: control (no tamoxifen), ADM+vehicle, ADM+FTY720. In the late intervention model (LIM), treatments began at 6 weeks, when adenomyotic lesions were established, mice were treated daily for 3 weeks with FTY720 (5 mg/kg) or the SPHK1 inhibitor SKI-5C (10 mg/kg; Abcam, ab144410, dissolved in methyl acetate) (Abcam, Cambridge, UK). Vehicle-treated and untreated controls were included. An exploratory cohort (n = 5–6/group) was followed by a confirmatory experiment (n = 7/group) enabling immune profiling.

Histology and immunohistochemistry

Uteri were fixed in 4% paraformaldehyde, embedded in paraffin, and sectioned at 5 µm (Leica RM2125RT, Wetzlar, Germany). Sections were deparaffinized, rehydrated, and subjected to antigen retrieval (Target Retrieval Solution, Dako, S1699, Santa Clara, CA, USA, 1:10; autoclave, 126 °C, 1.4 bar). Endogenous peroxidase was blocked with 3% H_2O_2 (1:10, Carl ROTH, 22029501, Karlsruhe, Germany) for 20 min, followed by incubation in blocking buffer (Cell Signaling, 15019 L, 1:5, Danvers, MA, USA).

Tissues were incubated for 1 h at room temperature with primary antibodies: rabbit anti-EpCAM (1:400, Cell Signaling, 93790) to detect endometrial epithelial cells, and FITC-conjugated mouse anti-aSMA (1:400, Sigma-Aldrich, F3777) for smooth muscle cells. After PBS washes, EpCAM staining was revealed with HRP-conjugated secondary antibody (Dako ENVISION K4003, ready-to-use) for 30 min and TSA-Cy3 signal amplification (1:2000, PerkinElmer, Shelton, CT, USA). Slides were counterstained with DAPI (Fluoromount-G, SouthernBiotech, Birmingham, AL, USA) and scanned using an Olympus SLIDEVIEW VS2000 microscope (Olympus, Antwerp, Belgium). $EpCAM^+$ cells appeared red and $aSMA^+$ muscle cells green.

Quantification of adenomyosis lesions

Image analysis and measurements were performed using MATLAB R2024b (MathWorks, Natick, MA, USA). Fluorescence images of the endometrium–myometrium interface were recorded in the RGB (red, green, blue) color space, with EpCAM, aSMA, and DAPI signals appearing in the red, green, and blue channels, respectively. The RGB images were then split, and the red channel (containing only the EpCAM staining) was segmented using MATLAB's graythresh function. This allowed the generation of a binary image in which epithelial glands appear as white pixels (pixel value = 1) on a black background (pixel value = 0).

To quantify the invasion of endometrial glands into the myometrium, the endometrium–myometrium boundary was first manually delineated. The distance of each gland pixel to this boundary was then computed using MATLAB's distance function. The resulting values were used to determine the spatial distribution of glands relative to the endometrium–myometrium interface. Importantly, this method provides a quantitative assessment of glandular invasion in adenomyosis: a measurement that, to our knowledge, has not previously been described in the literature. Because glandular invasion can occur throughout the entire thickness of the myometrium, no fixed penetration limit was applied; the analysis captures the presence of EpCAM-positive glands across the full myometrial thickness.

Lesion severity was graded according to the extent of adenomyotic involvement of the inner one-third (grade I, superficial adenomyosis), two-thirds (grade II), or the entire myometrial thickness (grade III, deep adenomyosis), as previously described and illustrated (Squatrito *et al.*, 2024).

Flow cytometry analysis

Uteri were minced and digested enzymatically in Hank's balanced salt solution (HBSS) supplemented with 2.5 mg/ml collagenase Type IA (Sigma-Aldrich, C9891) to obtain single-cell

Table 1. Antibodies used for flow cytometry.

Marker	Clone	Fluorochrome	Supplier	City and country	Catalog no.
CD45	30-F11	PeCy7	BioLegend	San Diego, CA, USA	103114
CD3	17A2	BB700	BD Biosciences	San Jose, CA, USA	742175
CD4	GK1.5	BV711	BioLegend	San Diego, CA, USA	100447
CD8	53-6.7	APC-Cy7	BD Biosciences	San Jose, CA, USA	561967
NKp46	29A1.4	BV650	BioLegend	San Diego, CA, USA	137635
CD11b	M1/70	BV785	BioLegend	San Diego, CA, USA	101243
F4/80	BM8	BV605	BioLegend	San Diego, CA, USA	123133
CD86	GL-1	Pe-Dazzle594	BioLegend	San Diego, CA, USA	105041
CD163	S15049F	APC	BioLegend	San Diego, CA, USA	156705
Live/Dead Fixable Aqua	_	_	ThermoFisher Scientific	Waltham, MA, USA	L34957
Fc Block	2.4G2	_	BD Biosciences	San Jose, CA, USA	553142

Table 2. Primers sequences used for RT-qPCR analysis of murine uterine genes.

Gene	Forward primer	Reverse primer	Amplicon size (bp)
S1pr1	CTCTTCTGCACCACCGTCTT	CGACTGGCCTTGGAGATGTT	128
S1pr2	TGTTGCTGGTCCTCAGACGCTA	AGTGGGCTTTGTAGAGGACAGG	149
S1pr3	GCCTTGCAGAACGAGAGCCTA	CTGCCAGTTTCCCCACGTAA	246
S1pr4	GTGTATGGCTGCATCGGTCTGT	GAGCACATAGCCCTTGGAGTAG	135
S1pr5	GTGTACACCAAATGCCCAGC	AGCACTGTGCAAAAGTCTCCT	101
Sphk1	GCTTCTGTCAACCACTATGCTGG	ACTGAGCACAGAATAGAGCCGC	153
Sphk2	GGTGCCAATGATCTCTGAAGCTG	CTCCAGACACAGTGACAATGCC	128
Sgpp1	CTGGAGGTCTTCTACAACTCGG	GTGAACTCCAGCAGGGAATGAG	151
Sgpp2	ATGGCTGTGTTCTCTACGC	GGTAGGTCAGAGCAATGAGGAC	115
Sgpl	GGAAAGCCTCAGGAGCTGTGTA	CTGCCTCTAACTTCCGCAATCC	132
Il6	ACCTGGAGTACATGAAGAACAACTT	GCTCTTGGTTGAAGATATGAATTAGA	102
Tnfα	TCTTCTCATTCCTGCTTGTGG	GAGGCCATTTGGGAACTTCT	106
Il10	GCTCTTACTGACTGGCATGAG	CGCAGCTCTAGGAGCATGTG	105
TGFβ	CGTCACTGGAGTTGTACGGCAG	CGTTTGGGGCTGATCCCGTTG	109
Vegf	GTCCTGTGTGCCGCTGAT	AGGTTTGATCCGCATGATCT	101
Plau	AGAAGCGACCCTGGTGCTATGT	CCACACTGGAAGCCTTGTTGGT	145
Gapdh	GGTGGACCTCATGGCCTACA	CTCTCTTGCTCAGTGTCCTTGCT	82
Rplp0	GGACCCGAGAAGACCTCCTT	GCACATCACTCAGAATTTCAATGG	85

suspensions. After filtering, cells were washed and stained with fluorochrome-conjugated antibodies against CD45, CD11b, F4/80, CD86, CD163, CD3, CD4, CD8, and NKp46 (details in Table 1). Dead cells were excluded with the LIVE/DEAD Fixable Aqua reagent, and doublets were removed by FSC/SSC gating. Data were acquired on a BD FACS Aria III cell sorter (BD biosciences, San Jose, CA, USA) and analyzed with FlowJo software (version 10, BD Biosciences, Ashland, OR, USA). The gating strategy is shown in Supplementary Fig. S1. Briefly, after exclusion of doublets and dead cells, live cells were then gated for CD45 expression to define total leukocytes. Within the $CD45^+$ compartment, expression of CD11b and F4/80 was used to delineate major immune subsets. Macrophages were identified as $CD11b^+F4/80^+$ cells and further characterized by the independent expression of CD86 and CD163 as functional markers. Cells negative or low for both CD11b and F4/80 were analyzed for CD3 and CD19 expression to distinguish T cells ($CD3^+CD19^-$) and B cells ($CD3^-CD19^+$). Within the $CD3^+$ T-cell population, natural killer T (NKT)-like cells were defined as $CD3^+NKp46^+$ cells, and T cells were further subdivided based on CD4 and CD8 expression into $CD4^+$, $CD8^+$, double-negative ($CD4^-CD8^-$), and double-positive ($CD4^+CD8^+$) subsets. In parallel, NK cells were identified as $NKp46^+$ cells within the $CD45^+CD11b^+F4/80^-$ population. Compensation was verified using unstained, single-stain, and fluorescence-minus-one (FMO) controls, and intrinsic uterine autofluorescence was taken into account during gating and compensation validation.

Gene expression (RTq-PCR)

For mouse uterine horns, total RNA was isolated using RNeasy® Mini Kit (Qiagen, Hilden, Germany), following the manufacturer's protocol for tissue samples. For each sample, 1μg RNA was reverse transcribed into cDNA using FastGene Scriptase II Ready Mix (Nippon Genetics, LS64, Düren, Germany). Quantitative real-time PCR was performed with SYBR Green PCR Master Mix (Nippon Genetics, LS4005) on a QuantStudio 3 system (Thermo Fisher Scientific, Waltham, MA, USA). Gene expression analysis focused on S1P pathway receptors and metabolic enzymes as well as *Il6*, *Tnfα*, *Il10*, *Tgfβ*, *Vegf*, and *Plau*. Expression levels were normalized to *Gapdh* and *Rplp0* (Lin *et al.*, 2013). Relative expression was calculated using the 2−DCt method as recommended for comparisons across biological samples (Schmittgen and Livak, 2008). Primer sequences are listed in Table 2.

Primer design and validation

All primers were designed using NCBI Primer-BLAST to ensure target specificity and, when possible, to span exon–exon junctions. Primer specificity was verified experimentally by melt-curve analysis, which consistently showed a single amplification peak. Amplification efficiency was determined from standard curves generated using serial dilutions of pooled cDNA; only primer pairs with efficiencies between 90% and 110% and an $R^2 \geq 0.99$ were retained for analysis.

Statistical analysis

Data are presented as mean ± SEM or as median ± interquartile range (IQR), depending on data normality. For comparisons involving more than two groups, one-way ANOVA was performed using parametric or non-parametric tests according to the distribution of the data. Statistical comparisons of gland area distributions between experimental conditions were performed using the Kolmogorov–Smirnov test. A P-value < 0.05 was considered statistically significant. All statistical analyses were performed using GraphPad Prism software (San Diego, CA, USA). Additional details regarding the specific tests and *post hoc* analysis used are provided in the figure legends.

Results

Dynamic modulation of the S1P axis in the uterus of adenomyosis-induced mice at pre- and post-lesional stages

To investigate the potential involvement of the S1P signaling pathway in adenomyosis (ADM), we assessed the mRNA expression of S1P receptors and metabolic enzymes in the uteri of control and ADM mice at both 4 and 12 weeks of age (Fig. 1A). These time points correspond to an early pre-lesional stage and a later stage with well-established lesions, as previously reported (Squatrito *et al.*, 2024).

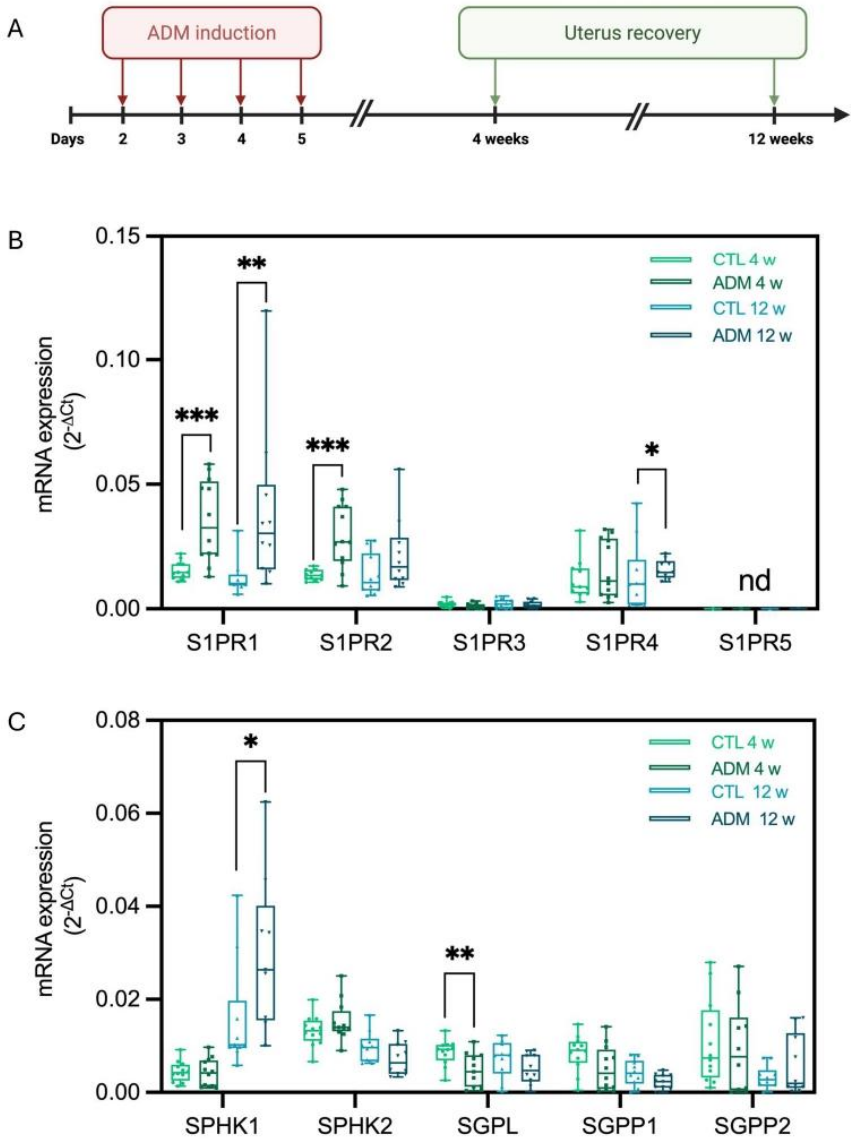


Figure 1. Stage-dependent dysregulation of the sphingosine-1-phosphate (S1P) pathway in uterine tissues from control (CTL) and adenomyosis (ADM) mice. (**A**) Experimental design for RT-qPCR analysis. (**B**) Relative mRNA expression of S1P receptors (*S1pr1*–*S1pr5*) at 4 and 12 weeks. (**C**) Relative expression of genes encoding S1P-metabolizing enzymes (*Sphk1*, *Sphk2*, *Sgpl*, *Sgpp1*, *Sgpp2*) at 4 and 12 weeks. At 4 weeks, adenomyotic uteri showed increased expression of *S1pr1* and *S1pr2* together with reduced *Sgpl*, whereas at 12 weeks, *S1pr1* remained elevated and *S1pr4* and *Sphk1* were upregulated, with no change in other S1P receptors or metabolic enzymes. Gene expression was normalized to the geometric mean of *Rplp0* and *Gapdh*. Data are presented as median with interquartile range (IQR). Group sizes were n = 12 mice at 4 weeks and n = 10 mice at 12 weeks. Statistical analyses were performed using parametric or non-parametric tests depending on data distribution. *$P < 0.05$; **$P < 0.01$; ***$P < 0.001$; nd, not detectable.

At 4 weeks, ADM mice displayed significant upregulation of *S1pr1* and *S1pr2* compared to controls ($P = 0.0009$; $P = 0.0005$, respectively), while *S1pr3* and *S1pr4* remained unchanged and *S1pr5* was undetectable. At 12 weeks, *S1pr1* expression remained elevated ($P = 0.003$) and *S1pr4* became upregulated ($P = 0.0232$) in ADM mice, whereas *S1pr2* and *S1pr3* were no longer different from controls; *S1pr5* stayed undetectable (Fig. 1B).

For metabolic enzymes, *Sgpl*, mediating irreversible S1P degradation, was reduced at 4 weeks in ADM mice ($P = 0.0076$), while the expression levels of *Sphk1*, *Sphk2*, *Sgpp1*, and *Sgpp2* were unchanged. At 12 weeks, *Sphk1*, driving S1P synthesis, was increased ($P = 0.0458$), whereas *Sgpl*, *Sgpp1*, *Sgpp2*, and *Sphk2* remained unchanged in ADM mice (Fig. 1C).

Preventive and therapeutic pharmacological modulation of the S1P pathway: effects on murine and uterine weights

Given the modulation of S1P signaling genes observed in uteri from ADM mice, we next investigated whether pharmacological inhibition could influence disease development and progression. Two *in vivo* treatment strategies were applied (Fig. 2A). In the EIM, mice received daily FTY720 from weaning for 3 weeks, targeting the pre-lesional stage. In the LIM, designed to mimic the clinical scenario in young adult women with established disease, treatments began at 6 weeks of age and included both FTY720 and the SPHK1 inhibitor SKI-5C.

As an initial step, we monitored body weight evolution and uterine weight at sacrifice to assess potential systemic and uterine effects of pharmacological modulation of the S1P pathway.

In the EIM, body weight increased similarly in CTL and ADM groups, with no effect of FTY720 (Fig. 2B, left panel). In the LIM, CTL, ADM, and SKI-5C groups exhibited similar weight gain, whereas FTY720-treated mice displayed a plateau in growth that did not reach a statistically significance difference (Fig. 2B, middle panel).

At sacrifice, uterine weight relative to body weight was lower in ADM mice than in CTL mice in both models. In the EIM, FTY720 did not modify this reduction. In the LIM, FTY720 again had no effect, whereas SKI-5C further decreased relative uterine weight compared to ADM mice (Fig. 2C). Given that uterine weight reflects both physiological myometrial growth and pathological remodeling, these changes are interpreted in conjunction with lesion prevalence and depth rather than as standalone indicators of treatment efficacy.

Although neither FTY720 nor SKI-5C restored uterine weight, we next investigated their impact on adenomyotic lesions, since lesion prevalence and severity are the main histological hallmarks of disease progression.

Impact of pharmacological modulation of the S1P pathway on adenomyosis lesion prevalence, grading, and depth

We first assessed the overall impact of pharmacological modulation of the S1P pathway on lesion prevalence and severity. Representative immunofluorescence images of uterine sections from CTL, ADM, and treated mice are shown in Fig. 2D. In the EIM, FTY720 significantly reduced lesion prevalence compared to ADM mice (Fig. 2E). In the LIM, SKI-5C markedly decreased lesion prevalence, whereas FTY720 had no effect.

Analysis of lesion grades (Fig. 2F) provided an insight into lesion severity independently of prevalence. In the EIM, FTY720 reduced the proportion of high-grade (grade 3) lesions compared to untreated ADM, indicating that preventive treatment is associated with a reduced proportion of high-grade lesions. In the LIM, no statistically significant differences in lesion grades were detected. Quantitative details of lesion prevalence and grades are provided in Supplementary Table S1.

These observations prompted a closer examination of glandular distribution within the myometrium to better characterize lesion architecture (Fig. 2G). In the EIM, gland distribution in ADM and FTY720-treated mice overlapped near the endometrial–myometrial junction, but FTY720 significantly reduced glandular area in deeper layers ($P = 0.0025$; Fig. 2H). In the LIM, FTY720 had no detectable effect, whereas SKI-5C markedly reduced gland area throughout the myometrium ($P = 0.0005$), with effects evident even close to the junction (Fig. 2I).

Modulation of uterine immune cell populations by pharmacological modulation of the S1P pathway

Previous studies in human adenomyosis and rodent models have reported alterations in macrophage infiltration and T-cell composition in the eutopic uterus (Bourdon *et al.*, 2021a, 2024; Bian *et al.*, 2025). To explore the immunomodulatory effects of targeting S1P signaling at distinct regulatory levels in our model, we analyzed uterine macrophage and T cell populations as well as B cells by flow cytometry in the LIM.

Total uterine macrophages ($CD45^+CD11b^+F4/80^+$) were modestly reduced in ADM compared to CTL mice, although this difference did not reach statistical significance (Fig. 3A). SKI-5C significantly reduced macrophage abundance compared with CTL ($P = 0.025$), whereas FTY720 had no effect. Macrophage polarization did not differ across groups as assessed by CD86 and CD163 expression within the $CD45^+CD11b^+F4/80^+$ population (Fig. 3B–D), indicating no major shift in these macrophage-associated functional markers across conditions. Representative flow cytometry panels illustrating macrophage gating and polarization are shown in Supplementary Fig. S2.

B cells constituted a minor fraction of uterine leukocytes and did not differ significantly between CTL, ADM, FTY720-treated or SKI-5C-treated mice (Fig. 3E).

We next examined the innate-like lymphoid population. NK-cell abundance did not differ significantly between CTL, ADM, and FTY720-treated groups. In contrast, SKI-5C treatment was associated with a significant increase in uterine NK cells compared with both ADM ($P = 0.0006$) and FTY720-treated mice ($P = 0.0112$) (Fig. 3F).

We subsequently examined the T-cell compartment. Total uterine T cells tended to be reduced in ADM mice compared with CTL mice, suggesting a modest alteration of T-cell homeostasis associated with adenomyosis. A significant decrease in total T-cell abundance was observed in FTY720-treated mice relative to CTL mice ($P = 0.0365$), consistent with the known lymphocyte-sequestering effects of S1P receptor modulation. In contrast, SKI-5C-treated mice exhibited total T-cell levels comparable to those of CTL mice, indicating that sphingosine kinase inhibition preserved uterine T-cell abundance despite disease induction and pharmacological intervention (Fig. 3G). Within this T-cell compartment, NKT-like cells were significantly increased in SKI-5C-treated mice compared with CTL mice ($P = 0.0054$) (Fig. 3H). Evaluation of conventional T-cell subsets showed a trend toward increased $CD4^+CD8^-$ T cells in ADM mice compared with CTL, as well as a significant increase in $CD4^+CD8^-$ T cells in SKI-5C-treated mice ($P = 0.02$). In contrast, the abundance of $CD8^+CD4^-$ T cells did not differ significantly between the experimental groups. Similarly, no significant differences were observed for double-negative or double-positive T-cell populations across groups. Overall, double-negative T cells represented the most

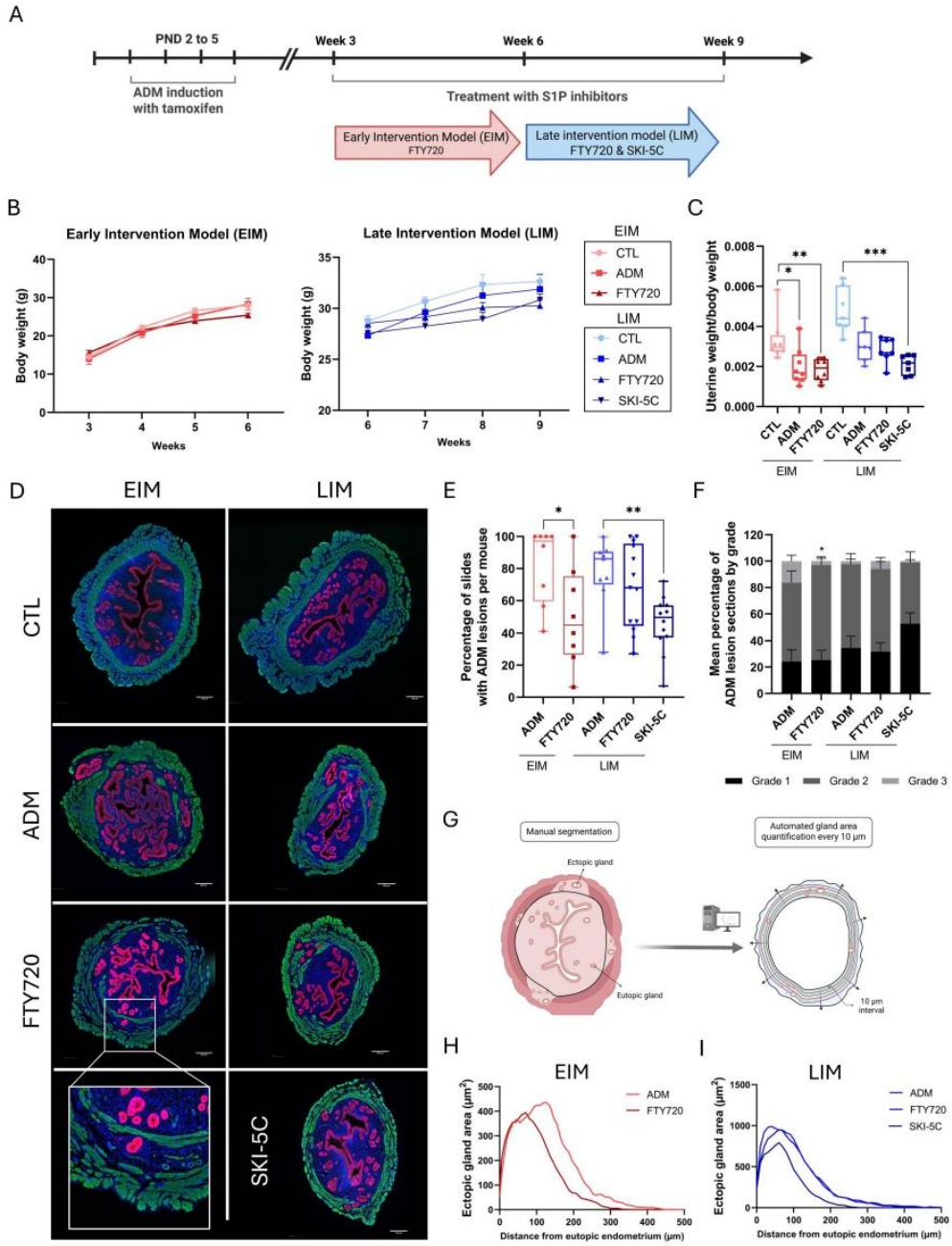


Figure 2. Preventive and therapeutic pharmacological modulation of the sphingosine-1-phosphate (S1P) pathway: systemic effects and lesion outcomes. (**A**) Experimental design: early intervention model (EIM) with daily FTY720 from weaning for 3 weeks, and late intervention model (LIM) with daily FTY720 or SKI-5C initiated at 6 weeks of age, when lesions were established. (**B**) Body weight evolution during treatment. Body-weight trajectories are shown to document potential systemic effects of FTY720 and SKI-5C during disease progression, as uterine-weight ratios can only be assessed at sacrifice. (**C**) Uterine weight at sacrifice normalized to body weight. Preventive and therapeutic pharmacological modulation of the S1P pathway did not restore uterine weight in adenomyotic (ADM) mice, although SKI-5C further reduced relative uterine weight in the late intervention model. (**D**) Representative uterine sections from control (CTL), ADM, and treated groups in EIM (FTY720) and LIM (FTY720, SKI-5C). Red highlights = epithelial glands (EpCam immunolabeling); green = myometrium (aSMA immunolabeling). Scale bar, 200 µm (**E**) Prevalence of adenomyotic lesions, expressed as percentage of uterine sections containing ectopic glands. An average of 19 ± 2 sections per animal (EIM) and 35 ± 4 (LIM) were analyzed spaced by ≥ 50 µm. (**F**) Distribution of lesion grades was defined according to adenomyotic involvement of the inner third (grade I), two-thirds (grade II), or entire myometrium (grade III). (**G**) Diagram illustrating the quantification pipeline: manual segmentation of ectopic glands and automated quantification of glandular area every 10 µm from the endometrial–myometrial junction. (**H–I**) Ectopic glandular invasion plotted as gland area versus distance from eutopic endometrium in EIM (**H**) and LIM (**I**). Preventive FTY720 treatment significantly reduced lesion prevalence, the proportion of high-grade lesions, and glandular invasion depth, whereas in established disease, only SKI-5C decreased lesion prevalence and reduced glandular invasion throughout the myometrium. Sample sizes: for body and uterine weights (B and C), n = 8 mice/group in EIM and n=7 mice/group in LIM; for lesion prevalence and invasion analyses (E, H–I), n = 8 mice/group in EIM, and n = 9 ADM, 13 FTY720, and 12 SKI-5C in LIM. Statistical significance was determined using the Kruskal–Wallis test followed by Dunn's *post hoc* test for panels B, C, E; the Kolmogorov–Smirnov test for panels H and I; the Kruskal–Wallis test for the analysis of lesion grades in the LIM group; and the Mann–Whitney *U* test in the EIM group for Panel F. *$P < 0.05$; **$P < 0.01$; ***$P < 0.001$.

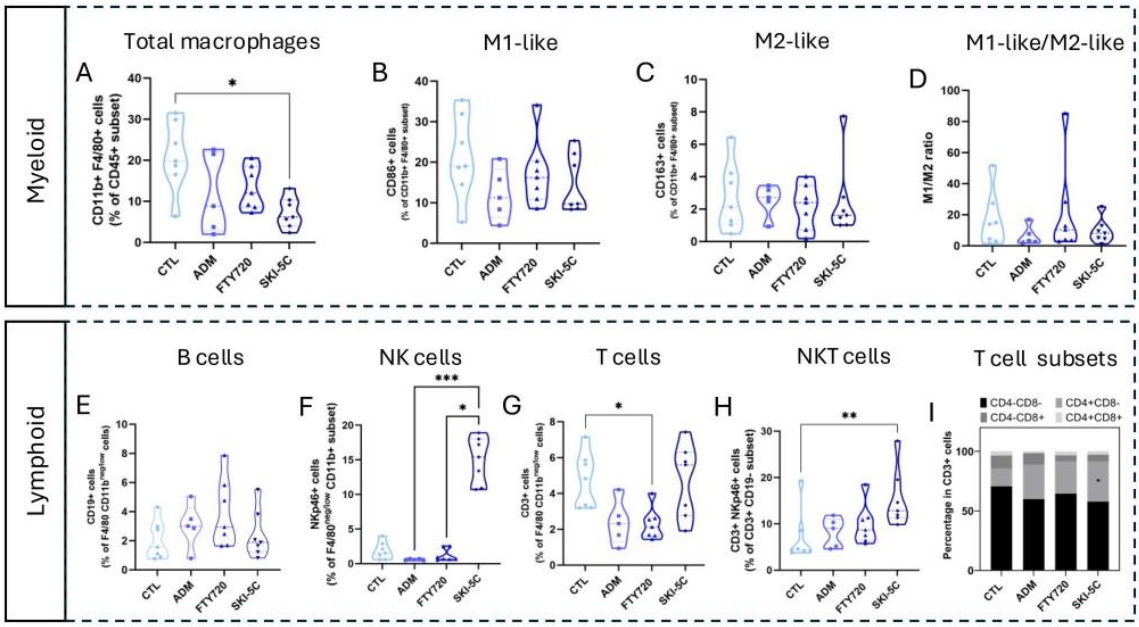


Figure 3. Immune profiling of adenomyosis following sphingosine-1-phosphate (S1P) pathway inhibition. Representative violin plots showing the percentage of (**A**) total macrophages ($CD45^+F4/80^+CD11b^+$), (**B**) M1-like macrophages ($F4/80^+CD11b^+CD86^+$), (**C**) M2-like macrophages ($F4/80^+CD11b^+CD163^+$), (**D**) M1-like/M2-like macrophages ratio, (**E**) B cells ($CD45^+F4/80^{low/neg}CD11^{low/neg}CD19^+$), (**F**) NK cells ($CD45^+F4/80^{low/neg}CD11b^+NKp46^+$), (**G**) total T cells ($CD45^+F4/80^{low/neg}CD11^{low/neg}CD3^+$), (**H**) NKT-like cells ($CD3^+NKp46^+$), and (**I**) T cells subsets: $CD4^-CD8^-$ (DN, black), $CD4^+CD8^-$ ($CD4^+$, light grey), $CD4^-CD8^+$ ($CD8^+$, dark grey), and $CD4^+CD8^+$ (DP, very light grey), in uteri of control (CTL), adenomyosis (ADM), and treated (FTY720 and SKI-5C) mice. Rows correspond respectively to CTL, ADM, FTY720, SKI-5C. The late intervention model revealed no major immune alterations associated with adenomyosis alone, with unchanged macrophage polarization and B-cell abundance. In contrast, SKI-5C selectively modulated uterine lymphoid populations by increasing NK and NKT-like cells and preserving total T-cell levels, whereas FTY70 reduced uterine T-cell abundance. Group sizes were n = 7. Statistical significance was determined using the Kruskal–Wallis test followed by Dunn's *post hoc* test. *$P < 0.05$; **$P < 0.01$.

abundant subset in all conditions, whereas double-positive T cells remained rare (Fig. 3I). Representative flow cytometry panels of B cells, NK cells, and T-cell populations subsets are shown in Supplementary Fig. S3.

Overall, pharmacological modulation of this S1P pathway, particularly through sphingosine kinase inhibition with SKI-5C, was associated with selective alterations in uterine immune cell populations, whereas adenomyosis alone induced limited changes in the immune compartments analyzed.

Modulation of inflammatory, angiogenic, and invasive gene expression by S1P inhibitors

Given the central role of S1P signaling in inflammation, angiogenesis, and tissue remodeling, we next explored whether pharmacological inhibition modulates the uterine expression of selected genes involved in these processes (Spiegel and Milstien, 2011; Donati *et al.*, 2021; Gomez-Larrauri *et al.*, 2025). We focused on cytokines with pro-inflammatory (*Il6*, *Tnfα*) or anti-inflammatory/immunoregulatory (*Il10*, *Tgfβ*) functions, the angiogenic factor *Vegf*, and the invasion-associated protease urokinase-type plasminogen activator (*Plau*), comparing expression patterns across CTL, ADM, and treated groups in both intervention models (EIM and LIM).

In ADM mice, *Il6* expression was significantly increased in the EIM ($P = 0.0479$), and FTY720 treatment did not counteract this increase. In the LIM, *Il6* did not differ between CTL and ADM, but both inhibitors induced *Il6* upregulation compared to CTL ($P < 0.01$, Fig. 4A). *Tnfa* remained unchanged between CTL and ADM in both models, and neither inhibitor modified *Tnfa* levels relative to ADM (Fig. 4B). *Il10* expression was increased by FTY720 in the EIM ($P = 0.0486$, FTY720 vs CTL) and by both inhibitors in the LIM ($P < 0.001$; Fig. 4C). *Tgfb* did not differ markedly between CTL and ADM in either model. Neither FTY720 nor SKI-5C significantly modified *Tgfb* expression compared with ADM in the EIM or LIM (Fig. 4D). The apparent reductions observed in both models occur only when treatments are compared with CTL ($P < 0.05$), a comparison that is not biologically informative in this context. *Vegf* expression was significantly lower in ADM mice compared to CTL in the EIM ($P = 0.0497$) and remained low in FTY720 treated mice ($P = 0.05$; Fig. 4E). In the LIM, *Vegf* expression in ADM uteri was comparable to CTL, whereas both FTY720 and SKI-5C significantly decreased *Vegf* compared with CTL (FTY720 $P = 0.0036$ and SKI-5C $P = 0.0051$), without significant differences relative to ADM (Fig. 4E). Finally, *Plau* expression tended to be elevated in ADM mice, but this increase was not statistically significant, and levels were normalized by both inhibitors in the LIM (ADM vs FTY720 $P = 0.0066$; ADM vs SKI-5C $P = 0.003$; Fig. 4F).

Overall, targeting S1P signaling at distinct regulatory levels variably affected inflammatory cytokines, consistently suppressed *Vegf* in treated groups, and robustly normalized *Plau*, indicating convergent effects on angiogenic and invasive-associated readouts, which complement the histological readouts.

Discussion

Our study provides evidence for a dynamic, stage-dependent dysregulation of the S1P signaling pathway in a murine model of adenomyosis and evaluates the therapeutic potential of targeting this pathway with two pharmacological inhibitors, FTY720 and SKI-5C. By integrating gene expression analysis, histological

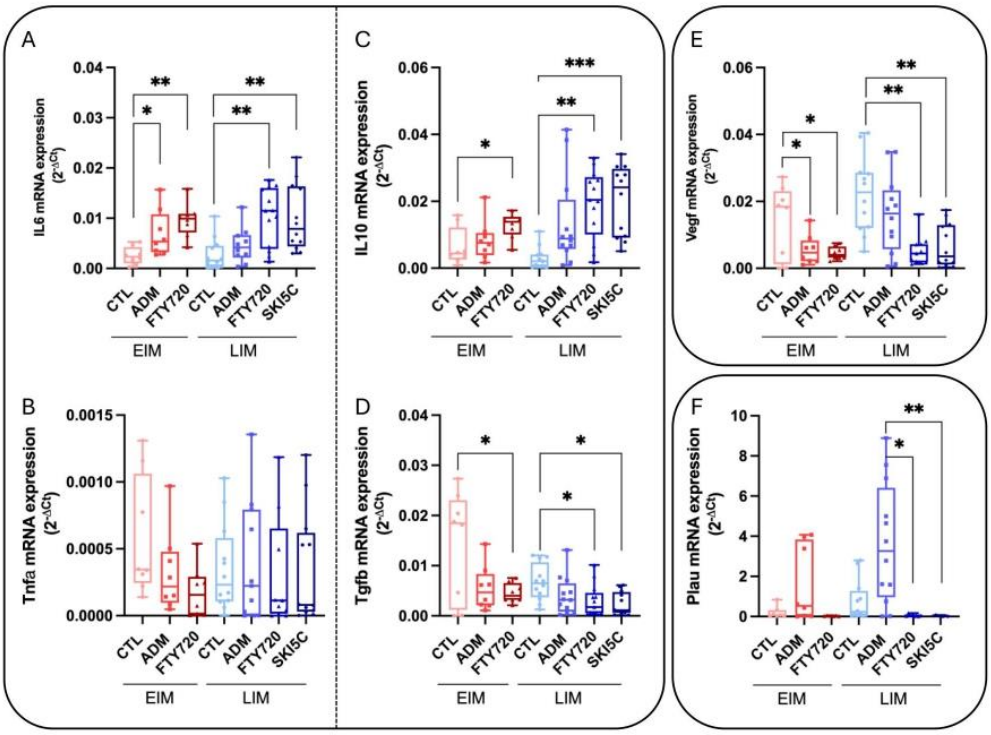


Figure 4. Modulation of inflammatory, angiogenic, and invasive gene expression in uterine tissues following sphingosine-1-phosphate (S1P) pathway inhibition in early (EIM) and late (LIM) intervention models. (**A** and **B**) Relative mRNA expression of inflammatory (*Il6*, *Tnfα*) and (**C** and **D**) regulatory (*Il10*, *Tgfβ*) cytokines, as well as (**E**) angiogenic (*Vegf*) and (**F**) invasive (*Plau*) mediators. Expression was normalized to *Gapdh* and *Rplp0*. Data are presented as median with interquartile range (IQR). Pharmacological modulation of the S1P pathway variably affected inflammatory cytokine gene expression, with both FTY720 and SKI-5C decreasing *Vegf* expression and normalizing *Plau* levels, indicating convergent effects on angiogenic and invasion-related pathways that parallel the histological findings. Sample sizes: n = 8 mice/group in EIM and n = 12 CTL, n = 9 ADM, n = 13 FTY720, and n = 12 SKI-5C in LIM. Statistical significance was determined using the Kruskal–Wallis test with Dunn's *post hoc* correction. *$P < 0.05$; **$P < 0.01$; ***$P < 0.001$.

assessment, and immune profiling, we demonstrated that pharmacological inhibition of S1P signaling modulates lesion burden and invasion depth and is associated with changes in immune cell composition and selected inflammatory and angiogenic transcripts such as *Vegf* and *Plau*. The rationale for focusing on the S1P pathway stems from its established role in inflammation, fibrosis, angiogenesis, and immune cell trafficking: processes that are central to the adenomyosis pathogenesis (Spiegel and Milstien, 2011; Donati *et al.*, 2021; Gomez-Larrauri *et al.*, 2025). Importantly, our study design captured potential temporal differences in S1P signaling by analyzing both early and late disease stages and linking these findings to therapeutic interventions.

Our data support a temporal modulation of S1P pathway components, with early disease showing reduced expression of degradation enzymes and later stage marked by sustained *Sphk1* upregulation, consistent with increased S1P synthetic capacity rather than direct ligand quantification. *S1pr1* remains persistently upregulated across phases. These findings align with human data reporting altered S1P receptor expression in adenomyotic tissue, including increased *S1pr3*, decreased *S1pr2*, and correlation with the fibrosis marker ACTA2 (Vannuzzi *et al.*, 2022), as well as in endometriotic cysts and peritoneal fluid, positioning S1P as an important regulator of inflammation and angiogenesis (Santulli *et al.*, 2012; Bernacchioni *et al.*, 2021, 2024; Zhang and Lu, 2023). Beyond uterine pathology, S1P signaling has well-established roles in vascular and immune regulation. S1PR1 regulates lymphocyte trafficking and vascular integrity through mechanisms involving VE-cadherin and VEGFR2 (Gaengel *et al.*, 2012), reinforcing its relevance as a therapeutic target in adenomyosis.

This stage-dependent hypothesis is directly supported by our pharmacological experiments. FTY720 was effective only in early disease, whereas SKI-5C exerted significant effects in established lesions, consistent with their distinct modes of action and with the stage-specific expression patterns observed *in vivo*. It is important to note that FTY720 (fingolimod) is a pro-drug that requires phosphorylation by sphingosine kinase-2 (SPHK2) to generate FTY720-phosphate, which induces internalization and degradation of S1PR1, S1PR3, S1PR4, and S1PR5 while sparing S1PR2 (Brinkmann *et al.*, 2002). These pharmacological properties provide a plausible framework to interpret the observation that receptor functional antagonism and synthesis inhibition display efficacy at different stages of the disease, without implying differences in ligand availability. Similar effects have been reported in endometriosis models, where FTY720 reduced inflammation and fibrosis and SKI-5C inhibited lesion growth and vascularization (Rudzitis-Auth *et al.*, 2021; Zhang *et al.*, 2023). Although relative uterine weight was reduced in ADM groups compared with CTL mice in EIM, neither FTY720 in the EIM nor both inhibitors in the LIM significantly modified this parameter compared with untreated ADM. In the neonatal tamoxifen model, decreased uterine weight mainly reflects myometrial remodeling rather

than lesion burden, and we therefore considered it as a non-specific structural read-out rather than a prognostic marker. The absence of uterine weight normalization despite clear effects on lesion prevalence and invasion further supports the notion that S1P pathway modulation primarily targets lesion biology rather than reversing established myometrial architecture. Accordingly, uterine weight changes should not be overinterpreted, and a more refined assessment of myometrial architecture would be required to determine whether SPHK1 inhibition could influence this parameter.

Our findings indicate that S1P dysregulation contributes to the altered immune landscape of adenomyosis. SKI-5C significantly reduced macrophage abundance compared with CTL, whereas macrophage levels in ADM were not significantly altered by treatment. Macrophage polarization markers remained unchanged across groups in our model. This profile differs from some reports in human studies emphasizing M2-like dominance as a key mediator of invasion, fibrosis, and epithelial-to-mesenchymal transistion in ADM and endometriosis (Bourdon *et al.*, 2021b; Stratopoulou *et al.*, 2023; Qiu *et al.*, 2024). In line with the view that the classical M1/M2 paradigm is overly simplistic (Nahrendorf and Swirski, 2016), CD86 and CD163 in our study were therefore interpreted as proxy markers of pro-inflammatory/antigen-presenting versus more tolerogenic/tissue-repair oriented programs, rather than as strict M1/M2 lineages. It is therefore conceivable, based on previous studies, that macrophages may play a more prominent role during the early phases of the disease; however, this was not directly addressed in the present late-stage model.

In contrast, adaptive immunity appeared more dynamically modulated. In our model, total T-cell abundance showed only limited changes in adenomyotic uteri, with a non-significant decrease compared with controls. FTY720 treatment was associated with a significant reduction in total T cells, consistent with its known effects on lymphocyte trafficking. In contrast, SKI-5C-treated mice exhibited same levels of T cells as controls, suggesting a distinct impact on lymphoid homeostasis.

Pharmacological modulation of the S1P pathway further influenced T-cell composition. While $CD4^+$ T cells tended to be increased in ADM mice, this difference did not reach statistical significance, suggesting that alterations in helper T-cell representation may be subtle at this stage of disease progression. These findings partially align with reports of $CD4^+$ T cells predominance and Th17/Treg imbalance in patients (Gui *et al.*, 2014; Lin *et al.*, 2022). $CD8^+$ cytotoxic T cells remained unchanged, which does not support a major contribution of $CD8^+$ cytotoxic responses in this model of disease progression (Liu *et al.*, 2022). A particularly intriguing finding was the SKI-5C-induced increase in NK cells as well as in NKT cells. NKT cells are a heterogeneous lymphocyte population known to exert immunomodulatory functions in various inflammatory and autoimmune contexts (Marrero *et al.*, 2015; Ahmadi *et al.*, 2022). However, their specific role in adenomyosis has not been defined. The increase in NK and NKT-like cells following SKI-5C treatment therefore reflects a treatment-associated shift in lymphoid composition rather than immune normalization. In the absence of functional or lineage-specific analyses, no conclusion can be drawn regarding their contribution to inflammation control or disease resolution in this model.

Across all experimental groups, double-negative ($CD4^-CD8^-$) T cells constituted the predominant T-cell subset in the uterine compartment. This compartment has been reported to include a significant proportion of γδ T cells, which represents a major lymphocyte subset in the murine uterus (Kang *et al.*, 2020; Foyle and Robertson, 2024). These cells regulate inflammation, tissue surveillance, and tissue repair through hormone-sensitive mechanisms (Kang *et al.*, 2020; Pawłowska *et al.*, 2022; Foyle and Robertson, 2024). Within this overall distribution, SKI-5C treatment was associated with an increase in $CD4^+CD8^-$ helper T cells. Collectively, these findings suggest that SKI-5C is associated with measurable changes in uterine T cell composition. Whether these changes are functionally immunoregulatory or directly contribute to disease attenuation cannot be determined from the present data.

Cytokine profiling revealed that *Il6* was elevated in ADM, while *Il10* changes were treatment dependent. These alterations indicate a shift in inflammatory signaling but do not define a consistent pro-inflammatory signature linked to $CD4^+$ T cell accumulation. S1P–S1PR1/3 signaling can induce IL6 via ERK5 activation in endometrial stromal cells (Seidita *et al.*, 2023), and S1P has been shown to promote IL6 expression and proliferation in endometriotic cells (Yoshino *et al.*, 2019). Strikingly, pharmacological modulation of the S1P pathway increased IL10 and IL6 expression in both models. As these changes did not mirror ADM-associated alterations, they are unlikely to reflect a reversal of disease-driven cytokine dysregulation. In parallel, *Vegf* was unexpectedly reduced or unchanged in ADM in both models, despite *S1pr1* overexpression, possibly reflecting compensatory or hormonal regulation (Jung *et al.*, 2012; Bouquerel *et al.*, 2016; Cartier and Hla, 2019). FTY720 significantly reduced *Vegf* expression in both models, while SKI-5C decreased *Vegf* only relative to CTL. These changes suggest that S1P modulation can influence angiogenic signaling, although the relevance to ADM-associated alterations remains limited. Given the known role of S1PR1 in maintaining vascular integrity and regulating angiogenesis through VE-cadherin and VEGFR2 (Gaengel *et al.*, 2012), the observed transcriptional changes suggest that targeting S1P signaling may alter angiogenic and immune-related pathways. Nonetheless, additional studies will be required to confirm whether these changes impact vascular remodeling or immune cell recruitment *in vivo* (Kono *et al.*, 2004; Gaengel *et al.*, 2012).

Beyond these processes, S1P also governs the invasive behavior of endometrial cells through modulation of proteolytic activity. In our model, *Plau* expression was elevated in ADM, consistent with its known role in extracellular matrix degradation. Both FTY720 and SKI-5C normalized *Plau* levels in LIM, pointing to a shared anti-invasive effect. This aligns with the reduced lesion depth under SKI-5C and preventive FTY720. Taken together, these findings indicate that *Plau* may participate in S1P-related invasive programs, although additional pathways are likely involved (Kono *et al.*, 2004; Huang *et al.*, 2017; Fu *et al.*, 2021; Yang *et al.*, 2021).

Strengths and limitations

A major strength of our study lies in its integrative design, combining a stage-dependent murine model of adenomyosis with two pharmacological inhibitors acting through distinct mechanisms. This approach allowed us to capture the temporal evolution of S1P signaling, from early receptor-driven to later synthesis-driven alterations, and to identify stage-specific therapeutic vulnerabilities. Another strength is the integration of transcriptomic, histological, and immunological analyses, which linked molecular dysregulation to immune remodeling and lesion invasion.

Nevertheless, several limitations should be acknowledged. First, the murine model, while highly informative for dissecting temporal and mechanistic dynamics, does not fully replicate the complexity and chronicity of human adenomyosis, which develops over years and under cyclical hormonal influences. Second, immunological profiling focused on selected macrophage and T

cell subsets, leaving other innate and adaptative immune cells compartments unexplored. Furthermore, the low absolute number of CD45$^+$ leukocytes acquired per sample limited the resolution of our flow-cytometric analyses, particularly for rare subsets. Future studies specifically designed to increase the number of CD45$^+$ events per sample will be required to perform more detailed stratification of uterine immune cell populations. Given the already low number of immune cells in late-stage uteri, immune profiling at early stage was not feasible due to even lower cellularity. Third, in the EIM, no SKI-5C group was included. This choice reflected the molecular profile at 4 weeks, where *Sphk1* expression was not yet increased; however, because *S1pr2* is already upregulated early and is not antagonized by FTY720, early SPHK1 inhibition may also be relevant, and the absence of both an early SKI-5C arm and an S1PR2-targeted intervention represents a limitation of the present study. Fourth, pharmacological treatments were of relatively short duration and long-term effects, recurrence, and systemic consequences were not assessed.

Another important limitation relates to the interpretation of gene expression data. Gene expression analyses were performed on whole-uterus lysates, reflecting averages expression across the tissue rather than lesion-specific changes. Because lesion incidence and severity vary between animals in this model, this approach does not allow precise determination of the contribution of lesion-bearing regions.

Protein-level mapping of S1P receptors or SPHK1 was not performed. Available antibodies lack the specificity required for reliable immunohistochemistry in uterine tissues, and Western blotting of whole-uterus lysates would not allow lesion-specific resolution in this diffuse model. For these reasons, we relied on transcript-level profiling, which provided robust comparative information despite these methodological constraints.

In addition, S1P levels were not quantified by LC–MS/MS, which will be required in future studies to directly validate the biochemical impact of pathway modulation. Lastly, translation to the clinical setting will require careful patient stratification according to disease stage, which will be a challenge given the current limitations in diagnostic tools. Together, these limitations highlight the need for validations in human tissues, broader immune and cytokine profiling, and studies addressing combinatorial and long-term treatment strategies.

Conclusion

S1P signaling is dynamically dysregulated in adenomyosis, with early receptor-driven and later synthesis-driven abnormalities. Pharmacological inhibition attenuates disease severity in a stage-dependent manner, with FTY720 being more effective pre-lesion and SKI-5C more effective post-lesion development, without restoring uterine weight. Together, our data identify S1P signaling as a stage-dependent regulator of adenomyosis progression and indicate that distinct levels of pathway targeting, i.e. receptor modulation versus synthesis inhibition, may be required at different disease phases. While these findings provide a strong preclinical rationale for S1P-directed interventions, their translational relevance will depend on precise disease staging and validation in human tissues.

Supplementary data

Supplementary data are available at *Molecular Human Reproduction* online.

Data availability

The data underlying this article will be shared on reasonable request to the corresponding author.

Acknowledgements

We gratefully acknowledge Prof. Michelle Nisolle for her support at the outset of this project, particularly in helping to secure the initial funding. The authors thank Prof. Jacques Donnez for his scientific input during discussions and Emilie Feyereisen and Isabelle Dasoul for their excellent technical assistance. We are furthermore grateful to the GIGA Flow cytometry Platform (University of Liège) for their expertise and support in cell phenotyping.

Authors' roles

Conceptualization, C.M. and M.S.; methodology, M.S., C.M., and S.B.; validation, M.S., J.V., and C.M.; formal analysis, M.S., S.B., L. B., and C.M.; investigation, M.S. and J.V. resources, M.S., J.V., S.B., L.B., and C.M., writing of original draft, M.S. and C.M.; review and editing, M.S., C.M., J.V., L.B. M.-M.D., and A.C.; supervision, C.M., project administration, C.M., A.C.; funding acquisition, C.M., A.C. All authors have read and agreed to the published version of the manuscript.

Funding

This research was funded by the Fonds de la Recherche Scientifique (F.R.S.-FNRS, Belgium), grant numbers T.0171.21, J.0169.25, F 5/4/130/5 (awarded to J.V.) and F 5/4/150/5 (awarded to M.-M.D.), the Fondation contre le Cancer grant number 2018-072 (awarded to A.C.), and the Foundation Léon Fredericq (University of Liège), grant numbers 2023-016 and 2024-085.

Conflict of interest

The authors declare no conflict of interest. The funders had no role in the design of the study, in the collection, analyses or interpretation of data, in the writing of the manuscript, or in the decision to publish the results.

References

Abbott JA. Adenomyosis and Abnormal Uterine Bleeding (AUB-A)—pathogenesis, diagnosis, and management. *Best Pract Res Clin Obstet Gynaecol* 2017;**40**:68–81.

Ahmadi A, Fallah Vastani Z, Abounoori M, Azizi M, Labani-Motlagh A, Mami S, Mami S. The role of NK and NKT cells in the pathogenesis and improvement of multiple sclerosis following disease-modifying therapies. *Health Sci Rep* 2022;**5**:e489.

Bernacchioni C, Capezzuoli T, Vannuzzi V, Malentacchi F, Castiglione F, Cencetti F, Ceccaroni M, Donati C, Bruni P, Petraglia F. Sphingosine 1-phosphate receptors are dysregulated in endometriosis: possible implication in transforming growth factor β–induced fibrosis. *Fertil Steril* 2021;**115**:501–511.

Bernacchioni C, Rossi M, Vannuzzi V, Prisinzano M, Seidita I, Raeispour M, Muccilli A, Castiglione F, Bruni P, Petraglia F *et al.* Sphingosine-1-phosphate receptor 3 is a non-hormonal target to counteract endometriosis-associated fibrosis. *Fertil Steril* 2024;**121**:631–641.

Bian X, Sun Z, Lai J, Li B, Dong X, Guan H, Vankelecom H, Sun Y. Metabolic reprogramming and M2 macrophage depletion define

the microenvironment of adenomyosis. *Front Endocrinol (Lausanne)* 2025;**16**:1602814.
Bird CC, McElin TW, Manalo-Estrella P. The elusive adenomyosis of the uterus-revisited. *Am J Obstet Gynecol* 1972;**112**:583–593.
Bouquerel P, Gstalder C, Müller D, Laurent J, Brizuela L, Sabbadini RA, Malavaud B, Pyronnet S, Martineau Y, Ader I *et al.* Essential role for SphK1/S1P signaling to regulate hypoxia-inducible factor 2α expression and activity in cancer. *Oncogenesis* 2016;**5**:e209.
Bourdon M, Maget AS, Jeljeli M, Doridot L, Marcellin L, Thomas M, Chene C, Chouzenoux S, Batteux F, Chapron C *et al.* Reduced fertility in an adenomyosis mouse model is associated with an altered immune profile in the uterus during the implantation period. *Hum Reprod* 2024;**39**:119–129.
Bourdon M, Santulli P, Doridot L, Jeljeli M, Chêne C, Chouzenoux S, Nicco C, Marcellin L, Chapron C, Batteux F. Immune cells and Notch1 signaling appear to drive the epithelial to mesenchymal transition in the development of adenomyosis in mice. *Mol Hum Reprod* 2021a;**27**:gaab053.
Bourdon M, Santulli P, Jeljeli M, Vannuccini S, Marcellin L, Doridot L, Petraglia F, Batteux F, Chapron C. Immunological changes associated with adenomyosis: a systematic review. *Hum Reprod Update* 2021b;**27**:108–129.
Brinkmann V, Davis MD, Heise CE, Albert R, Cottens S, Hof R, Bruns C, Prieschl E, Baumruker T, Hiestand P *et al.* The immune modulator FTY720 targets sphingosine 1-phosphate receptors. *J Biol Chem* 2002;**277**:21453–21457.
Cartier A, Hla T. Sphingosine 1-phosphate: lipid signaling in pathology and therapy. *Science* 2019;**366**:eaar5551.
Di Paolo A, Vignini A, Alia S, Membrino V, Delli Carpini G, Giannella L, Ciavattini A. Pathogenic role of the sphingosine 1-phosphate (S1P) pathway in common gynecologic disorders (GDs): a possible novel therapeutic target. *Int J Mol Sci* 2022;**23**:13538.
Donati C, Cencetti F, Bernacchioni C, Vannuzzi V, Bruni P. Role of sphingosine 1-phosphate signalling in tissue fibrosis. *Cell Signal* 2021;**78**:109861.
Foyle KL, Robertson SA. Gamma delta (γδ) T cells in the female reproductive tract: active participants or indifferent bystanders in reproductive success? *Discov Immunol* 2024;**3**:kyae004.
Fu X, Yao M, Ye C, Fang T, Wu R. Osteopontin regulates endometrial stromal cell migration in endometriosis through the PI3K pathway osteopontin regulates endometrial cell migration in endometriosis. *Reprod Sci* 2021;**28**:435–446.
Gaengel K, Niaudet C, Hagikura K, Laviña B, Muhl L, Hofmann JJ, Ebarasi L, Nyström S, Rymo S, Chen LL *et al.* The sphingosine-1-phosphate receptor S1PR1 restricts sprouting angiogenesis by regulating the interplay between VE-cadherin and VEGFR2. *Dev Cell* 2012;**23**:587–599.
Gomez-Larrauri A, Larrea-Sebal A, Martín C, Gomez-Muñoz A. The critical roles of bioactive sphingolipids in inflammation. *J Biol Chem* 2025;**301**:110475.
Green AR, Styles JA, Parrott EL, Gray D, Edwards RE, Smith AG, Gant TW, Greaves P, Al-Azzawi F, White INH. Neonatal tamoxifen treatment of mice leads to adenomyosis but not uterine cancer. *Exp Toxicol Pathol* 2005;**56**:255–263.
Gui T, Chen C, Zhang Z, Tang W, Qian R, Ma X, Cao P, Wan G. The disturbance of TH17-Treg cell balance in adenomyosis. *Fertil Steril* 2014;**101**:506–514.
Huang W, Jin A, Zhang J, Wang C, Tsang LL, Cai Z, Zhou X, Chen H, Chan HC. Upregulation of CFTR in patients with endometriosis and its involvement in NFκB-uPAR dependent cell migration. *Oncotarget* 2017;Mar 22**8**:66951–66959.
Jung B, Obinata H, Galvani S, Mendelson K, Ding BS, Skoura A, Kinzel B, Brinkmann V, Rafii S, Evans T *et al.* Flow-regulated endothelial S1P receptor-1 signaling sustains vascular development. *Dev Cell* 2012;**23**:600–610.
Kang S, Wu Q, Huang J, Yang B, Liang C, Chi P, Wu C. Tissue resident memory γδT cells in murine uterus expressed high levels of IL-17 promoting the invasion of trophocytes. *Front Immunol* 2020;**11**:588227.
Kono M, Mi Y, Liu Y, Sasaki T, Allende ML, Wu YP, Yamashita T, Proia RL. The sphingosine-1-phosphate receptors S1P1, S1P2, and S1P3 function coordinately during embryonic angiogenesis. *J Biol Chem* 2004;**279**:29367–29373.
Lin P, Lan X, Chen F, Yang Y, Jin Y, Wang A. Reference gene selection for real-time quantitative PCR analysis of the mouse uterus in the peri-implantation period. *PLoS One* 2013;**8**:e62462.
Lin J, Liu L, Zheng F, Chen S, Yang W, Li J, Mo S, Zeng DY. Exploration the global single-cell ecological landscape of adenomyosis-related cell clusters by single-cell RNA sequencing. *Front Genet* 2022;**13**:1020757.
Liu D, Yin X, Guan X, Li K. Bioinformatic analysis and machine learning to identify the diagnostic biomarkers and immune infiltration in adenomyosis. *Front Genet* 2022;**13**:1082709.
Liu Z, Sun Z, Liu H, Niu W, Wang X, Liang N, Wang X, Wang Y, Shi Y, Xu L *et al.* Single-cell transcriptomic analysis of eutopic endometrium and ectopic lesions of adenomyosis. *Cell Biosci* 2021;**11**:51.
Loring M, Chen TY, Isaacson KB. A systematic review of adenomyosis: it is time to reassess what we thought we knew about the disease. *J Minim Invasive Gynecol* 2021;**28**:644–655.
Maceyka M, Harikumar KB, Milstien S, Spiegel S. Sphingosine-1-phosphate signaling and its role in disease. *Trends Cell Biol* 2012;**22**:50–60.
Marrero I, Ware R, Kumar V. Type II NKT cells in inflammation, autoimmunity, microbial immunity, and cancer. *Front Immunol* 2015;**6**:316.
Moawad G, Fruscalzo A, Youssef Y, Kheil M, Tawil T, Nehme J, Pirtea P, Guani B, Afaneh H, Ayoubi JM *et al.* Adenomyosis: an updated review on diagnosis and classification. *J Clin Med* 2023;**12**:4828.
Nahrendorf M, Swirski FK. Abandoning M1/M2 for a network model of macrophage function. *Circ Res* 2016;**119**:414–417.
Pawłowska A, Natochina Y, Zardzewiały W, Skiba W, Włodarczyk K, Maciejczyk A, Suszczyk D, Wertel I. γδ T lymphocytes as a double-edged sword—state of the art in gynecological diseases. *Int J Mol Sci* 2022;**23**:14797.
Qiu Y, Cao J, Li S, Liu Y, Wan G, Gui T. Macrophage polarization in adenomyosis: a review. *Am J Reprod Immunol* 2024;**91**:e13841.
Rudzitis-Auth J, Christoffel A, Menger MD, Laschke MW. Targeting sphingosine kinase-1 with the low MW inhibitor SKI-5C suppresses the development of endometriotic lesions in mice. *Br J Pharmacol* 2021;**178**:4104–4118.
Santulli P, Marcellin L, Noël JC, Borghese B, Fayt I, Vaiman D, Chapron C, Méhats C. Sphingosine pathway deregulation in endometriotic tissues. *Fertil Steril* 2012;**97**:904–911.
Schmittgen TD, Livak KJ. Analyzing real-time PCR data by the comparative CT method. *Nat Protoc* 2008;**3**:1101–1108.
Seidita I, Tusa I, Prisinzano M, Menconi A, Cencetti F, Vannuccini S, Castiglione F, Bruni P, Petraglia F, Bernacchioni C *et al.* Sphingosine 1-phosphate elicits a ROS-mediated proinflammatory response in human endometrial stromal cells via ERK5 activation. *FASEB J* 2023;**37**:e23061.
Sharara FI, Kheil MH, Feki A, Rahman S, Klebanoff JS, Ayoubi JM, Moawad GN. Current and prospective treatment of adenomyosis. *J Clin Med* 2021;**10**:3410.
Spiegel S, Milstien S. The outs and the ins of sphingosine-1-phosphate in immunity. *Nat Rev Immunol* 2011;**11**:403–415.
Squatrito M, Vervier J, Bernet L, Camboni A, Dolmans MM, Munaut C. Temporal dynamics of uterine immune microenvironment remodeling in a murine model of adenomyosis. *Mol Hum Reprod* 2025;**31**:2025. gaaf057.

Squatrito M, Vervier J, Bindels J, Bernet L, Blacher S, Nisolle M, Munaut C. Impaired fertility in adenomyosis: a murine model reveals endometrial receptivity and progesterone resistance imbalances. *Reproduction* 2024;**167**:e240019.

Stratopoulou CA, Cussac S, d'Argent M, Donnez J, Dolmans M-M. M2 macrophages enhance endometrial cell invasiveness by promoting collective cell migration in uterine adenomyosis. *Reprod Biomed Online* 2023;**46**:729–738.

Vannuccini S, Luisi S, Tosti C, Sorbi F, Petraglia F. Role of medical therapy in the management of uterine adenomyosis. *Fertil Steril* 2018;**109**:398–405.

Vannuccini S, Petraglia F. Recent advances in understanding and managing adenomyosis. *F1000Res* 2019;**8**:F1000 Faculty Rev-283.

Vannuccini S, Tosti C, Carmona F, Huang SJ, Chapron C, Guo SW, Petraglia F. Pathogenesis of adenomyosis: an update on molecular mechanisms. *Reprod Biomed Online* 2017;**35**:592–601.

Vannuzzi V, Bernacchioni C, Muccilli A, Castiglione F, Nozzoli F, Vannuccini S, Capezzuoli T, Ceccaroni M, Bruni P, Donati C *et al.* Sphingosine 1-phosphate pathway is dysregulated in adenomyosis. *Reprod Biomed Online* 2022;**45**:15–18.

Xiaoyu L, Weiyuan Z, Ping J, Anxia W, Liane Z. Comparative serum proteomic analysis of adenomyosis using the isobaric tags for relative and absolute quantitation technique. *Fertil Steril* 2013;**100**:505–510.

Yang B, Gu N, Shi S, Zhang C, Chen L, Ouyang J, Lin Y, Sun F, Xu H. Immunoreactivity of plasminogen activator inhibitor 1 and its correlation with dysmenorrhea and lesional fibrosis in adenomyosis. *Reprod Sci* 2021;**28**:2378–2386.

Yoshino O, Yamada-Nomoto K, Kano K, Ono Y, Kobayashi M, Ito M, Yoneda S, Nakashima A, Shima T, Onda T *et al.* Sphingosine 1 phosphate (S1P) increased IL-6 expression and cell growth in endometriotic cells. *Reprod Sci* 2019;**26**:1460–1467.

Zhai J, Vannuccini S, Petraglia F, Giudice LC. Adenomyosis: mechanisms and pathogenesis. *Semin Reprod Med* 2020;**38**:129–143.

Zhang F, Lu Y. The Sphingosine 1-phosphate axis: an emerging therapeutic opportunity for endometriosis. *Reprod Sci* 2023;**30**:2040–2059.

Zhang F, Peng M, Zheng X, Wang X, Liu X, Chen C, Lu Y. Blocking sphingosine 1-phosphate receptor 1 with modulators reduces immune cells infiltration and alleviates endometriosis in mice. *Reprod Biomed Online* 2023;**47**:103304.

© The Author(s) 2026. Published by Oxford University Press on behalf of European Society of Human Reproduction and Embryology. All rights reserved. For commercial re-use, please contact reprints@oup.com for reprints and translation rights for reprints. All other permissions can be obtained through our RightsLink service via the Permissions link on the article page on our site—for further information please contact journals.permissions@oup.com.
Molecular Human Reproduction, 2026, 32, 1–13
https://doi.org/10.1093/molehr/gaag009
Original Research

Cellular mechanisms of S1P pathway modulation on migration and uPA expression in hESC and 12Z cells.

To complete the *in vivo* findings presented in the previous article and to determine whether S1P pathway modulation exerts direct effects on human endometrial cells, we performed exploratory *in vitro* assays using immortalized endometriotic epithelial (12Z) and stromal (hESC) cell lines. These experiments were designed to evaluate whether S1P signaling, or its pharmacological inhibition, influences cellular processes relevant to adenomyosis pathophysiology, including cell migration and the expression of urokinase-type plasminogen activator (uPA). The methodologies and results of these complementary analyses are detailed below.

MATERIALS AND METHODS

Cell lines and culture conditions

Two human endometrial cell lines were used: 12Z (ABM, T0764) and hESC (ABM, T0533). The 12Z cell line consists of immortalized human endometrial epithelial cells derived from endometriotic lesions, transformed using the SV40 large T antigen. These cells were maintained in DMEM/F-12 medium supplemented with 10% charcoal-stripped fetal bovine serum (FBS), 1% penicillin-streptomycin (P/S), and 1% L-glutamine.

The hESC cell line consists of immortalized human endometrial stromal cells obtained from a healthy donor. These cells were cultured in DMEDM/F-12 medium supplemented with 10% charcoal-stripped FBS, 2% sodium bicarbonate, 1% P/S, 0.2% sodium pyruvate, and 0.1% gentamicin sulfate.

All cells were cultured at 37°C in a humidified incubator with 5% CO2.

Wound healing assay

Cell migration was assessed using an Incucyte® scratch wound assay (Sartorius). 12Z and hESC cells were seeded in their respective complete media into 96-well Incucyte® ImageLock plates (Sartorius, BA-04855) at a density of 10,000 cells/well for 12Z cells and 15,000 cells/well for hESCs. Plates were incubated at 37°C for four days to allow cells to reach confluence. Once the cells reached confluence, they were serum-starved in media containing 2% FBS for 6 hours. An uniform scratch was then created in each well using the Incucyte® WoundMaker Tool (Sartorius, Cat. No. 4563). Immediately after wounding, cells were treated with increasing concentrations (0.1 μM to 10 μM) of the S1P pathway inhibitors SKI-5C and FTY720. Vehicle

controls were also included: DMSO for FTY720 and methyl acetate for SKI-5C (<0.1%). All conditions were tested in triplicate.

Plates were then placed in the Incucyte System, configured to capture images of the scratch area every 6 hours using a 10x objective. Imaging was performed for 24 hours in 12Z and 48 hours in hESCs. Wound closure was automatically quantified using the Incucyte software, which calculates confluence over time, providing a dynamic measure of cell migration. The collected data and images were analyzed to compare the effects of different treatments on wound healing dynamics.

S1P stimulation and gene expression analysis

To assess transcriptional responses to S1P signaling, cells were stimulated with 100 nM S1P for 6h or 24h. In a second set of experiments, cells were pre-treated for 6h with SKI-5C or FTY720 prior to assessing *uPA* (*Plau*) expression. Total RNA was isolated using the High Pure RNA Isolation Kit (Roche, Cat. No. 11828665001), following the manufacturer's protocol for cultured cells. cDNA and qRT-PCR were performed as described above. Human gene expression was normalized to *Gapdh* and *B2M*, commonly housekeeping genes for human samples. Primer sequences are listed in Table 1.

Table 1: Primer sequences used for RT-qPCR analysis of human genes in 12Z and hESC cell lines.

Gene	Forward primer	Reverse primer	Amplicon size (bp)
S1pr1	CCTGTGACATCCTCTTCA	CACTTGCAGCAGGACAT	136
S1pr2	TGGAAACGCAGGAGACGACCT	CGAGTGGAACTTGCTGTTTCGG	125
S1pr3	CATCTGGCATTCGAGCGC	GTTGAAAAAGGGCTCCTC	108
S1pr4	GACAGCTCTCTGAGGCCAAG	TGCACACAGCTTCCTGTACC	183
S1pr5	TGCGCCTTCATCGTGCTAGAGA	TGCCAGCAGATCCGACAACG	117
Sphk1	CCTTCCTCCTTCCCTAGGG	TAGAAGGCCTTACATAGGCAG	174
Sphk2	AGCGTGGTAGCCACTTCAG	GAGCAGTGTACCGATGC	167
Sgpp1	GGTGCTGGAATTGCATGTGG	GGGGCCCAGCTAAAGGTAAT	91
Sgpp2	GGATGCATACGGTCCTGGAT	AACACAGGAAGAATGGCACAACT	153
Sgpl	GAACACTGCCATGCTCGTCTGT	GATGAGGAAGCCTCCCAGACAA	136
uPA	GGCTTAACTCCAACACGCAAGG	CCTCCTTGGAACGGATCTTCAG	129
Gadph	TGCACCACCAACTGCTTAGC	GGCATGGACTGTGGTCATGAG	117
B2m	GCTGTCTCCATGTTTGATGTATCT	CTCTGCTCCCCACCTCTAAGT	84

RESULTS

Baseline S1P pathway expression and transcriptional responses to S1P

Both epithelial (12Z) and stromal (hESC) endometrial cell lines expressed the main components of the S1P signaling pathway at baseline, including receptors and metabolic enzymes (Figure 1 A-B). In 12Z cells, all five S1P receptors were detected, although S1PR4 showed only very low expression levels. These cells also expressed the key metabolic enzymes involved in S1P synthesis and degradation. In contrast, hESC expressed all S1P receptors at varying levels but lacked detectable expression of SGPP2. Upon activation of exogenous S1P, transcriptional responses were modest and transient, observed mainly at 6h and returning to baseline by 24h. In hESC, S1P treatment did not affect the expression of receptors or enzymes (Figure 1 C-D). In contrast, 12Z cells exhibited transient modulation, particularly of S1PR3, S1PR4, and SPHK1 expression (Figure 1 E-F),

Effects of S1P pathway inhibition on cell migration

To explore potential functional consequences, wound-healing assays were performed. Representative images and quantification (Figure 2A-C) showed that FTY720 reduced migration of 12Z epithelial cells in a dose-dependent manner, with significant inhibition at concentrations above 5μM; however, signs of cytotoxicity were observed at 10 μM. SKI-5C did not significantly affect migration at the concentration tested, and similar results were obtained in hESCs (Figure 3).

Regulation of uPA expression by S1P signaling

We next evaluated the expression of urokinase-type plasminogen activator (uPA), a key mediator of tissue invasion. In 12Z cells, S1P stimulation induced a slight, non-significant increase in uPA mRNA levels at 6h, which returned to near baseline values by 24h (Figure 2D). Treatment with the S1P pathway modulators FTY720 and SKI-5C, at concentrations used in migration assays, did not affect uPA expression (Figure 2E). In hESC, uPA expression remained unchanged following S1P stimulation at both 6h and 24h, and was similarly unaffected by either modulator (Figure 3 D-E).

Conclusion and Discussion

Overall, these findings indicate that the S1P signaling machinery is present but only weakly responsive to exogenous stimulation in endometrial and endometriotic cells. However, the reduced migration observed upon S1P pathway inhibition with FTY720 suggests that S1P exerts a pro-migratory influence on endometrial cells. This effect appears to be independent of uPA regulation, pointing to alternative downstream mechanisms linking S1P signaling to endometrial motility.

In vitro, our data only partially overlap with previously published reports on S1P signaling in hESC et 12Z cells. Seidita et al. and Prisinzano et al. described S1P receptor and enzyme expression in these cell lines using TaqMan-based qPCR assays (281,282) and reported expression patterns that differ from those observed here, where SYBR Green and independent designed primers were used. These methodological differences, together with potential variations in cell line handling, passage number, or culture conditions, may account for the discrepancies and underline the need for cautious comparison across studies.

Functionally, prior work has shown that S1P promotes a pro-invasive phenotype in 12Z cells and that FTY720 does not counteract this effect (283), whereas in our monoculture conditions FTY720 reduced the migratory capacity of both 12Z cells and hESC. In the former work, this pro-invasive activity of FTY720 was observed at concentrations around 1μM, while in our study the most pronounced effects on migration were detected at doses > 5 μM, indicating that FTY720 responsiveness may be dose-dependent and influenced by experimental context.

Taken together, these *in vitro* findings suggest that S1P signaling contributes to endometrial cell behavior and adenomyosis progression through context-dependent mechanisms. In monoculture, S1P exerts only modest transcription effects but appeared to sustain baseline epithelial endometriotic and stromal motility independently of uPA regulation. *In vivo*, pharmacological inhibition of the pathway reduced lesion formation and severity, though with distinct profiles depending on the timing and type of intervention. FTY720 effectively prevented lesion progression when administered early, whereas SKI-5C markedly prevented lesion prevalence and glandular invasion in established disease, normalizing uPA expression. These results indicate that while S1P signaling may not strongly drive invasive behavior in

isolated cells, it likely supports pathological remodeling in a complex tissue environment, potentially through stromal-epithelial or inflammatory interactions.

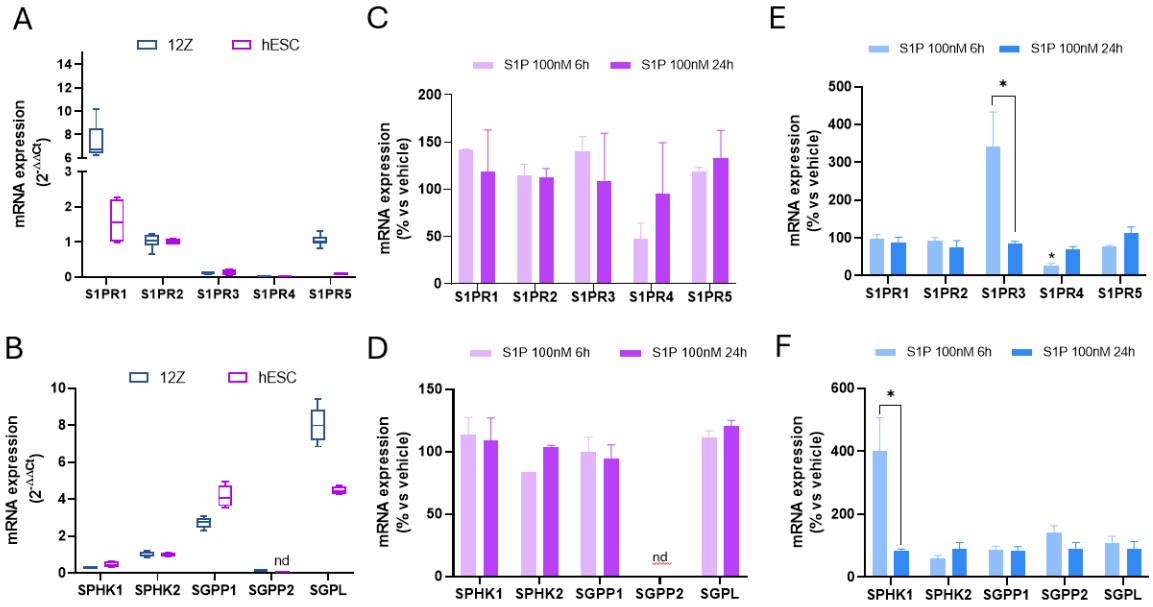


Figure 1. Basal expression and transcriptional responses of S1P in endometrial cell lines (12Z and hESC). *(A-B) Basal mRNA expression of S1P receptors (A) and metabolic enzymes (B) in 12Z and hESC cell lines. Data are expressed as relative expression levels normalized to the mean of reference genes (Gapdh and B2M) using $2^{-\Delta\Delta Ct}$ method. Data are presented as median with interquartile range. (C-D) Relative mRNA expression of S1P receptors (C) and enzymes (D) in hESC cells following stimulation with 100 nM S1P for 6h or 24h. (E-F) Relative mRNA expression of S1P receptors (E) and enzymes (F) in 12Z cells following stimulation with 100nM S1P for 6h or 24h. In panels C-F, data are expressed as percentage of vehicle, set at 100%. Data are presented as mean +/- SEM. Experiments were conducted independently three times in 12Z cells and twice in hESCs, each in technical duplicate. Nd= not detectable. *P<0.05.*

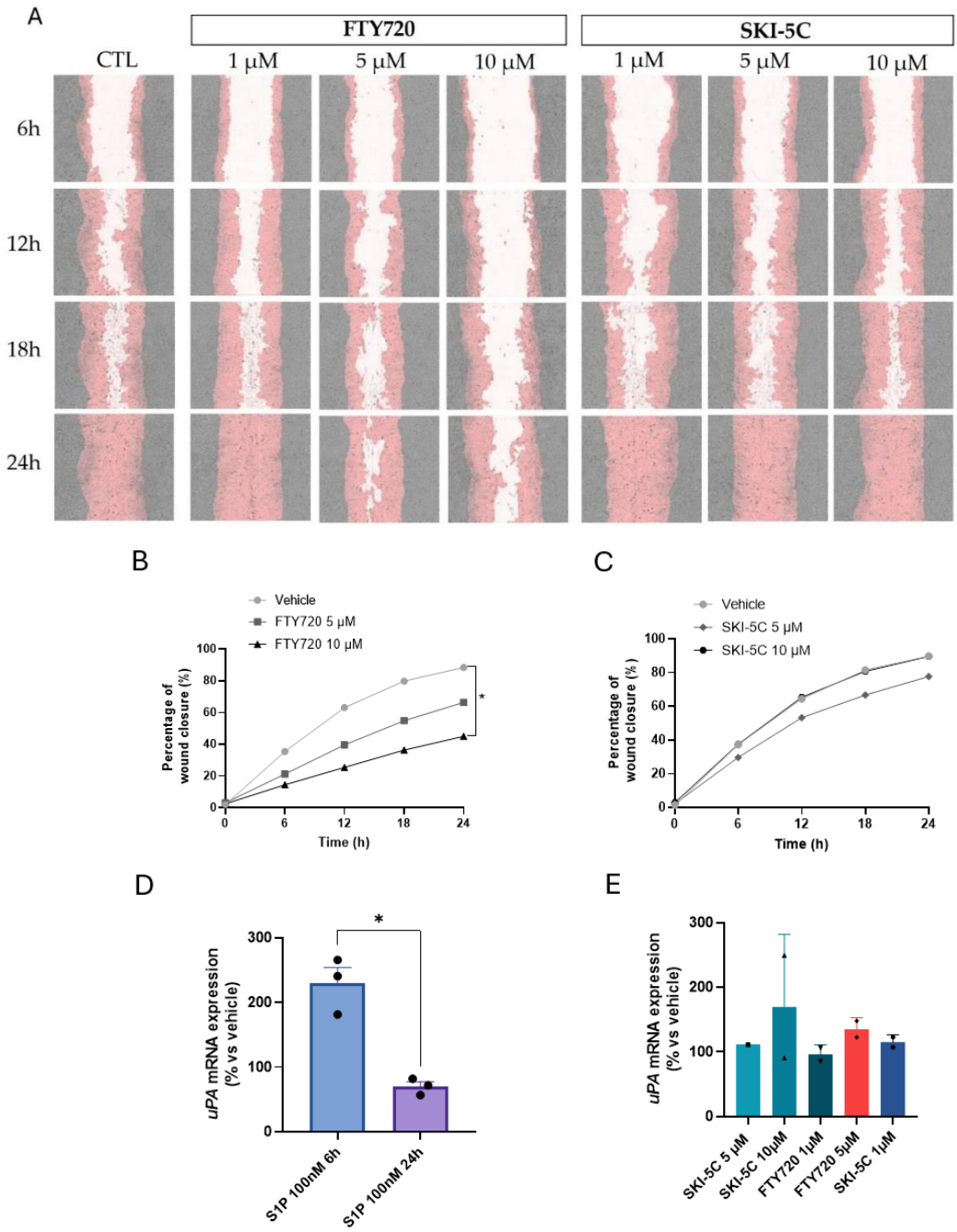


Figure 2. Dose-dependent effect of FTY720 and SKI-5C on the migration and uPA expression in 12Z human endometrial epithelial cells assessed by scratch wound healing assay. *(A) Representative images of wound closure at 6h, 12h, 18h and 24h after scratch in 12Z treated with increasing concentrations of FTY720 or SKI-5C (1µM, 5µM, and 10µM). (B-C) Quantification of wound closure in response to FTY720 (B) and SKI-5C (C). Experiments were performed in three independent biological replicates, each in triplicate. (D) Relative uPA mRNA expression following stimulation with 100 nM S1P for 6h or 24h. Experiments were performed in three independent biological replicates, each in duplicate. (E) Relative uPA mRNA expression after 6h treatment with FTY720 or SKI-5C at the indicated concentrations. Experiments were performed in two independent biological replicates, each in duplicate. In panels D and E, data are expressed as percentage of vehicle-treated cells, set at 100%. Data are presented as mean +/- SEM. Statistical significance was determined using Kruskal-Wallis test with Dunn's post-hoc correction; *p < 0.05.*

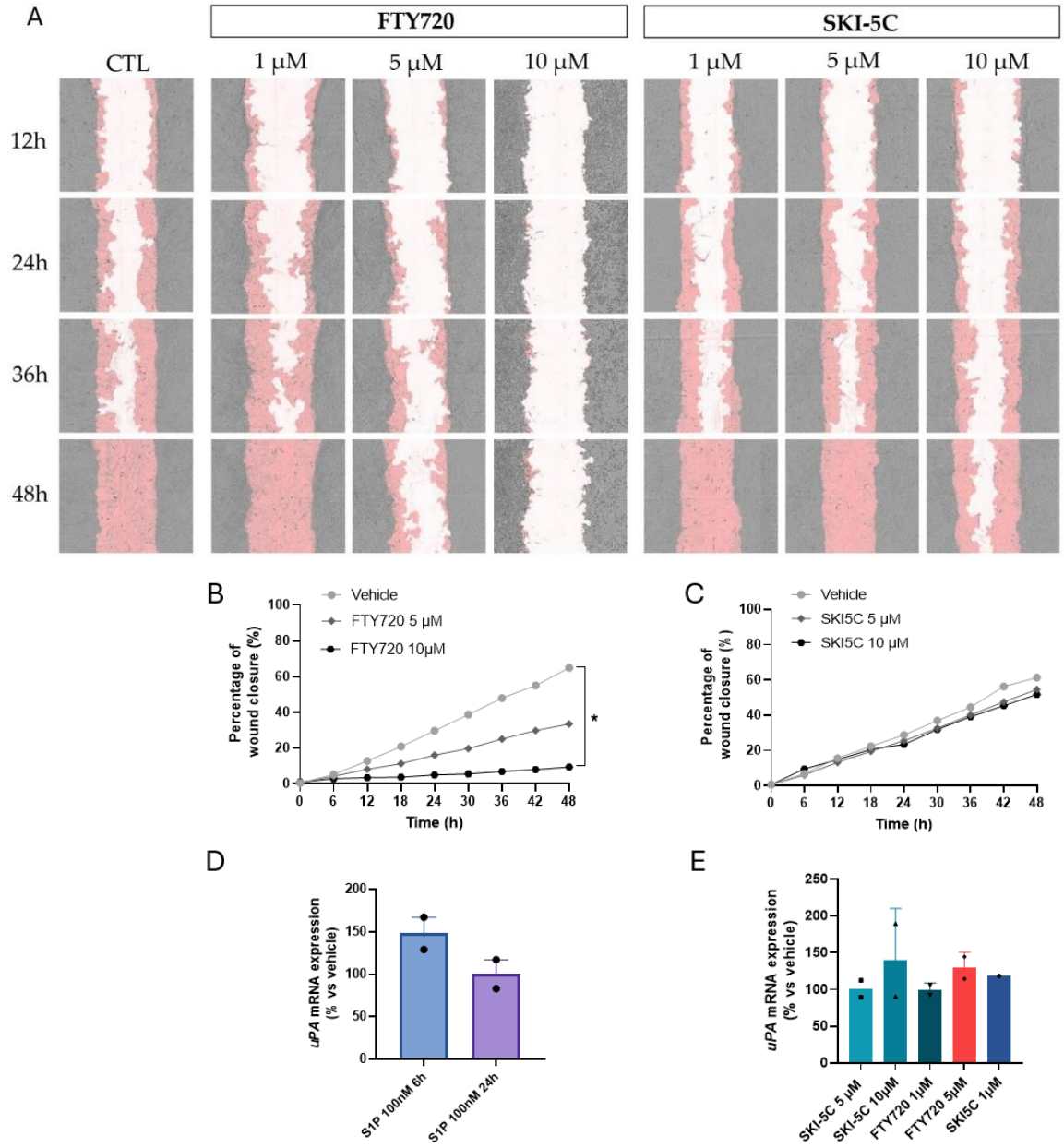


Figure 3. Dose-dependent effect of FTY720 and SKI-5C on the migration and uPA expression in hESC human endometrial stromal cells assessed by scratch wound healing assay. *(A) Representative images of wound closure at 6h, 12h, 18h, 24h and 48h after scratch in hESC treated with increasing concentrations of FTY720 or SKI-5C (1µM, 5µM, and 10µM). (B-C) Quantification of wound closure in response to FTY720 (B) and SKI-5C (C). Experiments were performed in three independent biological replicates, each in triplicate. (D) Relative uPA mRNA expression following stimulation with 100 nM S1P for 6h or 24h. Experiments were performed in two independent biological replicates, each in duplicate. (E) Relative uPA mRNA expression after 6h treatment with FTY720 or SKI-5C at the indicated concentrations. Experiments were performed in two independent biological replicates, each in duplicate. In panels D and E, data are expressed as percentage of vehicle-treated cells, set at 100%. Data are presented as mean +/- SEM. Statistical significance was determined using Kruskal-Wallis test with Dunn's post-hoc correction; *p < 0.05.*

DISCUSSION AND CONCLUSION

GENERAL DISCUSSION

Adenomyosis has long remained a clinical and biological enigma, partly because its symptoms and molecular signatures overlap with comorbid conditions such as endometriosis and fibroids, obscuring its specific contribution to infertility, menstrual dysfunction and pelvic pain. Beyond this symptomatic overlap, adenomyosis also shares inflammatory, endocrine and fibrotic features with these gynecological diseases, which has historically fostered a fragmented view of its pathophysiology rather than a unified disease process. Progress in imaging, genomics and immunology has undoubtedly refined the phenotypic characterization of the disease, yet major knowledge gaps persist regarding its early development, its impact on reproductive function, and the molecular pathways that may constitute actionable therapeutic targets. Human studies face inherent limitations, restricted access to early-stage tissue, substantial inter-individual variability, and the difficulty of disentangling adenomyosis-specific mechanisms from concomitant pathologies, highlighting the critical need for experimental models capable of capturing early disease dynamics in isolation. In this context, the neonatal tamoxifen-induced mouse model provides a window into the pre-lesional and lesional stages of adenomyosis development, enabling the interrogation of uterine, ovarian, immune and molecular processes within a unified biological system. This model therefore offers a unique opportunity to investigate, within the same experimental framework but through complementary studies, functional fertility outcomes, immune remodeling and molecular signaling pathways, and to relate these dimensions conceptually rather than experimentally combining them.

This thesis was built around the idea that adenomyosis is not merely a structural disorder arising from ectopic gland invasion, but rather a multifactorial disease emerging from early dysregulation of immune, endocrine, and inflammatory networks, eventually culminating in aberrant uterine remodeling and impaired reproductive outcomes. More specifically, the work supports a conceptual model in which adenomyosis may represent a pathological continuation of a wound-healing program in the junctional zone, in which failed resolution of inflammation, altered progesterone responsiveness and chronic microenvironmental stress progressively reshape the uterine niche. By integrating reproductive phenotyping, immune profiling, and S1P signaling pathway analyses, the three articles composing this thesis converge to define adenomyosis as a systemic disorder of the uterine microenvironment, structured by temporal transitions in receptivity, immune composition and S1P-dependent remodeling.

The first part of this work focused on fertility and asked whether adenomyosis by itself is sufficient to compromise fertility through combined ovarian and uterine mechanisms. Although clinical studies, particularly IVF and donor-oocyte cohorts, suggest that women with adenomyosis generally retain good ovarian reserve and produce high-quality embryos, they consistently exhibit reduced implantation, lower live-birth rates, and higher miscarriage rates compared with controls (192,299–301). These observations implicate a predominant uterine factor in infertility, yet clinical inference remains hindered by heterogeneity in diagnosis and frequent co-occurrence of endometriosis. The neonatal tamoxifen-induced CD1 model used in this thesis addresses these limitations by producing severe, diffuse adenomyosis in almost all exposed females by three months, in the absence of concurrent gynecological disease. This model allowed us to explore whether adenomyosis without concomitant pathologies may be sufficient to impair both ovarian and uterine parameters, thereby providing an experimental framework to investigate mechanisms that are difficult to isolate in clinical studies. Indeed, affected mice exhibit disrupted estrous cyclicity with prolonged estrus, a significant reduction in primordial, primary and growing follicles, and downregulation of key regulators of folliculogenesis, including FOXL2, BMP15, and FSHR, associated with markedly reduced fertility, litter number and litter size. These findings suggest that severe and diffuse adenomyosis may be associated with alterations in follicular development in this model, although the extent to which these ovarian alterations are directly attributable to adenomyosis itself remains difficult to determine with certainty. Because adenomyosis is induced through neonatal tamoxifen exposure, a period corresponding to a critical window of endocrine and ovarian development in mice, part of the follicular phenotype could theoretically be influenced by early tamoxifen-induced modulation of ovarian physiology rather than adenomyosis alone or by long-term programming effects resulting from early-life estrogen receptor modulation. Experimental studies have indeed reported that tamoxifen in adult mice can affect follicular activation and dynamics (97,98). In contrast, clinical data in women treated with tamoxifen generally indicate that ovarian reserve is largely preserved and that reduced pregnancy rates are not primarily explained by decreased follicular reserve highlighting important differences between developmental exposure in murine models and therapeutic exposure in adult patients (103). Neonatal exposure in mice therefore represents a biologically distinct context. Consequently, the ovarian phenotype observed here may reflect a combination of adenomyosis-associated systemic alterations and developmental endocrine perturbation related to neonatal tamoxifen exposure rather than a purely adenomyosis-driven phenotype which should be considered when interpreting causal relationships between uterine pathology and ovarian dysfunction in this model.

At the uterine level, this thesis identifies a temporal hierarchy of receptivity defects, with early molecular changes preceding overt progesterone resistance. At one month, uteri already showed myometrial disorganization but no invasive lesions, and exhibits decreased HoxA10 and Integrin β3 mRNA together with increased LIF, indicating an abnormal implantation-related signature in a pre-lesional uterus. By three months, progesterone receptor (PGR) expression becomes significantly reduced in stromal and glandular compartments, while HoxA10 downregulation persists, establishing a progesterone-resistant and hyporeactive endometrium. These results align with human data showing reduced stromal PGR expression during secretory phase, decreased HoxA10 in both proliferative and secretory phases, and reduced osteopontin in secretory stroma, whereas integrin β3 and glycodelin maintained largely physiological cyclic patterns (302). Ultrastructural analysis in the same cohort showed fewer and often regressing pinopodes during the window of implantation in adenomyosis patients, compared with abundant, fully developed pinopodes in controls, pointing to asynchronous epithelial maturation (302). Independent transcriptomic and functional studies in eutopic endometrium further revealed dysregulation of implantation and decidualization pathways, including HoxA10-dependent genes and LEF1/IL-11 signaling, reinforcing the notion that adenomyosis induced fundamental impairment of implantation competence (303). Together, these murine and human data support a model in which adenomyosis first impairs implantation-related gene networks, and only later progresses toward overt progesterone resistance, thereby creating a persistent window of suboptimal receptivity that can compromise fertility even before deep structural damage is established.

This interpretation is further supported by recent mechanistic models such as endometrial-myometrial interface disruption (EMID) mouse model, which induced adenomyosis through mechanical injury. Here, implantation sites become abnormally clustered, embryo spacing is reduced, and mid-gestational losses increase despite preserved ovarian histology. RNA-sequencing analyses pinpoint alterations in immune, metabolic and inflammatory pathways including PI3K-Akt, MAPK and TNF signaling that are tightly linked to implantation and placentation (304). Together with clinical IVF studies and our neonatal tamoxifen model, these data support a pathophysiological framework in which adenomyosis may contribute to a structurally and hormonally dysregulated uterus, with subtle ovarian dysfunction, which could collectively contribute to reduced implantation, increased pregnancy loss and fetal growth restriction observed in affected women. Importantly, this interpretation does not challenge clinical ART outcomes but rather suggests that such ovarian alterations are subtle and may be masked under conditions of controlled ovarian stimulation. In this framework, infertility and adverse pregnancy outcomes emerge not from a single dominant defect but

from the convergence of impaired folliculogenesis and uterine architecture and progressive loss of endometrial receptivity.

Taken together, the fertility study suggests that adenomyosis, when examined in isolation in this experimental model, may contribute to a dual ovarian-uterine dysfunction and to establishment of early, stage-dependent defects in endometrial receptivity, thereby supporting the hypothesis that adenomyosis could play an active role in subfertility rather than acting solely as a bystander condition.

The second article deepens this framework by demonstrating that such uterine dysfunction emerges within a profoundly remodeled immune microenvironment, detectable even before lesion formation. At one month, when the uterus still appears largely intact histologically, the tamoxifen-induced model already shows a significant reduction in total CD11b+F4/80+ macrophages with a skewing toward an M2-like phenotype, an increase in uterine B cells, and a remodeling of T-cells subsets characterized by increased CD4+ cells and decreased double-negative (DN) T cells. Concomitant upregulation of *Il6* and *Il10* mRNA, together with reduced expression of *Il6r* and *Stat3* and unchanged *Ptgs2* expression, indicates an IL6-rich immune milieu in which canonical IL6 receptor-STAT3 signaling is attenuated. This pattern suggests that, despite increased IL6 availability, downstream signaling through the IL-6R/STAT3 axis is functionally constrained during early disease priming. By three months, the immune landscape appears to evolve into a chronic state marked by selective reduction of M1-macrophages, persistent B-cell and CD4+ T cells enrichment, expansion of CD8+ T cells, and sustained Il6 expression with normalization of IL10. These observations support a model in which immune dysregulation is not a downstream consequence of gland invasion but rather an upstream driver shaping the uterine milieu in which lesions later expand. In other words, the adenomyotic uterus appears to enter an "immune-primed" state long before deep invasion, characterized by chronic IL-6 exposure and altered macrophages and T-cell compartments, which may be compatible with the progressive loss of receptivity described in the first article.

These immunological alterations uncovered in our model are further supported and nuanced by an important independent study using the same neonatal tamoxifen-induced adenomyosis model. PCR-based profiling of immune-related genes by Bourdon et al. revealed a partially different but complementary picture of early immune activation. At one month, they reported an increase in the M1-associated marker CD86 together with a decrease of the M2 marker Arg1, suggesting an early transcriptional shift toward a pro-inflammatory macrophage phenotype. In parallel, Ncr1, a marker associated with NK cells, was upregulated, CD19 (B-cells) and CD8 (T cytotoxic cells) were decreased (201). At first glance, these findings may appear discordant

with the flow-cytometry-based alterations we identified. However, these apparent discrepancies are likely explained by the different biological layers captured by each technique. Whole-uterus gene expression reflects activation states within a heterogeneous tissue, integrating contributions from epithelial, stromal, vascular and immune cells, while flow-cytometry quantifies the relative abundance and phenotype of immune cell subsets among viable immune cells. Rather than contradicting each other, the two datasets together provide a multi-dimensional, temporally coherent view converging on the same central conclusion: innate and adaptive immune compartments are modulated early in disease and remain altered as lesions develop, revealing an immunological "priming state" that likely predisposes the uterus to aberrant remodeling. This convergence between independent datasets reinforces the notion that immune remodeling is likely to represent a core component of adenomyosis pathogenesis rather than a model-specific artefact.

Nevertheless, the interpretation of immune alterations in this model also requires caution. Tamoxifen has been reported to exert immunomodulatory effects in several experimental systems, including modulation of macrophage activation, neutrophil activity and cytokine signaling pathways (106,107,305). However, these effects remain incompletely characterized and appear to be highly context-dependent. In particular, the impact of neonatal tamoxifen exposure on long-term uterine immune homeostasis is still poorly documented. It therefore cannot be entirely excluded that early pharmacological exposure contributes, at least partially, to the immune landscape observed in the uterus in this model. At the same time, several observations argue against a purely drug-induced effect. The immune alterations identified here persist long after the neonatal exposure and evolve dynamically between pre-lesional and lesional stages. Furthermore, our murine findings align closely with emerging high-resolution human studies. Recent single-cell RNA-seq and spatial transcriptomic studies of eutopic and ectopic adenomyotic endometrium have revealed distinct immune and stromal clusters characterized by macrophage-driven fibrosis programs, enhanced antigen-presentation signatures, and tight spatial interactions between macrophages, T cells and activated fibroblasts at the endometrial-myometrial interface (47,306,307). Independent bioinformatic analysis similarly describe increased infiltration of Th17 cells, CD56dim NK cells, monocytes and memory B cells, together with decreased proportions of activated CD4+, activated CD8+ and γδ T cells in eutopic endometrium of women with adenomyosis (308). While the direction of some T-cell subset changes differs between humans and mice, likely reflecting species-specific immunity as well as differences in disease stage, tissue compartment analyzed, and methodological approaches, two robust points of convergence emerge across systems: the T-cell compartment undergoes deep remodeling, and macrophage polarization states are profoundly altered in adenomyosis.

These early immune alterations may plausibly contribute to the receptivity defects described in the first part of this thesis, although direct causal evidence remains limited. Several human studies are consistent with potential mechanistic links: altered IL6 expression and a dysregulated cytokine milieu during the implantation window have been reported in adenomyosis and are known to interfere with epithelial maturation and decidualization (233,309). In addition, excessive accumulation of macrophages and NK cells has been associated with impaired implantation (223). Thus, while further causal and longitudinal studies are required to establish causality, the immune dysregulation observed here likely represents an additional contributing mechanism, alongside hormonal alterations, ovarian dysfunction and uterine structural changes, through which adenomyosis may compromise fertility. From an integrated perspective, the second article therefore suggests that immune remodeling may represent an early and important component of uterine microenvironmental dysregulation that could interact with endocrine and structural defects to shape the adenomyotic uterus.

Building on this immunological context, the third article of the thesis investigates S1P signaling as a potential upstream regulator of inflammation, invasion and tissue remodeling in adenomyosis. In the adenomyosis-induced mice model, uterine S1P signaling proved to be dynamically dysregulated in a stage-dependent manner. At one month, S1PR1 and S1PR2 mRNA levels are increased, SGPL expression is reduced, and synthetic enzymes remain unchanged, implying an increased S1P tone driven by impaired degradation. By three months, S1PR1 remains elevated but SPHK1 and S1PR4 become upregulated while SGPL normalizes, indicating a transition to increased S1P synthesis and broader receptor engagement in established lesions. This dynamic remodeling echoes human findings in adenomyotic and endometriosis, where altered S1P receptor expression and enzyme activity have been implicated in fibrosis and invasion processes (289,310,311). These patterns suggest that the S1P axis may act as a molecular bridge between chronic inflammation and invasive growth in the adenomyotic uterus.

To determine whether S1P dysregulation constitutes a therapeutically actionable pathway, we assessed two complementary pharmacological inhibitors: FTY720, a functional S1P receptor modulator, and SKI-5C, a selective SPHK1 inhibitor. Preventive FTY720, initiated at weaning before lesion establishment, reduced lesion depth and grade and limited the progression toward deeply invasive adenomyosis whereas therapeutic FTY720 given after lesion establishment had minimal impact, suggesting that receptor-driven processes may dominate early disease susceptibility. Conversely, SKI-5C exerted its main effect in the late therapeutic setting, markedly reducing lesion prevalence and glandular invasion throughout the

myometrium, consistent with the late upregulation of SPHK1. Together, these complementary outcomes support a temporal model in which early disease is shaped primarily by receptor overexpression and impaired degradation, while lesion progression becomes increasingly dependent on SPHK1-mediated S1P synthesis. This stage-dependent efficacy closely mirrors the temporal hierarchy described in the first two articles, where early receptivity and immune changes precede overt structural remodeling, and it suggests that optimal therapeutic strategies may need to be tailored to the pathophysiological phase of the disease.

Interestingly, the major effects of FTY720 and SKI-5C were not mediated by dramatic restructuring of the immune landscape. Although discrete modifications in T-cell subsets were observed under SKI-5C, neither inhibitor induced global depletion or expansion of immune cell populations. Instead, both compounds reprogrammed inflammatory cytokine and angiogenic factors: Il6 levels were maintained or increased, Il10 was elevated, and VEGF expression was consistently reduced. This pattern suggests a shift from a chronic inflammatory state toward a more regulated microenvironment with diminished angiogenic and invasive potential. Together, these findings suggest that S1P targeting acts mainly by modulating key cytokine and angiogenic pathways that condition tissue remodeling, rather than by inducing a global normalization of the immune infiltrate. The reduction of urokinase-type-plasminogen activator (uPA) *in vivo* under both inhibitors further illustrates how S1P targeting attenuates invasive behavior. *In vitro*, exogenous S1P did not significantly modify uPA mRNA in endometriotic epithelial cells, although a modest and transient trend toward increased expression was observed. Importantly for the interpretation of our results, neither FTY720 nor SKI-5C decreased uPA expression in monocultures, even though FTY720 significantly impaired cell migration in scratch assays at high concentrations. This divergence between *in vivo* and *in vitro* findings suggests that the normalization of uPA under S1P signaling inhibition likely depends on the complex uterine microenvironment, compromising epithelial-stromal crosstalk, immune-derived signals and vascular factors, rather than direct transcriptional repression. These results highlight that S1P contributes to adenomyosis through multifaceted programs involving invasion, angiogenesis and microenvironmental regulation, positioning the S1P axis as a central regulatory node. Within the overall thesis, this third study thus identified a potentially druggable lipid-signaling pathway that intersects with the immune changes described earlier and supports a temporal model in which early stages of disease are more dependent on S1P receptor-mediated signaling, whereas established lesions increasingly rely on sustained S1P synthesis, rather than a uniform, stage-independent effect of global pathway inhibition. Taken together, these findings provide preliminary evidence supporting stage-adapted, fertility-preserving strategies in adenomyosis that take into account the evolving dependence on S1P receptor signaling versus S1P production.

Altogether, the three articles of this thesis support a conceptual framework suggesting that adenomyosis may arise, at least in part, from a dysregulated uterine microenvironment shaped by early immune remodeling, impaired inflammatory resolution, progesterone resistance related defects and progressive S1P-driven tissue remodeling. In this view, adenomyosis could be interpreted not only as aberrant endometrial tissue migration but also as potentially reflecting a pathological continuation of a wound-healing program in the junctional zone, characterized by persistent Il6 signaling, M2-skewed macrophages, disrupted progesterone responsiveness and altered sphingolipid metabolism. From a clinical perspective, the management of adenomyosis remains particularly challenging in women wishing to preserve fertility. While hysterectomy is still the only definitive cure, available medical and conservative approaches mainly aim at symptom control, no drug is specifically approved for adenomyosis, and most therapies are extrapolated from endometriosis or abnormal uterine bleeding (312). In this context of limited, non-targeted options, the present work contributes to a more integrated understanding of adenomyosis pathophysiology and offers a conceptual basis for developing future stage-adapted, fertility-preserving therapeutic strategies.

Strengths and limitations

This thesis has several strengths that enhance the robustness and translational relevance of its findings. A major strength lies in the use of a single, well-characterized neonatal tamoxifen-induced murine model, which allows adenomyosis to be studied in isolation, without confounding endometriosis or fibroids, and at clearly defined pre-lesional and lesional stages. This design made it possible to interrogate, within the same biological system, fertility outcomes, immune remodeling and S1P pathway dynamics, and to integrate structural, functional, and molecular readouts rather than addressing these dimensions in separate, non-comparable models. Another strength is the multiparametric approach, combining *in vivo* reproductive assessment, detailed histopathology, flow cytometry, gene expression analyses and complementary *in vitro* assays in human cell lines. The focus on early time points, before lesion formation, is also a key strength, as it captures pre-clinical alterations that are rarely accessible in women and highlights potential windows of opportunity for preventive or stage-adapted interventions.

Several limitations of this thesis should also be acknowledged. First, the entire project is built around preclinical murine and *in vitro* models, which although powerful for mechanistic dissection, cannot fully capture the chronicity, hormonal cycling, heterogeneity and comorbidities that characterize adenomyosis in women. Translation to the clinical setting will therefore require cautious extrapolation and validation in well-phenotyped patient cohorts. In

addition, the neonatal tamoxifen-induced model itself presents inherent limitations. Some developmental or endocrine alterations observed in the model may partly reflect tamoxifen exposure rather than adenomyosis-specific mechanisms and the respective contribution of these two factors cannot be fully disentangled within the present experimental design. Second, the work adopts a reductionist strategy focusing on selected axes: fertility outcomes, uterine immune microenvironment and S1P signaling, while other relevant dimensions such as systemic metabolic factors, neural innervation, epigenetic regulation or microbiota were beyond its scope. As a result, the pathophysiological picture that emerges, although coherent is necessarily partial. A third global limitation lies in the temporal and technical resolution of the analyses. Only a limited number of time-points were examined, which provides a structured but necessarily incompletely resolved view of disease dynamics. Finer temporal mapping and higher dimensional approaches will be required to fully resolve cellular states and interactions across the different phases of disease. In addition, all experiments were conducted under controlled laboratory conditions that differ from the variability of real-world clinical practice, whether in terms of patient characteristics, environmental exposures or treatment histories, which may influence the generalizability of the conclusions. These constraints do not undermine the main messages of the work but should be kept in mind when considering how the present findings can be extended, refined and translated in future studies.

CONCLUSION

Adenomyosis is a major challenge for reproductive health, in a context where hysterectomy remains the only definitive treatment and no targeted medical therapy is approved, particularly for women wishing to preserve their fertility. Clinical management is largely empirical and symptom-oriented, and the frequent coexistence with other gynecological disorders makes it difficult to isolate the specific impact of adenomyosis on ovarian function, uterine receptivity and pregnancy outcomes.

Experimental work using a tamoxifen-induced murine model in the absence of gynecological comorbidities has shown that adenomyosis appears to be associated with alterations in ovarian reserve, estrous cyclicity, endometrial receptivity and fertility, supporting the concept of multifactorial reproductive dysfunctions rather than a purely uterine defect. These functional alterations arise within a remodeled uterine immune microenvironment, characterized at early stages by an “immune-primed” state involving macrophage reprogramming, redistribution of T-cell subsets and persistent Il-6 overexpression. In parallel, this altered immune landscape is accompanied by a dynamic dysregulation of the S1P signaling axis, which appears to integrate inflammatory, invasive, and remodeling processes during disease progression. Pharmacological modulation of the S1P pathway can reduce

lesion severity and invasion in a stage-dependent manner, without fully normalizing the immune cell infiltration, by reshaping cytokine and invasive programs rather than globally suppressing immune responses.

Given the current absence of disease-specific medical therapies and the clinical challenge of balancing symptom control with fertility preservation, these findings contribute to a more integrated understanding of adenomyosis pathophysiology and provide a conceptual framework for the future development of stage-adapted, uterus-preserving therapeutic strategies.

PERSPECTIVES

The findings of this thesis highlight several mechanistic, functional, and translational dimensions associated with adenomyosis, including impaired fertility, immune remodeling, and dysregulation of the S1P pathway. Together, these results provide a solid framework for future studies aimed at refining disease mechanisms and advancing translational strategies. The perspectives outlined below focus on priority research directions emerging directly from the present work.

Fertility: functional dissection of oocyte and uterine contributions

This thesis provides experimental evidence suggesting that adenomyosis may contribute to female fertility impairment through alterations of folliculogenesis, impaired endometrial receptivity, and progesterone resistance. However, the relative contributions of oocyte intrinsic defects versus uterine dysfunction remain to be clarified.

Future studies should therefore assess oocyte competence beyond morphological follicle staging, using functional IVF-based approaches combined with molecular profiling to determine whether adenomyosis directly impairs developmental potential at the gamete level.

Reciprocal embryo transfer experiments represent a key strategy to disentangle uterine versus gametic contributions to subfertility, by independently testing uterine receptivity and embryo developmental competence.

Long-term reproductive follow-up would further refine the impact of adenomyosis on reproductive lifespan by integrating time-to-pregnancy, cumulative pregnancy rates and pregnancy outcome parameters in relation to disease progression.

Immune remodeling: temporal, functional and spatial dissection

The immune analyses presented in this thesis demonstrate that uterine immune remodeling is an early and prominent feature of adenomyosis. Refining the temporal resolution of immune profiling would help to determine whether immune alterations precede structural lesion development or evolve concomitantly with early tissue remodeling.

Further functional characterization of uterine T-cell subsets would be particularly informative to determine whether altered T-cell composition reflects active immune effector programs contributing to lesion initiation, persistence or resolution. In addition, the flow cytometry panel used in this work identified $CD4^+$ T cells based on CD3 and CD4 expression, which does not allow discrimination between conventional $CD4^+$ T helper cells and regulatory T cells (Tregs), a subset of the $CD4^+$ compartment. The presence of Tregs may therefore partially contribute to the $CD4^+$ population quantified in this study, and more refined

immunophenotyping including markers such as FOXP3, CD25 or CD127 would be required to precisely define the functional composition of this compartment.

Macrophage heterogeneity also warrants further investigation, particularly to determine whether specific macrophage subpopulations actively support fibrosis, tissue remodeling, or lesion persistence beyond the classical binary M1/M2 framework.

An additional perspective is to determine whether adenomyosis represents a strictly local uterine pathology or is associated with a broader systemic immune signature, potentially identifiable through peripheral immune profiling.

Finally, probing the requirement of an intact immune system for lesion initiation represents an important mechanistic question. Although inducing adenomyosis in immunodeficient mice would be highly informative, our attempts in neonatal nude mice were unsuccessful due to poor tolerance of tamoxifen exposure, highlighting the technical and physiological limitations of combining severe immunodeficiency with neonatal hormonal induction.

Therapeutics perspectives: refining targets, strategies, and readouts

The therapeutic findings of this thesis demonstrate that modulation of the S1P pathway reduces lesion burden in a stage-dependent manner. Future studies should refine treatment timing and targeting within the S1P axis to optimize therapeutic windows and mechanistic specificity.

Importantly, the present work highlights a differential temporal use of S1P-targeting strategies, as FTY720 was evaluated in a preventive setting whereas SKI-5C was primarily tested at later disease stages. Extending early intervention studies to include SKI-5C would clarify whether inhibition of S1P synthesis can prevent immune remodeling and lesion establishment as efficiently as receptor modulation.

A critical perspective emerging from this work is the need to directly quantify S1P levels in uterine tissue. Measuring sphingolipid metabolites in adenomyotic lesions and adjacent eutopic compartments would validate the assumption of local S1P accumulation and clarify whether the observed effects of S1P-targeting therapies reflect altered ligand availability, receptor signaling or both.

Given the persistent elevation of IL6 observed across disease stages, targeting the IL-6/STAT3 axis represents a complementary therapeutic strategy with the potential to restore progesterone responsiveness, alleviate inflammation, and improve endometrial receptivity.

Combined endocrine and immune-targeted strategies may further enhance therapeutic efficacy by simultaneously restoring progesterone signaling and modulating the inflammatory microenvironment.

Finally, integrating clinically relevant symptomatic endpoints such as pain and bleeding would strengthen the translational relevance of therapeutic studies and help to evaluate the impact of S1P-targeting strategies on patient-centered outcomes.

Integration of MRI in preclinical therapeutic evaluation

An important translational perspective of this work is the integration of MRI for the non-invasive evaluation of adenomyosis in preclinical models. The adaptation of pelvic MRI to the tamoxifen-induced mouse model provides a powerful tool for longitudinal monitoring of lesion development, therapeutic response, and pregnancy progression. Beyond lesion quantification, preclinical MRI offers a unique opportunity to monitor pregnancy *in vivo*, enabling more accurate assessment of implantation success and early pregnancy loss in relation to uterine pathology.

Cross-cutting methodological perspectives: Spatial resolution and lesion-specific biology

Across the studies presented in this thesis, molecular analyses were largely performed on whole uterine tissue, providing global trends but limited spatial resolution. Future work should aim to isolate adenomyotic lesions and adjacent compartments in order to better resolve lesion-specific molecular signatures.

Translational validation: From mouse models to Human pathology

A critical translational perspective concerns the need to distinguish mechanisms intrinsic to adenomyosis from potential effects related to neonatal tamoxifen exposure. Validation across complementary mouse models and in human tissues will be essential to confirm disease-specific pathways. Comparative validation using alternative adenomyosis models and tamoxifen-treated non-susceptible strains would further strengthen mechanistic conclusions by disentangling lesion-driven from model-dependent effects. Together, these murine strategies will help define genuine hallmarks of adenomyosis pathophysiology. However, confirmation in human systems remains essential to establish the clinical relevance of pathways identified in mice.

Human validation should proceed along several complementary approaches combining molecular profiling of adenomyotic lesions and functional evaluation in patient-derived endometrial models. These strategies will determine whether pathways identified in mice are conserved in human disease and clinically relevant. Together, the perspectives outlined above

highlight how this thesis provides a strong mechanistic foundation and opens clearly defined avenues toward translational and fertility-preserving therapeutic strategies in adenomyosis.

REFERENCES

REFERENCES

1. Rokitansky K. Über Uterusdrüsen-Neubildung. Z Gesellschaft Aerzte (Wien). 1860;16:577–81.
2. Bird CC, McElin TW, Manalo-Estrella P. The elusive adenomyosis of the uterus. Am J Obstet Gynecol. 1972;112:583–93.
3. Antero MF, Ayhan A, Segars J, Shih IM. Pathology and Pathogenesis of Adenomyosis. Semin Reprod Med. 2020 May 1;38(2–3):108–18. doi:10.1055/s-0040-1718922 PubMed PMID: 33080632.
4. Santulli P, Vannuccini S, Bourdon M, Chapron C, Petraglia F. Adenomyosis: the missed disease. Reproductive BioMedicine Online. Elsevier Ltd; 2025. doi:10.1016/j.rbmo.2025.104837 PubMed PMID: 40287215.
5. Harmsen MJ, Trommelen LM, de Leeuw RA, Tellum T, Juffermans LJM, Griffioen AW, et al. Uterine junctional zone and adenomyosis: comparison of MRI, transvaginal ultrasound and histology. Ultrasound in Obstetrics and Gynecology. John Wiley and Sons Ltd; 2023. p. 42–60. doi:10.1002/uog.26117 PubMed PMID: 36370446.
6. Upson K, Missmer SA. Epidemiology of Adenomyosis. Semin Reprod Med. 2020 May 1;38(2–3):089–107. doi:10.1055/s-0040-1718920 PubMed PMID: 33105509.
7. Naftalin J, Hoo W, Pateman K, Mavrelos D, Holland T, Jurkovic D. How common is adenomyosis? A prospective study of prevalence using transvaginal ultrasound in a gynaecology clinic. Human Reproduction. 2012;27(12):3432–9. doi:10.1093/humrep/des332 PubMed PMID: 23001775.
8. Lonky NM, Chiu V, Portugal C, Estrada EL, Chang J, Fischer H, et al. Adenomyosis in women undergoing hysterectomy for abnormal uterine bleeding associated with uterine leiomyomas. PLoS One. 2023 Dec 1;18(12 December). doi:10.1371/journal.pone.0294925 PubMed PMID: 38079406.
9. Afzali N, Hafizi L, Abdollahi S. Risk factors for uterine adenomyosis diagnosed by MRI in women of reproductive age. Annals of Medicine & Surgery. 2025 Apr;87(4):1941–6. doi:10.1097/ms9.0000000000003175
10. Yıldırır M, Aytan H, Durukan H, Gürses İ. A clinical scoring system for the diagnosis of adenomyosis. Turk J Obstet Gynecol. 2022;19(2):138–44. doi:10.4274/tjod.galenos.2022.88289

11. Vercellini P, Buffo C, Bandini V, Cipriani S, Chiaffarino F, Viganò P, et al. Prevalence of adenomyosis in symptomatic adolescents and young women: a systematic review and meta-analysis. F and S Reviews. American Society for Reproductive Medicine; 2025. doi:10.1016/j.xfnr.2024.100083

12. Wilk K, Zieba-Domalik M, Wilk K, Bednarz K, Stojko R, Drosdzol-Cop A. Prevalence of adenomyosis in adolescents: diagnostic process and symptoms. Systematic review. Ginekol Pol. 2024 Oct 28. doi:10.5603/gpl.103105

13. Martire FG, d'Abate C, Schettini G, Cimino G, Ginetti A, Colombi I, et al. Adenomyosis and Adolescence: A Challenging Diagnosis and Complex Management. Diagnostics. Multidisciplinary Digital Publishing Institute (MDPI); 2024. doi:10.3390/diagnostics14212344

14. Niaz H, Nayab D, Khan AA. Understanding the Coexistence of Adenomyosis and Uterine Fibroids in Patients with Endometriosis to Enhance Treatment and Fertility Outcomes. Journal of Gandhara Medical and Dental Science. 2024 Dec 31;12(1):7–10. doi:10.37762/jgmds.12-1.617

15. Schrager S, Crystal M. M, Elizabeth A. S. Adenomyosis: Diagnosis and management. Am Fam Physician. 2022 Jan;105(1).

16. Munro MG, Mast AE, Powers JM, Kouides PA, O'Brien SH, Richards T, et al. The relationship between heavy menstrual bleeding, iron deficiency, and iron deficiency anemia. American Journal of Obstetrics and Gynecology. Elsevier Inc.; 2023. p. 1–9. doi:10.1016/j.ajog.2023.01.017 PubMed PMID: 36706856.

17. Fu Y, Wang X, Yang X, Zhao R. Analysis of dysmenorrhea-related factors in adenomyosis and development of a risk prediction model. Arch Gynecol Obstet. 2025 Apr 1;311(4):1081–9. doi:10.1007/s00404-025-07967-y PubMed PMID: 40095084.

18. Chen Q, Li YW, Wang S, Fan QB, Shi HH, Leng JH, et al. Clinical manifestations of adenomyosis patients with or without pain symptoms. J Pain Res. 2019;12:3127–33. doi:10.2147/JPR.S212117

19. Li N, Yuan M, Li Q, Ji M, Jiao X, Wang G. Higher Risk of Anxiety and Depression in Women with Adenomyosis as Compared with Those with Uterine Leiomyoma. J Clin Med. 2022 May 1;11(9). doi:10.3390/jcm11092638

20. Alcalde AM, Martínez-Zamora MÁ, Gracia M, Ros C, Rius M, Nicolás I, et al. Impact of Adenomyosis on Women's Psychological Health and Work Productivity: A Comparative Cross-Sectional Study. J Womens

Health. 2021 Nov 1;30(11):1653–9. doi:10.1089/jwh.2020.8789 PubMed PMID: 33464159.

21. Alcalde AM, Martínez-Zamora MÁ, Gracia M, Ros C, Rius M, Castelo-Branco C, et al. Assessment of Quality of Life, Sexual Quality of Life, and Pain Symptoms in Deep Infiltrating Endometriosis Patients With or Without Associated Adenomyosis and the Influence of a Flexible Extended Combined Oral Contraceptive Regimen: Results of a Prospective, Observational Study. Journal of Sexual Medicine. 2022 Feb 1;19(2):311–8. doi:10.1016/j.jsxm.2021.11.015 PubMed PMID: 34974988.

22. Campo S, Campo V, Benagiano G. Adenomyosis and infertility. Reproductive BioMedicine Online. 2012. p. 35–46. doi:10.1016/j.rbmo.2011.10.003 PubMed PMID: 22116070.

23. Bazot M, Cortez A, Darai E, Rouger J, Chopier J, Antoine JM, et al. Ultrasonography compared with magnetic resonance imaging for the diagnosis of adenomyosis: correlation with histopathology. Human Reproduction. 2001. Report.

24. Harmsen MJ, Van den Bosch T, de Leeuw RA, Dueholm M, Exacoustos C, Valentin L, et al. Consensus on revised definitions of Morphological Uterus Sonographic Assessment (MUSA) features of adenomyosis: results of modified Delphi procedure. Ultrasound in Obstetrics and Gynecology. 2022 Jul 1;60(1):118–31. doi:10.1002/uog.24786 PubMed PMID: 34587658.

25. Chatroux L, Maghsoudlou P, Ajao M, King L, Groszmann Y. Ultrasound diagnosis of adenomyosis- a blinded validation study of the 2022 MUSA guidelines. Am J Obstet Gynecol. 2024 Apr.

26. Champaneria R, Abedin P, Daniels J, Balogun M, Khan KS. Ultrasound scan and magnetic resonance imaging for the diagnosis of adenomyosis: Systematic review comparing test accuracy. Acta Obstetricia et Gynecologica Scandinavica. 2010. p. 1374–84. doi:10.3109/00016349.2010.512061 PubMed PMID: 20932128.

27. Novellas S, Chassang M, Delotte J, Toullalan O, Chevallier A, Bouaziz J, et al. MRI characteristics of the uterine junctional zone: From normal to the diagnosis of adenomyosis. American Journal of Roentgenology. 2011. p. 1206–13. doi:10.2214/AJR.10.4877 PubMed PMID: 21512093.

28. Tellum T, Matic G V., Dormagen JB, Nygaard S, Viktil E, Qvigstad E, et al. Diagnosing adenomyosis with MRI: a prospective study revisiting the junctional zone thickness cutoff of 12 mm as a diagnostic marker. Eur Radiol. 2019 Dec 1;29(12):6971–81. doi:10.1007/s00330-019-06308-3 PubMed PMID: 31264010.

29. Guo SW. The pathogenesis of adenomyosis vis-à-vis endometriosis. Journal of Clinical Medicine. MDPI; 2020. doi:10.3390/jcm9020485

30. Leyendecker G, Wildt L, Mall G. The pathophysiology of endometriosis and adenomyosis: Tissue injury and repair. Arch Gynecol Obstet. 2009 Oct;280(4):529–38. doi:10.1007/s00404-009-1191-0 PubMed PMID: 19644696.

31. García-Solares J, Donnez J, Donnez O, Dolmans MM. Pathogenesis of uterine adenomyosis: invagination or metaplasia? Fertility and Sterility. Elsevier Inc.; 2018. p. 371–9. doi:10.1016/j.fertnstert.2017.12.030 PubMed PMID: 29566849.

32. Curtis KM, Hillis SD, Marchbanks PA, Peterson HB. Disruption of the endometrial-myometrial border during pregnancy as a risk factor for adenomyosis. Am J Obstet Gynecol. 2002;187(3):543–4. doi:10.1067/mob.2002.124285

33. Schwab KE, Chan RWS, Gargett CE. Putative stem cell activity of human endometrial epithelial and stromal cells during the menstrual cycle. Fertil Steril. 2005 Oct;84(SUPPL. 2):1124–30. doi:10.1016/j.fertnstert.2005.02.056 PubMed PMID: 16210003.

34. Gargett CE. Uterine stem cells: What is the evidence? Human Reproduction Update. 2007. p. 87–101. doi:10.1093/humupd/dml045 PubMed PMID: 16960017.

35. Chapron C, Tosti C, Marcellin L, Bourdon M, Lafay-Pillet MC, Millischer AE, et al. Relationship between the magnetic resonance imaging appearance of adenomyosis and endometriosis phenotypes. Human Reproduction. 2017 Jul 1;32(7):1393–401. doi:10.1093/humrep/dex088 PubMed PMID: 28510724.

36. Kishi Y, Suginami H, Kuramori R, Yabuta M, Suginami R, Taniguchi F. Four subtypes of adenomyosis assessed by magnetic resonance imaging and their specification. Am J Obstet Gynecol. 2012;207(2):114.e1-114.e7. doi:10.1016/j.ajog.2012.06.027

37. Kobayashi H, Matsubara S, Imanaka S. Clinicopathological features of different subtypes in adenomyosis: Focus on early lesions. PLoS One. 2021 Jul 1;16(7 July). doi:10.1371/journal.pone.0254147 PubMed PMID: 34260636.

38. Marcellin L, Santulli P, Bourdon M, Maignien C, Campin L, Lafay-Pillet MC, et al. Focal adenomyosis of the outer myometrium and deep infiltrating endometriosis severity. Fertil Steril. 2020 Oct 1;114(4):818–27. doi:10.1016/j.fertnstert.2020.05.003 PubMed PMID: 32741618.

39. Zhai J, Vannuccini S, Petraglia F, Giudice LC. Adenomyosis: Mechanisms and Pathogenesis. Semin Reprod Med. 2020 May 1;38(2–3):129–43. doi:10.1055/s-0040-1716687 PubMed PMID: 33032339.

40. Guo SW. Cracking the enigma of adenomyosis: an update on its pathogenesis and pathophysiology. Reproduction. 2022;164:1741–899. doi:10.1530/REP

41. Zhou W, Peng Z, Zhang C, Liu S, Zhang Y. ILK-induced epithelial-mesenchymal transition promotes the invasive phenotype in adenomyosis. Biochem Biophys Res Commun. 2018 Mar 18;497(4):950–6. doi:10.1016/j.bbrc.2018.01.184 PubMed PMID: 29409901.

42. Polyak K, Weinberg RA. Transitions between epithelial and mesenchymal states: acquisition of malignant and stem cell traits. Nat Rev Cancer. 2009 Apr 5;9(4):265–73. doi:10.1038/nrc2620

43. Bourdon M, Santulli P, Jeljeli M, Vannuccini S, Marcellin L, Doridot L, et al. Immunological changes associated with adenomyosis: A systematic review. Human Reproduction Update. Oxford University Press; 2021. p. 108–29. doi:10.1093/humupd/dmaa038 PubMed PMID: 33099635.

44. Mehasseb MK, Panchal R, Taylor AH, Brown L, Bell SC, Habiba M. Estrogen and progesterone receptor isoform distribution through the menstrual cycle in uteri with and without adenomyosis. Fertil Steril. 2011;95(7). doi:10.1016/j.fertnstert.2011.02.051

45. Maclean A, Tipple L, Newton E, Hapangama DK. Hormone receptor profile of ectopic and eutopic endometrium in adenomyosis: a systematic review. Hum Reprod Open. 2025;2025(1). doi:10.1093/hropen/hoaf002

46. Harmsen MJ, Arduç A, Bleeker MCG, Juffermans LJM, Griffioen AW, Jordanova ES, et al. Increased Angiogenesis and Lymphangiogenesis in Adenomyosis Visualized by Multiplex Immunohistochemistry. Int J Mol Sci. 2022 Aug 1;23(15). doi:10.3390/ijms23158434 PubMed PMID: 35955568.

47. Chen T, Xu Y, Xu X, Wang J, Qiu Z, Yu Y, et al. Comprehensive transcriptional atlas of human adenomyosis deciphered by the integration of single-cell RNA-sequencing and spatial transcriptomics. Protein Cell. 2024 Jul 1;15(7):530–46. doi:10.1093/procel/pwae012 PubMed PMID: 38486356.

48. Vannuccini S, Tosti C, Carmona F, Huang SJ, Chapron C, Guo SW, et al. Pathogenesis of adenomyosis: an update on molecular mechanisms. Reproductive BioMedicine Online. Elsevier Ltd; 2017. p. 592–601. doi:10.1016/j.rbmo.2017.06.016 PubMed PMID: 28693952.

49. Wang X, Cai W, Liang T, Li H, Gu Y, Wei X, et al. The matrix stiffness is increased in the eutopic endometrium of adenomyosis patients: a study based on atomic force microscopy and histochemistry. European Journal of Histochemistry. 2024;68(4131).

50. Wang LN, Ren L, Li L, Liu SL, Lu HJ, Guo ML, et al. Role of SMOC2 in adenomyosis: implications for ECM remodeling and EMT pathogenesis. BMC Womens Health. 2025 Dec 1;25(1). doi:10.1186/s12905-025-03700-8 PubMed PMID: 40181364.

51. D'argent M, Stratopoulou CA, Cussac S, Camboni A, Jadoul P, Donnez J, et al. Are lower levels of apoptosis and autophagy behind adenomyotic lesion survival? Reprod Biomed Online. 2023;47:103248. doi:10.1016/j

52. Zhou Y, Zhao X, Zhang L, Xia Q, Peng Y, Zhang H, et al. Iron overload inhibits cell proliferation and promotes autophagy via PARP1/SIRT1 signaling in endometriosis and adenomyosis. Toxicology. 2022 Jan 15;465. doi:10.1016/j.tox.2021.153050 PubMed PMID: 34826546.

53. Bird CC, McElin TW, Manalo-Estrella P. The elusive adenomyosis of the uterus-revisited. Am J Obstet Gynecol. 1972 Mar 1;112(5):583–93. doi:10.1016/0002-9378(72)90781-8 PubMed PMID: 5059589.

54. Marques ALS, Andres MP, Mattos LA, Gonçalves MO, Baracat EC, Abrão MS. Association of 2d and 3d transvaginal ultrasound findings with adenomyosis in symptomatic women of reproductive age: A prospective study. Clinics. 2021;76. doi:10.6061/CLINICS/2021/E2981 PubMed PMID: 34406269.

55. Chung YJ, Rha SE, Kim MR, Shin YR. Correlation between MRI Features of Adenomyosis and Clinical Presentation. Diagnostics. 2023 Sep 1;13(17). doi:10.3390/diagnostics13172749

56. Szubert M, Koziróg E, Olszak O, Krygier-Kurz K, Kazmierczak J, Wilczynski J. Adenomyosis and infertility—review of medical and surgical approaches. International Journal of Environmental Research and Public Health. MDPI AG; 2021. p. 1–12. doi:10.3390/ijerph18031235 PubMed PMID: 33573117.

57. Yu O, Schulze-Rath R, Grafton J, Hansen K, Scholes D, Reed SD. Adenomyosis incidence, prevalence and treatment: United States population-based study 2006–2015. In: American Journal of Obstetrics and Gynecology. Mosby Inc.; 2020. p. 94.e1-94.e10. doi:10.1016/j.ajog.2020.01.016 PubMed PMID: 31954156.

58. Vannuccini S, Petraglia F. Recent advances in understanding and managing adenomyosis. F1000Research. F1000 Research Ltd; 2019. doi:10.12688/f1000research.17242.1 PubMed PMID: 30918629.

59. Sharma S, Bathwal S, Agarwal N, Chattopadhyay R, Saha I, Chakravarty B. Does presence of adenomyosis affect reproductive outcome in IVF cycles? A retrospective analysis of 973 patients. Reprod Biomed Online. 2019;38(1):13–21. doi:10.1016/j

60. Mishra I, Melo P, Easter C, Sephton V, Dhillon-Smith R, Coomarasamy A. Prevalence of adenomyosis in women with subfertility: systematic review and meta-analysis. Ultrasound in Obstetrics and Gynecology. John Wiley and Sons Ltd; 2023. p. 23–41. doi:10.1002/uog.26159 PubMed PMID: 36647238.

61. Horton J, Sterrenburg M, Lane S, Maheshwari A, Li TC, Cheong Y. Reproductive, obstetric, and perinatal outcomes of women with adenomyosis and endometriosis: A systematic review and meta-analysis. Hum Reprod Update. 2019 Sep 11;25(5):593–633. doi:10.1093/humupd/dmz012 PubMed PMID: 31318420.

62. Bulun SE, Yildiz S, Adli M, Chakravarti D, Parker JB, Milad M, et al. Endometriosis and adenomyosis: shared pathophysiology. Fertility and Sterility. Elsevier Inc.; 2023. p. 746–50. doi:10.1016/j.fertnstert.2023.03.006 PubMed PMID: 36925057.

63. Donnez J, Stratopoulou CA, Marie-Madeleine D. Endometriosis and adenomyosis: Similarities and differences. Best Practice and Research: Clinical Obstetrics and Gynaecology. Bailliere Tindall Ltd; 2024. doi:10.1016/j.bpobgyn.2023.102432 PubMed PMID: 38103509.

64. Habiba M, Guo SW, Benagiano G. Are Adenomyosis and Endometriosis Phenotypes of the Same Disease Process? Biomolecules. Multidisciplinary Digital Publishing Institute (MDPI); 2024. doi:10.3390/biom14010032 PubMed PMID: 38254632.

65. Martire FG, Costantini E, D'Abate C, Schettini G, Sorrenti G, Centini G, et al. Endometriosis and Adenomyosis: From Pathogenesis to Follow-Up. Current Issues in Molecular Biology. Multidisciplinary Digital Publishing Institute (MDPI); 2025. doi:10.3390/cimb47050298

66. Wang X, Benagiano G, Liu X, Guo SW. Unveiling the Pathogenesis of Adenomyosis through Animal Models. Journal of Clinical Medicine. MDPI; 2022. doi:10.3390/jcm11061744

67. Habiba M, Heyn R, Bianchi P, Brosens I, Benagiano G. The development of the human uterus: Morphogenesis to menarche. Human Reproduction Update. Oxford University Press; 2021. p. 1–26. doi:10.1093/humupd/dmaa036 PubMed PMID: 33395479.

68. Vue Z, R. Behringer R. Epithelial morphogenesis in the perinatal mouse uterus. Developmental dynamics. 2020 Nov;249(11):1377–86.

69. Hu J, Gray CA, Spencer TE. Gene expression profiling of neonatal mouse uterine development. Biol Reprod. 2004 Jun;70(6):1870–6. doi:10.1095/biolreprod.103.026336 PubMed PMID: 14985250.

70. Yamashita S, Newbold RR, Mclachlan JA, Korach KS. Development pattern of estrogene receptor expression in female mouse genital tracts. National Institutes of Health. 1989. Report.

71. Filant J, Zhou H, Spencer TE. Progesterone inhibits uterine gland development in the neonatal mouse uterus. Biol Reprod. 2012 May 1;86(5). doi:10.1095/biolreprod.111.097089 PubMed PMID: 22238285.

72. Ho SM, Cheong A, Adgent MA, Veevers J, Suen AA, Tam NNC, et al. Environmental factors, epigenetics, and developmental origin of reproductive disorders. Reproductive Toxicology. 2017 Mar 1;68:85–104. doi:10.1016/j.reprotox.2016.07.011 PubMed PMID: 27421580.

73. Elsherbini M, Koga K, Hiraoka T, Kumasawa K, Maki E, Satake E, et al. Establishment of a novel mouse model of adenomyosis suitable for longitudinal and quantitative analysis and perinatal outcome studies. Sci Rep. 2022 Dec 1;12(1). doi:10.1038/s41598-022-22413-8 PubMed PMID: 36266437.

74. Hao M, Liu X, Guo SW. Adenomyosis in mice resulting from mechanically or thermally induced endometrial–myometrial interface disruption and its possible prevention. Reprod Biomed Online. 2020 Nov 1;41(5):925–42. doi:10.1016/j.rbmo.2020.07.023 PubMed PMID: 32921577.

75. Mori TNH. Mechanisms of developemnt of prolactin-induced adenomyiosis in mice. Acta anat. 1983;116:46–54.

76. Mori T, Nagasawa H, Takahashi S. The induction of adenomyosis in mice by intrauterine pituitary isografts. Life Sciences. 1981. Report.

77. Koujyo T, Hatakeyama S, Yamada H, Iwabuchi K, Kajino K, Ogasawara K, et al. Induction of endometriosis and adenomyosis by transvaginal pituitary transplantation in mice with and without natural killer cell activity. American Journal of Reproductive Immunology. 1998;40(6):441–6. doi:10.1111/j.1600-0897.1998.tb00431.x PubMed PMID: 9894569.

78. Mori T, Kyokuwa M, Nagasawa H. Animal model of uterine adenomyosis: induction of the lesion in rats by ectopic pituitary isografting. Lab Anim Sci. 1998 Feb;48(1):64–8. PubMed PMID: 9517893.

79. Parrott E, Butterworth M, Green A, White INH, Greaves P. Adenomyosis-A Result of Disordered Stromal Differentiation. American Journal of Pathology. 2001;159(2).

80. Green AR, Styles JA, Parrott EL, Gray D, Edwards RE, Smith AG, et al. Neonatal tamoxifen treatment of mice leads to adenomyosis but not uterine cancer. Experimental and Toxicologic Pathology. 2005 Mar 21;56(4–5):255–63. doi:10.1016/j.etp.2004.10.001 PubMed PMID: 15816354.

81. Guo S, Li Z, Yan L, Sun Y, Feng Y. GnRH agonist improves pregnancy outcome in mice with induced adenomyosis by restoring endometrial receptivity. Drug Des Devel Ther. 2018 Jun 7;12:1621–31. doi:10.2147/DDDT.S162541 PubMed PMID: 29922037.

82. Kay N, Huang CY, Yu YC, Chen CC, Chang CC, Huang SJ. The Involvement of Mitochondrial Dysfunction during the Development of Adenomyosis. American Journal of Pathology. 2025 May 1;195(5):861–74. doi:10.1016/j.ajpath.2025.01.014 PubMed PMID: 40010668.

83. Jin Z, Wu X, Liu H, Xu C. Celecoxib, a selective COX-2 inhibitor, markedly reduced the severity of tamoxifen-induced adenomyosis in a murine model. Exp Ther Med. 2020 Mar 6. doi:10.3892/etm.2020.8580

84. Harmsen MJ, Juffermans LJM, Kroon MO, Griffioen AW, Huirne JAF. Anti-angiogenic therapy as potential treatment for adenomyosis. Angiogenesis. 2025 Mar 1;28(1). doi:10.1007/s10456-024-09960-6 PubMed PMID: 39862328.

85. Collins A, Miles GJ, Wood J, MacFarlane M, Pritchard C, Moss E. Patient-derived explants, xenografts and organoids: 3-dimensional patient-relevant pre-clinical models in endometrial cancer. Gynecologic Oncology. Academic Press Inc.; 2020. p. 251–9. doi:10.1016/j.ygyno.2019.11.020 PubMed PMID: 31767187.

86. Xu Y, Cheng T, Wang J, Qiu Z, Guan X, Yu Y, et al. Decoding adenomyosis pathogenesis using an assembloid model. Sci China Life Sci. 2025. doi:10.1007/s11427-025-2981-1

87. Gołąbek-Grenda A, Olejnik A. In vitro modeling of endometriosis and endometriotic microenvironment – Challenges and recent advances. Cellular Signalling. Elsevier Inc.; 2022. doi:10.1016/j.cellsig.2022.110375 PubMed PMID: 35690293.

88. Juárez-barber E, Francés-herrero E, Corachán A, Vidal C, Giles J, Alamá P, et al. Establishment of Adenomyosis Organoids as a Preclinical Model to Study Infertility. J Pers Med. 2022 Feb 1;12(2). doi:10.3390/jpm12020219 PubMed PMID: 35207707.

89. Park Y, Jung JG, Yu ZC, Asaka R, Shen W, Wang Y, et al. A novel human endometrial epithelial cell line for modeling gynecological diseases and for drug screening. Laboratory Investigation. 2021 Nov 1;101(11):1505–12. doi:10.1038/s41374-021-00624-3 PubMed PMID: 34376780.

90. Stratopoulou CA, Rossi M, Beaussart C, Zipponi M, Camboni A, Donnez J, et al. Generation of epithelial-stromal assembloids as an advanced in vitro model of impaired adenomyosis-related endometrial receptivity. Fertil Steril. 2025 Feb 1;123(2):350–60. doi:10.1016/j.fertnstert.2024.08.339 PubMed PMID: 39197515.

91. Krikun G, Mor G, Alvero A, Guller S, Schatz F, Sapi E, et al. A novel immortalized human endometrial stromal cell line with normal progestational response. Endocrinology. 2004 May;145(5):2291–6. doi:10.1210/en.2003-1606 PubMed PMID: 14726435.

92. Fang Z, Wang J, Li T, Yin M, Peng Y, Zhang X. A method for isolating and culturing ectopic epithelial and stromal cells to study human adenomyosis [Internet]. 2023. Available from: https://www.researchsquare.com/article/rs-3194957/v1 doi:10.21203/rs.3.rs-3194957/v1

93. Kim H, Kim M, Im SK, Fang S. Mouse Cre-LoxP system: general principles to determine tissue-specific roles of target genes. Laboratory Animal Research. BioMed Central Ltd; 2018. p. 147–59. doi:10.5625/lar.2018.34.4.147

94. Poulet FM, Roessler ML, Vancutsem PM. Initial uterine alterations caused by developmental exposure to tamoxifen. Reproductive Toxicology. Elsevier Science Inc; 1997. Report.

95. Mehasseb MK, Bell SC, Habiba MA. The effects of tamoxifen and estradiol on myometrial differentiation and organization during early uterine development in the CD1 mouse. Reproduction. 2009 Aug;138(2):341–50. doi:10.1530/REP-09-0054 PubMed PMID: 19451194.

96. Mehasseb MK, Bell SC, Habiba MA. Neonatal administration of tamoxifen causes disruption of myometrial development but not adenomyosis in the C57/BL6J mouse. Reproduction. 2010 Jun;139(6):1067–75. doi:10.1530/REP-09-0443 PubMed PMID: 20368191.

97. Wei W, Komatsu K, Osuka S, Murase T, Bayasula B, Nakanishi N, et al. Tamoxifen Activates Dormant Primordial Follicles in Mouse Ovaries. Reproductive Sciences. 2022 Dec 1;29(12):3404–12. doi:10.1007/s43032-022-00896-0 PubMed PMID: 35212933.

98. Akduman AT, Özerkan K, Zik B, Peker S, Avcı B, Ata B. Effect of tamoxifen on ovarian reserve: A randomized controlled assessor-blind trial in a mouse model. Journal of the Turkish German Gynecology Association. 2014;15(4):228–32. doi:10.5152/jtgga.2014.14166

99. Senkus-Konefka E, Konefka T, Jassem J. The effects of tamoxifen on the female geniatal tract. Cancer Treat Rev. 2004;30(3):291–301. doi:10.1016/j.ctrv.2003.09.004 PubMed PMID: 15059652.

100. Polin SA, Ascher SM. The effect of tamoxifen on the genital tract. Cancer Imaging. 2008. p. 135–45. doi:10.1102/1470-7330.2008.0020 PubMed PMID: 18603495.

101. Ryu KJ, Kim MS, Lee JY, Nam S, Jeong HG, Kim T, et al. Risk of Endometrial Polyps, Hyperplasia, Carcinoma, and Uterine Cancer after Tamoxifen Treatment in Premenopausal Women with Breast Cancer. JAMA Netw Open. 2022 Nov 28;5(11):E2243951. doi:10.1001/jamanetworkopen.2022.43951 PubMed PMID: 36441547.

102. Obstet G, Cohena I, Beytha Y, Shapirah J, Am RT, Fishmanc I, et al. O riginal Paper Gynecologic and Obstetric Investigation High Frequency of Adenomyosis in Postmenopausal Breast Cancer Patients Treated with Tamoxifen. Invest [Internet]. 1997. Report. Available from: http://BioMcdNet.com/kargcr

103. Goldfarb SB, Turan V, Bedoschi G, Taylan E, Abdo N, Cigler T, et al. Impact of adjuvant chemotherapy or tamoxifen-alone on the ovarian reserve of young women with breast cancer. Breast Cancer Res Treat. 2021 Jan 1;185(1):165–73. doi:10.1007/s10549-020-05933-7 PubMed PMID: 32930927.

104. Shandley LM, Spencer JB, Fothergill A, Mertens AC, Manatunga A, Paplomata E, et al. Impact of tamoxifen therapy on fertility in breast cancer survivors. Fertil Steril. 2017 Jan 1;107(1):243-252.e5. doi:10.1016/j.fertnstert.2016.10.020 PubMed PMID: 27887709.

105. Maiorano MFP, Cormio G, Loizzi V, Maiorano BA, D'Oronzo S, Silvestris E. Tamoxifen and Fertility in Women with Breast Cancer: A Systematic Review on Reproductive Outcomes and Oncological Safety of Treatment Interruption. International Journal of Molecular Sciences. Multidisciplinary Digital Publishing Institute (MDPI); 2025. doi:10.3390/ijms26083787 PubMed PMID: 40332441.

106. Corriden R, Hollands A, Olson J, Derieux J, Lopez J, Chang JT, et al. Tamoxifen augments the innate immune function of neutrophils through modulation of intracellular ceramide. Nat Commun. 2015 Oct 13;6. doi:10.1038/ncomms9369 PubMed PMID: 26458291.

107. Behjati S, Frank MH, Physician A. The Effects of Tamoxifen on Immunity. 2009. Report.

108. Hague S, Manek S, Oehler MK, Mackenzie IZ, Bicknell R, Rees M. Tamoxifen induction of angiogenic factor expression in endometrium. Br J Cancer. 2002;86:761–7. doi:10.1038/sj/bjc/6600157

109. Helmestam M, Andersson H, Stavreus-Evers A, Brittebo E, Olovsson M. Tamoxifen modulates cell migration and expression of angiogenesis-related genes in human endometrial endothelial cells. American Journal of Pathology. 2012 Jun;180(6):2527–35. doi:10.1016/j.ajpath.2012.02.026 PubMed PMID: 22531128.

110. Buonomo B, Brunello A, Noli S, Miglietta L, Del Mastro L, Lambertini M, et al. Tamoxifen Exposure during Pregnancy: A Systematic Review and Three More Cases. Breast Care. S. Karger AG; 2020. p. 148–56. doi:10.1159/000501473

111. Ved N, Curran A, Ashcroft FM, Sparrow DB. Tamoxifen administration in pregnant mice can be deleterious to both mother and embryo. Lab Anim. 2019 Dec 1;53(6):630–3. doi:10.1177/0023677219856918 PubMed PMID: 31248325.

112. Barrier BF, Allison J, Hubbard GB, Dick EJ, Brasky KM, Schust DJ. Spontaneous adenomyosis in the chimpanzee (Pan troglodytes): A first report and review of the primate literature: Case Report. Human Reproduction. 2007;22(6):1714–7. doi:10.1093/humrep/dem038 PubMed PMID: 17452396.

113. Ramírez-González JA, Vaamonde-Lemos R, Cunha-Filho JS, Varghese AC, Swanson RJ. Overview of the female reproductive system. In: Exercise and Human Reproduction: Induced Fertility Disorders and Possible Therapies. Springer New York; 2016. p. 19–46. doi:10.1007/978-1-4939-3402-7_2

114. Orsi NM, Baskind NE, Cummings M. Anatomy, Development, Histology and Normal Function of the Ovary. In: Essentials of diagnostic gynecological pathology. 2023. p. 1–33. doi:10.1007/978-3-031-39659-5_1

115. Sun YC, Sun XF, Dyce PW, Shen W, Chen H. The role of germ cell loss during primordial follicle assembly: A review of current advances. Int J Biol Sci. 2017 Jan 1;13(4):449–57. doi:10.7150/ijbs.18836 PubMed PMID: 28529453.

116. Westergaard CG, Byskov AG, Andersen CY. Morphometric characteristics of the primordial to primary follicle transition in the human ovary in relation to age. Human Reproduction. 2007;22(8):2225–31. doi:10.1093/humrep/dem135 PubMed PMID: 17580300.

117. Migale R, Neumann M, Mitter R, Rafiee MR, Wood S, Olsen J, et al. FOXL2 interaction with different binding partners regulates the dynamics of ovarian development. Sci Adv. 2024 Mar;10(10):788.

118. Migale R, Neumann M, Mitter R, Rafiee MR, Wood S, Olsen J, et al. FOXL2 interaction with different binding partners regulates the dynamics of ovarian development [Internet]. 2023. Available from: http://biorxiv.org/lookup/doi/10.1101/2023.04.14.536403 doi:10.1101/2023.04.14.536403

119. Omrizadeh M, Mokhtari P, Eftekhari-Yazdi P, Chekini Z, Meybodi AM. Altered Expression of GDF9 and BMP15 Genes in Granulosa Cells of Diminished Ovarian Reserve Patients: A Case-Control Study. Cell J. 2022 Sep 1;24(9):540–5. doi:10.22074/CELLJ.2022.8077

120. Otsuka F, McTavish KJ, Shimasaki S. Integral role of GDF-9 and BMP-15 in ovarian function. Molecular Reproduction and Development. 2011. p. 9–21. doi:10.1002/mrd.21265 PubMed PMID: 21226076.

121. Murray CM, Orr CJ. Hormonal Regulation of the Menstrual Cycle and Ovulation. In: Maternal-Fetal and Neonatal Endocrinology: Physiology, Pathophysiology, and Clinical Management. Elsevier; 2020. p. 159–67. doi:10.1016/B978-0-12-814823-5.00012-X

122. Rimon-Dahari N, Yerushalmi-Heinemann L, Alyagor L, Dekel N. Ovarian folliculogenesis. Results Probl Cell Differ. 2016 Jun 1;58:167–90. doi:10.1007/978-3-319-31973-5_7 PubMed PMID: 27300179.

123. Reed B, Carr B. Endotext. 2018. The normal menstrual cycle and the control of ovulation .

124. Hawkins SM, Matzuk MM. The menstrual cycle: Basic biology. In: Annals of the New York Academy of Sciences. Blackwell Publishing Inc.; 2008. p. 10–8. doi:10.1196/annals.1429.018 PubMed PMID: 18574203.

125. Critchley HOD, Maybin JA, Armstrong GM, Williams ARW. Physiology of the endometrium and regulation of menstruation. Physiological Reviews. American Physiological Society; 2020. p. 1149–79. doi:10.1152/physrev.00031.2019 PubMed PMID: 32031903.

126. Rosen Vollmar AK, Mahalingaiah S, Jukic AMZ. The menstrual cycle: a vital sign across the lifespan. The Lancet Obstetrics, Gynaecology, & Women's Health. 2025 Jul;100001. doi:10.1016/j.lanogw.2025.100001

127. Cha J, Sun X, Dey SK. Mechanisms of implantation: Strategies for successful pregnancy. Nature Medicine. 2012. p. 1754–67. doi:10.1038/nm.3012 PubMed PMID: 23223073.

128. Conti M, Franciosi F. Acquisition of oocyte competence to develop as an embryo: Integrated nuclear and cytoplasmic events. Human Reproduction Update. Oxford University Press; 2018. p. 245–66. doi:10.1093/humupd/dmx040 PubMed PMID: 29432538.

129. Martinez CA, Rizos D, Rodriguez-Martinez H, Funahashi H. Oocyte-cumulus cells crosstalk: New comparative insights. Theriogenology. Elsevier Inc.; 2023. p. 87–93. doi:10.1016/j.theriogenology.2023.04.009 PubMed PMID: 37105091.

130. Georges A, L'Hôte D, Todeschini AL, Auguste A, Legois B, Zider A, et al. The transcription factor FOXL2 mobilizes estrogen signaling to maintain the identity of ovarian granulosa cells. Elife. 2014 Nov 4;3(November):1–19. doi:10.7554/eLife.04207 PubMed PMID: 25369636.

131. Gilchrist RB, Lane M, Thompson JG. Oocyte-secreted factors: Regulators of cumulus cell function and oocyte quality. Hum Reprod Update. 2008;14(2):159–77. doi:10.1093/humupd/dmm040 PubMed PMID: 18175787.

132. Ulloa-Aguirre A, Reiter E, Crepieux P. FSH receptor signaling: Complexity of interactions and signal diversity. Endocrinology. Oxford University Press; 2018. p. 3020–35. doi:10.1210/en.2018-00452 PubMed PMID: 29982321.

133. Pasquariello R, Ermisch AF, Silva E, Mccormick S, Logsdon D, Barfield JP, et al. Alterations in oocyte mitochondrial number and function are related to spindle defects and occur with maternal aging in mice and humans. Biol Reprod. 2018. doi:10.1093/biolre/ioy248/5206053

134. Tora L, Vincent SD. What defines the maternal transcriptome? Biochemical Society Transactions. Portland Press Ltd; 2021. p. 2051–62. doi:10.1042/BST20201125 PubMed PMID: 34415300.

135. Innocenti F, Fiorentino G, Cimadomo D, Soscia D, Garagna S, Rienzi L, et al. Maternal effect factors that contribute to oocytes developmental competence: an update. Journal of Assisted Reproduction and Genetics. Springer; 2022. p. 861–71. doi:10.1007/s10815-022-02434-y PubMed PMID: 35165782.

136. Favetta LA, Saleh AC, Sabry R. Environmental Effects on Oocyte Quality and Competence. In: Comprehensive Biotechnology. Elsevier; 2019. p. 498–507. doi:10.1016/B978-0-444-64046-8.00470-5

137. Maclean JA, Hayashi K. Progesterone Actions and Resistance in Gynecological Disorders. Cells. MDPI; 2022. doi:10.3390/cells11040647 PubMed PMID: 35203298.

138. Okada H, Tsuzuki T, Murata H. Decidualization of the human endometrium. Reproductive Medicine and Biology. John Wiley and Sons Ltd; 2018. p. 220–7. doi:10.1002/rmb2.12088

139. Yue X, Wu L, Hu W. The Regulation of Leukemia Inhibitory Factor. Cancer Cell Microenviron. 2015 Oct 27. doi:10.14800/ccm.877 PubMed PMID: 26807429.

140. Song H, Lim H, Das Bibhash C Paria SK, Dey SK, Obstetrics Skd. Dysregulation of EGF Family of Growth Factors and COX-2 in the Uterus during the Preattachment and Attachment Reactions of the Blastocyst with the Luminal Epithelium Correlates with Implantation Failure in LIF-Deficient Mice. Molecular Endocrinology. 2000. Report.

141. Aghajanova L, Altmäe S, Bjuresten K, Hovatta O, Landgren BM, Stavreus-Evers A. Disturbances in the LIF pathway in the endometrium among women with unexplained infertility. Fertil Steril. 2009 Jun;91(6):2602–10. doi:10.1016/j.fertnstert.2008.04.010 PubMed PMID: 18684446.

142. Margioula-Siarkou C, Prapas Y, Petousis S, Milias S, Ravanos K, Dagklis T, et al. LIF endometrial expression is impaired in women with unexplained infertility while LIF-R expression in all infertility sub-groups. Cytokine. 2017 Aug 1;96:166–72. doi:10.1016/j.cyto.2017.04.009 PubMed PMID: 28432985.

143. Cai L, Cao Y, Duan E. Role of αVβ3 integrin in embryo implementation in the mouse. Chinese Science Bulletin. 2000;45(22):2077–81. doi:10.1007/BF03183530

144. Daftary GS, Troy PJ, Bagot CN, Young SL, Taylor HS. Direct Regulation of 3-Integrin Subunit Gene Expression by HOXA10 in Endometrial Cells. 2002. Report.

145. Elnaggar A, Farag AH, Gaber ME, Hafeez MA, Ali MS, Atef AM. AlphaVBeta3 Integrin expression within uterine endometrium in unexplained infertility: A prospective cohort study. BMC Womens Health. 2017 Sep 26;17(1). doi:10.1186/s12905-017-0438-3 PubMed PMID: 28950833.

146. Tei C, Maruyama T, Kuji N, Miyazaki T, Mikami M, Yoshimura Y. Reduced Expression of αvβ3 Integrin in the Endometrium of Unexplained Infertility Patients with Recurrent IVF-ET Failures: Improvement by Danazol Treatment 1. Journal of Assisted Reproduction and Genetics. 2003. Report.

147. Dorostghoal M, Ghaffari H o allah, Shahbazian N, Mirani M. Endometrial expression of β3 integrin, calcitonin and plexin-B1 in the

window of implantation in women with unexplained infertility. Int J Reprod BioMed. 2017. Report.

148. Pîrlog LM, Pătrășcanu AA, Ona MD, Cătană A, Rotar IC. HOXA10 and HOXA11 in Human Endometrial Benign Disorders: Unraveling Molecular Pathways and Their Impact on Reproduction. Biomolecules. Multidisciplinary Digital Publishing Institute (MDPI); 2025. doi:10.3390/biom15040563 PubMed PMID: 40305321.

149. Mishra A, Modi D. Role of HOXA10 in pathologies of the endometrium. Rev Endocr Metab Disord. 2025 Feb 1;26(1):81–96. doi:10.1007/s11154-024-09923-8 PubMed PMID: 39499452.

150. Wei Q, St. Clair JB, Fu T, Stratton P, Nieman LK. Reduced expression of biomarkers associated with the implantation window in women with endometriosis. Fertil Steril. 2009 May;91(5):1686–91. doi:10.1016/j.fertnstert.2008.02.121 PubMed PMID: 18672236.

151. Szczepańska M, Wirstlein P, Łuczak M, Jagodziński PP, Skrzypczak J. Reduced expression of HOXA10 in the midluteal endometrium from infertile women with minimal endometriosis. Biomedicine and Pharmacotherapy. 2010 Dec;64(10):697–705. doi:10.1016/j.biopha.2010.09.012 PubMed PMID: 20971605.

152. Godbole G, Suman P, Malik A, Galvankar M, Joshi N, Fazleabas A, et al. Decrease in expression of HOXA10 in the decidua after embryo implantation promotes trophoblast invasion. Endocrinology. 2017 Aug 1;158(8):2618–33. doi:10.1210/en.2017-00032 PubMed PMID: 28520923.

153. Halasz M, Szekeres-Bartho J. The role of progesterone in implantation and trophoblast invasion. J Reprod Immunol. 2013;97(1):43–50. doi:10.1016/j.jri.2012.10.011 PubMed PMID: 23432871.

154. Kim JJ, Fazleabas AT. Uterine receptivity and implantation: The regulation and action of insulin-like growth factor binding protein-1 (IGFBP-1), HOXA10 and forkhead transcription factor-1 (FOXO-1) in the baboon endometrium. Reproductive Biology and Endocrinology. 2004. doi:10.1186/1477-7827-2-34 PubMed PMID: 15200677.

155. Ng SW, Norwitz GA, Pavlicev M, Tilburgs T, Simón C, Norwitz ER. Endometrial decidualization: The primary driver of pregnancy health. International Journal of Molecular Sciences. MDPI AG; 2020. p. 1–20. doi:10.3390/ijms21114092 PubMed PMID: 32521725.

156. Lydon JP, Demayo FJ, Funk CR, Mani SK, Hughes AR, Montgomery CA, et al. Mice lacking progesterone receptor exhibit pleiotropic reproductive abnormalities. Genes Dev. 1995;2266–78.

157. Attia GR, Johns A, Carr BR, Bulun SE. Progesterone Receptor Isoform A But Not B Is Expressed in Endometriosis. J Clin Endocrinol Metab. 2000;85(8):2897–902.

158. Wu Y, Strawn E, Basir Z, Halverson G, Guo SW. Promoter hypermethylation of progesterone receptor isoform B (PR-B) in endometriosis. Epigenetics. 2006;1(2):106–11. doi:10.4161/epi.1.2.2766 PubMed PMID: 17965625.

159. Cakmak H, Taylor HS. Molecular mechanisms of treatment resistance in endometriosis: The role of progesterone-hox gene interactions. Seminars in Reproductive Medicine. 2010. p. 69–74. doi:10.1055/s-0029-1242996 PubMed PMID: 20104430.

160. Gebril M, Hirota Y, Aikawa S, Fukui Y, Kaku T, Matsuo M, et al. Uterine Epithelial Progesterone Receptor Governs Uterine Receptivity through Epithelial Cell Differentiation. Endocrinology (United States). 2020 Dec 1;161(12). doi:10.1210/endocr/bqaa195 PubMed PMID: 33099617.

161. Kim TH, Young SL, Sasaki T, Deaton JL, Schammel DP, Palomino WA, et al. Role of SIRT1 and Progesterone Resistance in Normal and Abnormal Endometrium. Journal of Clinical Endocrinology and Metabolism. 2022 Mar 1;107(3):788–800. doi:10.1210/clinem/dgab753 PubMed PMID: 34665857.

162. Suthaporn S, Jayaprakasan K, Thornton J, Walker K, Medrano JH, Castellanos M, et al. Suboptimal mid-luteal progesterone concentrations are associated with aberrant endometrial gene expression, potentially resulting in implantation failure. Reprod Biomed Online. 2021;42:595–608. doi:10.1016/j

163. Luo Y, Cen C, Liu H, Mo D, Fu P, Liu X, et al. Evaluation of Progesterone Resistance and the Role of Downregulation Protocols in Endometrial Preparation for Frozen Embryo Transfer in Patients with Recurrent Implantation Failure—A Retrospective Study [Internet]. 2025 Feb 24. doi:10.1101/2025.02.22.25322723

164. Chi RPA, Wang T, Adams N, Wu SP, Young SL, Spencer TE, et al. Human endometrial transcriptome and progesterone receptor cistrome reveal important pathways and epithelial regulators. Journal of Clinical Endocrinology and Metabolism. 2020 Apr 1;105(4):E1419–39. doi:10.1210/clinem/dgz117 PubMed PMID: 31665330.

165. Li R, Wang X, Huang Z, Balaji J, Kim TH, Wang T, et al. The role of epithelial progesterone receptor isoforms in embryo implantation. iScience. 2021 Dec 17;24(12). doi:10.1016/j.isci.2021.103487

166. Wetendorf M, Wu SP, Wang X, Creighton CJ, Wang T, Lanz RB, et al. Decreased epithelial progesterone receptor A at the window of receptivity is required for preparation of the endometrium for embryo attachment. Biol Reprod. 2017 Feb 1;96(2):313–26. doi:10.1095/biolreprod.116.144410 PubMed PMID: 28203817.

167. Wu HM, Chen LH, Hsu LT, Lai CH. Immune Tolerance of Embryo Implantation and Pregnancy: The Role of Human Decidual Stromal Cell- and Embryonic-Derived Extracellular Vesicles. International Journal of Molecular Sciences. MDPI; 2022. doi:10.3390/ijms232113382

168. Robson A, Harris/'^ LK, Innes BA, Lash GE, Aljunaidy MM, Aplin JD, et al. Uterine natural killer cells initiate spiral artery remodeling in human pregnancy. The FASEB Journal • Research Communication. doi:10.1096/fi.12-210310

169. Kanter JR, Mani S, Gordon SM, Mainigi M. Uterine natural killer cell biology and role in early pregnancy establishment and outcomes. F and S Reviews. Elsevier Inc.; 2021. p. 265–86. doi:10.1016/j.xfnr.2021.06.002

170. Rossi F, Luppi S, Fejza A, Giolo E, Ricci G, Andreuzzi E. Extracellular matrix and pregnancy: functions and opportunities caught in the net. Reproductive Biology and Endocrinology. BioMed Central Ltd; 2025. doi:10.1186/s12958-025-01348-5 PubMed PMID: 39953593.

171. Robertson SA, Moldenhauer LM, Green ES, Care AS, Hull ML. Immune determinants of endometrial receptivity: a biological perspective. Fertility and Sterility. Elsevier Inc.; 2022. p. 1107–20. doi:10.1016/j.fertnstert.2022.04.023 PubMed PMID: 35618356.

172. Zhao Y, Zhang T, Guo X, Wong CK, Chen X, Chan YL, et al. Successful implantation is associated with a transient increase in serum pro-inflammatory cytokine profile followed by a switch to anti-inflammatory cytokine profile prior to confirmation of pregnancy. Fertil Steril. 2021 Apr 1;115(4):1044–53. doi:10.1016/j.fertnstert.2020.10.031 PubMed PMID: 33272613.

173. Zhao Y, Zhang T, Guo X, Wong CK, Chen X, Chan YL, et al. Successful implantation is associated with a transient increase in serum pro-inflammatory cytokine profile followed by a switch to anti-inflammatory cytokine profile prior to confirmation of pregnancy. Fertil Steril. 2021 Apr 1;115(4):1044–53. doi:10.1016/j.fertnstert.2020.10.031 PubMed PMID: 33272613.

174. Zhou J, Yan P, Ma W, Li J. Cytokine modulation and immunoregulation of uterine NK cells in pregnancy disorders. Cytokine and Growth Factor

Reviews. Elsevier Ltd; 2025. p. 40–53. doi:10.1016/j.cytogfr.2024.11.007 PubMed PMID: 39603954.

175. Ono Y, Yoshino O, Hiraoka T, Sato E, Fukui Y, Ushijima A, et al. CD206+ M2-Like Macrophages Are Essential for Successful Implantation. Front Immunol. 2020 Oct 23;11. doi:10.3389/fimmu.2020.557184 PubMed PMID: 33193326.

176. Huang N, Chi H, Qiao J. Role of Regulatory T Cells in Regulating Fetal-Maternal Immune Tolerance in Healthy Pregnancies and Reproductive Diseases. Frontiers in Immunology. Frontiers Media S.A.; 2020. doi:10.3389/fimmu.2020.01023 PubMed PMID: 32676072.

177. Liu H, Zhang L. Decidual macrophage subsets and polarization puzzle during the human early pregnancy. Frontiers in Immunology. Frontiers Media SA; 2025. doi:10.3389/fimmu.2025.1610891 PubMed PMID: 40726980.

178. Weng J, Couture C, Girard S. Innate and Adaptive Immune Systems in Physiological and Pathological Pregnancy. Biology. MDPI; 2023. doi:10.3390/biology12030402

179. Waterston R, Lindblad-Toh K, Briney E, Rogers J, Abril J, Agarwal P, et al. Initial sequencing and comparative analysis of the mouse genome. Nature [Internet]. 2002;420. Available from: http://www.infor-

180. Rendi MH, Muehlenbachs A, Garcia RL. Female reproductive system. In: Comparative Anatomy and Histology. 2012. p. 253–83.

181. Kerr JB, Duckett R, Myers M, Britt KL, Mladenovska T, Findlay JK. Quantification of healthy follicles in the neonatal and adult mouse ovary: Evidence for maintenance of primordial follicle supply. Reproduction. 2006 Jul;132(1):95–109. doi:10.1530/rep.1.01128 PubMed PMID: 16816336.

182. Hirshfield AN. Development of Follicles in the Mammalian Ovary. Int Rev Cytol. 1991;124.

183. Kaprara A, Huhtaniemi IT. The hypothalamus-pituitary-gonad axis: Tales of mice and men. Metabolism: Clinical and Experimental. W.B. Saunders; 2018. p. 3–17. doi:10.1016/j.metabol.2017.11.018 PubMed PMID: 29223677.

184. Gaylord EA, Foecke MH, Samuel RM, Soygur B, Detweiler AM, McIntyre TI, et al. Comparative analysis of human and mouse ovaries across age. Science (1979). 2025 Oct 9. doi:10.1126/science.adx0659

185. Bellofiore N, Cousins F, Temple-Smith P, Dickinson H, Evans J. A missing piece: The spiny mouse and the puzzle of menstruating species.

Journal of Molecular Endocrinology. BioScientifica Ltd.; 2018. p. R25–41. doi:10.1530/JME-17-0278 PubMed PMID: 29789322.

186. Chemerinski A, Garcia de Paredes J, Blackledge K, Douglas NC, Morelli SS. Mechanisms of endometrial aging: lessons from natural conceptions and assisted reproductive technology cycles. Frontiers in Physiology. Frontiers Media SA; 2024. doi:10.3389/fphys.2024.1332946

187. Muter J, Lynch VJ, McCoy RC, Brosens JJ. Human embryo implantation. Development (Cambridge). Company of Biologists Ltd; 2023. doi:10.1242/dev.201507 PubMed PMID: 37254877.

188. Du H, Taylor HS. The role of hox genes in female reproductive tract development, adult function, and fertility. Cold Spring Harb Perspect Med. 2016 Jan 1;6(1). doi:10.1101/cshperspect.a023002 PubMed PMID: 26552702.

189. Justice MJ, Dhillon P. Using the mouse to model human disease: Increasing validity and reproducibility. DMM Disease Models and Mechanisms. Company of Biologists Ltd; 2016. p. 101–3. doi:10.1242/dmm.024547 PubMed PMID: 26839397.

190. Hashim HA, Elaraby S, Fouda AA, Rakhawy M El. The prevalence of adenomyosis in an infertile population: a cross-sectional study. Reprod Biomed Online. 2020;40:842–50. doi:10.1016/j

191. Puente JM, Fabris A, Patel J, Patel A, Cerrillo M, Requena A, et al. Adenomyosis in infertile women: Prevalence and the role of 3D ultrasound as a marker of severity of the disease. Reproductive Biology and Endocrinology. 2016 Sep 20;14(1). doi:10.1186/s12958-016-0185-6 PubMed PMID: 27645154.

192. Salim R, Riris S, Saab W, Abramov B, Khadum I, Serhal P. Adenomyosis reduces pregnancy rates in infertile women undergoing IVF. Reprod Biomed Online. 2012 Sep;25(3):273–7. doi:10.1016/j.rbmo.2012.05.003 PubMed PMID: 22832421.

193. Sharma S, Bathwal S, Agarwal N, Chattopadhyay R, Saha I, Chakravarty B. Does presence of adenomyosis affect reproductive outcome in IVS cycles? A retrospective analysis of 973 patients. Reprod Biomed Online. 2019;38(1):13–21. doi:10.1016/j

194. Pados G, Gordts S, Sorrentino F, Nisolle M, Nappi L, Daniilidis A. Adenomyosis and Infertility: A Literature Review. Medicina (Lithuania). Multidisciplinary Digital Publishing Institute (MDPI); 2023. doi:10.3390/medicina59091551 PubMed PMID: 37763670.

195. Squillace ALA, Simonian DS, Allegro MC, Júnior EB, Bianchi PH de M, Bibancos M. Adenomyosis and in vitro fertilization impacts-a literature review. J Bras Reprod Assist. 2021;25(2):303–9. doi:10.5935/1518-0557.20200104 PubMed PMID: 33656838.

196. Wu HM, Tsai TC, Liu SM, Pai AHY, Chen LH. The Current Understanding of Molecular Mechanisms in Adenomyosis-Associated Infertility and the Treatment Strategy for Assisted Reproductive Technology. International Journal of Molecular Sciences. Multidisciplinary Digital Publishing Institute (MDPI); 2024. doi:10.3390/ijms25168937

197. Harada T, Mon Khine Y, Kaponis A, Nikellis T, Decavalas G, Taniguchi F, et al. The Impact of Adenomyosis on Women's Fertility [Internet]. 2016. Report. Available from: www.obgynsurvey.com

198. Bourdon M, Pham B, Marcellin L, Bordonne C, Millischer AE, Maignien C, et al. Endometriosis increases the rate of spontaneous early miscarriage in women who have adenomyosis lesions. Reprod Biomed Online. 2022 Jan 1;44(1):104–11. doi:10.1016/j.rbmo.2021.10.003 PubMed PMID: 34819248.

199. Rees CO, Rupert IAM, Nederend J, Consten D, Mischi M, A.A.M. van Vliet H, et al. Women with combined adenomyosis and endometriosis on MRI have worse IVF/ICSI outcomes compared to adenomyosis and endometriosis alone: A matched retrospective cohort study. European Journal of Obstetrics and Gynecology and Reproductive Biology. 2022 Apr 1;271:223–34. doi:10.1016/j.ejogrb.2022.02.026 PubMed PMID: 35231748.

200. Meyer N, Zenclussen AC. Immune Cells in the Uterine Remodeling: Are They the Target of Endocrine Disrupting Chemicals? Frontiers in Immunology. Frontiers Media S.A.; 2020. doi:10.3389/fimmu.2020.00246 PubMed PMID: 32140155.

201. Bourdon M, Santulli P, Doridot L, Jeljeli M, Chêne C, Chouzenoux S, et al. Immune cells and Notch1 signaling appear to drive the epithelial to mesenchymal transition in the development of adenomyosis in mice. Mol Hum Reprod. 2021 Oct 1;27(10). doi:10.1093/molehr/gaab053 PubMed PMID: 34463756.

202. Liu W, Sheng S, Zhu C, Li C, Zou Y, Yang C, et al. Increased NKG2A+CD8+ T-cell exhaustion in patients with adenomyosis. Mucosal Immunol. 2023 Apr 1;16(2):121–34. doi:10.1016/j.mucimm.2023.02.003 PubMed PMID: 36828189.

203. Stratopoulou CA, Cussac S, Donnez J, Dolmans MM. M2 macrophages enhance endometrial cell invasiveness by promoting collective cell migration in uterine adenomyosis. Reprod Biomed Online. 2023;46:729–38. doi:10.1016/j

204. Kitazawa J, Kimura F, Nakamura A, Morimune A, Takahashi A, Takashima A, et al. Endometrial immunity for embryo implantation and pregnancy establishment. Tohoku Journal of Experimental Medicine. Tohoku University Medical Press; 2020. p. 49–60. doi:10.1620/tjem.250.49 PubMed PMID: 31996497.

205. Nahrendorf M, Swirski FK. Abandoning M1/M2 for a network model of macrophage function. Circ Res. 2016 Jul 25;115(2):414–7. doi:10.1161/CIRCRESAHA.115.303567 PubMed PMID: 24786973.

206. Wang X, Wu N, Xue Q. Macrophages in endometriosis: key roles and emerging therapeutic opportunities—a narrative review. Reproductive Biology and Endocrinology. BioMed Central Ltd; 2025. doi:10.1186/s12958-025-01471-3

207. Park M, Kim YS, Song H. Macrophages: a double-edged sword in female reproduction and disorders. Experimental and Molecular Medicine. Springer Nature; 2025. p. 285–97. doi:10.1038/s12276-025-01392-6 PubMed PMID: 39894821.

208. Shreeve N, Depierreux D, Colucci F. Natural Killer Cells in the Uterus. In: Natural Killer Cells. Springer Berlin Heidelberg; 2025. p. 1–27. doi:10.1007/978-3-662-68816-8_29-1

209. Moffett A, Colucci F. Uterine NK cells: Active regulators at the maternal-fetal interface. Journal of Clinical Investigation. The American Society for Clinical Investigation; 2014. p. 1872–9. doi:10.1172/JCI68107 PubMed PMID: 24789879.

210. Kalkunte SS, Mselle TF, Norris WE, Wira CR, Sentman CL, Sharma S. Vascular Endothelial Growth Factor C Facilitates Immune Tolerance and Endovascular Activity of Human Uterine NK Cells at the Maternal-Fetal Interface. The Journal of Immunology. 2009 Apr 1;182(7):4085–92. doi:10.4049/jimmunol.0803769 PubMed PMID: 19299706.

211. Yang JH, Chen MJ, Chen HF, Lee TH, Ho HN, Yang YS. Decreased expression of killer cell inhibitory receptors on natural killer cells in eutopic endometrium in women with adenomyosis. Human Reproduction. 2004;19(9):1974–8. doi:10.1093/humrep/deh372 PubMed PMID: 15217996.

212. Xie M, Li Y, Meng YZ, Xu P, Yang YG, Dong S, et al. Uterine Natural Killer Cells: A Rising Star in Human Pregnancy Regulation. Frontiers in

Immunology. Frontiers Media S.A.; 2022. doi:10.3389/fimmu.2022.918550 PubMed PMID: 35720413.

213. Wira CR, Rodriguez-Garcia M, Patel M V. The role of sex hormones in immune protection of the female reproductive tract. Nature Reviews Immunology. Nature Publishing Group; 2015. p. 217–30. doi:10.1038/nri3819 PubMed PMID: 25743222.

214. Kan AKC, Tang WT, Li PH. Helper T cell subsets: Development, function and clinical role in hypersensitivity reactions in the modern perspective. Heliyon. Elsevier Ltd; 2024. doi:10.1016/j.heliyon.2024.e30553

215. Lee SK, Kim CJ, Kim DJ, Kang J hyun. Immune Cells in the Female Reproductive Tract. Immune Netw. 2015;15(1):16. doi:10.4110/in.2015.15.1.16 PubMed PMID: 25713505.

216. Braun AS, Vomstein K, Reiser E, Tollinger S, Kyvelidou C, Feil K, et al. NK and T Cell Subtypes in the Endometrium of Patients with Recurrent Pregnancy Loss and Recurrent Implantation Failure: Implications for Pregnancy Success. J Clin Med. 2023 Sep 1;12(17). doi:10.3390/jcm12175585

217. Shen M, O'donnell E, Leon G, Kisovar A, Melo P, Zondervan K, et al. The role of endometrial B cells in normal endometrium and benign female reproductive pathologies: a systematic review. Human Reproduction Open. Oxford University Press; 2022. doi:10.1093/hropen/hoab043

218. Antsiferova YS, Sotnikova NY, Posiseeva L V., Shor AL. Changes in the T-helper cytokine profile and in lymphocyte activation at the systemic and local levels in women with endometriosis. Fertil Steril. 2005 Dec;84(6):1705–11. doi:10.1016/j.fertnstert.2005.05.066 PubMed PMID: 16359969.

219. Randall GW, Gantt PA, Poe-Zeigler RL, Bergmann CA, Noel ME, Strawbridge WR, et al. Serum antiendometrial antibodies and diagnosis of endometriosis. American Journal of Reproductive Immunology. 2007 Oct;58(4):374–82. doi:10.1111/j.1600-0897.2007.00523.x PubMed PMID: 17845208.

220. Bourdon M, Santulli P, Jeljeli M, Vannuccini S, Marcellin L, Doridot L, et al. Immunological changes associated with adenomyosis: A systematic review. Human Reproduction Update. Oxford University Press; 2021. p. 108–29. doi:10.1093/humupd/dmaa038 PubMed PMID: 33099635.

221. Yang JH, Wu MY, Chang DY, Chang CH, Yang YS, Ho HN. Increased interleukin-6 messenger RNA expression in macrophage-cocultured endometrial stromal cells in adenomyosis. American Journal of

Reproductive Immunology. 2006 Mar;55(3):181–7. doi:10.1111/j.1600-0897.2005.00363.x PubMed PMID: 16451352.

222. Artemova D, Vishnyakova P, Elchaninov A, Gantsova E, Sukhikh G, Fatkhudinov T. M1 macrophages as promising agents for cell therapy of endometriosis. Heliyon. 2024 Aug 30;10(16). doi:10.1016/j.heliyon.2024.e36340

223. Tremellen KP, Russell P. The distribution of immune cells and macrophages in the endometrium of women with recurrent reproductive failure. II: Adenomyosis and macrophages. J Reprod Immunol. 2012 Jan;93(1):58–63. doi:10.1016/j.jri.2011.12.001 PubMed PMID: 22209314.

224. Maclean A, Barzilova V, Patel S, Bates F, Hapangama DK. Characterising the immune cell phenotype of ectopic adenomyosis lesions compared with eutopic endometrium: A systematic review. Journal of Reproductive Immunology. Elsevier Ireland Ltd; 2023. doi:10.1016/j.jri.2023.103925 PubMed PMID: 36870297.

225. Wu Q, Shao W, Zhen J, Li Z, Zhao Z, Shi W. Complex causal association between immunophenotypes and adenomyosis: Univariable, bidirectional, and multivariable Mendelian randomization. J Reprod Immunol. 2025 Aug 1;170. doi:10.1016/j.jri.2025.104551 PubMed PMID: 40505456.

226. Bulmer JN, Jones RK, Searle RF. Intraepithelial leukocytes in endometriosis and adenomyosis: comparison of eutopic and ectopic endometrium with normal endometrium. Human Reproduction. 1998. Report.

227. Scheerer C, Bauer P, Chiantera V, Sehouli J, Kaufmann A, Mechsner S. Characterization of endometriosis-associated immune cell infiltrates (EMaICI). Arch Gynecol Obstet. 2016 Sep 1;294(3):657–64. doi:10.1007/s00404-016-4142-6 PubMed PMID: 27358184.

228. Jones RK, Bulmer JN, Searle RF. Phenotypic and functional studies of leukocytes in human endometrium and endometriosis. Human Reproduction Update. 1998. Report.

229. Gui T, Chen C, Zhang Z, Tang W, Qian R, Ma X, et al. The disturbance of TH17-Treg cell balance in adenomyosis. Fertil Steril. 2014 Feb;101(2):506–14. doi:10.1016/j.fertnstert.2013.10.050 PubMed PMID: 24331831.

230. Sotnikova N, Antsiferova I, Malyshkina A. Cytokine Network of Eutopic and Ectopic Endometrium in Women with Adenomyosis. American Journal of Reproductive Immunology. 2022;47:251–5.

231. Murata H, Tanaka S, Okada H. The Regulators of Human Endometrial Stromal Cell Decidualization. Biomolecules. MDPI; 2022. doi:10.3390/biom12091275 PubMed PMID: 36139114.

232. Mahajan N, Kaur S, Alonso MR. Window of implantation is significantly displaced in patients with adenomyosis with previous implantation failure as determined by endometrial receptivity assay. J Hum Reprod Sci. 2018 Oct 1;11(4):353–8. doi:10.4103/jhrs.JHRS_52_18

233. Zhihong N, Yun F, Pinggui Z, Sulian Z, Zhang A. Cytokine profiling in the eutopic endometrium of adenomyosis during the implantation window after ovarian stimulation. Reproductive Sciences. 2016 Jan 1;23(1):124–33. doi:10.1177/1933719115597761 PubMed PMID: 26239388.

234. Wang J, Huang C, Jiang R, Du Y, Zhou J, Jiang Y, et al. Decreased endometrial IL-10 impairs endometrial receptivity by downregulating HOXA10 expression in women with adenomyosis. Biomed Res Int. 2018;2018. doi:10.1155/2018/2549789 PubMed PMID: 30687738.

235. He B, Teng XM, Hao F, Zhao M, Chen ZQ, Li KM, et al. Decreased intracellular IL-33 impairs endometrial receptivity in women with adenomyosis. Front Endocrinol (Lausanne). 2022 Jul 22;13. doi:10.3389/fendo.2022.928024

236. Chen LH, Chan SH, Li CJ, Wu HM, Huang HY. Altered Expression of Interleukin-18 System mRNA at the Level of Endometrial Myometrial Interface in Women with Adenomyosis. Curr Issues Mol Biol. 2022 Nov 1;44(11):5550–61. doi:10.3390/cimb44110376 PubMed PMID: 36354688.

237. Prašnikar E, Kunej T, Gorenjak M, Potočnik U, Kovačič B, Knez J. Transcriptomics of receptive endometrium in women with sonographic features of adenomyosis. Reproductive Biology and Endocrinology. 2022 Dec 1;20(1). doi:10.1186/s12958-021-00871-5 PubMed PMID: 34980152.

238. Bourdon M, Maget AS, Jeljeli M, Doridot L, Marcellin L, Thomas M, et al. Reduced fertility in adenomyosis mouse model is associated with an altered immune profile in the uterus during the implantation period. Human Reproduction. 2024 Jan 1;39(1):119–29. doi:10.1093/humrep/dead246 PubMed PMID: 38011900.

239. Cai QY, Tang WZ, Li ZM, Li JZ, Zhi XQ, Yang QH, et al. Efficacy of glucocorticoids treatment in recurrent embryo implantation failure. Cell Death Discovery. Springer Nature; 2025. doi:10.1038/s41420-025-02753-w

240. McLaughlin K, Hobson SR, Chandran AR, Agrawal S, Windrim RC, Parks WT, et al. Circulating maternal placental growth factor responses to low-molecular-weight heparin in pregnant patients at risk of placental

dysfunction. Am J Obstet Gynecol. 2022 Feb 1;226(2):S1145-S1156.e1. doi:10.1016/j.ajog.2021.08.027 PubMed PMID: 34461078.

241. Scarrone M, Salmeri N, Buzzaccarini G, Canti V, Pasi F, Papaleo E, et al. Low-molecular-weight heparin in the prevention of unexplained recurrent miscarriage: a systematic review and meta-analysis. Sci Rep. 2024 Dec 1;14(1). doi:10.1038/s41598-024-62949-5 PubMed PMID: 38898143.

242. Parsa Nezhad ME, Fathi Fathikaljahi E, Dousfatemeh S. Thrombo-Prophylactic Effects of Low Molecular Weight Heparin in Women Without Thrombophilic Disorder Undergoing Assisted Reproductive Technology: A Double-Blind, Randomized, Placebo-Controlled Clinical Trial. Journal of Obstetrics, Gynecology and Cancer Research. 2024 Jan 1;9(1):63–9. doi:10.30699/jogcr.9.1.63

243. Canella PRBC, Barini R, Carvalho P de O, Razolli DS. Lipid emulsion therapy in women with recurrent pregnancy loss and repeated implantation failure: The role of abnormal natural killer cell activity. Journal of Cellular and Molecular Medicine. Blackwell Publishing Inc.; 2021. p. 2290–6. doi:10.1111/jcmm.16257 PubMed PMID: 33544456.

244. Liu M, Li Y, Yuan Y, Jiang M, Yin P, Yang D. Peri-implantation treatment with TNF-α inhibitor for endometriosis and/or adenomyosis women undergoing frozen-thawed embryo transfer: A retrospective cohort study. J Reprod Immunol. 2025 Feb 1;167. doi:10.1016/j.jri.2024.104415 PubMed PMID: 39700679.

245. Jiang Y, Zhao Q, Zhang Y, Zhou L, Lin J, Chen Y, et al. Treatment of G-CSF in unexplained, repeated implantation failure: A systematic review and meta-analysis. J Gynecol Obstet Hum Reprod. 2020 Dec 1;49(10). doi:10.1016/j.jogoh.2020.101866 PubMed PMID: 32663652.

246. Pourmoghadam Z, Soltani-Zangbar MS, Sheikhansari G, Azizi R, Eghbal-Fard S, Mohammadi H, et al. Intrauterine administration of autologous hCG- activated peripheral blood mononuclear cells improves pregnancy outcomes in patients with recurrent implantation failure; A double-blind, randomized control trial study. J Reprod Immunol. 2020 Nov 1;142. doi:10.1016/j.jri.2020.103182 PubMed PMID: 32781360.

247. Ren R, Pang B, Han Y, Li Y. A Glimpse of the Structural Biology of the Metabolism of Sphingosine-1-Phosphate. Contact. SAGE Publications Inc.; 2021. doi:10.1177/2515256421995601

248. Maceyka M, Sankala H, Hait NC, Le Stunff H, Liu H, Toman R, et al. SphK1 and SphK2, sphingosine kinase isoenzymes with opposing functions in sphingolipid metabolism. Journal of Biological Chemistry.

2005 Nov 4;280(44):37118–29. doi:10.1074/jbc.M502207200 PubMed PMID: 16118219.

249. Diaz Escarcega R, McCullough LD, Tsvetkov AS. The Functional Role of Sphingosine Kinase 2. Frontiers in Molecular Biosciences. Frontiers Media S.A.; 2021. doi:10.3389/fmolb.2021.683767

250. Tolksdorf C, Moritz E, Wolf R, Meyer U, Marx S, Bien-Möller S, et al. Platelet-Derived S1P and Its Relevance for the Communication with Immune Cells in Multiple Human Diseases. International Journal of Molecular Sciences. MDPI; 2022. doi:10.3390/ijms231810278 PubMed PMID: 36142188.

251. Venkataraman K, Lee YM, Michaud J, Thangada S, Ai Y, Bonkovsky HL, et al. Vascular endothelium as a contributor of plasma sphingosine 1-phosphate. Circ Res. 2008 Mar;102(6):669–76. doi:10.1161/CIRCRESAHA.107.165845 PubMed PMID: 18258856.

252. Pappu R, Schwab SR, Cornelissen I, Pereira JP, Regard JB, Xu Y, et al. Promotion of Lymphocyte Egress into Blood and Lymph by Distinct Sources of Sphingosine-1-Phosphate [Internet]. Report. Available from: https://www.science.org

253. Leiber D, Banno Y, Tanfin Z. Exogenous sphingosine 1-phosphate and sphingosine kinase activated by endothelin-1 induced myometrial contraction through differential mechanisms. Am J Physiol Cell Physiol. 2007;292:240–50. doi:10.1152/ajpcell.00023.2006.-Sphingosine

254. Saurabh K, Mbadhi MN, Prifti KK, Martin KT, Frolova AI. Sphingosine 1-Phosphate Activates S1PR3 to Induce a Proinflammatory Phenotype in Human Myometrial Cells. Endocrinology (United States). 2023 Jun 1;164(6). doi:10.1210/endocr/bqad066 PubMed PMID: 37120767.

255. Santulli P, Marcellin L, Noël JC, Borghese B, Fayt I, Vaiman D, et al. Sphingosine pathway deregulation in endometriotic tissues. Fertil Steril. 2012;97(4). doi:10.1016/j.fertnstert.2011.12.051

256. Ishimaru K, Yoshioka K, Kano K, Kurano M, Saigusa D, Aoki J, et al. Sphingosine kinase-2 prevents macrophage cholesterol accumulation and atherosclerosis by stimulating autophagic lipid degradation. Sci Rep. 2019 Dec 1;9(1). doi:10.1038/s41598-019-54877-6 PubMed PMID: 31797978.

257. Joshi JC, Joshi B, Rochford I, Rayees S, Akhter MZ, Baweja S, et al. SPHK2-Generated S1P in CD11b+ Macrophages Blocks STING to Suppress the Inflammatory Function of Alveolar Macrophages. Cell Rep. 2020 Mar 24;30(12):4096-4109.e5. doi:10.1016/j.celrep.2020.02.112 PubMed PMID: 32209471.

258. Weigert A, Johann AM, Von Knethen A, Schmidt H, Geisslinger G, Brüne B. Apoptotic cells promote macrophage survival by releasing the antiapoptotic mediator sphingosine-1-phosphate. Blood. 2006 Sep 1;108(5):1635–42. doi:10.1182/blood-2006-04-014852 PubMed PMID: 16690965.

259. Hisano Y, Kobayashi N, Yamaguchi A, Nishi T. Mouse SPNS2 functions as a Sphingosine-1-Phosphate transporter in vascular endothelial cells. PLoS One. 2012 Jun 12;7(6). doi:10.1371/journal.pone.0038941 PubMed PMID: 22723910.

260. Burg N, Salmon JE, Hla T. Sphingosine 1-phosphate receptor-targeted therapeutics in rheumatic diseases. Nature Reviews Rheumatology. Nature Research; 2022. p. 335–51. doi:10.1038/s41584-022-00784-6 PubMed PMID: 35508810.

261. Scotti L, Di Pietro M, Pascuali N, Irusta G, I de Zúñiga, Gomez Peña M, et al. Sphingosine-1-phosphate restores endothelial barrier integrity in ovarian hyperstimulation syndrome. Mol Hum Reprod. 2016 Dec 1;22(12):852–66. doi:10.1093/molehr/gaw065 PubMed PMID: 27645281.

262. Bernacchioni C, Rossi M, Vannuzzi V, Prisinzano M, Seidita I, Raeispour M, et al. Sphingosine-1-phosphate receptor 3 is a non-hormonal target to counteract endometriosis-associated fibrosis. Fertil Steril. 2024 Apr 1;121(4):631–41. doi:10.1016/j.fertnstert.2023.12.007 PubMed PMID: 38072366.

263. Hu Y, Dai K. Sphingosine 1-Phosphate Metabolism and Signaling. In: Advances in Experimental Medicine and Biology. Springer; 2022. p. 67–76. doi:10.1007/978-981-19-0394-6_6 PubMed PMID: 35503175.

264. Wang W, Zhao Y, Zhu G. The role of sphingosine-1-phosphate in the development and progression of Parkinson's disease. Frontiers in Cellular Neuroscience. Frontiers Media SA; 2023. doi:10.3389/fncel.2023.1288437

265. Constantinescu V, Haase R, Akgün K, Ziemssen T. S1P receptor modulators and the cardiovascular autonomic nervous system in multiple sclerosis: a narrative review. Therapeutic Advances in Neurological Disorders. SAGE Publications Ltd; 2022. doi:10.1177/17562864221133163

266. Drouillard A, Mathieu AL, Marçais A, Belot A, Viel S, Mingueneau M, et al. S1PR5 is essential for human natural killer cell migration toward sphingosine-1 phosphate. Journal of Allergy and Clinical Immunology. 2018 Jun 1;141(6):2265-2268.e1. doi:10.1016/j.jaci.2017.11.022 PubMed PMID: 29248494.

267. Maas JWM, Groothuis PG, Dunselman GAJ, De Goeij AFPM, Struyker Boudier HAJ, Evers JLH. Endometrial angiogenesis throughout the human menstrual cycle. Human Reproduction. 2001. Report.

268. Hughes SM, Levy CN, Katz R, Lokken EM, Anahtar MN, Hall MB, et al. Changes in concentrations of cervicovaginal immune mediators across the menstrual cycle: a systematic review and meta-analysis of individual patient data. BMC Med. 2022 Dec 1;20(1). doi:10.1186/s12916-022-02532-9 PubMed PMID: 36195867.

269. Hao X, Zhang M. Roles of sphingosine-1-phosphate in follicle development and oocyte maturation. Animal Research and One Health. John Wiley and Sons Inc; 2024. p. 314–22. doi:10.1002/aro2.53

270. Hernández-Coronado CG, Guzmán A, Castillo-Juárez H, Zamora-Gutiérrez D, Rosales-Torres AM. Sphingosine-1-phosphate (S1P) in ovarian physiology and disease. Ann Endocrinol (Paris). 2019 Nov 1;80(5–6):263–72. doi:10.1016/j.ando.2019.06.003 PubMed PMID: 31455516.

271. Di Paolo A, Vignini A, Alia S, Membrino V, Delli Carpini G, Giannella L, et al. Pathogenic Role of the Sphingosine 1-Phosphate (S1P) Pathway in Common Gynecologic Disorders (GDs): A Possible Novel Therapeutic Target. International Journal of Molecular Sciences. MDPI; 2022. doi:10.3390/ijms232113538 PubMed PMID: 36362323.

272. Jeng YJ, Suarez VR, Izban MG, Wang HQ, Soloff MS. Progesterone-induced sphingosine kinase-1 expression in the rat uterus during pregnancy and signaling consequences. Am J Physiol Endo-crinol Metab. 2007;292:1110–21. doi:10.1152/ajpendo.00373.2006.-Sphingosine

273. Kaneko-Tarui T, Zhang L, Austin KJ, Henkes LE, Johnson J, Hansen TR, et al. Maternal and embryonic control of uterine sphingolipid-metabolizing enzymes during murine embryo implantation. Biol Reprod. 2007 Oct;77(4):658–65. doi:10.1095/biolreprod.107.061044 PubMed PMID: 17582011.

274. Yamamoto Y, Olson DM, Van Bennekom M, Brindley DN, Hemmings DG. Increased expression of enzymes for sphingosine 1-phosphate turnover and signaling in human decidua during late pregnancy. Biol Reprod. 2010 Mar;82(3):628–35. doi:10.1095/biolreprod.109.081497 PubMed PMID: 20007411.

275. Skaznik-Wikiel ME, Kaneko-Tarui T, Kashiwagi A, Pru JK. Sphingosine-1-phosphate receptor expression and signaling correlate with uterine prostaglandin-endoperoxide synthase 2 expression and angiogenesis

during early pregnancy. Biol Reprod. 2006 Mar;74(3):569–76. doi:10.1095/biolreprod.105.046714 PubMed PMID: 16319286.

276. Kharel Y, Huang T, Salamon A, Harris TE, Santos WL, Lynch KR. Mechanism of sphingosine 1-phosphate clearance from blood. Biochemical Journal. 2020;477(5):925–35. doi:10.1042/BCJ20190730 PubMed PMID: 32065229.

277. Dunlap KA, Kwak H Il, Burghardt RC, Bazer FW, Magness RR, Johnson GA, et al. The sphingosine 1-phosphate (S1P) signaling pathway is regulated during pregnancy in sheep. Biol Reprod. 2010 May;82(5):876–87. doi:10.1095/biolreprod.109.081604 PubMed PMID: 20107206.

278. Zhang F, Lu Y. The Sphingosine 1-Phosphate Axis: an Emerging Therapeutic Opportunity for Endometriosis. Reproductive Sciences. Institute for Ionics; 2023. p. 2040–59. doi:10.1007/s43032-023-01167-2 PubMed PMID: 36662421.

279. Ono Y, Kawakita T, Yoshino O, Sato E, Kano K, Ohba M, et al. Sphingosine 1-phosphate (S1p) in the peritoneal fluid skews m2 macrophage and contributes to the development of endometriosis. Biomedicines. 2021 Nov 1;9(11). doi:10.3390/biomedicines9111519

280. Yoshino O, Yamada-Nomoto K, Kano K, Ono Y, Kobayashi M, Ito M, et al. Sphingosine 1 Phosphate (S1P) Increased IL-6 Expression and Cell Growth in Endometriotic Cells. Reproductive Sciences. 2019 Nov 1;26(11):1460–7. doi:10.1177/1933719119828112 PubMed PMID: 30782093.

281. Seidita I, Tusa I, Prisinzano M, Menconi A, Cencetti F, Vannuccini S, et al. Sphingosine 1-phosphate elicits a ROS-mediated proinflammatory response in human endometrial stromal cells via ERK5 activation. FASEB Journal. 2023 Aug 1;37(8). doi:10.1096/fj.202300323R PubMed PMID: 37389926.

282. Prisinzano M, Bernacchioni C, Seidita I, Rossi M, Raeispour M, Cencetti F, et al. Sphingosine 1-phosphate signaling axis mediates neuropeptide S-induced invasive phenotype of endometriotic cells. FEBS Journal. 2024 Apr 1;291(8):1744–58. doi:10.1111/febs.17071 PubMed PMID: 38287231.

283. Prisinzano M, Seidita I, Bruni P, Petraglia F, Bernacchioni C, Meyer zu Heringdorf D, et al. Characterization of functionally relevant G protein-coupled receptors in endometriotic epithelial cells. Cell Signal. 2025 Sep 1;133. doi:10.1016/j.cellsig.2025.111876 PubMed PMID: 40381972.

284. Bernacchioni C, Capezzuoli T, Vannuzzi V, Malentacchi F, Castiglione F, Cencetti F, et al. Sphingosine 1-phosphate receptors are dysregulated in endometriosis: possible implication in transforming growth factor β–

induced fibrosis. Fertil Steril. 2021 Feb 1;115(2):501–11. doi:10.1016/j.fertnstert.2020.08.012 PubMed PMID: 32907751.

285. Houshdaran S, Nezhat C. Transforming growth factor β–sphingosine 1-phosphate axis in pathogenesis of endometriosis. Fertility and Sterility. Elsevier Inc.; 2021. p. 338–9. doi:10.1016/j.fertnstert.2020.09.147 PubMed PMID: 33272634.

286. Bernacchioni C, Ciarmela P, Vannuzzi V, Greco S, Vannuccini S, Malentacchi F, et al. Sphingosine 1-phosphate signaling in uterine fibroids: implication in activin A pro-fibrotic effect. Fertil Steril. 2021 Jun 1;115(6):1576–85. doi:10.1016/j.fertnstert.2020.12.022 PubMed PMID: 33500141.

287. Yang YL, Ji C, Cheng L, He L, Lu CC, Wang R, et al. Sphingosine kinase-1 inhibition sensitizes curcumin-induced growth inhibition and apoptosis in ovarian cancer cells. Cancer Sci. 2012 Aug;103(8):1538–45. doi:10.1111/j.1349-7006.2012.02335.x PubMed PMID: 22594559.

288. Hart PC, Chiyoda T, Liu X, Weigert M, Curtis M, Chiang CY, et al. SPHK1 is a novel target of metformin in ovarian cancer. Molecular Cancer Research. 2019;17(4):870–81. doi:10.1158/1541-7786.MCR-18-0409 PubMed PMID: 30655321.

289. Vannuzzi V, Bernacchioni C, Muccilli A, Castiglione F, Nozzoli F, Vannuccini S, et al. Sphingosine 1-phosphate pathway is dysregulated in adenomyosis. Reprod Biomed Online. 2022 Jul 1;45(1):15–8. doi:10.1016/j.rbmo.2022.03.026 PubMed PMID: 35562234.

290. Rudzitis-Auth J, Christoffel A, Menger MD, Laschke MW. Targeting sphingosine kinase-1 with the low MW inhibitor SKI-5C suppresses the development of endometriotic lesions in mice. Br J Pharmacol. 2021 Oct 1;178(20):4104–18. doi:10.1111/bph.15601 PubMed PMID: 34185874.

291. Zhang F, Peng M, Zheng X, Wang X, Liu X, Chen C, et al. Blocking sphingosine 1-phosphate receptor 1 with modulators reduces immune cells infiltration and alleviates endometriosis in mice. Reprod Biomed Online. 2023 Nov 1;47(5). doi:10.1016/j.rbmo.2023.103304 PubMed PMID: 37757611.

292. Shida D, Takabe K, Kapitonov D, Milstien S, Spiegel S. Targeting SphK1 as a New Strategy against Cancer [Internet]. Report. Available from: http://www.ncbi.nlm.nih.gov

293. Gupta P, Taiyab A, Hussain A, Alajmi MF, Islam A, Hassan MI. Targeting the sphingosine kinase/sphingosine-1-phosphate signaling axis in drug discovery for cancer therapy. Cancers. MDPI AG; 2021. doi:10.3390/cancers13081898

294. Li ZH, Tao YF, Xu LX, Zhao H, Li XL, Fang F, et al. Original Article A novel sphingosine kinase 1 inhibitor (SKI-5C) induces cell death of Wilms' tumor cells in vitro and in vivo. Am J Transl Res [Internet]. 2016. Report. Available from: http://www.genome.jp/

295. Strader CR, Pearce CJ, Oberlies NH. Fingolimod (FTY720): A recently approved multiple sclerosis drug based on a fungal secondary metabolite. Journal of Natural Products. 2011. p. 900–7. doi:10.1021/np2000528 PubMed PMID: 21456524.

296. Chun J, Hartung HP. Mechanism of action of oral fingolimod (FTY720) in multiple sclerosis. Clinical Neuropharmacology. 2010. p. 91–101. doi:10.1097/WNF.0b013e3181cbf825 PubMed PMID: 20061941.

297. Chaudhry BZ, Cohen JA, Conway DS. Sphingosine 1-Phosphate Receptor Modulators for the Treatment of Multiple Sclerosis. Neurotherapeutics. Springer New York LLC; 2017. p. 859–73. doi:10.1007/s13311-017-0565-4 PubMed PMID: 28812220.

298. Liu J, Zhang L, Liu L, Wu T, Wang L, Han Q. The potential capacities of FTY720: Novel therapeutic functions, targets, and mechanisms against diseases. European Journal of Medicinal Chemistry. Elsevier Masson s.r.l.; 2025. doi:10.1016/j.ejmech.2025.117508 PubMed PMID: 40120496.

299. Arlıer S, Kükrer S, Adıgüzel FI, Nessar AZ, Uysal G, Adıgüzel C, et al. The impact of adenomyosis on intrauterine insemination success in unexplained infertile women: a retrospective cross-sectional study. BMC Pregnancy Childbirth. 2025 Dec 1;25(1). doi:10.1186/s12884-025-07769-9 PubMed PMID: 40462001.

300. Wang Y, Yi YC, Guu HF, Chen YF, Kung HF, Chang JC, et al. Impact of adenomyosis and endometriosis on IVF/ICSI pregnancy outcome in patients undergoing gonadotropin-releasing hormone agonist treatment and frozen embryo transfer. Sci Rep. 2023 Dec 1;13(1). doi:10.1038/s41598-023-34045-7 PubMed PMID: 37185812.

301. Cozzolino M, Cosentino M, Loiudice L, Martire FG, Galliano D, Pellicer A, et al. Impact of adenomyosis on in vitro fertilization outcomes in women undergoing donor oocyte transfers: a prospective observational study. Fertil Steril. 2024 Mar 1;121(3):480–8. doi:10.1016/j.fertnstert.2023.11.034 PubMed PMID: 38043844.

302. Stratopoulou CA, El Grari I, Camboni A, Donnez J, Dolmans MM. Expression of Endometrial Receptivity Markers throughout the Menstrual Cycle in Women with and without Uterine Adenomyosis. J Clin Med. 2024 Sep 1;13(17). doi:10.3390/jcm13175016

303. Duan J, Zhou X, Zhu H, Zhou M, Liu M, Zhou Y, et al. Decreased expression of LEF1 caused defective decidualization by inhibiting IL-11 expression in patients with adenomyosis. Molecular Medicine. 2025 Dec 1;31(1). doi:10.1186/s10020-024-01054-9 PubMed PMID: 39794729.

304. Zheng H, Liu M, Su Q, Li H, Wang F. Impaired fertility and perinatal outcomes in adenomyosis: insights from a novel murine model and uterine gene profile alterations during implantations. Am J Obstet Gynecol. 2025 Sep 1;233(3):180.e1-180.e18. doi:10.1016/j.ajog.2025.02.033 PubMed PMID: 39986340.

305. Sfogliarini C, Pepe G, Dolce A, Della Torre S, Cesta MC, Allegretti M, et al. Tamoxifen Twists Again: On and Off-Targets in Macrophages and Infections. Frontiers in Pharmacology. Frontiers Media S.A.; 2022. doi:10.3389/fphar.2022.879020

306. Niu W, Zhang Y, Liu H, Liang N, Xu L, Li Y, et al. Single-Cell Profiling Uncovers the Roles of Endometrial Fibrosis and Microenvironmental Changes in Adenomyosis. J Inflamm Res. 2023;16:1949–65. doi:10.2147/JIR.S402734

307. Liu Z, Sun Z, Liu H, Niu W, Wang X, Liang N, et al. Single-cell transcriptomic analysis of eutopic endometrium and ectopic lesions of adenomyosis. Cell Biosci. 2021 Dec 1;11(1). doi:10.1186/s13578-021-00562-z

308. Liu D, Yin X, Guan X, Li K. Bioinformatic analysis and machine learning to identify the diagnostic biomarkers and immune infiltration in adenomyosis. Front Genet. 2023 Jan 4;13. doi:10.3389/fgene.2022.1082709

309. Zhou M, Xu H, Zhang D, Si C, Zhou X, Zhao H, et al. Decreased PIBF1/IL6/p-STAT3 during the mid-secretory phase inhibits human endometrial stromal cell proliferation and decidualization. J Adv Res. 2021 May 1;30:15–25. doi:10.1016/j.jare.2020.09.002

310. Bernacchioni C, Capezzuoli T, Vannuzzi V, Malentacchi F, Castiglione F, Cencetti F, et al. Sphingosine 1-phosphate receptors are dysregulated in endometriosis: possible implication in transforming growth factor β–induced fibrosis. Fertil Steril. 2021 Feb 1;115(2):501–11. doi:10.1016/j.fertnstert.2020.08.012 PubMed PMID: 32907751.

311. Prisinzano M, Seidita I, Bruni P, Petraglia F, Bernacchioni C, Meyer zu Heringdorf D, et al. Characterization of functionally relevant G protein-coupled receptors in endometriotic epithelial cells. Cell Signal. 2025 Sep 1;133. doi:10.1016/j.cellsig.2025.111876 PubMed PMID: 40381972.

312. Sharara FI, Kheil MH, Feki A, Rahman S, Klebanoff JS, Ayoubi JM, et al. Current and prospective treatment of adenomyosis. Journal of Clinical Medicine. MDPI; 2021. doi:10.3390/jcm10153410

APPENDIXES

APPENDIX 1

Autophagy downregulation emerges early in murine adenomyosis and persists selectively in human stromal lesions.

Julie Vervier, Marlyne Squatrito, Silvia Blacher, Michelle Nisolle and Carine Munaut.

Frontiers – Under review

As a co-author of this study, I contributed to the *in vivo* experiments, including the induction of adenomyosis in the neonatal tamoxifen-treated mouse model, as well as to the conceptual design and discussion of experimental approaches throughout the project.

This study was prompted by the limited and inconsistent evidence regarding the role of autophagy in adenomyosis, despite its well-established involvement in endometrial homeostasis and implantation. To address this gap, we employed a neonatal tamoxifen-induced CD1 mouse model, analyzing both early pre-lesional and established disease stages, and complemented these findings with human uterine samples. Our results revealed an early downregulation of autophagy in mice, characterized by reduced LC3B expression and modulation of a restricted set of autophagy/apoptosis-related genes, coinciding with initial myometrial disorganization and stromal invasion. At later stages, autophagy markers return to baseline levels despite the progression of lesions, whereas in human adenomyotic foci, LC3B loss was selectively maintained in stromal cells. Collectively, these findings demonstrate that autophagy regulation in adenomyosis is neither binary or static but instead dynamically modulated in a time- and compartment-specific manner, highlighting stromal autophagy impairment as a potential therapeutic target.

Autophagy downregulation emerges early in murine adenomyosis and persists selectively in human stromal lesions

Vervier Julie[1,2], Squatrito Marlyne[1], Blacher Silvia[1], Nisolle Michelle[2], Munaut Carine[1]

1: Laboratory of Tumor and Development Biology, Giga-Cancer, University of Liège, 4000 Liege, Belgium

2: Obstetrics and Gynecology Department, University of Liège, Boulevard du 12ème de Ligne 1, 4000 Liege, Belgium

Corresponding author: Carine Munaut (c.munaut@uliege.be)

Keywords: Adenomyosis; Autophagy; LC3B; Endometrial stroma; Tamoxifen-induced murine model; Uterine pathophysiology; Immunohistochemistry; Endometrial–myometrial interface.

Abstract

Background

Adenomyosis is a heterogeneous uterine disorder characterized by the presence of endometrial tissue within the myometrium. Autophagy, a key homeostatic process involved in tissue remodeling and stress adaptation, has been inconsistently described in adenomyosis. This study aimed to define the temporal and compartment-specific regulation of autophagy during disease progression, using a tamoxifen-induced CD1 mouse model and human uterine samples.

Methods

Female neonatal CD1 mice were exposed to oral tamoxifen from postnatal days 1-4 and evaluated at 1 and 3 months. Uterine tissues were examined for autophagy- and apoptosis-related transcripts (RT-qPCR) autophagy protein expression (Western blot) and LC3B distribution (immunohistochemistry and immunofluorescence). LC3B expression was also assessed in paraffin-embedded-human uterine

samples from women with histologically confirmed adenomyosis and from controls without uterine pathology.

Results

At one month, a restricted set of autophagy/apoptosis-related transcripts (*Ulk2, Bax, Bcl2, Bcl2l1, Akt1, Mapk1, Nfkb1, Cxcr4*) was modulated, and LC3B protein levels were decreased, coinciding with early myometrial disorganization and stromal invasion. By three months, , gene and protein expression normalized despite established lesions, suggesting biological adaptation or involvement of compensatory pathways. In human adenomyosis tissues, LC3B reduction was confined to the stromal compartment of ectopic lesions, whereas glandular and eutopic endometrium remained comparable to controls, indicating a persistent stromal-specific autophagy defect.

Conclusions

Autophagy downregulation is an early and transient event in murine adenomyosis initiation, whereas in human disease, it persists selectively in stromal cells of established lesions. These findings demonstrate that autophagy is regulated in a temporally and spatially distinct manner in adenomyosis and identify stromal autophagy impairment as a potential therapeutic target

1. Introduction

Adenomyosis is a chronic benign condition defined by the ectopic presence of endometrial glands and stroma within the uterine myometrium, usually surrounded by reactive smooth-muscle hyperplasia (1). The disease affects approximatively one in five women of reproductive age and is associated with abnormal uterine bleeding, pelvic pain and infertility (2). These symptoms, however, lack specificity and frequently overlap with those of endometriosis and uterine myomas which often coexist with adenomyosis and confound both diagnosis and mechanistic inference (1).

Multiple hypotheses have been proposed to explain lesion initiation, including invagination of the endometrial basalis into the myometrium though mechanisms related to tissue-injury and repair, metaplasia transformation of Müllerian remnants, aberrant differentiation of displaced endometrial/stromal stem cells, enhanced invasion across the endometrial–myometrial interface (EMI), local hormonal dysregulation, and genetic/epigenetic alterations such as KRAS mutations (3–5). Disease progression may further involve the epithelial-mesenchymal transition (EMT), inflammation, hormonal imbalance, altered PI3K/AKT/mTOR and autophagic pathways ((4)6). Data on the role of autophagy in adenomyosis remain scarce and elucidating these mechanisms in patients is hindered by phenotypic heterogeneity and frequent comorbidities.

Controlled animal models provide a tractable framework to dissect early disease mechanisms under defined hormonal and experimental conditions. We therefore used a tamoxifen-induced CD1 mouse model to characterize the temporal regulation of autophagy during disease development. While CD1 mice can spontaneously develop adenomyosis after 6 months at low incidence, neonatal tamoxifen exposure dramatically increases penetrance, improving reproducibility and the confounding effects of coexisting uterine pathologies (7).

Macroautophagy (hereafter referred to as “autophagy”) is a conserved cellular recycling process in which LC3-decorated autophagosomes sequester cytoplasmic cargo for lysosomal degradation (8). Autophagy maintains cellular homeostasis, adapts metabolism to stress, and intersects with development, immunity, inflammation, and cell death (9). While primarily cytoprotective, excessive self-degradation can be harmful, and defective autophagy has been implicated in diverse human pathologies, including neurodegenerative and metabolic diseases, cancers, ageing, inflammatory and autoimmune disorders (10). In the endometrium, autophagy is hormonally regulated: estrogen generally restrains it, whereas progesterone promotes autophagic activity during the secretory phase. Autophagic activity peaks late in the menstrual cycle, contributing to controlled apoptosis and shedding (11), and supports endometrial receptivity and implantation (12). Dysregulated autophagy has been reported in endometrial hyperplasia, carcinoma, infertility, and endometriosis (12). In adenomyosis, however, available studies show heterogeneous and sometimes contradictory findings, and whether autophagy contributes lesion initiation or maintenance remains unclear (13).

The aim of this study was to investigate the contribution of autophagy to the development of adenomyosis across experimental and clinical settings. Using a neonatal tamoxifen-induced CD1 mouse model, we evaluated autophagy at an early pre-lesional stage (1 month) and at a lesion-established stage (3 months), thereby capturing different phases of disease evolution. To bridge these findings to the human condition, we analyzed uterine specimens from women with histologically confirmed adenomyosis obtained at hysterectomy, representing advanced disease.

2. Material and methods

2.1. Mouse model of adenomyosis and estrus cycle stage assessment

Animal experiments were approved by the Animal Ethics Committee of the University of Liège (#2387) and conducted in strict accordance with institutional guidelines for the care and use of laboratory

88 animals. Mice were kept under controlled conditions of temperature (+/- 21°C) and light (12h/12h
89 light/dark cycle) with ad libitum access to food and water. Animal welfare was monitored daily.
90 Female neonatal CD1 mice, obtained from pregnant dams provided by Charles River Laboratories (Italy),
91 received oral doses of 2.7µmol/kg tamoxifen (=1mg/kg) (Sigma, T5648) suspended in a mixture of
92 peanut oil, lecithin, and condensed milk (2:0.2:3, v/v) from postnatal days 1 to 4 after birth (day of birth
93 = day 0). Control mice received vehicle only. As previously reported by our group and others, this
94 protocol induces adenomyosis with a high penetrance (> 98%) (14).
95 To minimize hormonal variability affecting on autophagy, only mice in the proliferative stage of the
96 estrus cycle (proestrus or estrus phase) were analyzed. Cycle synchronization was achieved by 3
97 consecutive daily subcutaneous injections of 17ß-estradiol (100ng/100µl) prior to sacrifice (15). On the
98 day of sacrifice, estrous stage was confirmed by vaginal cytology according to *Caligioni*. (16) Briefly,
99 vaginal lavage samples were smeared on glass slides, dried, fixed in 100% ethanol (30 min), rehydrated,
100 and stained with hematoxylin–eosin. The stage was determined by the relative abundance and
101 morphology of leukocytes and epithelial cells under light microscopy (40×), as described by Byers et al.
102 (17)

103 ### 2.2. Tissue collection

104 The mice were euthanized at either 1 or 3 months old, and uteri were collected. In 1-month-old mice,
105 one uterine horn was divided into 2 parts, while in 3-month-old mice it was divided in 3 parts, which
106 were snap-frozen for RNA and protein extraction. The contralateral horn was fixed in 4% formalin and
107 paraffin-embedded. Histological analyses were performed on hematoxylin and eosin (H&E) stained
108 sections, as well as by immunofluorescence (IF) and immunohistochemistry (IHC), as described below.
109 Human paraffin-embedded uterine samples were obtained by the Biothèque Hospitalo-Universitaire de
110 Liège (BHUL) from anonymized hysterectomy specimens. Adenomyosis cases (mean age 43.2 years)
111 were selected based on histological confirmation. Control samples (mean age 29 years) were derived
112 from hysterectomies performed for gender-affirming surgery or prophylactic hysterectomy, with no

underlying uterine pathology. The study was conducted under institutional and national ethical approval (CE1267).

2.3. Real time PCR analysis for mRNA

Total RNA was extracted from individual uterine samples using the RNeasy Mini Kit for tissues (Qiagen) following the manufacturer's instructions. RNA concentration and integrity were assessed and 1µg samples was reverse transcribed into complementary DNA (cDNA) using FastGene Scriptase II Ready mix (Nippon Genetics) according to the manufacturer's instructions. Primers were designed and purchased from Eurogentec (Table 1). RT-qPCR was performed using SYBER-green PCR Master Mix on an Applied Biosystems 7500 Fast Real-Time PCR System (QuantStudio 3, Thermo Fisher Scientific).

Gene expression was normalized to the geometric mean of *Rplp0* and *Gapdh* genes in line with Lin et al. (18). Relative expression levels were calculated using the $2^{-\Delta\Delta CT}$ method. All samples were assayed in duplicate reactions.

2.4. Western blot analysis

Proteins were extracted from half uterine horns of 1-month-old mice using RIPA buffer supplemented with protease and phosphatase inhibitors (Roche). Protein concentrations were determined with a protein assay kit (Bio-Rad Laboratories). Equal protein amounts were denatured and separated by SDS–polyacrylamide gel electrophoresis then transferred onto a polyvinylidene difluoride membrane (PerkinElmer). Membranes were blocked with 5% non-fat milk for 2 hours at room temperature and incubated overnight at 4 °C with primary antibodies (Table 2). After washing, HRP-conjugated secondary antibodies were applied for 1-hour at room temperature. Detection was performed using enhanced chemiluminescence (ECL kit, PerkinElmer) and imaged on a LAS4000 imager (Fujifilm). Protein band intensities were quantified using QuantityOne Analysis software and normalized to GAPDH as a loading control. Data were presented as fold-change compared to the control group. For AKT and MAPK1, the ration of phosphorylated to total protein was calculated prior to fold-change determination.

2.5. Immunohistochemistry (IHC) and Immunofluorescence (IF)

Serial uterine sections were immune-stained to (i) quantify LC3B as a readout of autophagic activity across uterine compartments and (ii) precisely localize glands relative to myometrial depth when H&E-based grading was equivocal, using αSMA/EpCAM double immunofluorescence.

Mouse and human uterine samples were deparaffinized, rehydrated, and subjected to antigen retrieval using an autoclave (11 min, 126°C, 1.3 bar). After cooling down for 20 min, endogenous peroxidase activity was blocked by incubating the sections in 3% hydrogen peroxide for 20 min at room temperature (RT). Non-specific binding was blocked with Animal-Free Blocking Solution (Cell Signaling, 20 min at RT). Primary antibodies were diluted in REAL antibody diluent (Dako). Sections were incubated 1h at RT for anti-αSMA/FITC (Sigma, F377, 1/400) and anti-EpCAM (Cell Signaling, 93790, 1/400), or overnight at 4°C with anti-LC3B (Cell signaling 3868, 1/1500). After PBS washout, sections were incubated with the secondary antibody linked to horseradish peroxidase (ENVISION/HRP ready to use, Dako) for 30 min at RT.

For IHC, sections were incubated with Envision HRP-linked secondary antibody (Dako), revealed with DAB+ (Dako), counterstained with hematoxylin, and mounted with Entellan (Sigma-Aldrich). Slides were scanned using a NanoZoomer 2.0HT digital scanner (Hamamatsu). LC3B expression was identified as cytoplasmic brown staining.

For IF, LC3B signal was amplified with fluorescein tyramide (PerkinElmer, 10 min), then mounted with DAPI Fluoromount-G (SouthernBiotech) and scanned with a SLIDEVIEW VS200 slide scanner (Olympus). For α-SMA/EpCAM double immunostaining, fluorescence amplification was performed similarly with tyramide, and slides were mounted and imaged under the same conditions.

2.6. Classification and grading of adenomyotic lesions

To evaluate the extent and severity of adenomyotic infiltration, lesions were graded according to the criteria of Bird et al. (19), based on the maximal depth of myometrial infiltration by ectopic endometrial glands and stroma on hematoxylin and eosin (H&E) stained sections. For each uterine horn, twelve serial sections were systematically examined at x20 magnification, and the section showing the deepest

extent of adenomyotic foci was used to assign the grade. Grade 1: invasion limited to the inner one-third of the myometrium; grade 2: invasion extending into the inner two-thirds; grade 3: invasion through the full myometrial thickness. In cases where H&E grading was uncertain (e.g., distorted architecture, or subtle stromal invasion in 1 month-old mice), matched sections stained for α-SMA (smooth muscle) and EpCAM (epithelium) by immunofluorescence were reviewed to confirm gland position. This approach increased sensitivity while preserving comparability with the H&E-based system. Overall, this semi-quantitative grading method provided a reproducible measure of adenomyosis severity, serving as a baseline to compare lesion progression across experimental conditions.

2.7. Quantification of LC3B staining

Quantification of LC3B-IHC staining was performed using an H-score method. Staining intensity was classified into four categories (Supplementary figure 1), the percentage of positively stained cells was estimated across multiple representative fields. The H-score was calculated as: (0 x % cells with intensity 0) + (1 x % cells with intensity 1) + (2 x % cells with intensity 2) + (3 x % cells with intensity 3), yielding a score ranged from 0 (no staining) to 300 (100% of cells with strong staining).

For immunofluorescence staining, image analysis and quantitative measurements were performed using MATLAB R2024b (MathWorks). Fluorescence images of transverse uterine sections were acquired in the RGB (red, green, blue) color space. In these images, LC3B, α-SMA, and DAPI signals were visualized in the red, green, and blue channels, respectively. Regions corresponding to lesions, eutopic endometrium, glandular and luminal epithelium, were manually delineated, and a binary mask was generated for each region. Stroma was deduced by substracting luminal and glandular epithelia from the eutopic endometrium. Subsequently, the RGB images were separated into their individual channels, and the red channel—containing the LC3B staining—was automatically segmented using MATLAB's graythresh function. This procedure produced a binary image in which LC3B-positive areas appeared white (pixel value = 1) on a black background (pixel value = 0). Finally, the area (in mm^2) corresponding to LC3B-positive staining within each mask was quantified.

All statistical analyses were performed using GraphPad Prism 10.1.1 (GraphPad Inc). Data normality was evaluated using the Shapiro-Wilk test and visually confirmed with QQ plot. Normally distributed data were analyzed with Welch's t-test and are presented as mean ± SD, while non-normally distributed data were analyzed with the Mann-Whitney U-test and are reported as median with interquartile ranges (IQR). Statistical significance was set at $P<0.05$ and indicated as $*P < 0.05$, $**P < 0.01$, $***P < 0.001$.

3. Results

3.1. Adenomyosis severity increases with age.

Histological analysis of uterine sections revealed a marked clear age-dependent differences in lesion severity (Figure 1) of adenomyotic lesions between 1-month and 3-month-old mice.

At 1 month, tamoxifen-treated mice (ADM, n = 16) showed early or mild disease. Thirteen percent of mice showed no detectable lesions (grade 0), 56% had grade 1 lesions, 25% grade 2 lesions, and only 6% exhibited grade 3 lesions. Even in mice without overt lesions, early disruption of myometrial architecture was observed, including loss of the normal inner circular and outer longitudinal layers. Occasional focal stromal invasion without glandular elements was also detected, consistent with the earliest stages of adenomyosis development (Supplementary Figure 2).

By 3 months, lesions were more severe and widespread. Nearly all tamoxifen-treated mice (ADM, n = 15) exhibited extensive grade 3 adenomyosis (93%), with the remaining animals showing grade 2 lesions (7%). These lesions were diffuse, multifocal, and infiltrated the full thickness of the myometrium.

3.2. Modulation of autophagy and apoptosis pathways in the early phase of adenomyosis.

3.2.1. Gene expressions are modulated at one month but not at 3 months

At 1 month, RT-qPCR revealed significant modulation of a subset of autophagy- and apoptosis-related genes, including *Ulk2, Bax, Bcl2, Bcl2l1, Akt1, Mapk1, Nfkb1, and Cxcr4* (Figure 2). No significant differences were observed for *Ulk1, Beclin1, Pik3c3, Atg9, Lc3b, Tnfsf10, Dapk1, Bid*, or *Igf1*.

By 3 months, expression levels of all tested genes were comparable between ADM and control groups, with only a non-significant tendency toward lower expression in ADM mice (Figure 2).

3.2.2. Protein expression of LC3B, MAPK and BAX are modulated at 1 month

Western Blot analysis at 1 month confirmed significant modulation of MAPK and Bax protein levels in adenomyosis mice compared with controls. In addition, LC3B protein was significantly altered despite the absence of transcriptional changes at the mRNA level (Figure 3). No significant differences were observed for p-AKT/AKT, BCL-2, BCL-XL, NF-KB, or cleaved caspase-3 (Figure 3).

Given the absence of transcriptional modulation at 3 months, protein analyses were limited to 1-month samples.

3.2.3. Reduced LC3B staining in the uterus of younger mice

Immunohistochemistry at 1-month showed a significant reduction of LC3B staining in the endometrium of adenomyosis mice compared with controls (Figure 4 A-C). In parallel, immunofluorescence quantification revealed a similar trend with an even more pronounced decrease of LC3B staining area in the stroma compartment (Figure 4 D-F)

At 3-months, LC3B staining was comparable between adenomyosis and control groups (Figure 5).

3.3. Decreased LC3B staining in the stroma of human adenomyosis lesions

LC3B expression was evaluated in human uterine samples (n = 12 adenomyosis, n = 10 controls; Figure 6). Endometrium from control patients showed robust LC3B staining across luminal epithelium, glandular epithelium, and stroma. In adenomyosis specimens, ectopic lesions displayed a selective and significant reduction of LC3B staining in the stromal compartment, while glandular epithelium retained expression levels comparable to controls. The eutopic endometrium of adenomyosis patients retained expression levels comparable to controls.

4. Discussion

This study identifies autophagy as a temporally and spatially regulated process in adenomyosis, based on complementary mouse and human analyses. In the neonatal tamoxifen-induced CD1 model,

238 autophagy- and apoptosis-related pathways were significantly altered during the early phase of lesion
239 establishment but normalized at later stages. In contrast, human adenomyosis specimens displayed a
240 persistent and selective reduction of LC3B staining in the stromal compartment, while epithelial
241 components remained comparable to controls. Together, these findings suggest that autophagy
242 impairment is transient during disease initiation in mice but compartmentalized within stromal cells in
243 established human lesions.

244 ### 4.1. Clinical heterogeneity and alignment of our model with diffuse disease

245 Clinically, adenomyosis presents as a heterogeneous condition ranging from junctional-zone thickening
246 to full-thickness infiltration, with focal or diffuse phenotypes (20). Focal adenomyosis- including cystic
247 adenomyoma- is often associated with deep endometriosis (21)(22), whereas diffuse adenomyosis
248 consists of multifocal gland-stroma aggregates throughout the myometrium (19). Our tamoxifen-
249 induced CD1 model reproduces this diffuse pattern: lesions arise at the endometrial–myometrial
250 interface (EMI) and extend centripetally into the myometrium, consistent with the basalis-invagination
251 hypothesis and recent NGS-based clonal evidence (5).
252 Several pathogenetic frameworks have been proposed, including invagination of basalis endometrium
253 across a disrupted junctional zone, metaplasia of Müllerian remnants or progenitor cells and
254 endometrial-myometrial disruption (EMID) after iatrogenic injury (23) (24). The EMID hypothesis is
255 supported by experimental mouse models and by epidemiological associations with uterine procedures
256 such as curettage or cesarean delivery (25). Although our model induces adenomyosis
257 pharmacologically rather than mechanically, both approaches converge on interface instability, a
258 context in which the early autophagy dampening observed here could promote stromal survival and
259 invasion (7).
260 Viewed together, this clinical heterogeneity has a practical consequence: phenotype matters. The
261 autophagy and signaling features described in our study are aligned with diffuse adenomyosis and may
262 not generalize to focal phenotypes. In particular, focal adenomyosis located in the outer myometrium
263 (FOAM) could involve distinct migratory routes, hormonal milieus, or mechanical constraints (22) (26).

This phenotypic diversity plausibly underlies conflicting reports in literature. Future investigations should therefore stratify by subtype, incorporate compartment-resolved endpoints (stromal vs epithelial; eutopic vs ectopic), and align sampling with cycle phase and hormonal exposure when interrogating autophagy and related pathways.

4.2. Autophagy impairment as an early pathogenic trigger

Our findings indicate that autophagy impairment occurs at the earliest stages of adenomyosis, coinciding with myometrial disorganization and initial stromal invasion. In tamoxifen-exposed uteri, smooth-muscle layers were disrupted, creating permissive planes for endometrial invasion. However, C57BL/6J mice can exhibit similar remodeling without developing adenomyosis, suggesting that additional molecular cues are required (25). Acquisition of invasive properties, through epithelial-mesenchymal transition (EMT), a process promoted by hyperestrogenic conditions, has been implicated in both human and preclinical models (4,27). Estrogen is also known to inhibit autophagy, providing a mechanistic link with the early reduction of LC3B observed in our model (11). We used cycle synchronization via estrogen administration, which could have affected the autophagic activity monitored in our research. However, both adenomyosis and control group received the hormonal treatment mitigating the risk of bias. During estrus, autophagy is dampened but not completely inhibited, which is why autophagic variation can still be monitored during this phase.

Beclin1, a major autophagy initiator, connects autophagy and apoptosis through its interaction with Bcl-2 (28). Reduced Beclin-1 expression is associated with proliferation, migration, and EMT via PI3K/AKT/mTOR activation, while its overexpression enhances apoptosis (13)(27). Consistent with this, we observed early modulation of apoptotic regulators such as *Cxcr4, Bax* and *Mapk*, supporting a crosstalk between autophagy and apoptosis during lesion initiation. The absence of cleaved caspase-3 modulation suggests that apoptosis execution may not be fully engaged, potentially allowing survival of invasive stromal cells. In other systems, autophagy and apoptosis are bidirectionally coupled, and dysregulated autophagy can trigger caspase-independent cell death through ERK/MAPK signaling (29) (30) (31).

290 Interestingly, *Lc3b* mRNA was unchanged at 1 month, whereas Western blot and immunohistochemistry
291 consistently showed reduced LC3B protein. This divergence underscores the complexity of autophagy
292 regulation beyond transcriptional control. Post-transcriptional mechanisms, altered protein turnover,
293 or impaired flux may explain reduced LC3B protein levels despite stable transcripts (32,33)(34). Similar
294 mRNA-protein discrepancies have been reported in endometriosis and cancers (35,36), emphasizing the
295 need for dynamic autophagy assays rather than static readouts (37).

296 ### 4.3. Persistent stromal-specific impairment of autophagy in human adenomyosis

297 Interestingly, in one month old mice, LC3B staining area is strongly dampened in the stromal
298 compartment. However, by three months in the murine model, transcriptional and protein differences
299 between adenomyosis and controls were no longer detectable, and LC3B staining had normalized. This
300 may reflect biological adaptation, a shift toward other processes such as angiogenesis, fibrosis, or
301 chronic inflammation or signal dilution in whole-tissue analyses. Collectively, these data support the
302 notion that autophagy downregulation acts primarily as a disease-initiating rather than a sustaining
303 mechanism in mice.

304 In contrast, human adenomyosis samples displayed a persistent stromal-specific reduction of LC3B,
305 whereas glandular epithelium and the eutopic endometrium showed levels comparable to controls. This
306 observation, consistent with reports of compartment-specific autophagy defects in endometriosis
307 (38,39)(40), highlights stromal cells as a critical niche for disease persistence, given their roles in matrix
308 remodeling, cytokine signaling, and invasive behavior (41–43). Sustained autophagy downregulation
309 may thus contribute to stromal survival, apoptosis resistance, and tissue remodeling in established
310 lesions.

311 Mechanistic links have been proposed. Decreased expression of TSC2, LC3B and mTOR expression has
312 been reported in human endometrium, activating mTORC1, suppressing autophagy, and enhancing
313 proliferation and EMT (44). Beclin-1 is also reduced in eutopic endometrium from adenomyosis patients
314 and correlates inversely with CA125 levels and pain scores (45). Together, these findings reinforce the
315 plausibility of autophagy defects as contributors to lesion persistence.

However, the literature remains heterogeneous: while many studies report reduced LC3B or Beclin1 in adenomyosis (38,39,44,44,45), others describe no change (46) or even increased autophagy markers expression (47–50). Such variability likely reflects differences in disease stage (early vs established disease), compartment analyzed (stromal vs epithelial vs whole tissue), menstrual phase, phenotype, or technical approaches. Future work should therefore stratify by phenotype and cycle stage and integrate flux-based assays to resolve whether stromal autophagy impairment consistently underlies disease maintenance.

4.4. Limitations & perspectives

This study has several limitations that should be considered when interpreting the findings. First, gene and protein analyses were performed on whole uterine tissue, which may dilute cell-type restricted effects. Compartment-specific alterations might therefore be underestimated and future work should incorporate laser-capture microdissection, stromal/epithelial cell sorting, or single-cell/spatial transcriptomic and proteomic approaches.

Second, autophagy in the endometrium is tightly regulated by cycle phase. In this study, mice were synchronized with estradiol and analyzed specifically in proliferative states to reduce inter-animal variability. While this approach increases internal consistency, it may also mask phase-dependent fluctuations in autophagy. Future work should therefore adopt phase-stratified designs in both mice (e.g., estrus vs diestrus) and humans (proliferative vs secretory endometrium) to fully capture hormonal influences on autophagy regulation.

Third, conclusions about autophagy relied on static markers rather than direct flux assays, which will require validation by dynamic in vivo approaches such as p62/LC3 turnover under lysosomal inhibition or fluorescent LC3 reporter mice (36). Complementary ex vivo approaches using endometrial organoids or primary stromal cell cultures could provide additional mechanistic insight under controlled hormonal conditions (51).

Fourth, the tamoxifen-induced CD1 mouse reproduces diffuse adenomyosis but does not fully capture the chronicity, heterogeneity, or menstruation-linked physiology of human disease, which limits

generalizability. Validation in complementary systems including human endometrial organoids, would strengthen translational relevance.

Fifth, the human cohort was limited in size and confounded by age differences and by the context of gender-affirming surgery for controls, with potential exposure to exogenous hormones. Larger cohorts with age-matched controls and detailed hormonal information are warranted to strengthen these findings.

Finally, Western blot analysis was not extended to 3-month samples since gene expression levels were already normalized at this stage. However, we acknowledge that transcriptional stability does not preclude potential post-transcriptional or post-translational regulation, and this remains a limitation of the present study

Despite these limitations, our study has notable strengths. It combines a well-characterized experimental model with human validation, applies complementary readouts at transcript, protein, and histological levels, and integrates a temporal dimension by analyzing pre-lesional (1 month) and lesion-established (3 months) stages. This design enabled us to distinguish early, transient changes in mice from persistent, compartment-specific alterations in human lesions.

Together, these strengths and limitations outline a clear path forward: future studies should apply cell type-resolved analyses across defined hormonal contexts, integrate autophagic flux assays in vivo and ex vivo, and validate findings in larger human cohorts. Such approaches will clarify whether stromal autophagy impairment consistently contributes to adenomyosis persistence and could be exploited as a therapeutic target.

5. Conclusion

Across complementary mouse and human analyses, this study identifies autophagy impairment as a temporally and spatially constrained feature of adenomyosis. In the tamoxifen-induced CD1 model, autophagy downregulation was early and transient, coinciding with myometrial disorganization and initial stromal invasion, but normalized by three months. In contrast, human adenomyosis specimens

showed a persistent stromal-specific reduction of LC3B, implicating the stroma as a key compartment for lesion maintenance.

The combined use of a time-resolved murine model and human validation represents a major strength, allowing us to distinguish early initiating events from compartment-specific alterations in established disease. These findings highlight autophagy as a potential contributor to adenomyosis pathogenesis and suggest that stromal autophagy impairment may represent a targetable vulnerability.

Future work should integrate dynamic flux assays, cell type–resolved analyses, and larger, stratified human cohorts to determine whether defective autophagy is a consistent driver of disease persistence and a viable therapeutic entry point.

6. Declaration

6.1. Ethics approval and consent to participate

Animal procedures were approved by the Animal Ethics Committee of the University of Liège (protocol #2387). Human uterine samples were obtained from the Biothèque Hospitalo-Universitaire de Liège (BHUL) under ethical approval CE1267.

6.2. Consent for publication

Not applicable.

6.3. Availability of data and materials

All data generated and analyzed for this study are available from the corresponding author on reasonable request. All raw images (IHC/IF), Western blot original files, MATLAB scripts for image segmentation, and RT-qPCR raw values will be provided upon request.

6.4. Conflict of Interest

The authors declare no commercial or financial relationships that could be construed as a potential conflict of interest.

6.5. Funding

This research was funded by the Fonds de la Recherche Scientifique (F.R.S.-FNRS, Belgium; grants T.0171.21, J.0169.25, F 5/4/130/5) and by the Fondation Léon Fredericq (University of Liège; grants 2023-016, 2023-171, 2023-291, 2024-061, 2025-046).

6.6. Authors' contributions

JV: Investigation, Data curation, Formal analysis, Methodology, Visualization, Writing – original draft. MS: Investigation, Formal analysis, Resources, Validation, Writing – review & editing. SB: Conceptualization, Methodology, Resources, Supervision. MN: Funding acquisition, Writing – review & editing. CM: Conceptualization, Project administration, Supervision, Methodology, Validation, Funding acquisition, Writing – original draft, Writing – review & editing.

6.7. Acknowledgements

We gratefully acknowledge Isabelle Dasoul, Emilie Feyereisen, and Erika Kondarowski for their excellent technical assistance.

6.8. Figures Legends

Figure 1. Severity of adenomyosis increases with age in mice.

Histological and quantitative analysis of adenomyotic lesions in uteri from 1-month and 3-month-old mice. (A) Representative transverse uterine sections from adenomyosis mice at 1 month and (B) at 3 months with corresponding zooms (orange square) on area of interest. The white line delineates the border between eutopic endometrium and myometrium. Sections were stained by

immunofluorescence with EpCAM (red, endometrial glands), α-SMA (green, smooth muscle cells), and DAPI (blue, nuclei). Adenomyosis foci (white arrows) are defined by the presence of glands and stroma within the myometrium. At 1 month, lesions were mild and focal, occasionally showing stromal invasion and partial distortion of myometrial organization (red circle). At 3 months, lesions were diffuse, multifocal, and deeply infiltrative. (C) Quantification of lesion severity based on depth of myometrial infiltration: grade I: inner third; grade II: inner two-thirds; grade III: entire thickness. Data are shown as absolute counts (n = 16 for 1 month; n = 15 for 3 months).

Figure 2. mRNA expression of autophagy-, apoptosis-, and signaling-related genes in adenomyosis. Relative mRNA expression levels of (A) signaling-, (B) apoptosis- and (C) autophagy- related genes in uterine tissues from control (CTL) and adenomyosis (ADM) mice at 1 and 3 months. Gene expression was normalized to *Gapdh* and calculated using the ΔΔCt method. Data are presented as median ± min-max. Statistical comparisons were performed using Welch's *t*-tests after confirming normality, or Mann–Whitney tests otherwise. **p* < 0.05; ***p* < 0,01; ****p* < 0,001.

Figure 3. Altered expression of autophagy- and apoptosis-related proteins in early adenomyosis.
(A) Representative Western blots of LC3B, BAX, total and phosphorylated-MAPK (p-MAPK), BCL2, total and phosphorylated NF-κB (p-NF-κB), total and phosphorylated AKT (p-AKT), and cleaved caspase-3 in uterine tissues from control (CTL) and adenomyosis (ADM) mice at 1 month (n = 5 per group). GAPDH served as a loading control.
(B) Quantification of relative protein levels. Data are presented as mean ± SD for normally distributed variables (LC3B, BAX, MAPK, BCL2, AKT, cleaved caspase-3) and as median ± IQR for non-normal variables (NF-κB). Group comparisons were performed using Welch's t-tests or Mann–Whitney tests as appropriate. *p < 0.05; ns: not significant.

Figure 4. Decreased LC3B expression in the uteri of adenomyosis mice.

(A, B) Representative images of LC3B expression by immunohistochemistry in uterine transverse sections from 1 month control (A) and adenomyosis (B) mice.

(C) Quantification of lc3b staining index (H-score) across luminal epithelium, glandular epithelium, and stroma. (D, E) Representative images of LC3B expression by immunofluorescence (LC3B red; α-SMA green; DAPI blue) in uterine sections from control (D) and adenomyosis (E) mice. From left to right: original transverse uterine section; delimitation of eutopic endometrium (white line) and lesions (red lines); delimitation of luminal (white line) and glandular epithelium (red lines) within the eutopic endometrium. Stroma was identified by subtracting luminal et glandular epithelium from total eutopic endometrium. (F) Quantification of LC3B stained area in different compartments of eutopic endometrium: luminal epithelium, glandular epithelium, and stroma and across eutopic and ectopic endometrium.

Data are presented as mean ± SD. Group comparisons were performed using Welch's t-test after confirming normality. ***$p < 0.001$; ns: not significant. N = 12 in each group.

Figure 5. LC3B expression in 3-month-old adenomyosis mice.

Representative IHC images of LC3B expression in uterine sections from control (A) and adenomyosis (B) mice. For each image, focus on a zone including luminal epithelium and stroma. No significant difference in lc3b staining intensity was observed between groups.

Figure 6. Decreased stromal LC3B expression in human adenomyosis lesions.

Representative IHC images of LC3B expression in human endometrial tissue from control women (A), eutopic endometrium of adenomyosis patients (B), and ectopic endometrial lesions (C).

(D) Quantification of LC3B staining index (H-score) in luminal epithelium, glandular epithelium, and stroma. Data are presented as mean ± SD for normally distributed variables (luminal epithelium) and as median ± IQR for non-normal variables (glandular epithelium, stroma). Group comparisons were performed using Welch's t-tests or Mann–Whitney tests as appropriate. *$p < 0.05$; ns: not significant.

7. References

1. Chapron C, Vannuccini S, Santulli P, Abrão MS, Carmona F, Fraser IS, et al. Diagnosing adenomyosis: an integrated clinical and imaging approach. Human Reproduction Update. 2020 Apr 15;26(3):392–411.

2. Vannuccini S, Petraglia F. Recent advances in understanding and managing adenomyosis. F1000Res. 2019 Mar 13;8:283.

3. Zhai J, Vannuccini S, Petraglia F, Giudice LC. Adenomyosis: Mechanisms and Pathogenesis. Semin Reprod Med. 2020 May;38(02/03):129–43.

4. García-Solares J, Donnez J, Donnez O, Dolmans MM. Pathogenesis of uterine adenomyosis: invagination or metaplasia? Fertility and Sterility. 2018 Mar;109(3):371–9.

5. Bulun SE, Yildiz S, Adli M, Wei JJ. Adenomyosis pathogenesis: insights from next-generation sequencing. Human Reproduction Update. 2021 Oct 18;27(6):1086–97.

6. Vannuccini S, Tosti C, Carmona F, Huang SJ, Chapron C, Guo SW, et al. Pathogenesis of adenomyosis: an update on molecular mechanisms. Reproductive BioMedicine Online. 2017 Nov;35(5):592–601.

7. Wang X, Benagiano G, Liu X, Guo SW. Unveiling the Pathogenesis of Adenomyosis through Animal Models. JCM. 2022 Mar 21;11(6):1744.

8. Parzych KR, Klionsky DJ. An Overview of Autophagy: Morphology, Mechanism, and Regulation. Antioxidants & Redox Signaling. 2014 Jan 20;20(3):460–73.

9. Mizushima N, Levine B. Autophagy in Human Diseases. Longo DL, editor. N Engl J Med. 2020 Oct 15;383(16):1564–76.

10. Wirawan E, Berghe TV, Lippens S, Agostinis P, Vandenabeele P. Autophagy: for better or for worse. Cell Res. 2012 Jan;22(1):43–61.

11. Choi J, Jo M, Lee E, Oh YK, Choi D. The Role of Autophagy in Human Endometrium1. Biology of Reproduction [Internet]. 2012 Mar 1 [cited 2024 Feb 20];86(3). Available from: https://academic.oup.com/biolreprod/article-lookup/doi/10.1095/biolreprod.111.096206

12. Yang S, Wang H, Li D, Li M. Role of Endometrial Autophagy in Physiological and Pathophysiological Processes. J Cancer. 2019;10(15):3459–71.

13. Vervier J, Squatrito M, Nisolle M, Henry L, Munaut C. Controversial Roles of Autophagy in Adenomyosis and Its Implications for Fertility Outcomes—A Systematic Review. JCM. 2024 Dec 10;13(24):7501.

14. Squatrito M, Vervier J, Bindels J, Bernet L, Blacher S, Nisolle M, et al. Impaired Fertility in Adenomyosis: a Murine Model Reveals Endometrial Receptivity and Progesterone Resistance Imbalances. Reproduction. 2024 Mar;REP-24-0019.

15. De Clercq K, Hennes A, Vriens J. Isolation of Mouse Endometrial Epithelial and Stromal Cells for In Vitro Decidualization. JoVE. 2017 Mar 2;(121):55168.

16. Caligioni CS. Assessing Reproductive Status/Stages in Mice. CP Neuroscience [Internet]. 2009 July [cited 2023 Dec 8];48(1). Available from: https://currentprotocols.onlinelibrary.wiley.com/doi/10.1002/0471142301.nsa04is48

17. Byers SL, Wiles MV, Dunn SL, Taft RA. Mouse Estrous Cycle Identification Tool and Images. Singh SR, editor. PLoS ONE. 2012 Apr 13;7(4):e35538.

18. Lin P, Lan X, Chen F, Yang Y, Jin Y, Wang A. Reference Gene Selection for Real-Time Quantitative PCR Analysis of the Mouse Uterus in the Peri-Implantation Period. Müller R, editor. PLoS ONE. 2013 Apr 24;8(4):e62462.

19. Bird CC, McElin TW, Manalo-Estrella P. The elusive adenomyosis of the uterus—revisited. American Journal of Obstetrics and Gynecology. 1972 Mar;112(5):583–93.

20. Van den Bosch T, Dueholm M, Leone FPG, Valentin L, Rasmussen CK, Votino A, et al. Terms, definitions and measurements to describe sonographic features of myometrium and uterine masses: a consensus opinion from the Morphological Uterus Sonographic Assessment (MUSA) group. Ultrasound Obstet Gynecol. 2015 Sept;46(3):284–98.

21. Donnez J, Donnez O, Dolmans MM. Introduction: Uterine adenomyosis, another enigmatic disease of our time. Fertility and Sterility. 2018 Mar;109(3):369–70.

22. Chapron C, Tosti C, Marcellin L, Bourdon M, Lafay-Pillet MC, Millischer AE, et al. Relationship between the magnetic resonance imaging appearance of adenomyosis and endometriosis phenotypes. Human Reproduction. 2017 July;32(7):1393–401.

23. Guo SW. The Pathogenesis of Adenomyosis vis-à-vis Endometriosis. JCM. 2020 Feb 10;9(2):485.

24. Elsherbini M, Koga K, Hiraoka T, Kumasawa K, Maki E, Satake E, et al. Establishment of a novel mouse model of adenomyosis suitable for longitudinal and quantitative analysis and perinatal outcome studies. Sci Rep. 2022 Oct 20;12(1):17515.

25. Marquardt RM, Jeong JW, Fazleabas AT. Animal Models of Adenomyosis. Semin Reprod Med. 2020 May;38(02/03):168–78.

26. Chen T, Xu Y, Xu X, Wang J, Qiu Z, Yu Y, et al. Comprehensive transcriptional atlas of human adenomyosis deciphered by the integration of single-cell RNA-sequencing and spatial transcriptomics. Protein & Cell. 2024 July 1;15(7):530–46.

27. Chen Y, Li H, Huang C, Twu N, Yen M, Wang P, et al. Oestrogen-induced epithelial–mesenchymal transition of endometrial epithelial cells contributes to the development of adenomyosis. The Journal of Pathology. 2010 Nov;222(3):261–70.

28. Pattingre S, Tassa A, Qu X, Garuti R, Liang XH, Mizushima N, et al. Bcl-2 Antiapoptotic Proteins Inhibit Beclin 1-Dependent Autophagy. Cell. 2005 Sept;122(6):927–39.

29. Xue L, Fletcher GC, Tolkovsky AM. Autophagy Is Activated by Apoptotic Signalling in Sympathetic Neurons: An Alternative Mechanism of Death Execution. Molecular and Cellular Neuroscience. 1999 Sept;14(3):180–98.

30. Espert L. Autophagy is involved in T cell death after binding of HIV-1 envelope proteins to CXCR4. Journal of Clinical Investigation. 2006 Aug 1;116(8):2161–72.

31. Yee KS, Wilkinson S, James J, Ryan KM, Vousden KH. PUMA- and Bax-induced autophagy contributes to apoptosis. Cell Death Differ. 2009 Aug;16(8):1135–45.

32. Kang HM, Noh KH, Chang TK, Park D, Cho HS, Lim JH, et al. Ubiquitination of MAP1LC3B by pVHL is associated with autophagy and cell death in renal cell carcinoma. Cell Death Dis. 2019 Mar 22;10(4):279.

33. Franks A, Airoldi E, Slavov N. Post-transcriptional regulation across human tissues. Vogel C, editor. PLoS Comput Biol. 2017 May 8;13(5):e1005535.

34. Zhang Z, Li M, Hou Y, Huang T, Zhang B, Lin Q, et al. SETD7 promotes LC3B methylation and degradation in ovarian cancer. Journal of Biological Chemistry. 2025 Feb;301(2):108134.

35. Yang M, Jiang H, Ding X, Zhang L, Zhang H, Chen J, et al. Multi-omics integration highlights the role of ubiquitination in endometriosis fibrosis. J Transl Med. 2024 May 12;22(1):445.

36. Chen G, Gharib TG, Huang CC, Taylor JMG, Misek DE, Kardia SLR, et al. Discordant Protein and mRNA Expression in Lung Adenocarcinomas. Molecular & Cellular Proteomics. 2002 Apr;1(4):304–13.

37. Kaizuka T, Morishita H, Hama Y, Tsukamoto S, Matsui T, Toyota Y, et al. An Autophagic Flux Probe that Releases an Internal Control. Molecular Cell. 2016 Nov;64(4):835–49.

38. Mei J, Sheng X, Yan Y, Cai X, Zhang C, Tian J, et al. Decreased Krüppel-like factor 4 in adenomyosis impairs decidualization by repressing autophagy in human endometrial stromal cells. BMC Mol and Cell Biol. 2022 June 27;23(1):24.

39. d'Argent M, Stratopoulou CA, Cussac S, Camboni A, Jadoul P, Donnez J, et al. Are lower levels of apoptosis and autophagy behind adenomyotic lesion survival? Reproductive BioMedicine Online. 2023 Sept;47(3):103248.

40. Shen HH, Zhang T, Yang HL, Lai ZZ, Zhou WJ, Mei J, et al. Ovarian hormones-autophagy-immunity axis in menstruation and endometriosis. Theranostics. 2021;11(7):3512–26.

41. Lebovic DI, Mueller MD, Taylor RN. Immunobiology of endometriosis. Fertility and Sterility. 2001 Jan;75(1):1–10.

42. Lv H, Zhao G, Jiang P, Wang H, Wang Z, Yao S, et al. Deciphering the endometrial niche of human thin endometrium at single-cell resolution. Proc Natl Acad Sci USA. 2022 Feb 22;119(8):e2115912119.

43. Owusu-Akyaw A, Krishnamoorthy K, Goldsmith LT, Morelli SS. The role of mesenchymal–epithelial transition in endometrial function. Human Reproduction Update. 2019 Jan 1;25(1):114–33.

44. Gu NH, Li GJ, Yang BX, You M, Lin Y, Sun F, et al. Hypo-Expression of Tuberin Promotes Adenomyosis via the mTOR1-Autophagy Axis. Front Cell Dev Biol. 2021 July 29;9:710407.

45. Ren Y, Mu L, Ding X, Zheng W. Decreased expression of Beclin 1 in eutopic endometrium of women with adenomyosis. Arch Gynecol Obstet. 2010 Oct;282(4):401–6.

46. Tantanavipas S, Aojanepong T, Waiyaput W, Sophonsritsuk A. The expression of *BECN1, LC3B* , and *BCL2* genes in eutopic endometrium of patients with adenomyosis: A cross-sectional study. Journal of Endometriosis and Pelvic Pain Disorders. 2021 Dec;13(4):250–5.

47. Chen M, Wang W, Fu X, Yi Y, Wang K, Wang M. Role of Pink1-mediated mitophagy in adenomyosis. PeerJ. 2023 Nov 30;11:e16497.

48. Zhou Y, Zhao X, Zhang L, Xia Q, Peng Y, Zhang H, et al. Iron overload inhibits cell proliferation and promotes autophagy via PARP1/SIRT1 signaling in endometriosis and adenomyosis. Toxicology. 2022 Jan;465:153050.

49. Huang Y, Zhao Y, Liu H, Yang Y, Cheng L, Deng X, et al. Decreased expression of *GRIM-19* induces autophagy through the *AMPK* / *ULK1* signaling pathway during adenomyosis. Biology of Reproduction. 2022 July 31;ioac151.

50. Zhou Y, Peng Y, Xia Q, Yan D, Zhang H, Zhang L, et al. Decreased Indian hedgehog signaling activates autophagy in endometriosis and adenomyosis. Reproduction. 2021 Feb;161(2):99–109.

51. Boretto M, Cox B, Noben M, Hendriks N, Fassbender A, Roose H, et al. Development of organoids from mouse and human endometrium showing endometrial epithelium physiology and long-term expandability. Development. 2017 May 15;144(10):1775–86.

8. TABLES

Table 1. Primers for qRT-PCR

GENE NAME	PRIMER SEQUENCES (5' – 3')	PRODUCT SIZE (BP)
Atg9b	Forward: GAACCATACAAGACGTGGACCAT Reverse: CCCAGGGTACCGAGCTGAG	248
Akt1	Forward: TCGTGTGGCAGGATGTGTAT Reverse: ACCTGGTGTCAGTCTCAGAGG	78
Bcl2	Forward: AACATCGCCCTGTGGATGAC Reverse: TATGCACCCAGAGTGATGCAG	191
Bcl2l1	Forward: GCCACCTATCTGAATGACCACC Reverse: AGGAACCAGCGGTTGAAGCGC	134
Bid	Forward: GCGTCTGCGTGGTGATTC Reverse: TCCCAGTAAGCTTGCACAGG	211
Cxcr4	Forward: CCATGGAACCGATCAGTCTGA Reverse: CGGTACTTGTCCGTCATGCT	238
Dapk1	Forward: GGCGCACGAAGCGAC Reverse: AGACCGGTACTTTTCTCACGAC	245
Igf1	Forward: AAGCGATGGGGAAAATCAGC Reverse: ATAGCCTGTGGGCTTGTTGAA	242
Lc3b	Forward: GTCCTGGACAAGACCAAGTTCC Reverse: CCATTCACCAGGAGGAAGAAGG	119
Pik3c3	Forward: TGCAGTTCATCCAGTCGGTT Reverse: TCACACAGTATCCAGCACAGC	159
Tnfs10	Forward: GGAAGACCTCAGAAAGTGGCAG Reverse: TTTCCGAGAGGACTCCCAGGAT	129
Ulk1	Forward: GCATCGAGCAAAACCTGCAA Reverse: CCACTTGGGGAGAAGGTGTG	195
Ulk2	Forward: TATTGCAATGGTGGAGACCTGG Reverse: CTGCCGCAATCTGATGGAGA	94
Gapdh	Forward: GGTGGACCTCATGGCCTACA Reverse: CTCTCTTGATCAGTGTCCTTGCT	82
Rplp0	Froward: GGACCCGAGAAGACCTCCTT Reverse: GCACATCACTCAGAATTTCAATGG	85

Abbreviations: qRT-PCR, quantitative reverse transcription polymerase chain reaction; Bp, number of base pairs; GAPDH, glyceraldehyde 3-phosphate dehydrogenase.

591
592 **Table 2.** Antibody used for Western Blot
593

Target (Antigen)	Dilution	Company	# Catalog
LC3B	1/1000	Novusbio	nb100-2220
BCL2	1/1000	Cell signaling	3498
BCLXL	1/1000	Cell signaling	2764
P-AKT	1/1000	Cell signaling	9271
AKT	1/1000	Cell signaling	9272
BAX	1/1000	Cell signaling	14796
MAPK1	1/1000	Cell signaling	9102
P-MAPK1	1/1000	Cell signaling	9101
NFKB1	1/1000	Cell signaling	8242
Caspase3	1/1000	Cell signaling	9661
GAPDH	1/10 000	Chemicon international	mab374

594 9.
595

Figures

Figure 1

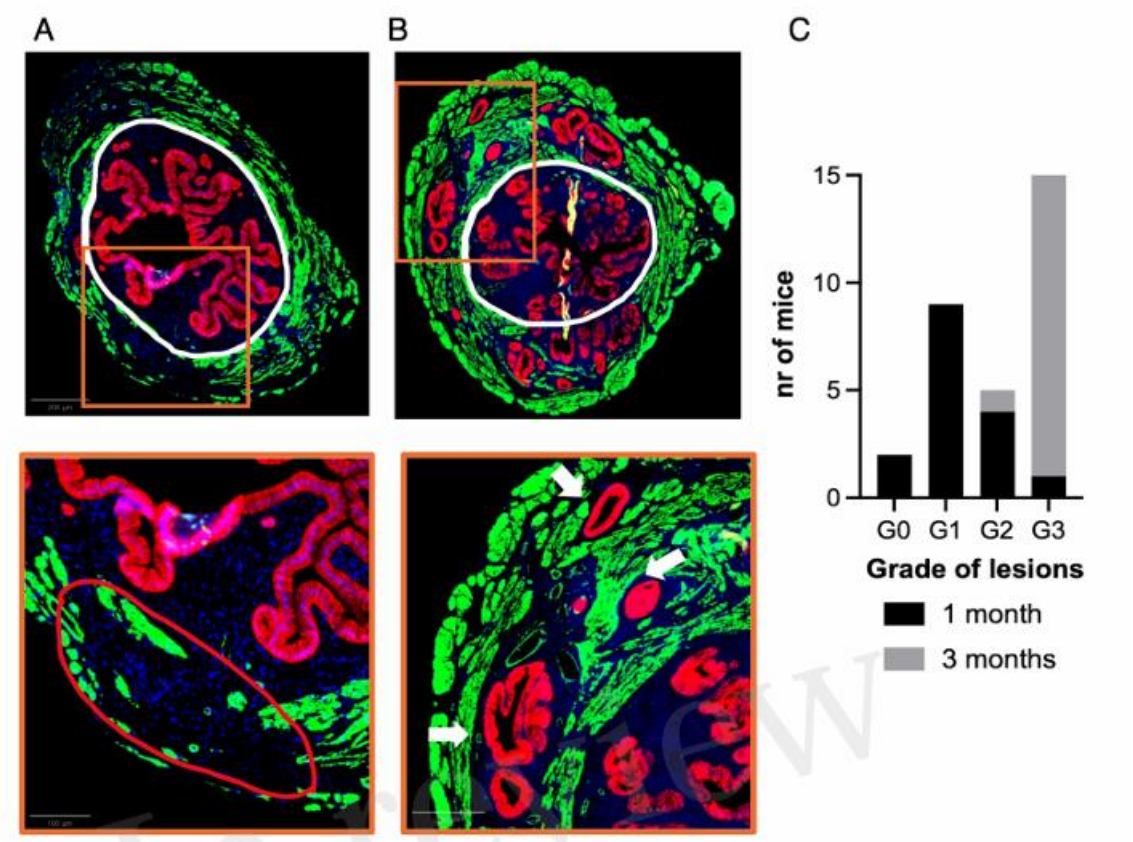
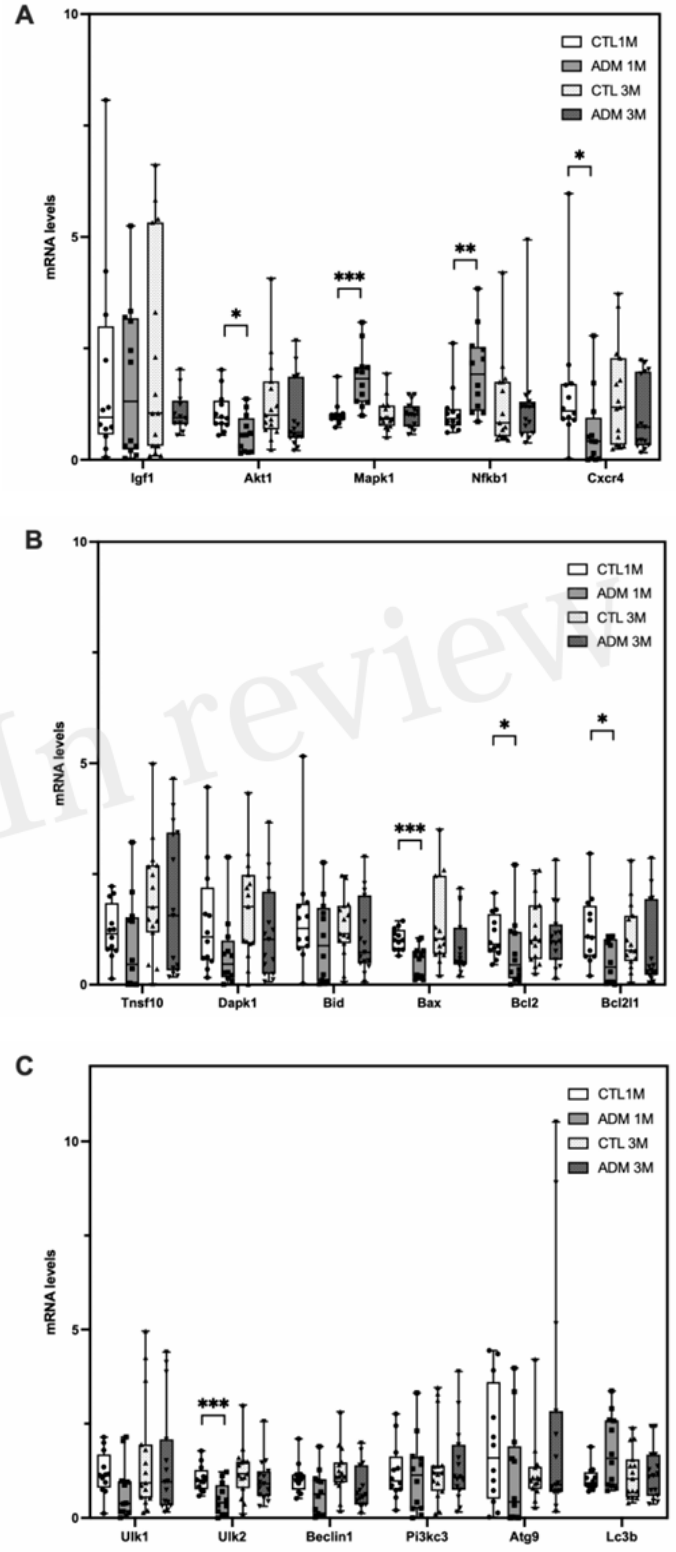
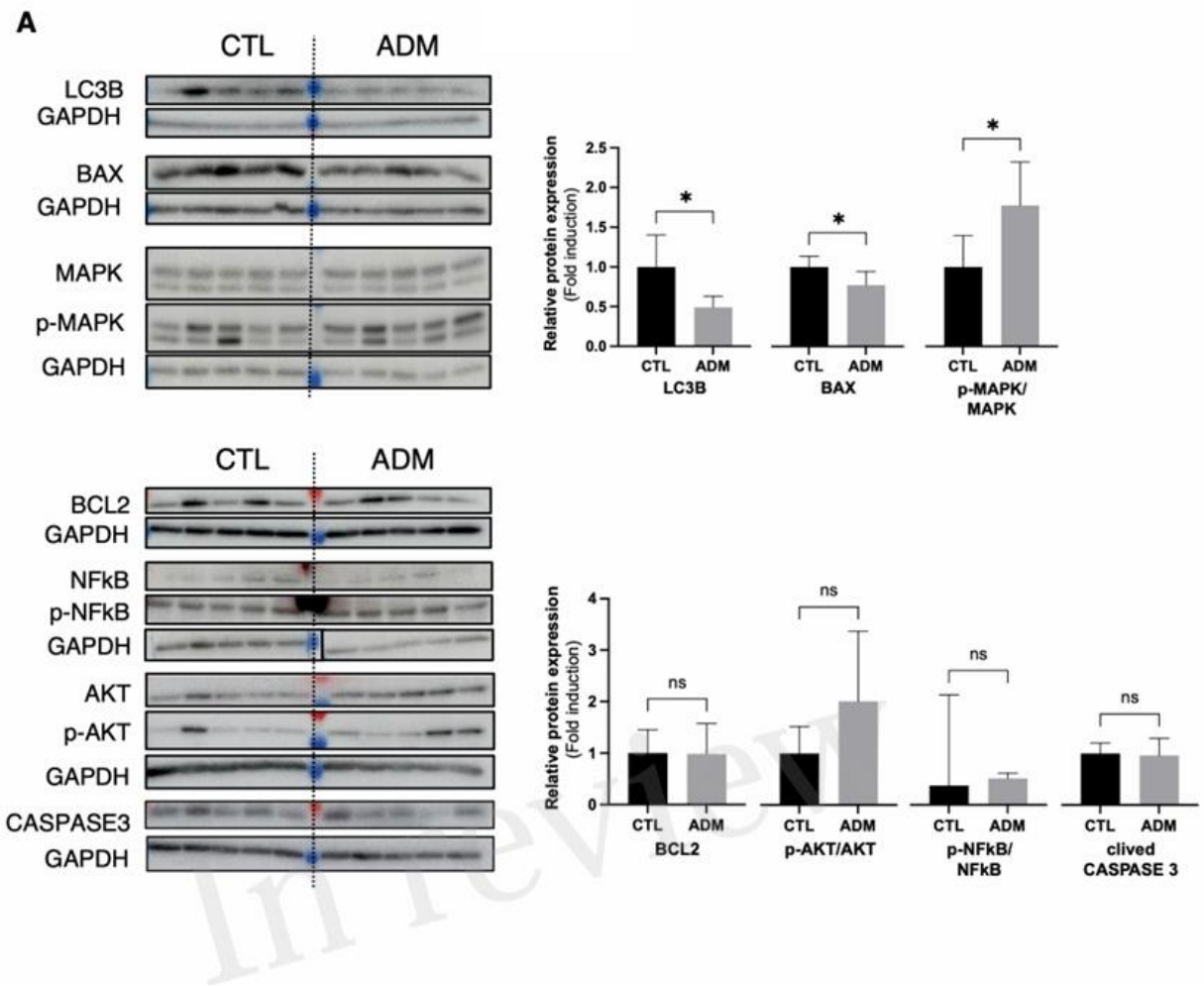


Figure 2



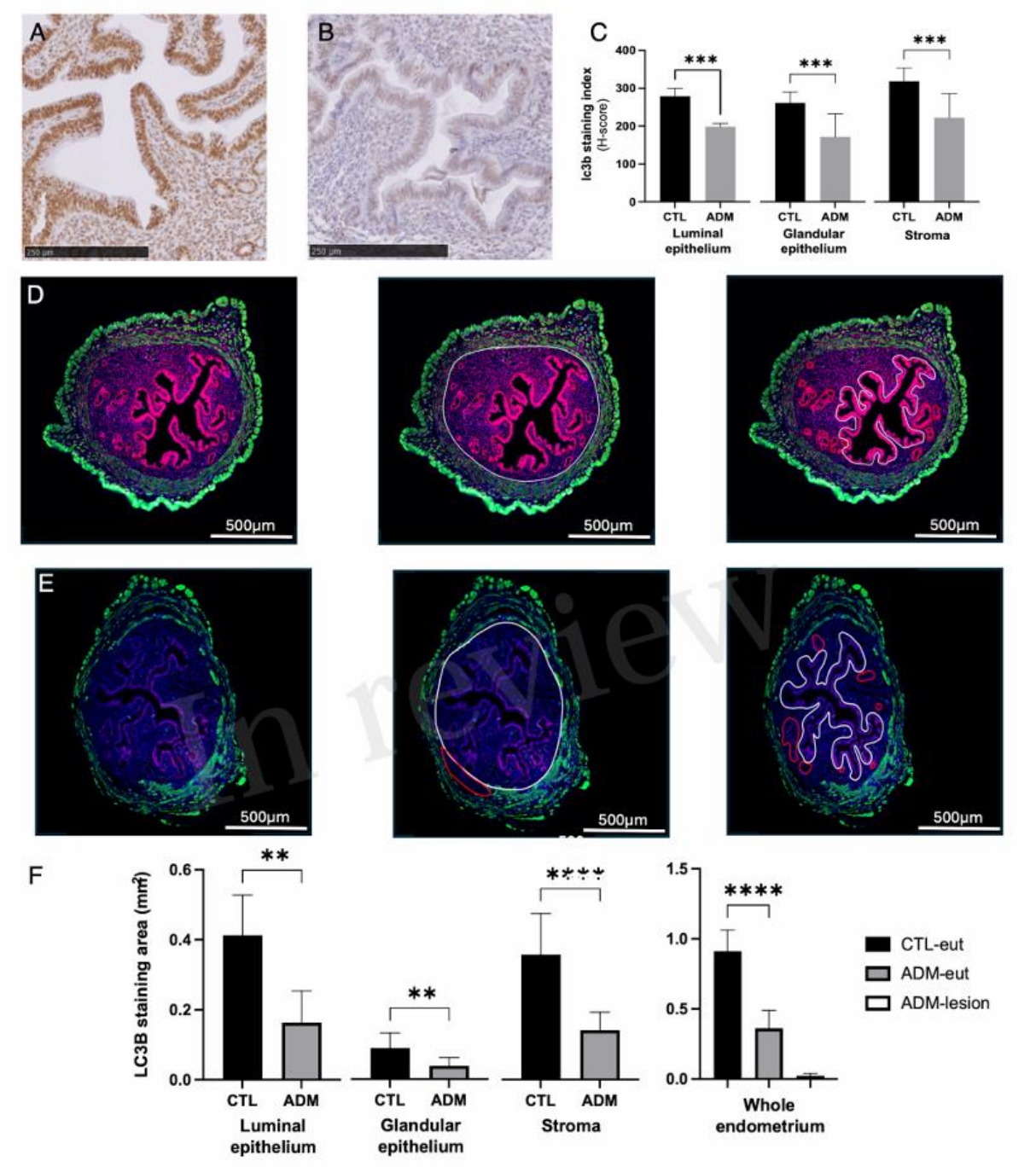
In review

Figure 3



In review

Figure 4



In review

Figure 5

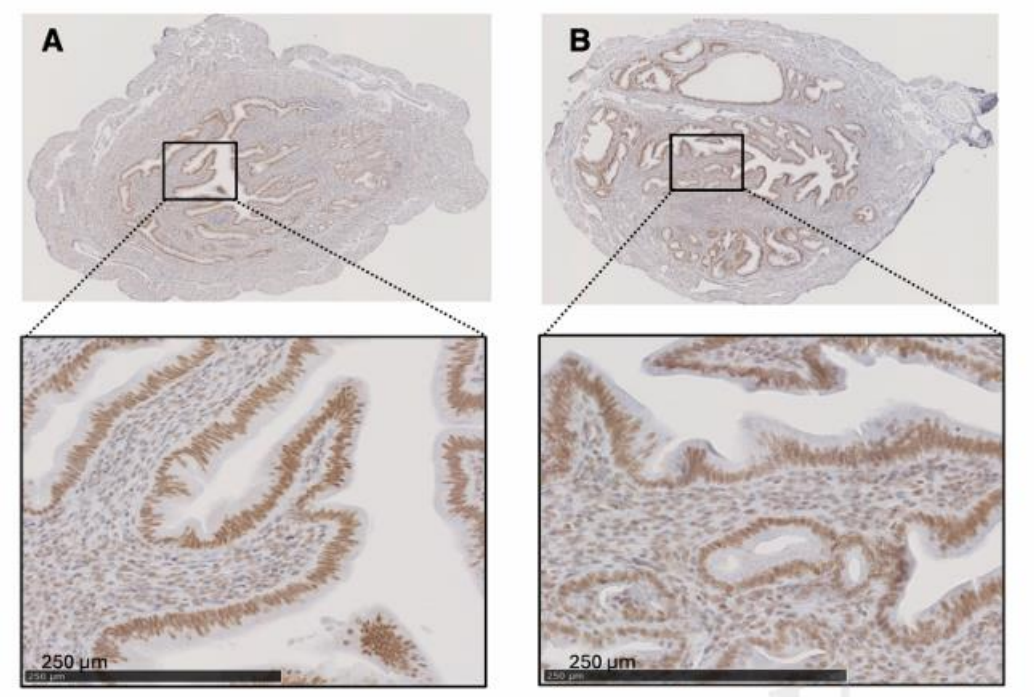
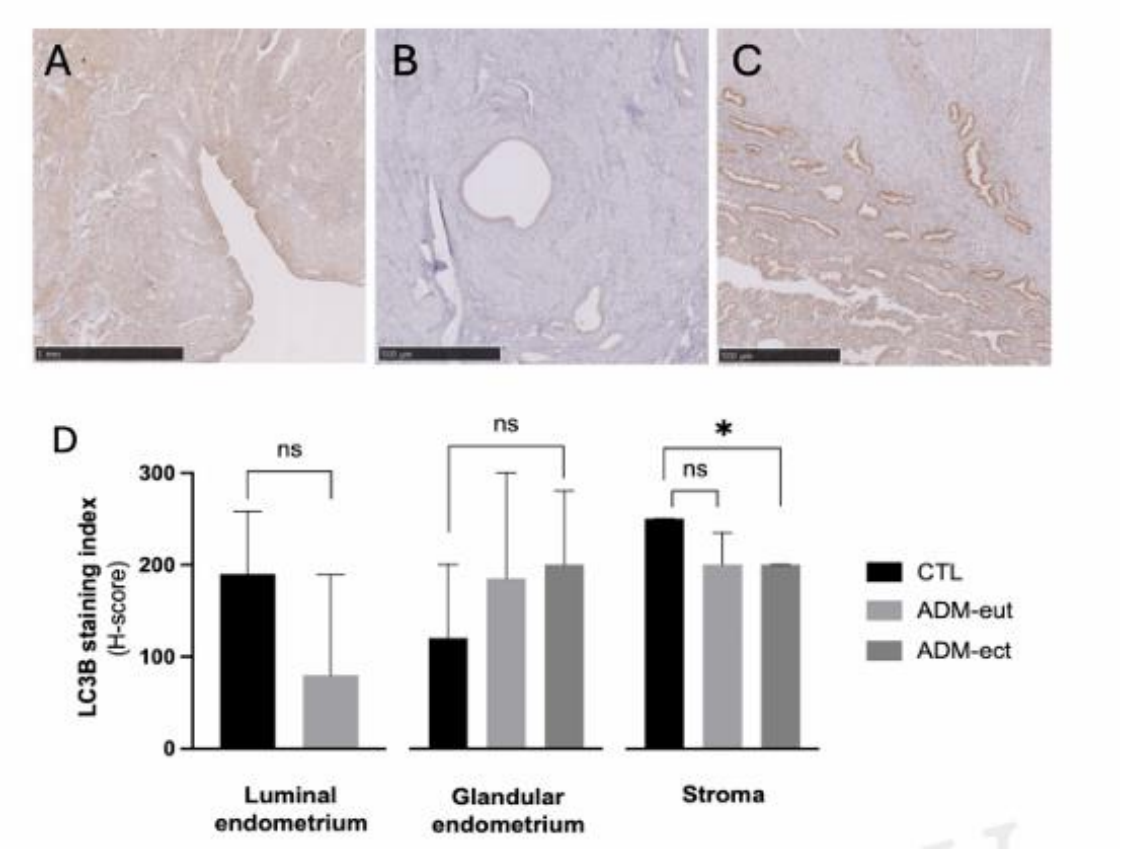


Figure 6



APPENDIX 2

Comparison of morphological and digital-assisted analysis for BCL6 endometrial expression in women with endometriosis.

Marlyne Squatrito, Silvia Blacher, Laurie Henry, Soraya Labied, Agnès Noël, Michelle Nisolle and Carine Munaut.

Journal of clinical Medicine (2022), 11, 6164

At the beginning of my PhD, while animal ethics approval for the murine adenomyosis model was still pending, previously generated Master's thesis data were validated and published to avoid losing time and to strengthen the clinical foundation of the project. That work, entitled "Contribution to the study of the pathophysiology of endometriosis and its non-invasive diagnosis", focused on endometrial expression of the transcriptional repressor BCL6, a promising tissue biomarker for endometriosis and endometriosis-associated infertility.

The article compared the conventional semi-quantitative HSCORE method with a new computer-assisted digital image analyses to quantify BCL6 staining on whole-slide images of eutopic endometrium from fertile and infertile women with or without endometriosis. It showed higher BCL6 expression in infertile women with endometriosis, particularly in advanced stage disease, and demonstrated a strong correlation between HSCORE and the automated digital measurements, confirming that the new method is objective, robust and reproductible. Overall, this work both reinforced the link between endometrial BCL6 overexpression, endometriosis and infertility, and provided a validated digital tool for more reliable BCL6 quantification in future diagnostic and research settings.

Journal of
Clinical Medicine

MDPI

Article

Comparison of Morphological and Digital-Assisted Analysis for BCL6 Endometrial Expression in Women with Endometriosis

Marlyne Squatrito [1], Silvia Blacher [1], Laurie Henry [2], Soraya Labied [2], Agnès Noel [1], Michelle Nisolle [1,2] and Carine Munaut [1,*]

[1] Laboratory of Tumor and Development Biology, GIGA-Cancer, University of Liège, 4000 Liège, Belgium
[2] Obstetrics and Gynecology Department, University of Liege, 4000 Liège, Belgium
* Correspondence: c.munaut@uliege.be; Tel.: +32-43-662-453

Abstract: BCL6 (B-cell lymphoma 6) is a proto-oncogene and transcriptional repressor initially described as being involved in B-cell lymphoma. Recently, this factor has been identified as a promising tissue biomarker which could be used to diagnose women affected by endometriosis. Previous studies used HSCORE for BCL6 staining quantification in the endometrium. However, this semi-quantitative technique of analysis has some limitations, including a lack of objectivity, robustness, and reproducibility that may lead to intra- and inter-observer variability. Our main goal was to develop an original computer-assisted method to quantify BCL6 staining from whole-slide images reliably. In order to test the efficiency of our new digital method of quantification, we compared endometrial BCL6 expression between fertile and infertile women without or with different stages of endometriosis by using the widely used HSCORE analysis and our new automatic digital image analysis. We find a higher expression of BCL6 in the endometrium of infertile women with endometriosis and women with stage IV endometriosis. Furthermore, we demonstrate a significant correlation between the two types of independent measurements, indicating the robustness of results and also the reliability of our computer-assisted method for BCL6 quantification. In conclusion, our work, by using this original computer-assisted method, enables BCL6 quantification more objectively, reliably, robustly, and promptly compared to HSCORE analysis.

Keywords: B-cell lymphoma 6; endometriosis; infertility; diagnosis; HSCORE; computer-assisted analysis

check for updates

Citation: Squatrito, M.; Blacher, S.; Henry, L.; Labied, S.; Noel, A.; Nisolle, M.; Munaut, C. Comparison of Morphological and Digital-Assisted Analysis for BCL6 Endometrial Expression in Women with Endometriosis. *J. Clin. Med.* **2022**, *11*, 6164. https://doi.org/10.3390/jcm11206164

Academic Editor: Jacek Szamatowicz

Received: 19 September 2022
Accepted: 13 October 2022
Published: 19 October 2022

Publisher's Note: MDPI stays neutral with regard to jurisdictional claims in published maps and institutional affiliations.

Copyright: © 2022 by the authors. Licensee MDPI, Basel, Switzerland. This article is an open access article distributed under the terms and conditions of the Creative Commons Attribution (CC BY) license (https://creativecommons.org/licenses/by/4.0/).

1. Introduction

Initially described as a proto-oncogene and transcriptional repressor implicated in the pathogenesis of B-cell lymphoma, BCL6 has recently been identified as a promising tissular biomarker which could be used to diagnose women affected by endometriosis [1–4]. The recent identification of actors acting in conjunction with BCL6, and the delineation of several target genes have helped to better determine its biological functions [5]. BCL6 contributes to cell cycle control and differentiation, as well as apoptosis inhibition [6–8]. The underlying pathophysiological mechanisms leading to endometriosis, a gynecological disease defined by the presence of endometrial tissue outside of the uterine cavity, also include proliferation, apoptosis, autophagy, migration, invasion, fibrosis, angiogenesis, oxidative stress, inflammation, and immune escape [9–11].

This disorder is mainly associated with both pelvic pain and infertility and affects about 10–15% of reproductive-age women [12]. Endometriosis is most often classified into four stages according to revised criteria described by the American Society of Reproductive Medicine (rASRM). To define the disease stage, a score taking into account the size of the lesions, their location, and the extent of the adhesions is used [9,13,14]. However, no association between the severity of symptoms and this stage has been shown [15]. The current time span between the onset of women's perceived symptoms and diagnosis is

approximately 8–12 years [16]. Indeed, the range of symptoms can be confusing for the patient and care provider [17–19]. This lack of early diagnosis has many consequences for patient health since they are not treated for endometriosis during this period. A late diagnosis, sometimes at an advanced stage of the disease, can already represent a loss of chance for the patient regarding her fertility. Endometriosis, as well as its surgical management, can compromise the chances of pregnancy, particularly by altering the ovarian reserve. This is why an early diagnosis, which may allow oocyte vitrification to be carried out in order to preserve the patient's chances of fertility, is essential in the management of these women [20]. In addition to the physical consequences, endometriosis induces a deleterious effect on the psychosocial and sexual wellbeing of women and imposes a substantial economic burden from a personal and societal point of view [21,22].

Currently, to reliably diagnose endometriosis, laparoscopy with inspection of the abdominal cavity and histological confirmation of the suspicious lesion must be performed. While alternative methods such as medical imaging, genetic tests, or biomarkers are aimed at alleviating invasive diagnosis, none of them can adequately substitute for surgery at present [23–27]. Recent studies have identified a promising tissular biomarker called B-cell lymphoma 6 (BCL6), which could be used to diagnose women affected by endometriosis [1–4].

Indeed, Evans-Hoeker et al. examined BCL6 expression in the human eutopic endometrium across the menstrual cycle in women with and without endometriosis and found that BCL6 was overexpressed in the eutopic endometrium of patients with endometriosis, especially during the secretory phase of the menstrual cycle [1]. BCL6 is a promising candidate as a unique diagnostic tissular biomarker for the detection of endometriosis in women. On the contrary, use of BCL6 as a protein biomarker in bodily fluids (such as serum and urine) for a less invasive diagnosis of endometriosis is not appropriate [2]. Furthermore, this factor was also overexpressed in the endometrium of women who suffer from unexplained infertility, recurrent miscarriages, or implantation failure during in vitro fertilization cycles [28–30]. These observations prompted researchers to investigate the potential role of BCL6 in the pathophysiological process of endometriosis, especially in infertility [30,31].

All the previous studies describing BCL6 expression in the endometrium of women with or without proven endometriosis use HSCORE for the quantification of BCL6 staining [1–4]. Evans-Hoeker et al. established an immunostaining cutoff to better discriminate normal versus elevated BCL6 expression [1]. Manual evaluation by an experienced researcher remains a time-consuming and subjective procedure that might lead to intra- and inter-observer variability. The main objective of this study was to compare BCL6 expression in human eutopic endometrium samples by using digital image analysis to obtain objective and highly reproducible quantification from whole-slide images with an adequate dynamic range and the previously widely used HSCORE.

2. Materials and Methods

2.1. Human Endometrial Tissue Samples

The human endometrial samples were collected from two cohorts of patients recruited in the Gynecology-Obstetrics Department and the Center for Medically Assisted Procreation of the University of Liège (Citadelle Hospital). The first population included endometrium samples obtained from women who underwent laparoscopy for suspicion of endometriosis. The second one included eutopic endometrium samples from infertile women (associated or not with endometriosis). In the first population, the presence of the disease was confirmed by clinicians at the time of laparoscopy in the endometriosis group and classified according to the revised American Society of Reproductive Medicine (ASRM) [14,32]. Women without endometriosis at laparoscopy constituted the control group. All the endometria analyzed were in the secretory phase as determined by the pathologist. The first cohort was further divided into 3 groups: the control fertile group (n = 11), the stage I endometriosis group (n = 6), and the stage IV endometriosis group (n = 10) (subdivided into fertile (n = 5) and infertile group (n = 5)) (Table 1).

Table 1. Demographics of patients who underwent laparoscopy.

Characteristics	Endometriosis (n = 16)	Control (n = 11)	p Value
Age (y), mean (SD)	32.4 ± 6.1	38.4 ± 5.7	0.018
Body mass index (kg/m^2), mean (SD)	22.9 ± 4.5	25.5 ± 4.8	0.112
Pregnancy history (%)			
>1	3 (18.75)	7 (63.6)	0.042 *
≤1	13 (81.25)	4 (26.4)	
Endometriosis stage, n (%)			
I	6 (37.5)		
IV	10 (62.5)		

* Chi-squared and Fisher's exact test analysis; ns = non-significant.

The second cohort was divided into 2 groups: the control infertile group (n = 29) and the laparoscopically previously proven endometriosis-infertile group (n = 17) (Table 2).

Table 2. Demographics of infertile patients with or without endometriosis.

Characteristics	Endometriosis (n = 17)	No endometriosis (n = 29)	p Value
Age (y), mean (SD)	34.5 ± 5.0	36.2 ± 3.4	0.244
Body mass index (kg/m^2), mean (SD)	22.0 ± 7.6	26.04 ± 5.8	0.166
Infertility type, n (%)			
Primary	6 (35.3)	13 (44.8)	0.565 *
Secondary	11 (64.7)	15 (51.7)	
Not available	0 (0)	1 (3.45)	
Previous miscarriages, n (%)			
>1	10 (58.8)	16 (55.2)	0.774 *
≤1	7 (41.2)	13 (44.8)	

* Chi-squared and Fisher's exact test analysis; ns = non-significant.

2.2. Immunofluorescence Analyses

Endometrial samples fixed in 4% formaldehyde were paraffin-embedded and serially sectioned (5 µm sections). Sections were deparaffinized and rehydrated before endogenous peroxidase activity was blocked by incubating the sections in 3% hydrogen peroxide for 20 min at room temperature (RT). Nonspecific binding sites were blocked by incubation in the "Free Blocking Solution" (Cell Signaling, Danvers, USA) for 1 h at RT. The primary antibody was diluted at 1:100 in the "Dako diluent" (Dako, Jena, Germany) and incubated overnight at 4 °C (rabbit monoclonal anti-BCL6 (Cell Signaling 89369, Danvers, MA, USA)), followed by incubation with the secondary antibody HRP (ENVISION/HRP ready to use, Dako, Glostrup, Denmark) for 30 min at RT. The reaction was revealed using TSA-FITC (Akoya Biosciences, Marlborough, Massachusetts, USA), and the sections were mounted with DAPI FluoromountG mounting medium (SouthernBiotech, Birmingham, AL, USA).

2.3. Quantification of Immunostaining

The slides were scanned at 20× magnification using a high-resolution digital slide scanner (NanoZoomer 2.0HT (Hamamatsu Photonics, K.K., Hamamastsu, Japan)). The semi-quantitative analysis of the nuclear labeling of BCL6 was performed using HSCORE (0–4), calculated using the following equation: HSCORE = $\sum$ Pi (i + 1)/100, with i = the intensity of fluorescence with values of 1, 2, or 3 (weak, moderate, or intense, respectively), and Pi = the percentage of epithelial cells labeled for each intensity, which can range from 0 to 100%. The use of HSCORE is a semi-quantitative immunohistological analysis method that has been previously validated [33]. The HSCORE analyses were performed blinded by two different observers.

J. Clin. Med. **2022**, *11*, 6164

Scanned slides were also analyzed with computer-assisted image analysis. In this case, image processing and automatic quantification of BCL6 expression in the epithelial compartment of the endometrium were performed using the image analysis toolbox of MATLAB R2021b according to the following steps: The original images were registered in the full-color red, green, and blue (RGB) space where BCL6 labeling appeared in green and DAPI nuclear staining in blue. Both in the original color image (Figure 1A) as well as in its grey-level green-component (Figure 1B), both epithelial and stromal cells are stained. All cell types appear clearly when an automatic thresholding technique is used to extract the green stained regions (Figure 1C) [34]. The criterion used to discriminate between glandular epithelial cells and stromal cells is their different sizes and morphology. Indeed, as stromal cells appear as small and isolated objects, glandular epithelial cells are connected together as ring-like structures of greater size. Taking into account these differences, morphological filters were applied to the binary images (erosion and open transformations of appropriate sizes) followed by a geodesic reconstruction (Figure 1D) [35]. Finally, the resulting binary image was then multiplied by the grey level green component in order to eliminate the background (Figure 1E). By this process, BCL6 intensities were visualized in 256 grey levels. Eventually, a histogram of intensities was calculated (Figure 1E,F). It must be noticed that the filtering process is strongly dependent on the quality of the images. Indeed, "noise-characteristics" depend on the technical process (tissue fixation, immunofluorescence staining, microscopy-image registration, etc.). For this reason, filtering techniques must be adapted to the particular situation.

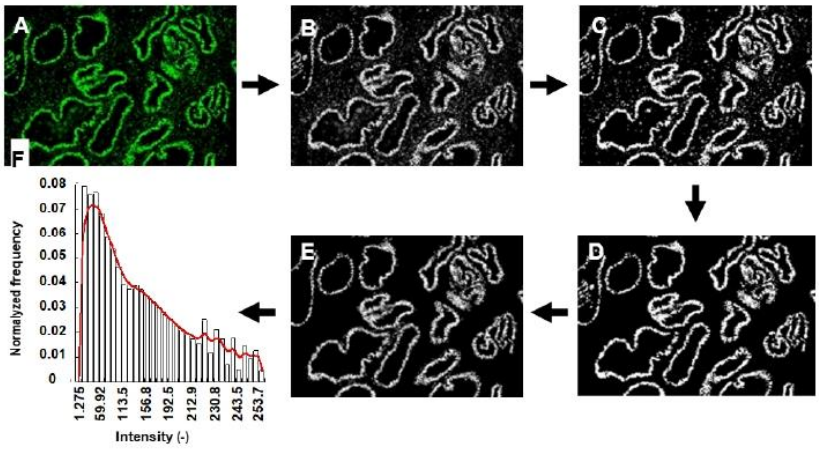


Figure 1. Image processing workflow to quantify epithelial endometrial BCL6 expression: (**A**) original image of one isolated region from the whole scanned image registered in RGB space, (**B**) grey level green component of the RGB image (**C**) automatic thresholding to extract all BCL6 expression (green labeling in stromal and epithelial compartments), (**D**) resulting binary image after filtering stromal cells, (**D**) visualization of the resulting image in 256 gray levels) after background elimination by multiplying the binary image with the grey level green component, (**E**) resulting intensity distribution, (**F**) Histogram of intensities.

The whole methodological process was applied to sections containing at least 20 glands where the intensity distribution was measured simultaneously. A mean intensity distribution of sections corresponding to the patients within the same group was then calculated point by point and in order to produce underling distributions, a smooth operator was applied on histograms Meg Noah (2022). Smooth Operator (Stineman 1D Interpolation) (https://www.mathworks.com/matlabcentral/fileexchange/104195-smooth-operator-stineman-1d-interpolation), MATLAB Central File Exchange. Retrieved 11 October 2022.

2.4. Statistical Analysis

For statistical HSCORE analyses, the Mann–Whitney nonparametric test was applied for comparisons between two groups. HSCORE data are presented as the median (min. to max.), with $p \leq 0.05$ considered statistically significant. To characterize mean intensity distribution curves, percentiles were determined. Taking into account that each point of the mean intensity distribution is the mean ± SEM value of the individual distributions corresponding to each patient of the same group, the Mann–Whitney nonparametric test was applied point by point to perform comparisons between the different experimental groups. To establish possible correlations between HSCOREs and computer-assisted image analysis measurements, mean distribution curves were fitted with the Gaussian model, and the amplitude, the mean, and the standard deviation were determined. Statistical analyses were performed using GraphPad Prism Software (GraphPad 8.0, San Diego, CA, USA).

3. Results

3.1. BCL6 Expression in Different Endometriosis Stages

BCL6 expression was first evaluated by immunofluorescence in the endometrium of a control group and compared to the endometrial expression in women suffering from endometriosis (stage I or stage IV associated with/without infertility, patients from Table 1). Epithelial BCL6 expression levels were found to be comparable in the endometrium of control women and of women with endometriosis stage I. However, higher BCL6 glandular epithelial cell expression was observed in the endometrium of infertile women with stage IV endometriosis (Figure 2A). The HSCORE analysis confirmed those observations. While no difference in BCL6 HSCORE between patients without endometriosis and those with minimal endometriosis (stage I) could be demonstrated (HSCORE 2.095 ($p25 = 1.890$; $p75 = 2.425$) versus 2.012 ($p25 = 1.825$; $p75 = 2.645$), $p = 0.9829$), in the case of severe endometriosis (stage IV) associated with infertility, a higher HSCORE for BCL6 was observed (HSCORE 3.625 ($p25 = 2.948$; $p75 = 3.875$) versus 2.095 ($p25 = 1.890$; $p75 = 2.425$, $p = 0.0053$) (Figure 2B).

A digital computer-assisted quantification of BCL6 was performed on the same sections. BCL6 intensity distributions were calculated in the four different groups of patients (Figure 2C). For the control group, intensities were spread in the range of 11.033–78.448 (Table 3). For women with endometriosis, distributions remained almost within the same ranges (between 4.219 and 56.204 and between 10.819 and 59.447 for stage I and IV endometriosis, respectively). However, in the endometrium of women with stage IV endometriosis associated with infertility, the intensity distribution was spread out in a larger range between 26.138–125.93 (Figure 2C and Table 3), indicating a higher and more heterogeneous BCL6 expression. Statistical analyses evidenced no difference between the intensity distribution of control, stage I, and fertile stage IV endometriosis, whereas a significant difference was observed between those conditions and infertile stage IV endometriosis, mostly in the highest intensity range.

Table 3. Percentiles of BCL6 intensity and distribution in control, endometriosis (Stage I and IV), and infertility-associated endometriosis stage IV patients.

Percentiles	Fertile Control	Fertile Stage I	Fertile Stage IV	Infertile Stage IV
10	11.033	4.2194	10.819	26.138
25	22.021	11.996	16.810	40.352
50	34.980	21.942	27.304	64.295
75	54.108	36.508	42.114	95.765
90	78.448	56.204	59.477	125.93

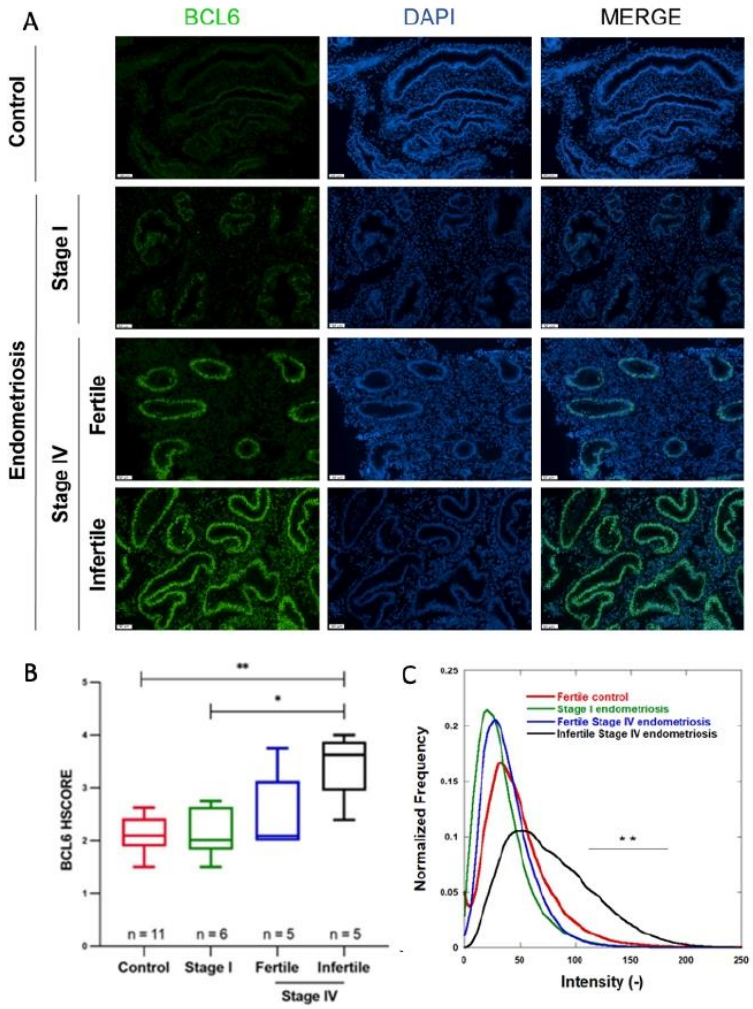


Figure 2. BCL6 expression in endometrium collected during laparoscopy: (**A**) Representative images of BCL6 expression in the endometrium of patients without endometriosis (controls), patients with stage I or stage IV endometriosis with or without associated fertility (▬ 50 µm); (**B**) BCL6 HSCOREs in control patients (n = 11) and (**B**) patients with stage I (n = 6) or stage IV, fertile (n = 5) or infertile (n = 5); (**C**) mean normalized BCL6 intensity distributions measured on all scanned sections in each group of patients. * $p \leq 0.05$, and ** $p \leq 0.01$.

3.2. BCL6 Expression and Fertility Status

In order to further study the role of BCL6 in endometriosis-related infertility, a comparison of its expression in the endometrium of infertile patients without and with endometriosis was performed on a second set of patients (Table 2). The same methodology was used. In all patients suffering from infertility, clear endometrial BCL6 expression was observed (Figure 3A). HSCORE was indeed the highest in the group of infertile women with endometriosis (HSCORE 2.335 ($p25$ = 1.876; $p75$ = 3.521) versus 3.202 ($p25$ = 2.241; $p75$ = 4.000), p = 0.0348) (Figure 3B). When the digital computer-assisted image analysis was used, distribution intensities showed significant differences at low and large intensities (Figure 3C). In fertile or infertile women without endometriosis, BCL6 intensities were spread in a narrow range (see Tables 3 and 4), with a median at 34.980 (range 11.033–78.448) and at 14.786 (range 0.724–48.51), respectively. The median of BCL6 intensity distribution in the endometrium of infertile women was found at 21.493 in the range of 4.451–54.822.

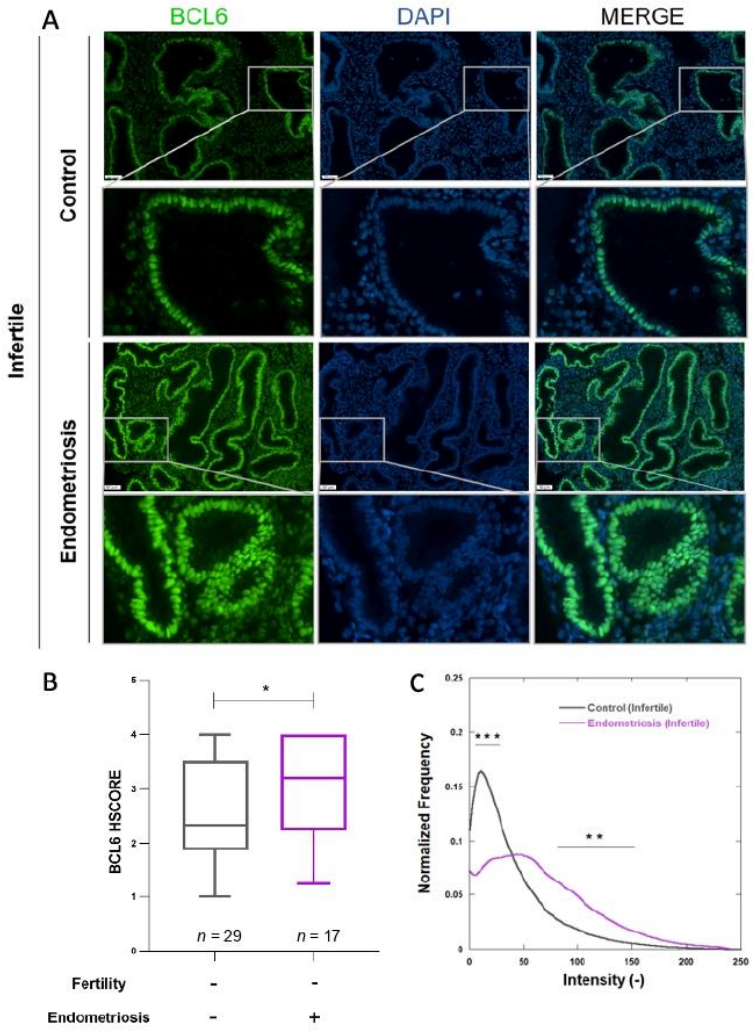


Figure 3. BCL6 expression in the endometrium of infertile patients with and without endometriosis: (**A**) representative images of BCL6 expression (▬ 50 µm); (**B**) HSCOREs in the endometrium of infertile women without endometriosis (controls, $n = 29$ and infertile patients with endometriosis ($n = 17$); (**C**) mean normalized BCL6 intensity distributions measured on all scanned sections in each group of patients. * $p \leq 0.05$, ** $p \leq 0.01$, and *** $p \leq 0.001$.

Table 4. Percentiles of BCL6 intensity and distribution in infertile patients without or with associated endometriosis.

Percentiles	Infertile Control	Infertile with Endometriosis
10	0.724	4.4512
25	4.912	11.464
50	14.786	21.493
75	28.596	34.918
90	48.512	54.822

The question arises about a possible correlation between the two independent measurements performed on the same samples, i.e., determination of HSCOREs by independent and blinded observers and automatic image analysis.

The linear regression between the HSCOREs and the mean values of the corresponding intensity distributions showed a significant correlation between the two types of measurements, indicating the robustness of results (Figure 4).

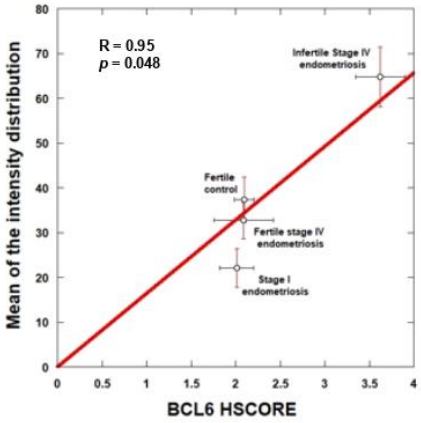


Figure 4. Correlation between computer-assisted image quantification and HSCORE analyses for endometrial BCL6 expression.

4. Discussion

In our study, we confirmed the recently described overexpression of endometrial BCL6 in endometriotic patients by using HSCORE analysis. Indeed, we found that endometrial BCL6 expression was higher in the endometrium of women with stage IV endometriosis. Moreover, the highest HSCORE for BCL6 expression was found in infertile women suffering from endometriosis as compared to infertile women without endometriosis. As previously demonstrated by others, our data suggests a potential role for BCL6 in infertility. Indeed, for up to 50–80% of women having difficulties conceiving, endometriosis has been found to be the main reason for infertility [30,36]. Several hypotheses have been formulated about the way endometriosis impacts fertility. It is known that endometriosis, especially ovarian endometrioma and its surgical treatment, can impair the ovarian reserve. However, this is not the only impact of this pathology on fertility, and one recent theory is linked to progesterone resistance and endometrial receptivity [37]. Endometriosis is clearly associated with a systemic and reversible inflammatory condition that impairs endometrial function [38]. So far, a limited number of studies have investigated the possible involvement of BCL6 in infertility. Interestingly, high levels of endometrial BCL6 in women with unexplained infertility have been recently revealed [1,29] as demonstrated and confirmed in our study by the higher expression of this factor in our infertile group of patients without endometriosis. Increased endometrial BCL6 has been recently considered to be a negative predictor for patients with endometriosis undergoing IVF [3]. Stimulation of pro-inflammatory cytokines by BCL6 in the peritoneal fluid of these women could be responsible for infertility as well as recurrent miscarriages. In addition to its inflammatory power, IL-6 may also be able to directly induce the expression of BCL6. Once transcribed, BCL6, with the help of SIRT1, could inactivate regulators of progesterone but also lead to implantation defects and repeated miscarriages in patients with endometriosis [3].

To date, none of the medical treatments have been able to cure endometriosis, and symptoms recur as soon as the medication is stopped. The development of new biomedical targets, aimed at the cellular and molecular mechanisms responsible for endometriosis, is clearly needed [39]. The use of molecules targeting BCL6 could be a new approach to be investigated in order to treat these numerous patients suffering from endometriosis.

In our study, we used the same semi-quantitative analysis method of BCL6 expression as previously validated [1]. We are perfectly aware that we used the scoring method established for a different experimental method. In the study of Evans-Hoeker et al.,

negative, medium, or high BCL6 labeling was defined as <1.4, from ≥1.4 to <2.7, and ≥2.7 [1]. Using the cutoff value of 1.4 in HSCORE analysis, BCL6 expression displayed an accuracy of 94% for diagnosing endometriosis. In our study, we used a different antibody for BCL6 detection and performed immunofluorescence for immunostaining. We did not determine HSCORE cutoffs in our setting. However, by using computer-assisted image analysis, a method based on whole pixel quantification and computerization, we were able to clearly demonstrate a good correlation between the two different methods of quantification. The purpose of our work was to compare HSCORE analysis using an automatic quantitative computer-assisted method. It must be noted that the proposed methodology can be implemented with any commercial or free image analysis software as it uses the basic functions in this domain. Moreover, this original computer-assisted method is a robust and reproducible method since it allows one to quantify objectively a large number of endometrial tissue sections.

5. Conclusions

By using this original computer-assisted method, our work confirmed that endometrial BCL6 is proportionally expressed with endometriosis stage and that BCL6 overexpression is associated with endometriosis, especially with infertility caused by this gynecological disease. Our quantification method is objective, reliable, robust, and prompt compared to HSCORE analysis.

Author Contributions: Experimental work, M.S.; data acquisition, analysis, and interpretation of data, M.S, S.B. and C.M; writing—draft manuscript, M.S.; software analysis design—computer-assisted image analysis, S.B.; patient selection, M.N., L.H. and S.L.; writing and review—final manuscript and supervision, C.M.; funding acquisition, M.N., C.M. and A.N. All authors have read and agreed to the published version of the manuscript.

Funding: This research was supported by grants from the Fonds de la Recherche Scientifique—FNRS (F.R.S.-FNRS, Belgium, grant number T.0171.21 attributed to M.N. and grant J.0143.22 attributed to C.M.), the Foundation against Cancer (foundation of public interest, Belgium), the Fonds spéciaux de la Recherche (University of Liège), the Centre Anticancéreux près l'Université de Liège, and the Fondation Hospitalo Universitaire Léon Fredericq (FHULF, University of Liège).

Institutional Review Board Statement: The study was conducted in accordance with the Declaration of Helsinki and approved by the Institutional Ethics Committee (707) of the University of Liege (protocol code 2020/397, approved 18 January 2021).

Informed Consent Statement: Informed consent was obtained from all subjects.

Data Availability Statement: Not applicable.

Acknowledgments: The authors acknowledge Isabelle Dasoul and Emilie Feyereisen for their excellent technical assistance. The authors also thank Marie Timmermans for her administrative help.

Conflicts of Interest: The authors declare no conflict of interest.

References

1. Evans-Hoeker, E.; Lessey, B.A.; Jeong, J.W.; Savaris, R.F.; Palomino, W.A.; Yuan, L.; Schammel, D.P.; Young, S.L. Endometrial BCL6 Overexpression in Eutopic Endometrium of Women with Endometriosis. *Reprod. Sci.* **2016**, *23*, 1234–1241. [CrossRef] [PubMed]
2. Sansone, A.M.; Hisrich, B.V.; Young, R.B.; Abel, W.F.; Bowens, Z.; Blair, B.B.; Funkhouser, A.T.; Schammel, D.P.; Green, L.J.; Lessey, B.A.; et al. Evaluation of BCL6 and SIRT1 as Non-Invasive Diagnostic Markers of Endometriosis. *Curr. Issues Mol. Biol.* **2021**, *43*, 96. [CrossRef] [PubMed]
3. Nezhat, C.; Rambhatla, A.; Miranda-Silva, C.; Asiaii, A.; Nguyen, K.; Eyvazzadeh, A.; Tazuke, S.; Agarwal, S.; Jun, S.; Nezhat, A.; et al. BCL-6 Overexpression as a Predictor for Endometriosis in Patients Undergoing In Vitro Fertilization. *J. Soc. Laparosc. Robot. Surg.* **2020**, *24*, e2020.00064. [CrossRef] [PubMed]
4. Nezhat, C.; Agarwal, S.; Lee, D.A.; Tavallaee, M. Can we accurately diagnose endometriosis without a diagnostic laparoscopy? *J. Turk. Ger. Gynecol. Assoc.* **2022**, *23*, 117–119. [CrossRef]
5. Bunting, K.L.; Melnick, A.M. New effector functions and regulatory mechanisms of BCL6 in normal and malignant lymphocytes. *Curr. Opin. Immunol.* **2013**, *25*, 339–346. [CrossRef]

6. Kumagai, T.; Miki, T.; Kikuchi, M.; Fukuda, T.; Miyasaka, N.; Kamiyama, R.; Hirosawa, S. The proto-oncogene Bc16 inhibits apoptotic cell death in differentiation-induced mouse myogenic cells. *Oncogene* **1999**, *18*, 467–475. [CrossRef]
7. Hatzi, K.; Nance, J.P.; Kroenke, M.A.; Bothwell, M.; Haddad, E.K.; Melnick, A.; Crotty, S. BCL6 orchestrates Tfh cell differentiation via multiple distinct mechanisms. *J. Exp. Med.* **2015**, *212*, 539–553. [CrossRef]
8. Valls, E.; Lobry, C.; Geng, H.; Wang, L.; Cardenas, M.; Rivas, M.; Cerchietti, L.; Oh, P.; Yang, S.N.; Oswald, E.; et al. BCL6 Antagonizes NOTCH2 to Maintain Survival of Human Follicular Lymphoma Cells. *Cancer Discov.* **2017**, *7*, 506–521. [CrossRef]
9. Zondervan, K.T.; Becker, C.M.; Missmer, S.A. Endometriosis. *N. Engl. J. Med.* **2020**, *382*, 1244–1256. [CrossRef]
10. Vallve-Juanico, J.; Houshdaran, S.; Giudice, L.C. The endometrial immune environment of women with endometriosis. *Hum. Reprod. Update* **2019**, *25*, 564–591. [CrossRef]
11. Giacomini, E.; Minetto, S.; Li Piani, L.; Pagliardini, L.; Somigliana, E.; Vigano, P. Genetics and Inflammation in Endometriosis: Improving Knowledge for Development of New Pharmacological Strategies. *Int. J. Mol. Sci.* **2021**, *22*, 9033. [CrossRef] [PubMed]
12. Nisolle, M.; Alvarez, M.L.; Colombo, M.; Foidart, J.M. Pathogenesis of endometriosis. *Gynecol. Obstet. Fertil.* **2007**, *35*, 898–903. [CrossRef] [PubMed]
13. Zondervan, K.T.; Becker, C.M.; Koga, K.; Missmer, S.A.; Taylor, R.N.; Vigano, P. Endometriosis. *Nat. Rev. Dis. Primers* **2018**, *4*, 9. [CrossRef] [PubMed]
14. Adamson, G.D. Endometriosis classification: An update. *Curr. Opin. Obstet. Gynecol.* **2011**, *23*, 213–220. [CrossRef]
15. Vercellini, P.; Fedele, L.; Aimi, G.; Pietropaolo, G.; Consonni, D.; Crosignani, P.G. Association between endometriosis stage, lesion type, patient characteristics and severity of pelvic pain symptoms: A multivariate analysis of over 1000 patients. *Hum. Reprod.* **2007**, *22*, 266–271. [CrossRef]
16. Agarwal, S.K.; Chapron, C.; Giudice, L.C.; Laufer, M.R.; Leyland, N.; Missmer, S.A.; Singh, S.S.; Taylor, H.S. Clinical diagnosis of endometriosis: A call to action. *Am. J. Obstet. Gynecol.* **2019**, *220*, 354.e1–354.e12. [CrossRef]
17. Kiesel, L.; Sourouni, M. Diagnosis of endometriosis in the 21st century. *Climacteric* **2019**, *22*, 296–302. [CrossRef]
18. Hudson, N. The missed disease? Endometriosis as an example of 'undone science'. *Reprod. Biomed. Soc. Online* **2022**, *14*, 20–27. [CrossRef]
19. Koninckx, P.R.; Ussia, A.; Adamyan, L.; Tahlak, M.; Keckstein, J.; Wattiez, A.; Martin, D.C. The epidemiology of endometriosis is poorly known as the pathophysiology and diagnosis are unclear. *Best Pract. Res. Clin. Obstet. Gynaecol.* **2021**, *71*, 14–26. [CrossRef]
20. Henry, L.; Vervier, J.; Boucher, A.; Brichant, G.; Gaspard, O.; Labied, S.; Munaut, C.; Ravet, S.; Nisolle, M. Oocyte Cryopreservation in Patients with Endometriosis: Current Knowledge and Number Needed to Treat. *J. Clin. Med.* **2022**, *11*, 4559. [CrossRef]
21. Simoens, S.; Dunselman, G.; Dirksen, C.; Hummelshoj, L.; Bokor, A.; Brandes, I.; Brodszky, V.; Canis, M.; Colombo, G.L.; DeLeire, T.; et al. The burden of endometriosis: Costs and quality of life of women with endometriosis and treated in referral centres. *Hum. Reprod.* **2012**, *27*, 1292–1299. [CrossRef]
22. Eisenberg, V.H.; Decter, D.H.; Chodick, G.; Shalev, V.; Weil, C. Burden of Endometriosis: Infertility, Comorbidities, and Healthcare Resource Utilization. *J. Clin. Med.* **2022**, *11*, 1133. [CrossRef]
23. Hudelist, G.; English, J.; Thomas, A.E.; Tinelli, A.; Singer, C.F.; Keckstein, J. Diagnostic accuracy of transvaginal ultrasound for non-invasive diagnosis of bowel endometriosis: Systematic review and meta-analysis. *Ultrasound Obstet. Gynecol.* **2011**, *37*, 257–263. [CrossRef]
24. Aas-Eng, M.K.; Montanari, E.; Lieng, M.; Keckstein, J.; Hudelist, G. Transvaginal Sonographic Imaging and Associated Techniques for Diagnosis of Ovarian, Deep Endometriosis, and Adenomyosis: A Comprehensive Review. *Semin. Reprod. Med.* **2020**, *38*, 216–226. [CrossRef]
25. Agrawal, S.; Tapmeier, T.; Rahmioglu, N.; Kirtley, S.; Zondervan, K.; Becker, C. The miRNA Mirage: How Close Are We to Finding a Non-Invasive Diagnostic Biomarker in Endometriosis? A Systematic Review. *Int. J. Mol. Sci.* **2018**, *19*, 599. [CrossRef]
26. May, K.E.; Conduit-Hulbert, S.A.; Villar, J.; Kirtley, S.; Kennedy, S.H.; Becker, C.M. Peripheral biomarkers of endometriosis: A systematic review. *Hum. Reprod. Update* **2010**, *16*, 651–674. [CrossRef]
27. Nisenblat, V.; Hull, M.L. Biomarkers in Endometriosis. In *How to Perform Ultrasonography in Endometriosis*; Guerriero, S., Condous, G., Alcázar, J.L., Eds.; Springer International Publishing: Cham, Switzerland, 2018; pp. 169–183. [CrossRef]
28. Slizewski, D.; Crowe, R.; Young, S.L.; Lessey, B.A. Endometriosis is a common denominator in unexplained pregnancy loss and infertility based on BCL6 testing. *Fertil. Steril.* **2015**, *104*, e83–e84. [CrossRef]
29. Almquist, L.D.; Likes, C.E.; Stone, B.; Brown, K.R.; Savaris, R.; Forstein, D.A.; Miller, P.B.; Lessey, B.A. Endometrial BCL6 testing for the prediction of in vitro fertilization outcomes: A cohort study. *Fertil. Steril.* **2017**, *108*, 1063–1069. [CrossRef]
30. Likes, C.E.; Cooper, L.J.; Efird, J.; Forstein, D.A.; Miller, P.B.; Savaris, R.; Lessey, B.A. Medical or surgical treatment before embryo transfer improves outcomes in women with abnormal endometrial BCL6 expression. *J. Assist. Reprod. Genet.* **2019**, *36*, 483–490. [CrossRef]
31. Louwen, F.; Kreis, N.N.; Ritter, A.; Friemel, A.; Solbach, C.; Yuan, J. BCL6, a key oncogene, in the placenta, pre-eclampsia and endometriosis. *Hum. Reprod. Update* **2022**, dmac027. [CrossRef]
32. Canis, M.; Donnez, J.G.; Guzick, D.S.; Halme, J.K.; Rock, J.A.; Schenken, R.S.; Vernon, M.W. Revised American Society for Reproductive Medicine classification of endometriosis: 1996. *Fertil. Steril.* **1997**, *67*, 817–821. [CrossRef]
33. Fedchenko, N.; Reifenrath, J. Different approaches for interpretation and reporting of immunohistochemistry analysis results in the bone tissue—A review. *Diagn. Pathol.* **2014**, *9*, 221. [CrossRef] [PubMed]
34. Otsu, N. A Threshold Selection Method from Gray-Level Histograms. *IEEE Trans. Syst. Man Cybern.* **1979**, *9*, 62–66. [CrossRef]

35. Soille, P. *Morphological Image Analysis: Principles and Applications*; Springer: Berlin/Heidelberg, Germany, 1999. [CrossRef]
36. Lessey, B.A. Implantation defects in infertile women with endometriosis. *Ann. N. Y. Acad. Sci.* **2002**, *955*, 265–280. [CrossRef]
37. Lessey, B.A.; Kim, J.J. Endometrial receptivity in the eutopic endometrium of women with endometriosis: It is affected, and let me show you why. *Fertil. Steril.* **2017**, *108*, 19–27. [CrossRef]
38. Vannuccini, S.; Clifton, V.L.; Fraser, I.S.; Taylor, H.S.; Critchley, H.; Giudice, L.C.; Petraglia, F. Infertility and reproductive disorders: Impact of hormonal and inflammatory mechanisms on pregnancy outcome. *Hum. Reprod. Update* **2016**, *22*, 104–115. [CrossRef]
39. Brichant, G.; Laraki, I.; Henry, L.; Munaut, C.; Nisolle, M. New Therapeutics in Endometriosis: A Review of Hormonal, Non-Hormonal, and Non-Coding RNA Treatments. *Int. J. Mol. Sci.* **2021**, *22*, 10498. [CrossRef]